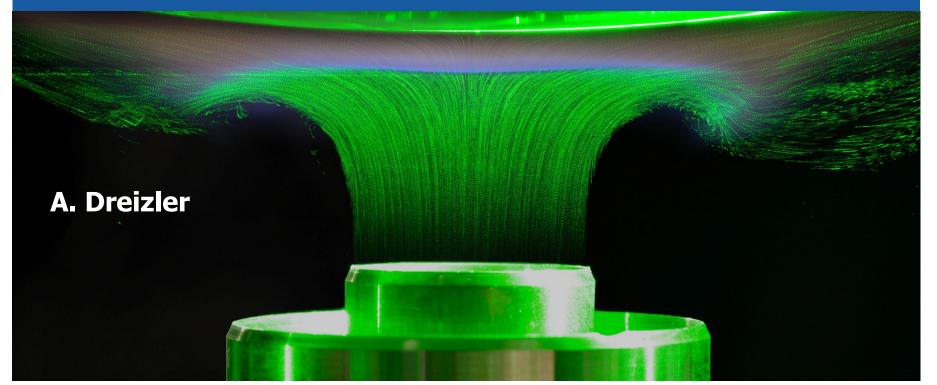
Advanced Laser Diagnostics in Combustion

TU Darmstadt, Germany Dept. of Mechanical Engineering Institute for Reactive Flows and Diagnostics



TECHNISCHE

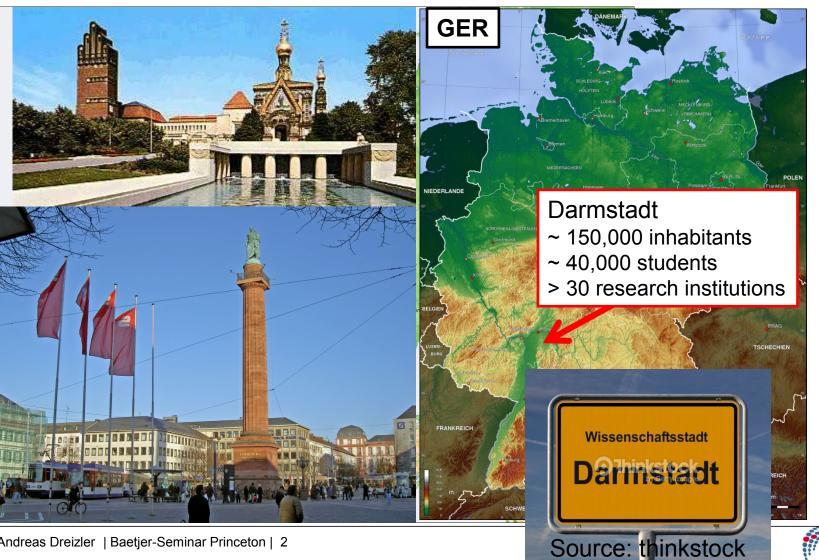
UNIVERSITÄT DARMSTADT



Copyright ©2017 by Andreas Dreizler. This material is not to be sold, reproduced or distributed without prior written permission of the owner, Andreas Dreizler

Where to find the city of Darmstadt?



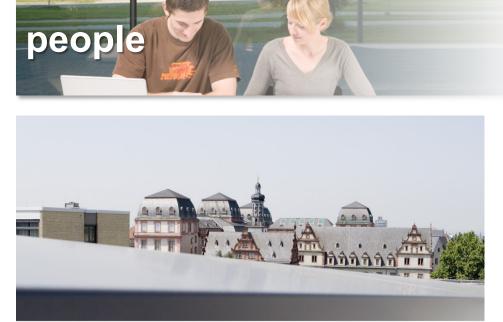


Andreas Dreizler | Baetjer-Seminar Princeton | 2



TU Darmstadt in numbers





Students	25,900
Professors	300
Research associates	2,150
Administrative and technical employees	1,750

One focus: "energy conversion"

Engineering	50%
Natural Sciences	35%
Social Sciences	15%



TU Darmstadt: Dept. of Mechanical Engineering





Students	3,000
Professors/institutes	27
Research associates	>400
Third party funding (2015)	46 Mio €



Institute Reactive Flows and Diagnostics http://www.rsm.tu-darmstadt.de/rsm/index.en.jsp

- Prof. Dreizler (director)
- Dr. Böhm, Dr. Wagner, Prof. Ebert
- 25 Research associates (ph.D.)
- 9 technical and administrative staff
- Third party funding in 2015 >3 Mio €
- \rightarrow Focus on Turbulent Combustion
- → Advanced Laser Diagnostics



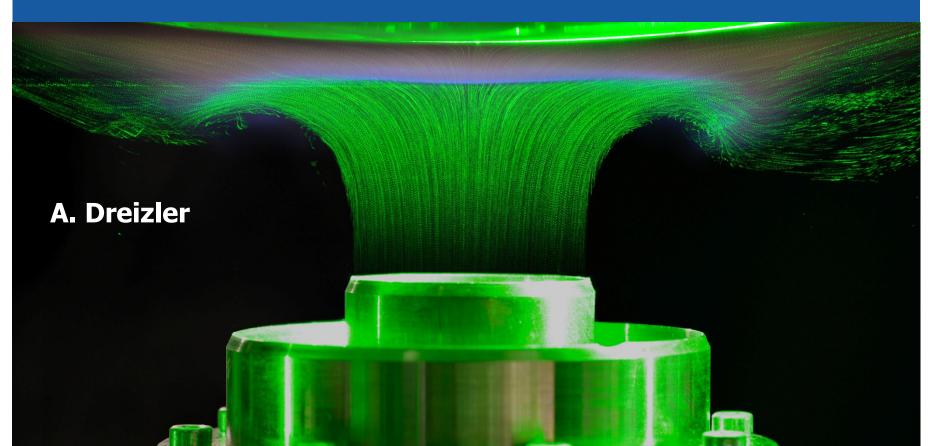
Advanced Laser Diagnostics in Combustion

TU Darmstadt, Germany Dept. of Mechanical Engineering Institute for Reactive Flows and Diagnostics



TECHNISCHE

UNIVERSITÄT



Andreas Dreizler | 5

Challenges in combustion research



- → Need for efficient, clean and flexible combustion technology
- → Coherent action of combustion-community: experiments, theory/modeling and simulation
- \rightarrow Objective of this lecture series:
 - Highlight role of combustion diagnostics
 - Provide some basics of light matter interaction
 - Discussion of most important laser combustion diagnostic methods
 - Present some topical application examples

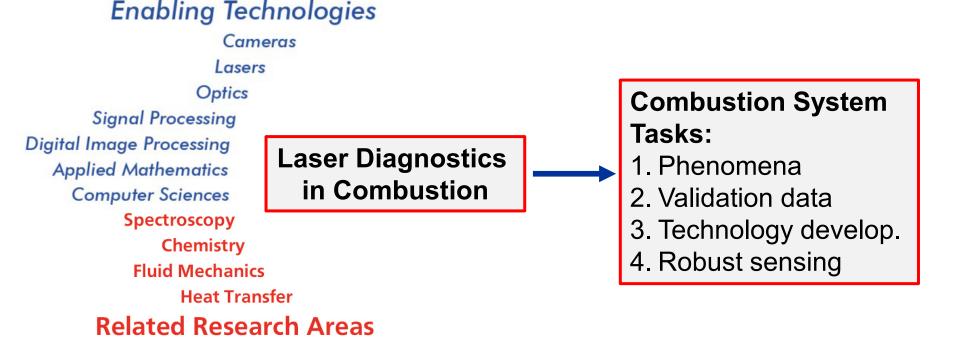


Content



- Introduction
- Benchmark experiments
- General requirements for laser combustion diagnostics
- Particle-based velocimetry
- Gas-phase thermometry
- Surface thermometry
- Gas-phase concentration measurements
- Towards 4D-imaging
- Application examples
 - Flame-wall interactions in canonical configurations
 - Effusion cooling in gas turbine combustor
 - IC Engine: Technology development









TECHNISCHE UNIVERSITÄT

DARMSTADT

Quantities of primary interest in combustion



• Flow field

- Mean velocities, fluctuations, Reynold-stresses
- Strain, dilatation, vorticity
- Integral length and time scales
- Power spectral densities
- Scalar field
 - Means and fluctuation of temperature and chemical species concentrations
 - Structural information based on 2D- or quasi 3D-diagnostics
 - Scalar gradients
 - Wall/ nozzle temperatures
- Inflow conditions, boundary conditions
- Information on **unsteadiness**, temporal sequences of flow/ scalar fields



Using light – matter interaction for diagnostics



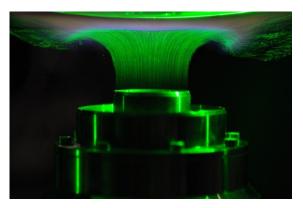
Methods from physics

Engineering sciences

Transfer of methods

- Measuring by laser light
- Insitu-diagnostics → measuring inside combustors
- Non- or minimal intrusive
- High temporal resolution (~10⁻⁸s)
- Reasonable spatial resolution (>10µm)







Laser diagnostic methods



- Flow field
 - Laser Doppler Velocimetry (LDV), 1 to 3 components
 - Particle Image Velocimetry (10 Hz 30 kHz)
 - 2 dimensional and 2 components (2D2C)
 - 2 dimensional and 3 components (2D3C stereo PIV)
 - 3 dimensional and 3 components (3D3C tomographic PIV)
- Two-phase flows
 - Mie scattering
 - Phase Doppler Anemometry (PDA)
- Scalar field
 - Mie scattering
 - Laser absorption spectroscopy (LAS) but line-of-sight
 - Planar Laser-Induced Fluorescence (PLIF)
 - 1D Raman/Rayleigh scattering
 - Coherent anti-Stokes Raman Spectroscopy (CARS)
 - Thermographic Phosphors (TG)



Towards complex combustion systems



- Laser diagnostic methods have been used primarily in unconfined
 gaseous flames
- Additional challenges in practical
 - Enclosure, high pressure –
 - High turbulence levels \rightarrow s



syst

es

Darmstadt Stratified flame





Task 1: Studying phenomena by laser diagnostics



- Mimic specific properties of practical combustion systems in canonical configurations
- Adapt/develop laser diagnostics for monitoring of a specific property
- Exploit rapid developments in laser and camera technology to break new ground
 - From single-parameter to multi-parameter diagnostics
 - From 0-D towards 3-D measurements

AMBRIDGE

- From statistical independent measurements at low sampling rates towardshigh-speed diagnostics for statistically correlated measurements
- → Ultimate goal: summarize phenomenological understanding in physically consistent and predictive mathematical schematic of flame kernel

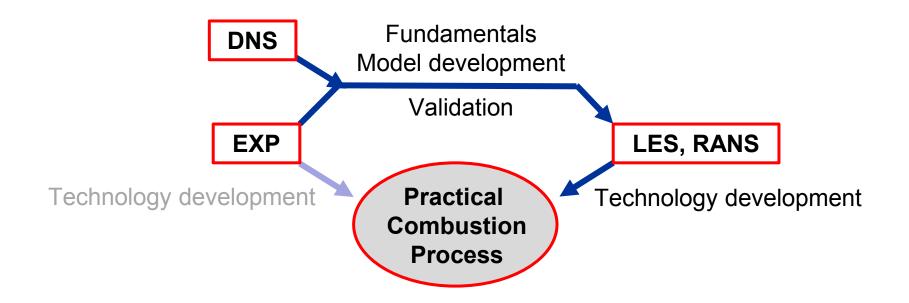
expansion following local ignition



Task 2: Provide validation data



• Interplay of experimental and numerical methods for developing future combustion technologies





Task 2: Provide validation data

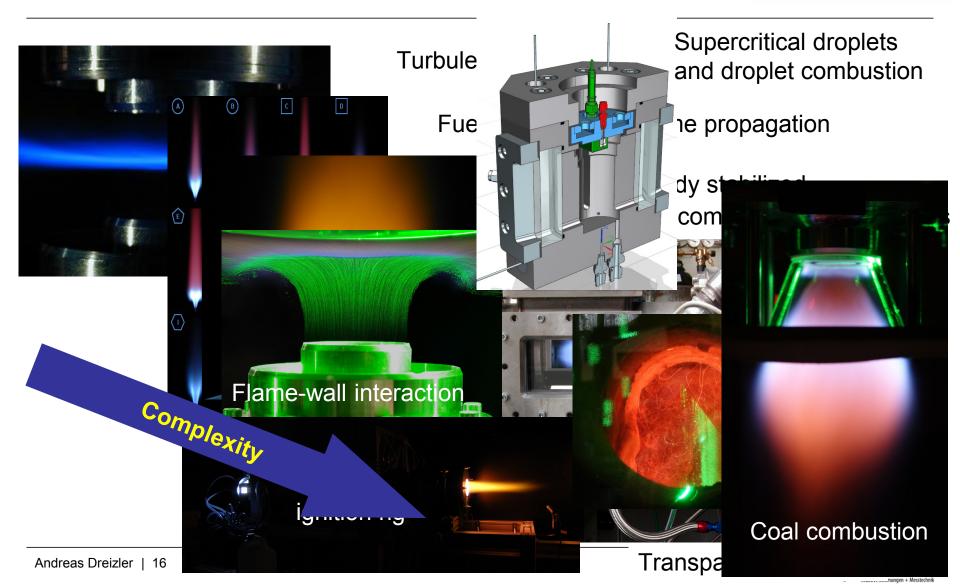


- Validation sequence: from simple to complex
 - Stepwise approach: select specific sub-processes and build experiment to develop and validate models for this specific subprocess
 - Example:
 - Turbulence-chemistry interaction
 - Soot formation
 - Spray breakup
 - ...



Task 2: Provide validation data - from simple to complex, strategy at TUD





Task 3: Support technology development



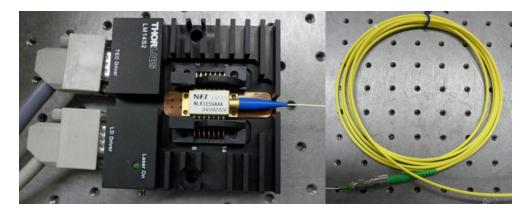
- Development of future combustion technology requires billions of Euro (IC engine, gas turbine combustor, coal power plant, rocket motor, ...)
- \rightarrow Not the core-business of universities
- University task: development of methods (experimental, theoretical, numerical) supporting technology development and educate well-trained engineers
- \rightarrow In this context: Transfer of measurement methods to industry
 - By graduated students
 - Bilateral industry projects

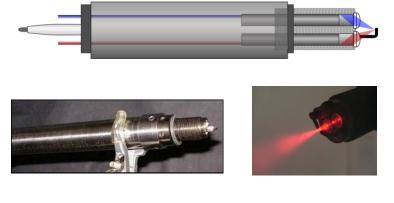


Task 4: Develop robust sensors



- Reliable components and easy operation without special training
- Applicable to real-world combustion systems
- → Fiber-based optical sensors in combination with (direct) absorption spectroscopy





DFB-diode laser, mounted

Glass fiber SMF-28

Fiber-coupled spark plug sensor

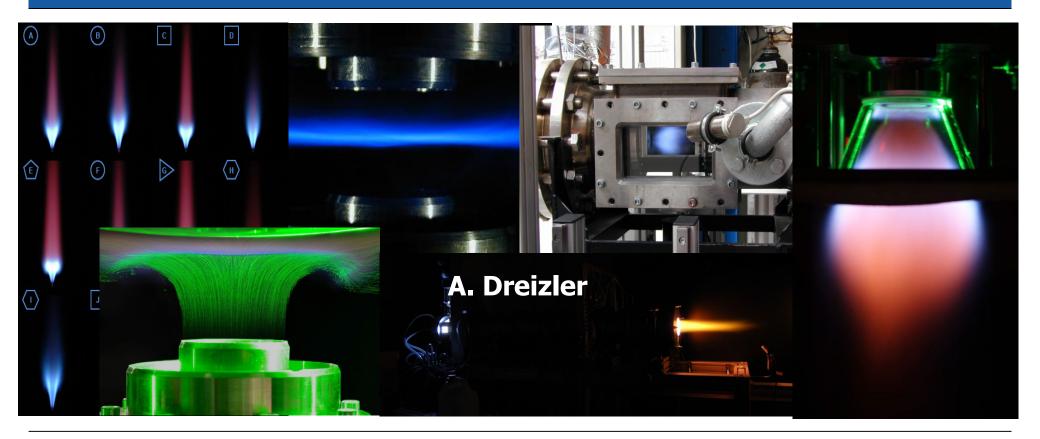


Chapter 2: Benchmark Experiments

TU Darmstadt, Germany Dept. of Mechanical Engineering Institute for Reactive Flows and Diagnostics



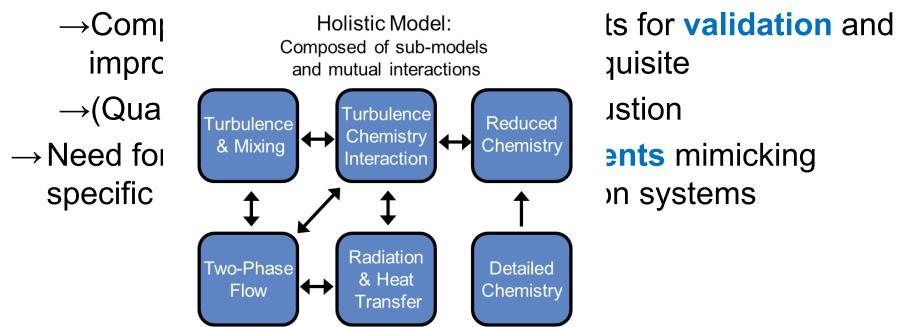




Validation of numerical simulations



- Experimental research in turbulent flames needs suitable generic combustion systems
- Numerical simulations are based on models
 - Turbulence model
 - Combustion model
 - Turbulence-chemistry interaction model
 - Spray model ...



Bench mark flames/ configurations



- Requirements for optical diagnostics
 - Optical access from three sides to enable application of different laser diagnostics
 - Nozzle exit accessible, such that radial profiles can be recorded as close as possible (~1mm)
 - Optical access to interior of nozzle (if possible)
 - In case of atmospheric flames shielding from the lab (coflowing air)
 - Decoupling of the flame from the exhaust gas system
 - Fuel composition that does not interfere with the laser/ detection wavelength

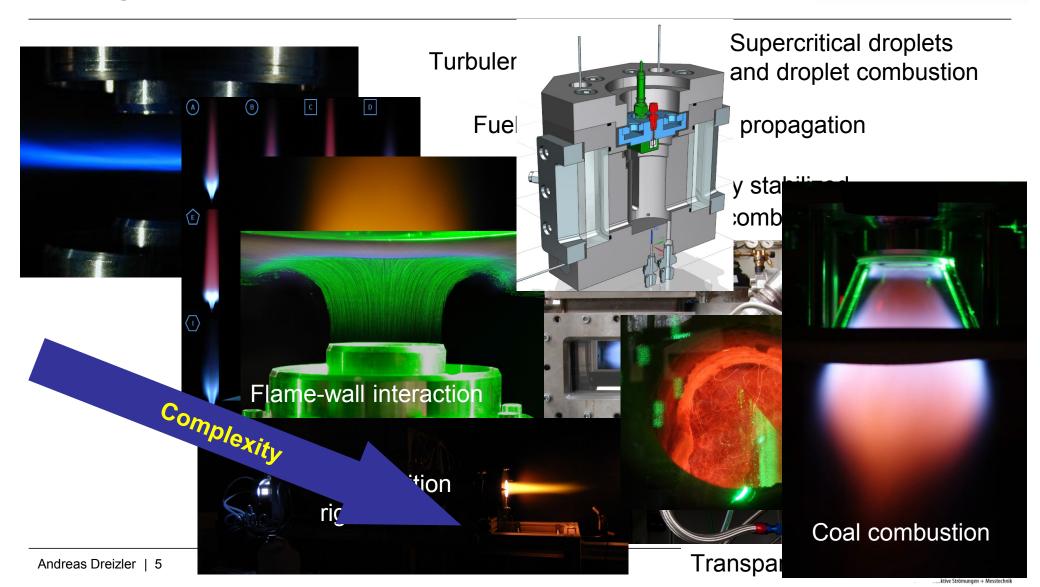
Bench mark flames/ configurations



- Requirements for validation of numerical simulations
 - Known or measurable inflow conditions
 - Well-defined boundary conditions
 - Parametric variation ("flame sequence") of key-quantities such as
 - Fuel composition, equivalence ratio
 - Reynolds-number, thermal load
 - Swirl intensity
 - Pressure
 - Geometry
 - \rightarrow Identify sensitivities

From simple to complex – benchmark configurations at TUD

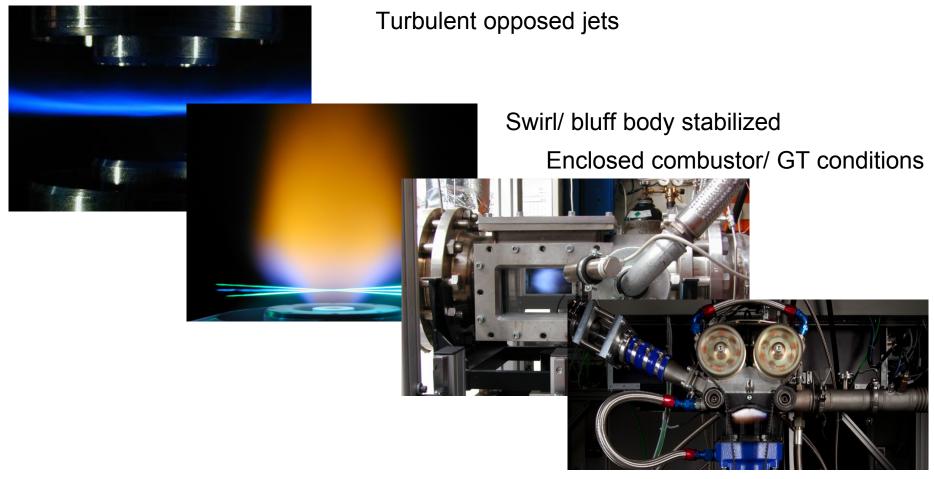




Bench mark configurations



• 1 Example of optically accessible IC-engine



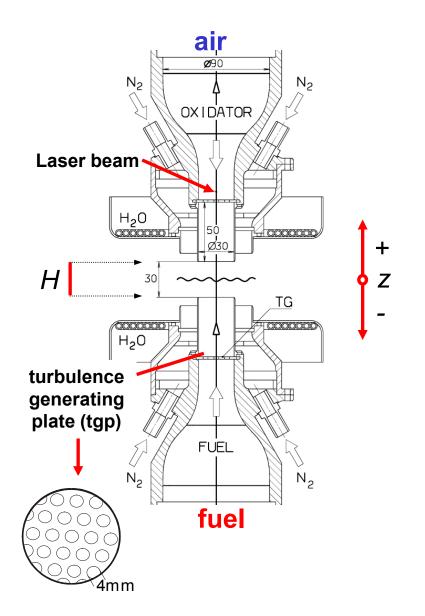
TECHNISCHE

UNIVERSITÄT DARMSTADT

Example 1: Turbulent opposed jet flame



- Two identical opposed nozzles, D=H=30mm
- Turbulence intensity ~0.07 at nozzle exit, enhanced by turb. grid (tgp)
- N₂ coflow prevents ambient air mixing
- Access laser beam along burner axis
 → no beam steering
- Horizontal stagnation plane → symmetric influence of gravity
- Water cooling for stable long term operation
- Parametric variation
 - Fuel composition
 - Reynolds-No. (stable to extinction)





- "Flame sequence" \rightarrow Variation of fuel composition and Re
- Fuel: partially premixed methane/air (avoiding soot)

	Re _{air}	<i>a</i> _m (1/s)	Φ = 3.18	Φ = 2.0	Φ = 1.6	Φ = 1.2
	3300	115	TOJ1A			
	4500	158	TOJ1B	TOJ2B	TOJ3B	TOJ4B
	5000	175	TOJ1C	TOJ2C		
	6650	235	TOJ1D	TOJ2D		
Extinction limit	7200	255		TOJ2E		



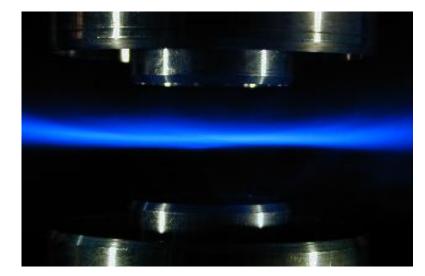
• Flow field quantities for TOJ2D

Bulk velocity $W_{\rm b}$	3.4m/s
Turbulent Re-number Re _t	90
Bulk strain rate $a_{b} = (-W_{b,O} + W_{b,F})/H$	231s ⁻¹
Residence time in mixing layers $t_{res} = a_b^{-1}$	4.3ms
Large-eddy turnover time $t_{ov} = l_0 / (2k)^{1/2}$	16.2ms
Integral time scale <i>T</i> at nozzle exit	1.6ms
Integral length scale <i>I</i> ₀ at nozzle exit	4.7mm
Kolmogorov length scale $\eta_{\rm K}$ at nozzle exit	0.16mm
Batchelor scale at nozzle exit η_c	0.18mm



Visual impression

Time-averaged flame luminosity

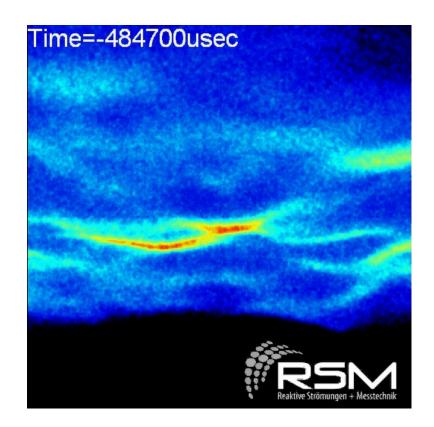


Transient flame luminosity @ 500 Hz





- Special feature of turbulent opposed jet flames:
 - Investigation of flame extinction by increasing strain close to critical value
 - Extinction monitored by temporally resolved chemiluminescence, 10 kHz



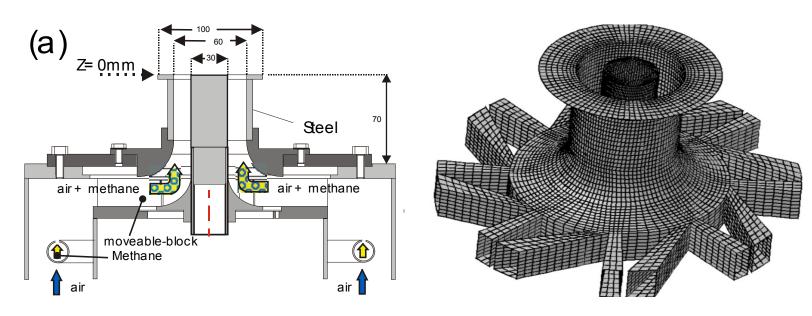
Bench mark configurations



- Example 2: Swirling lean premixed flame
 - Relevant for flame stabilization in real combustors
 - Complex chemistry <u>and</u> complex flow field properties



- Need for reliable data sets of premixed flames
- Parametric variation of
 - Reynolds number
 - Swirl number
 - Equivalence ratio

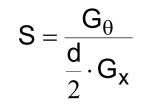


TECHNISCHE

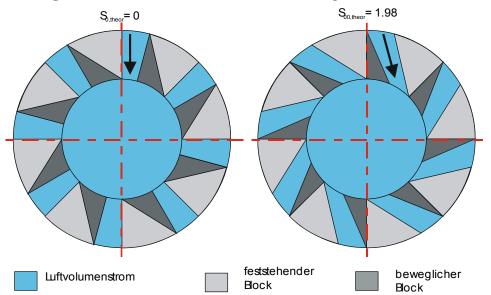
UNIVERSITÄT DARMSTADT



• Swirl number



- G_{θ} Axial flux of tangential momentum
- G_x Axial flux of axial momentum
- Variation by moveable block (motor driven, gear reduction)



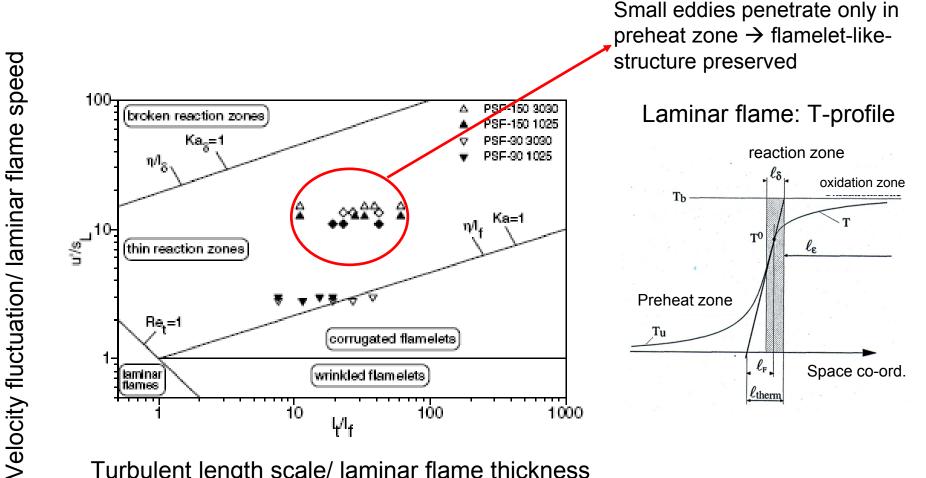


• Parametric variation: Re

		PSF-30	PSF-90	PSF-150
S _{0,th}	[-]	0.75	0.75	0.75
Ρ	[kW]	30	90	150
ϕ	[-]	0.833	0.833	1.0
Q _{gas}	[m _n ³ /h]	3.02	9.06	15.1
Q _{air}	[m _n ³/h]	34.91	104.33	145.45
Re _{tot.}	[-]	10000	29900	42300
s _L	[m/s]	0.36	0.36	0.42
I _F	[m]	0.26 [.] 10 ⁻³	0.26 [.] 10 ⁻³	0.18 [.] 10 ⁻³



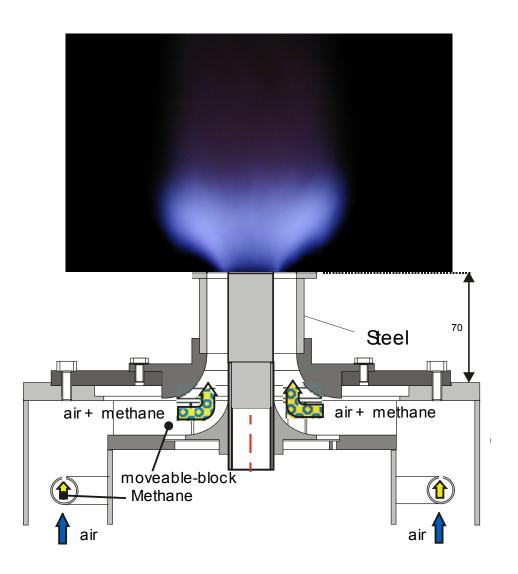
Classification in regime diagram •



Turbulent length scale/ laminar flame thickness

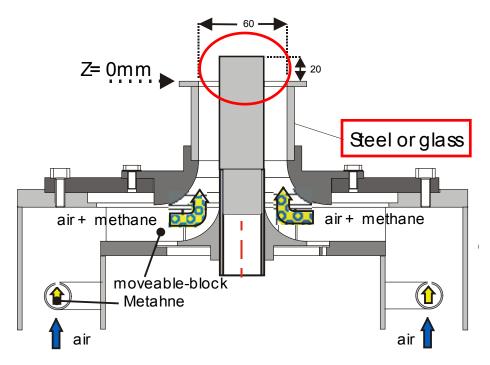


Visual impression



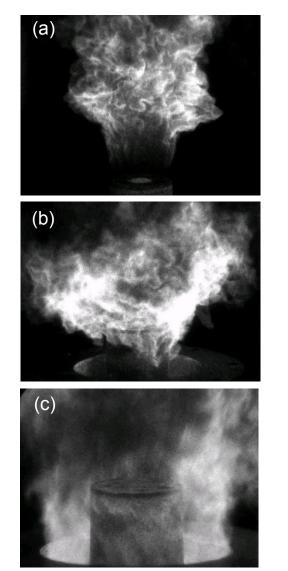


- Transition into flashback
 - Variation of swirl number
 - Variation of equivalence ratio
- Slight adaptation of nozzle geometry
 - Extension of bluff body





Three states of operation



Stable: stabilization at the edge of the bluff body

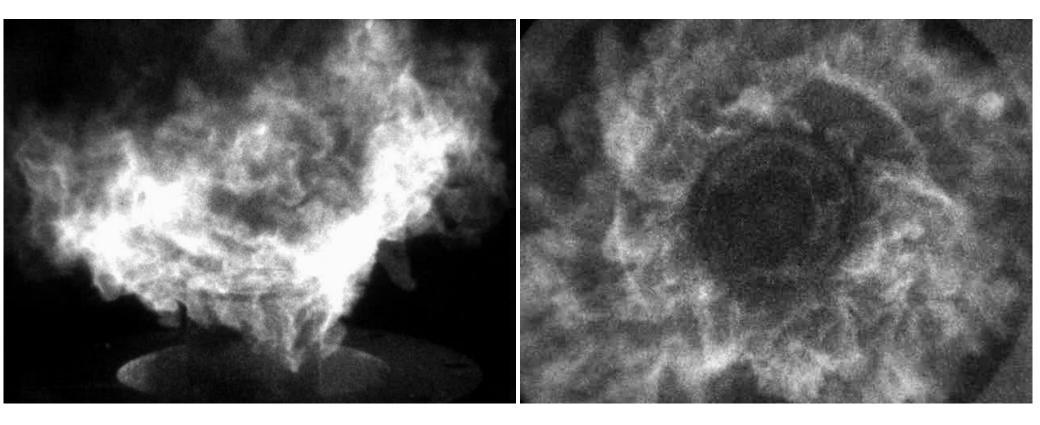
Spinning: flame precesses around the shell of the bluff body

After flashback: the flame is stabilized at the swirler



• Precessing flame

Meta-stable





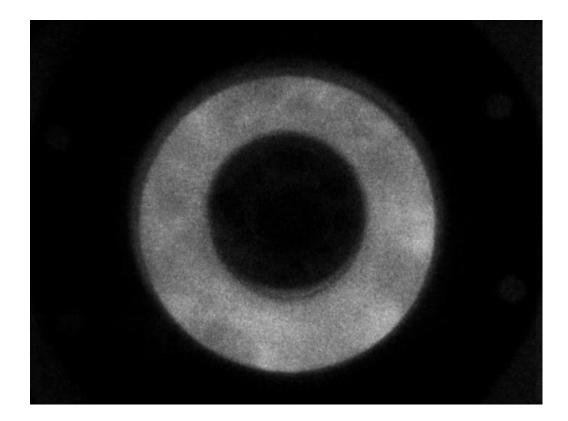
• Precessing flame

Flashback



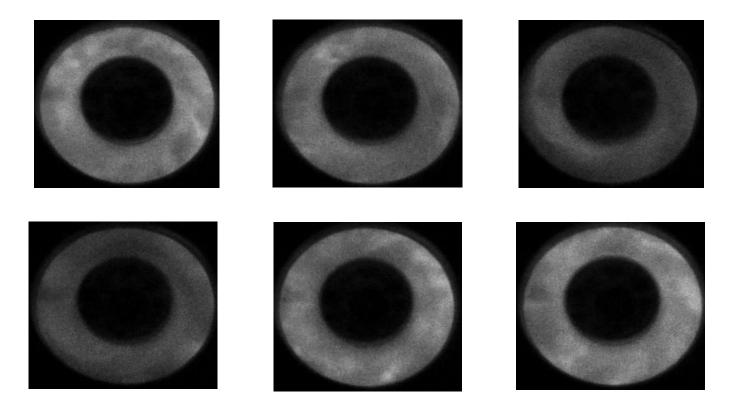


• After flash back: view from top (slightly tilted)





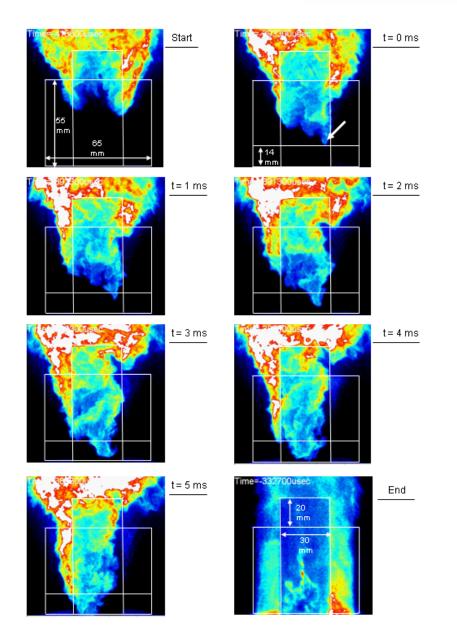
• After flash back: view from top (slightly tilted)



- Flame luminescence monitored by intensified CMOS-camera at a frame rate of 7kHz
- Only 6 exposures of a full cycle are shown
- Cycle duration ~7.5±0.6ms.

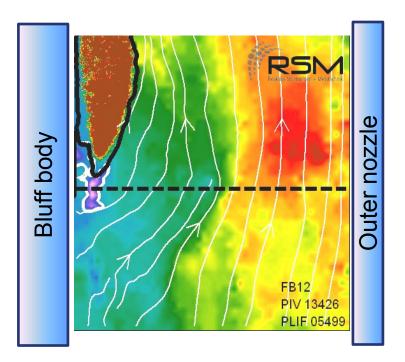


- Transition from spinning
 into flashback
 - Transparent nozzle
 - Chemiluminescence recorded at high repetition rates (kHzregime)

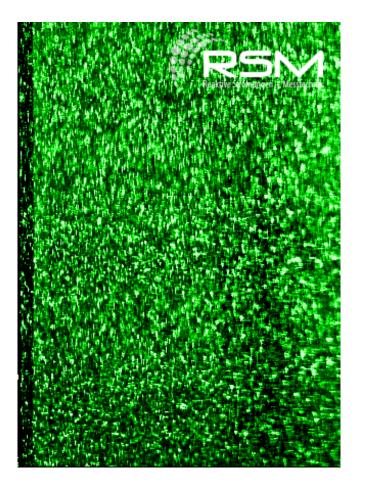


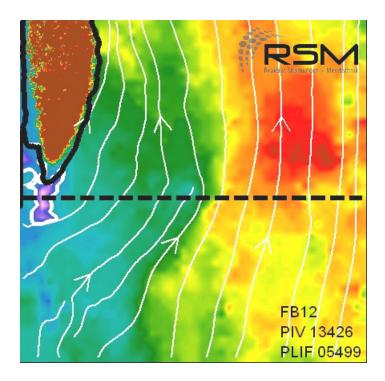


- Transition from spinning into flashback
 - Transparent nozzle
 - OH-PLIF and 2C-PIV recorded at high repetition rates (kHzregime)



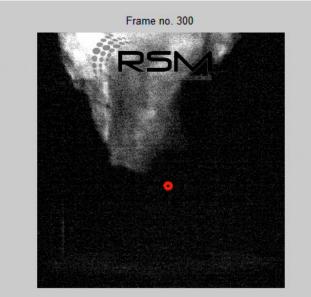


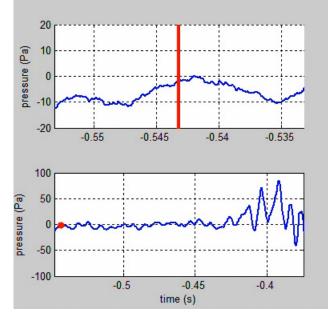






- Transition from spinning into flashback
 - Simultaneous optical and pressure measurements
 - <u>Multi-parameter</u>
 <u>diagnostics</u> crucial for
 better understanding

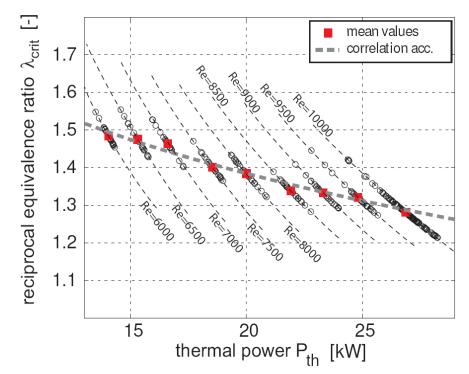






Stability map

- For fixed geometrical swirl number



- Flashback is favored by
 - Lower Reynolds numbers
 - Higher laminar flame speeds
 - Higher swirl intensity (not shown in this graph)

Bench mark configurations



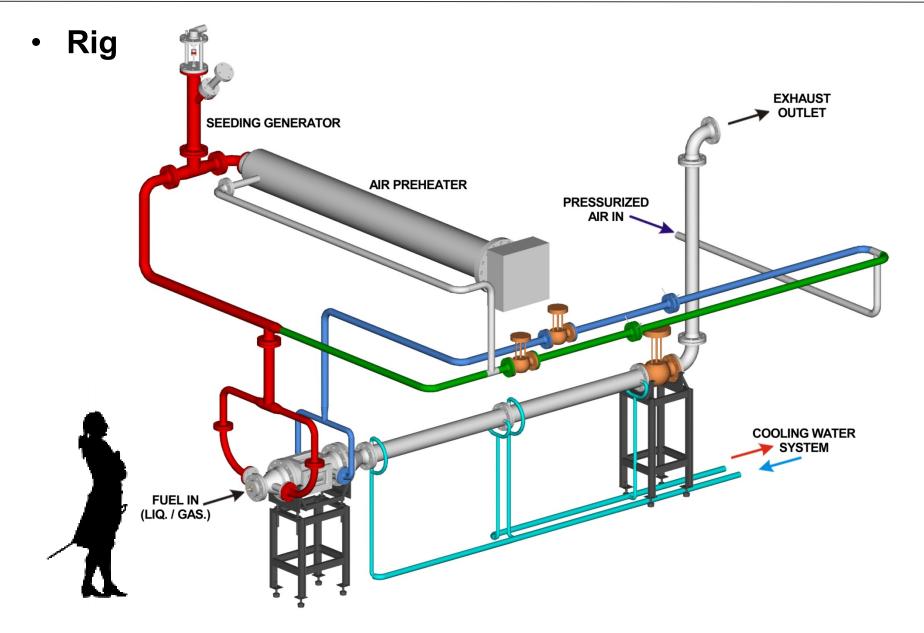
- Example 3: enclosed pressurized flames
 - Non-premixed natural gas flames or spray flames and lean premixed flames
 - Mimicking performance of real combustors but only single nozzle (for example circumferential modes in annular combustors not accessible)



Modular setup

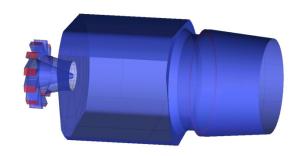
- Pressure housing
- Optically accessible flame tube
- Complex infrastructure
 - Pressurized air supply
 - Electrical heating of combustion air to mimic inlet conditions of GT-combustor
 - Pressurized fuel supply (natural gas compressor, for liquid fuels high pressure pump and large storage capacity)
 - Exhaust gas treatment (cooling)
 - Safety equipment (sensors and explosion protection)

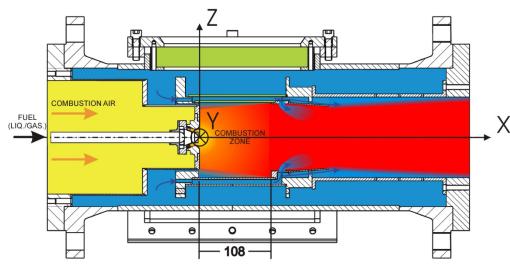


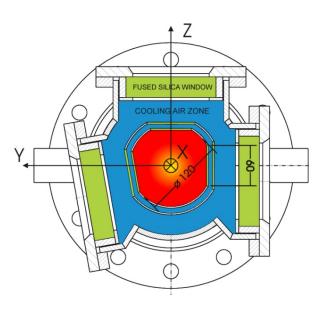




- Optically accessible combustor
- "Can-combustor-concept"
- P_{max}=10bar, T_{max}=773K
- Modular to adapt different geometries/ combustion concepts
- Optical access from three sides for LDA/PDA, PIV, LIF, CARS, etc.
- No disturbance of primary reaction zone by cooling air
- CAD-design for computational meshes



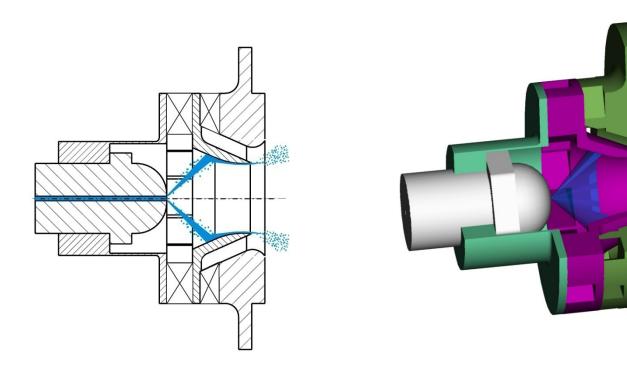






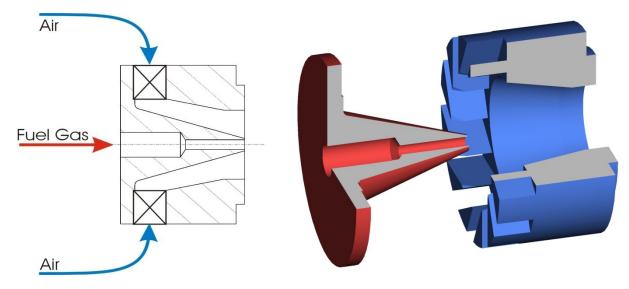
Nozzles

- Spray flames: n-heptane / air
- Surrogate n-heptane advantageous compared to kerosene due to chemical kinetics modeling and spectroscopic properties





- Nozzles
 - Non-premixed gaseous flame: Natural gas / air



- Simple, generic design
- Non-reactive conditions: Mixture of helium and air to match density
- Swirl number from geometry S=1

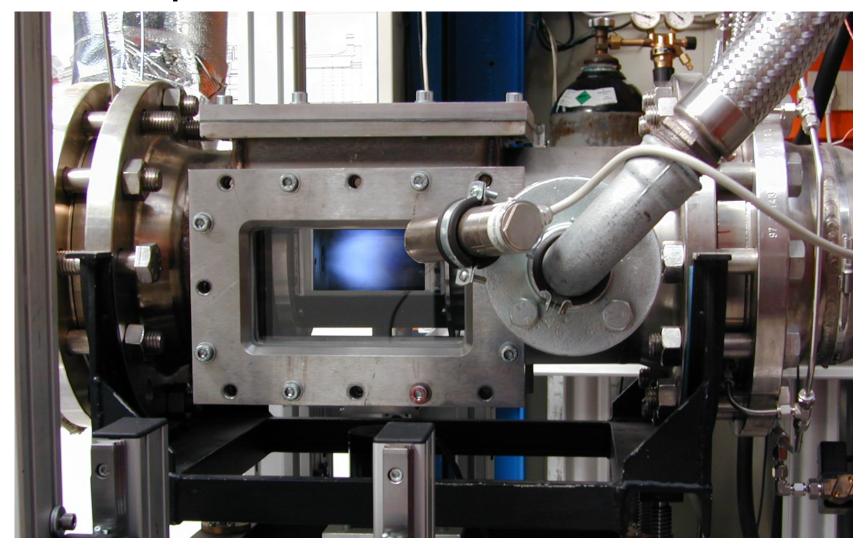


Operational conditions

Pressure	2bar	4bar	6bar
Combustion air temperature	623K	623K	623K
Fuel temperature	373K	373K	373K
Combustion air mass flow	30g/s	60g/s	90g/s
Re _{Air}	46000	92000	138000
<i>Re</i> _{Fuel}	33000	67000	100000

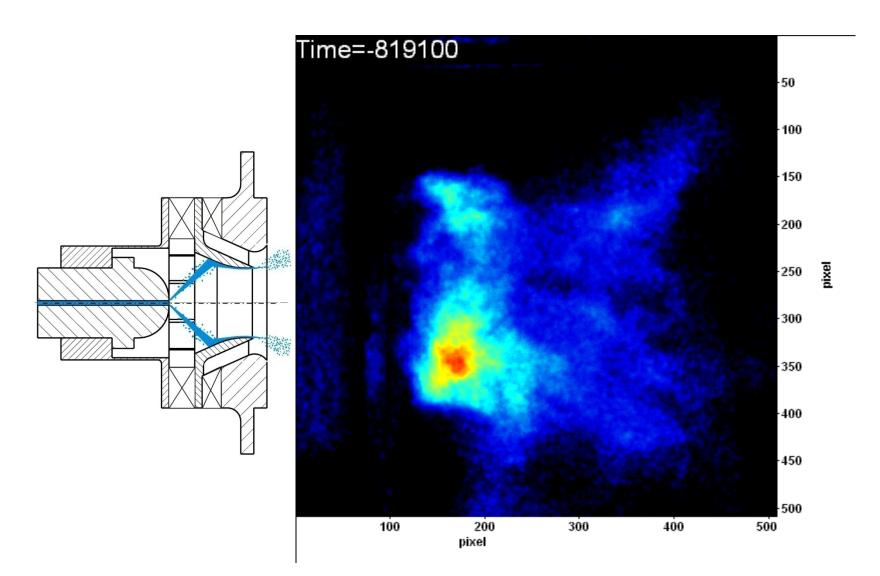


• Visual impression



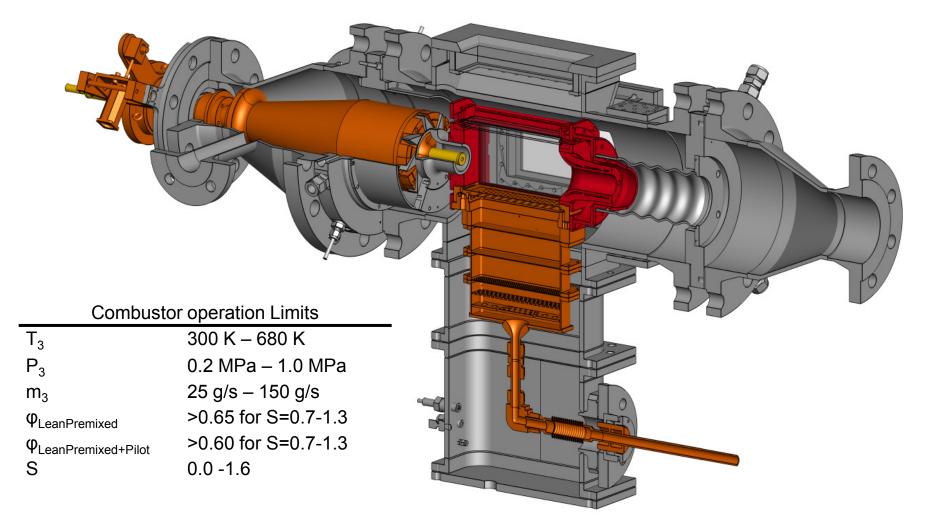


• Visual impression – chemoluminescence of spray flame



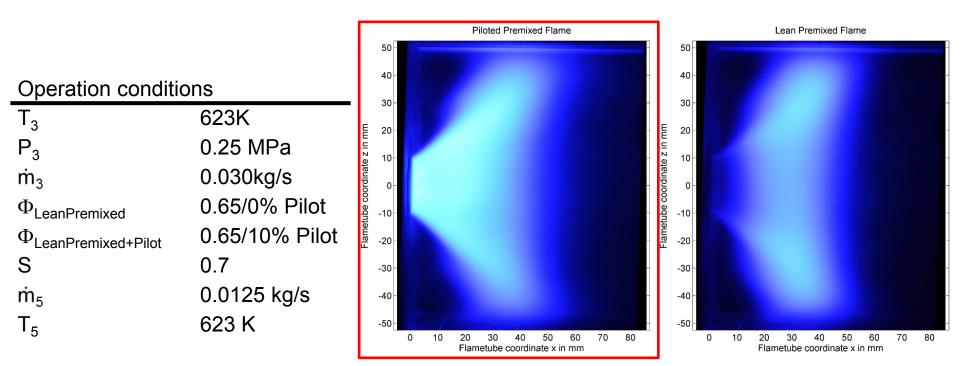


Present research: Effusion cooling





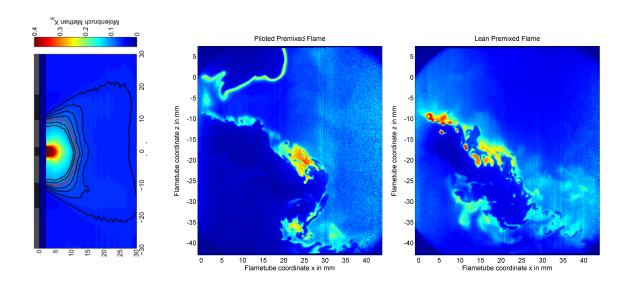
Present research: Effusion cooling

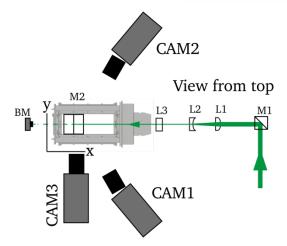


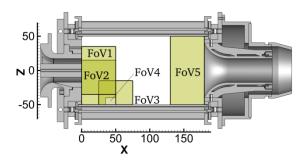
Low-pass (490nm) filtered Chemiluminescence images from piloted and premixed flames



- Present research: Effusion cooling
 - Flow field: 2C and 3C PIV
 - Flame brush: OH-PLIF
 - Mixing fields: Acetone PLIF
 - Gas temp: CARS
 - Surface temp: phosphor thermometry

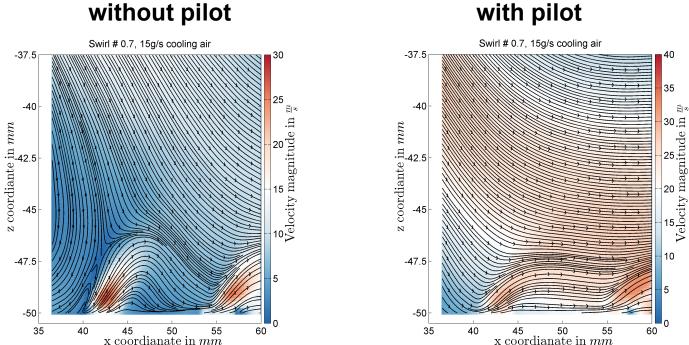








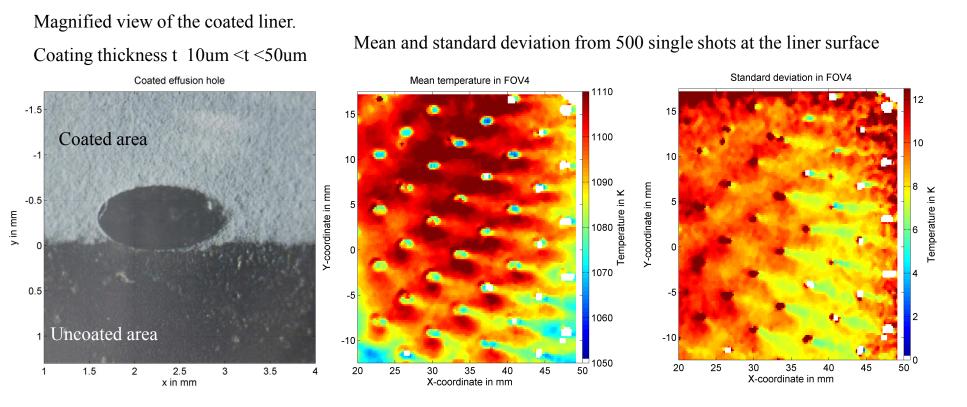
- Present research: Effusion cooling
- **Particle Image Velocimetry PIV** •



with pilot

TECHNISCHE UNIVERSITÄT DARMSTADT

2D wall temperature

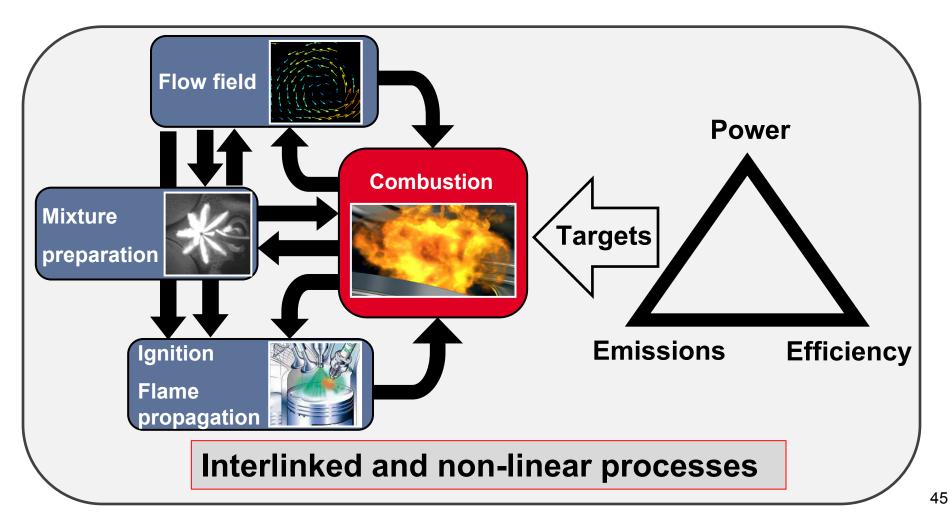


- Temperature measurement in flame wall contact zone at 20mm < x < 45mm
- Influence of cooling film visible in wakes behind single holes

Generic bench mark configurations

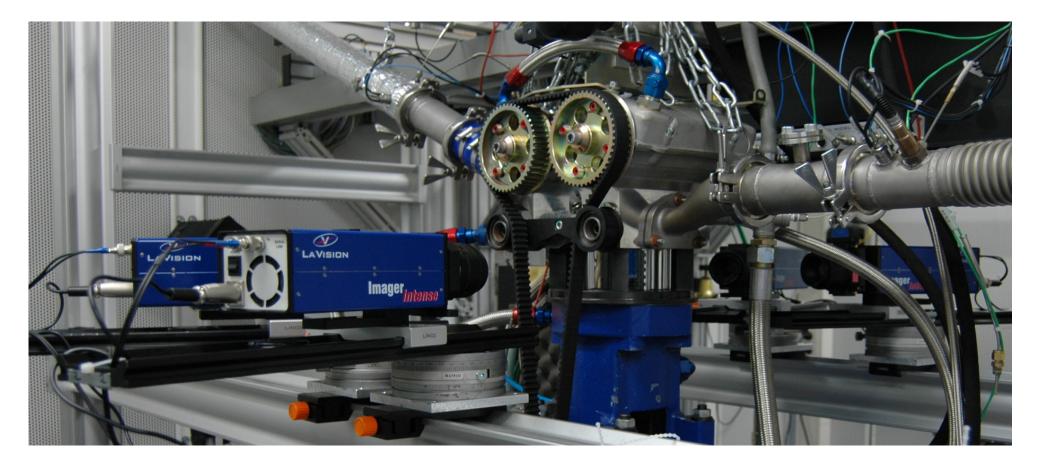


- Example 4: Optically accessible IC-engine
 - Different to GT-combustion there does not exist a simplified generic configuration where important and relevant effects can be studied!



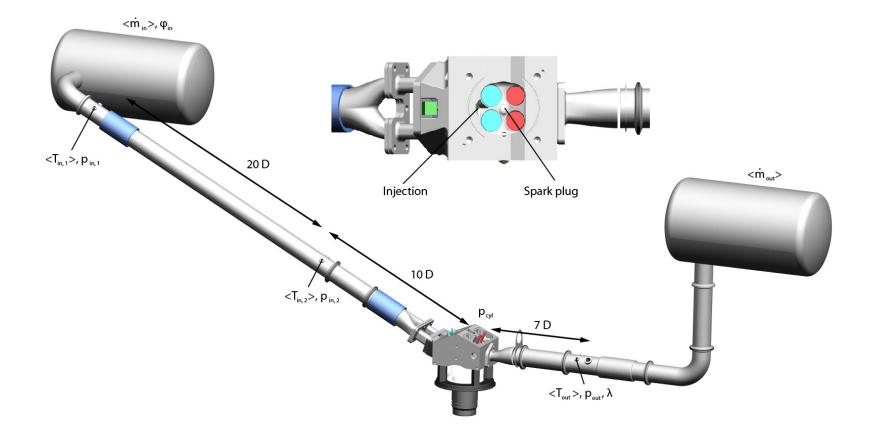
Transparent DISI engine





Boundary conditions





Specifications



Optical accessible IC Engine

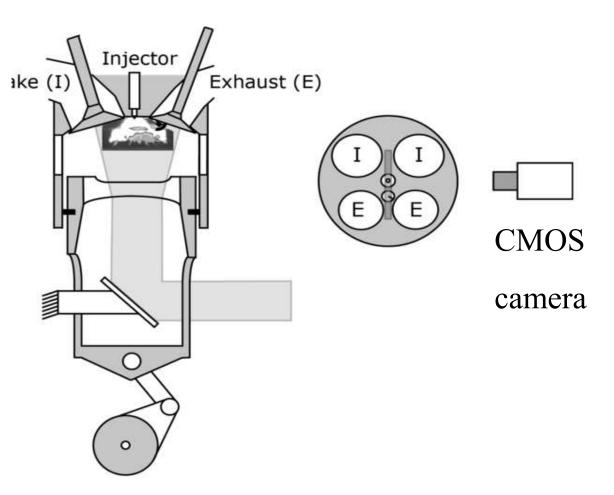
- Capacity: 499 ccm
- Bore: 86 mm
- Stroke: 86 mm
- Compression ratio: 8.5
- Optically accessible liner: 55 mm
- Motored or fired operation:
 - ≤ 3000 rpm
 - Manifold pressure: variable
- Seeding
 - Silicon oil (~1µm) or BN-particles



In-cylinder flow field measurements – 2C PIV



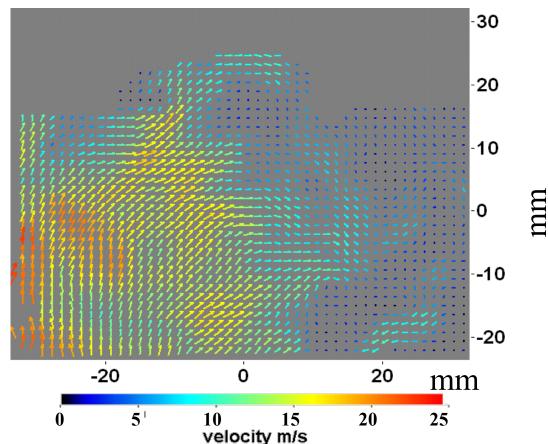
- Particle Image Velocimetry (PIV)
 - -@ 16 kHz
 - -100-0 °bTDC
 - -~40x30mm²
 - -768x592px²
 - -273 cycles/run
- <u>Challenges:</u>
- Scattered light off surfaces
- Contamination optical accesses
- Suitable PIV-seeding particles
- Optimized interval between laser illumination



In-cylinder flow field measurements – 2C PIV

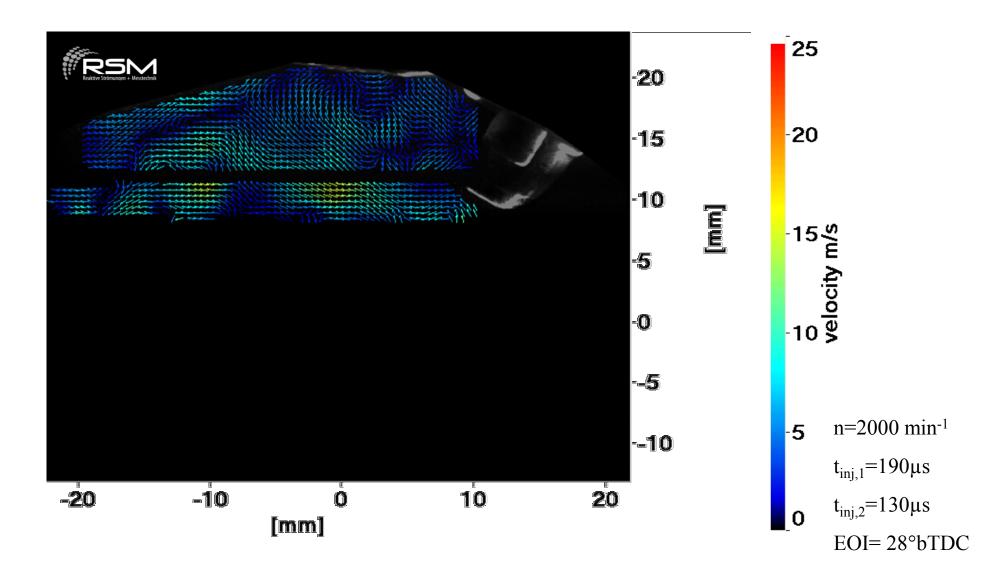


- Particle Image Velocimetry (PIV)
 - -@16 kHz
 - -100-0 °bTDC
 - -~40x30mm²
 - -768x592px²
 - -273 cycles/run
- <u>Challenges:</u>
- Scattered light off surfaces
- Contamination optical accesses
- Suitable PIV-seeding particles
- Optimized interval between laser illumination



Stratified engine operation: Single cycle with double-injection





Towards volumetric imaging: example TomoPIV

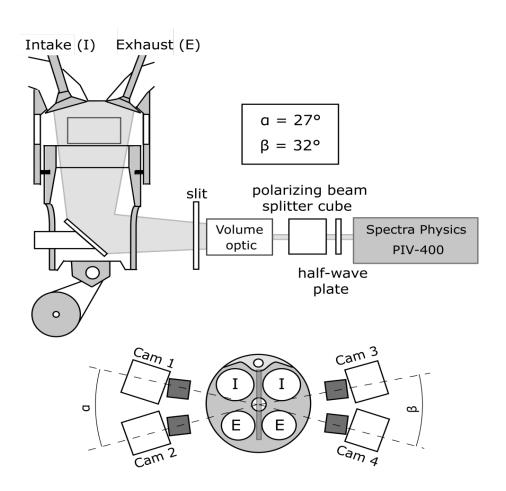


Illumination

- Dual-cavity laser (PIV400, Spectra Physics)
- Avg. 375 mJ per single pulse
- Phase-locked acquisition during intake and compression (<5 Hz)
- Volume of: 48 x 35 x 4/8 mm

Detection

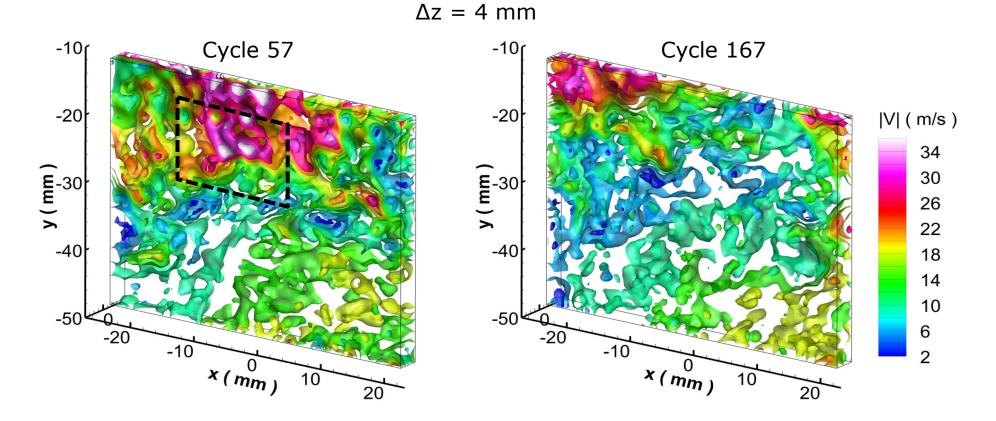
- Interline transfer CCD (ImagerIntense, LaVision, 1376x1040 pixels)
- Nikon 50 mm, 1.4 (f# 16)
- Limitation of Camera angles due to cylinder head bolts





Iso-surfaces of instantaneous velocity magnitudes

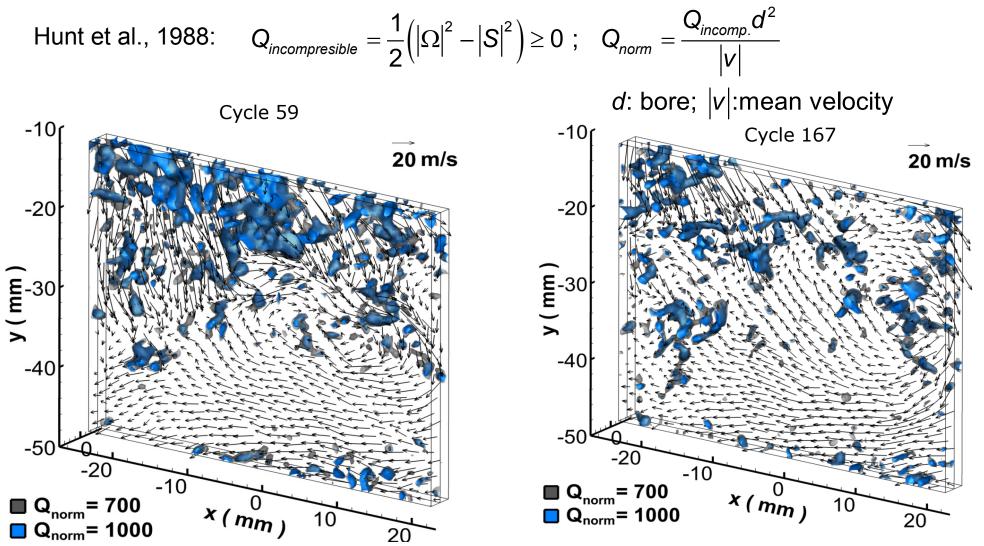
Intake stroke (270° bTDC)



Baum et al. PCI 2013



• Vortex region by second invariant of the velocity gradient tensor



Conclusions – bench mark configurations



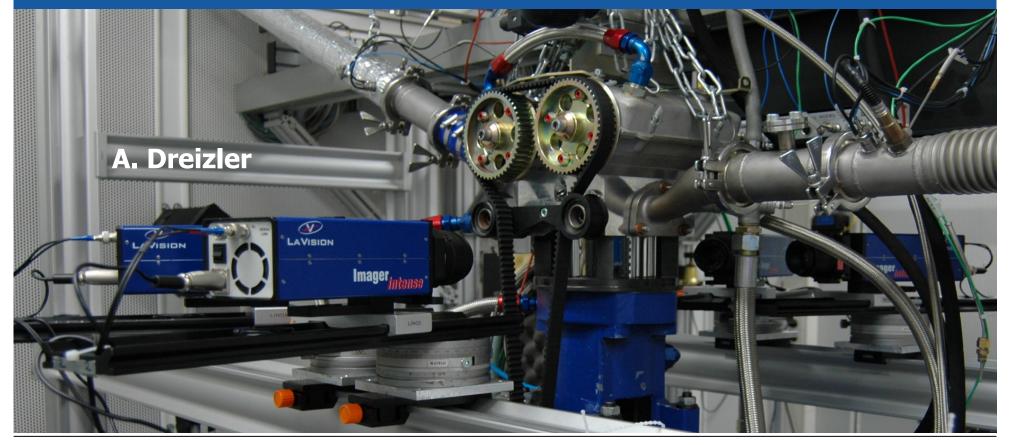
- Configurations of rising complexity and different geometries necessary to study different phenomena
- Optical access in atmospheric flames no problem
- Pressurized combustion (GT-combustor or IC-engine)
 - causes large investments for reliable, safe and reproducible operation
 - realization of optical access more difficult
- Improved characterization of inflow conditions needs more attention

Chapter 3: General Requirements for Laser Combustion Diagnostics

TU Darmstadt, Germany Dept. of Mechanical Engineering Institute for Reactive Flows and Diagnostics







Quantities of primary interest in combustion



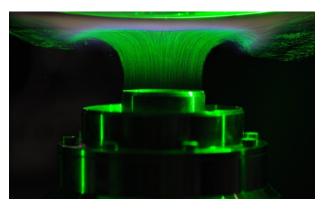
Methods from physics

Engineering sciences

Transfer of methods

- Measuring by laser light
- Insitu-diagnostics → measuring inside combustors
- Non- or minimal intrusive
- High temporal resolution (~10⁻⁸s)
- Reasonable spatial resolution (>10µm)



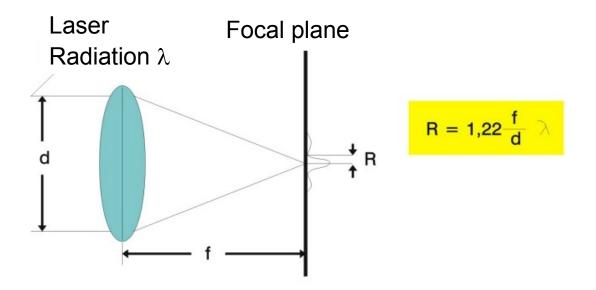






Laser properties

- Coherent radiation \rightarrow well focusable \rightarrow small spot sizes = small probe volumes
- For TEM₀₀-mode operation:



- Typical values f=350mm, d=10mm, λ =532nm
- \rightarrow Spot size diameter 2R~45µm
- In practice for pulsed lasers worse (~200µm)

Spatial resolution



Typical spatial scales in turbulent flows

- Integral length scale
$$L_{ij,k}(\vec{x},t) = \frac{1}{2} \int_{-\infty}^{\infty} \rho_{ij}(\vec{x},t,r_k,0) dr_k$$

- Spatial covariance
$$\rho_{ij}(\vec{x},\vec{r},t) = \frac{u'_i(\vec{x},t)u'_j(\vec{x}+\vec{r},t)}{\sqrt{{u'_i}^2}(\vec{x},t)\sqrt{{u'_j}^2}(\vec{x}+\vec{r},t)}$$

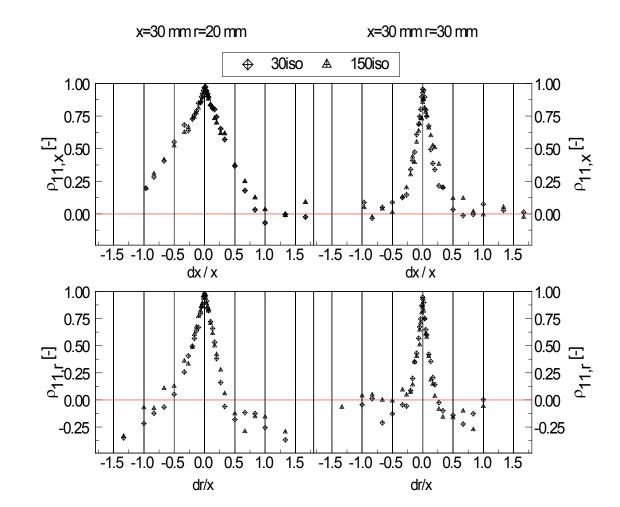
Kolmogorov (smallest) length scale
 (v kinematic viscosity m²/s)

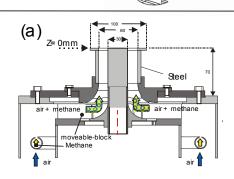
$$\eta_k = \left(\frac{\nu^3}{\varepsilon}\right)^{1/4} \qquad \varepsilon = \frac{k^{\frac{3}{2}}}{L}$$

$$\eta_k = \frac{L}{Re_t^{0.75}} \qquad Re_t = \frac{k^{\frac{1}{2}}L}{\nu}$$

Spatial resolution

- Full optical resolution:
 2R (spot diameter) ≤ η_k (Kolmogorov scale)
- Example non-reacting swirling flow

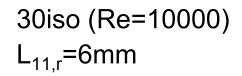




TECHNISCHE

UNIVERSITÄT DARMSTADT

30iso (Re=10000) L_{11,x}=10mm





Spatial resolution



- Comparison optical resolution and Kolmogorov scale
 - Spot size 2R~45μm (f=350mm, d=10mm, λ=532nm)
 - Kolmogorov scale $\eta_k \sim 50 \mu m$ (swirled air flow at Re=10000)
 - \rightarrow Same order of magnitude but in practice often not fully resolved
- \rightarrow To be considered when comparing experimental data to numerical results
 - Smoothing of measurands is an important issue but <u>not yet any</u> <u>commonly agreed advice for best practice</u> when comparing "filtered" measurands with "filtered" quantities from CFD



- Quality (q-) switch allows ns-pulses (10⁻⁹ s)
- 1ns pulse corresponds to ~30cm
- Pulsed operation increases intensity dramatically \rightarrow non-linear optical methods become feasible (most prominent method CARS)
- Typical time scales in turbulent flames

- Integral time scale
$$T_{ij}(\vec{x},t) = \frac{1}{2} \int_{-\infty}^{\infty} \rho_{ij}(\vec{x},t,0,\tau) d\tau$$

- Temporal auto-covariance $\rho_{ij}(\vec{x},t,0,\tau) = \frac{\overline{u'_i(\vec{x},t)u'_j(\vec{x},t+\tau)}}{\sqrt{u'_i^2}(\vec{x},t)\sqrt{u'_j^2}(\vec{x},t+\tau)}$

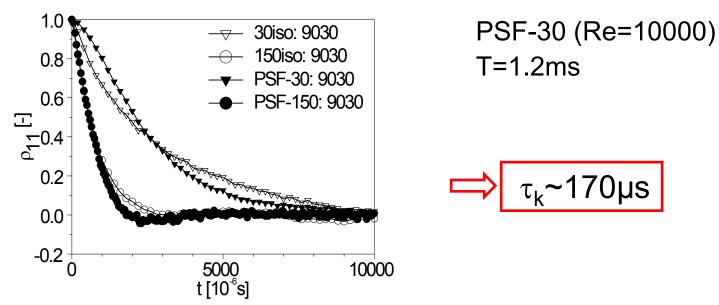
- Kolmogorov time scale
$$\tau_k = \left(\frac{v}{s}\right)^2$$

$$\varepsilon = \frac{k^{\frac{3}{2}}}{L}$$

TECHNISCHE



• Example reacting swirling lean premixed flame

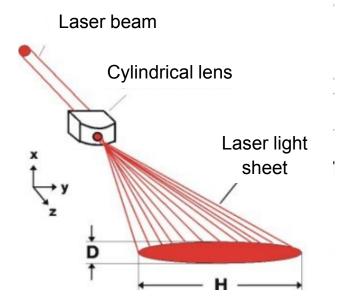


- Comparison optical resolution and Kolmogorov time scale
 - Laser pulses are much shorter than any time scales in turbulent flames
 - Temporal resolution is no problem
 - → Comparison of calculated and measured power spectra better in frequency domain

0D – 3D measurements by laser diagnostics



- Up to 3 spatial dimensions are observable
 - 0D/ 1D: generation of a thin laser beam
 - 2D: generation of a laser light sheet



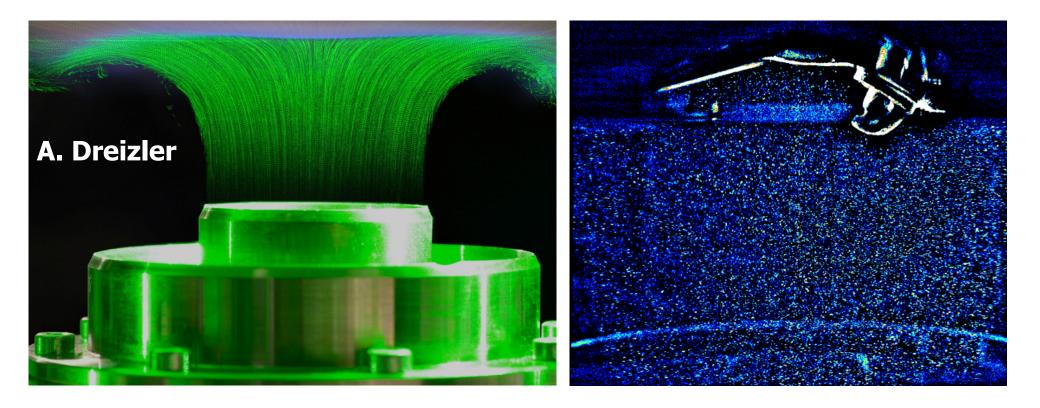
- (Quasi-)3D: multiple and parallel laser light sheets
- Extension to cinematographic (quasi-)3D imaging

Chapter 4: Particle-Based Velocimetry

TU Darmstadt, Germany Dept. of Mechanical Engineering Institute for Reactive Flows and Diagnostics



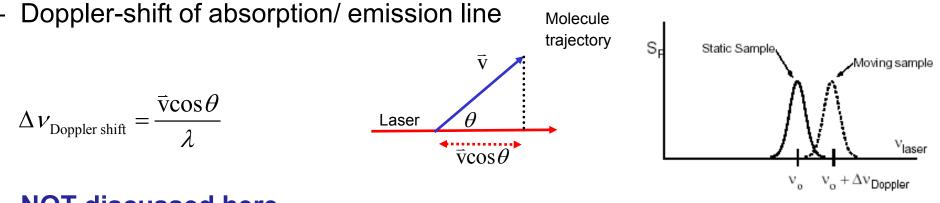




Flow field measurements

TECHNISCHE UNIVERSITÄT DARMSTADT

Spectroscopic methods



NOT discussed here

Particle based methods

- Doppler shift during Mie scattering process (Laser Doppler Velocimetry, LDV, using heterodyne technique)
- Sequential exposures of instantaneous particle positions by Mie scattering (Particle Image Velocimetry, PIV)



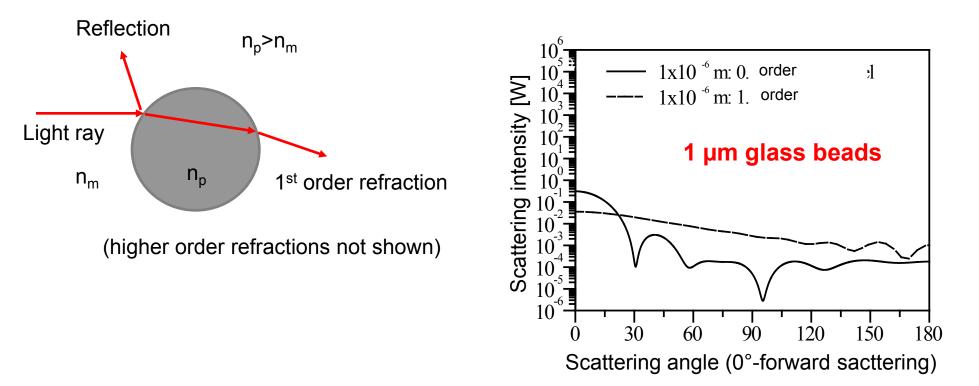
Mie scattering: Scattering of electro-magnetic waves off spherical particles



Particle-based flow field measurements



- Mie scattering: spherical particles seeded to the flow
 - Intensity of Mie scattered light in dependence of scattering angle
 - Example: transparent glass bead, 1µm diameter



- Forward scattering highest intensities
- Use of Mie scattering for tracking gas velocities

Particle-based flow field measurements



- Seeding material for turbulent flame research
 - Chemically inert
 - Melting point exceeding adiabatic flame temperatures (>2500K), oil droplets as in aerodynamic studies often not feasible
 - Sufficiently small to reduce slip *s* between particle (u_p) and gaseous fluid (u_f)

$$s = \left| \frac{u_f - u_p}{u_f} \right| < 1\%$$

Cut-off frequency exceeding slip of 1%

$$f_{c} = \frac{\sqrt{(2s-s^{2})}}{2\pi\tau_{0}\sqrt{(1-s^{2})\left(1+\frac{\rho_{f}}{2\rho_{p}}\right)^{2} - \left(\frac{3\rho_{f}}{2\rho_{p}}\right)^{2}}}$$

$$\tau_0 = \frac{\rho_P d_P^2}{18\eta}$$
 η : dynamic viscosity



• Typical seeding materials

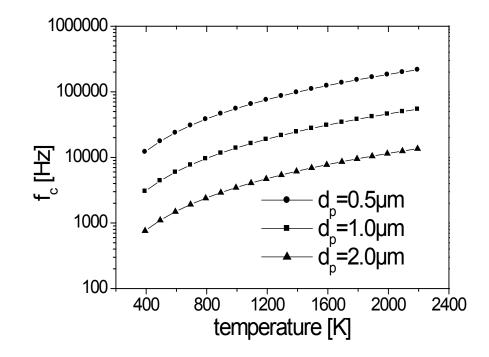
Material	Short notation	Density [kg/m³]	Melting point [K]
Magnesium oxide	MgO	3500	2800
Zirconium silicate	ZrSiO ₄	3900 - 4700	2420
Titanium dioxide	TiO ₂	4000	1780

Particle-based flow field measurements



• Example

- MgO
- f_c : maximal turbulent fluctuations that can be resolved, slip < 1%

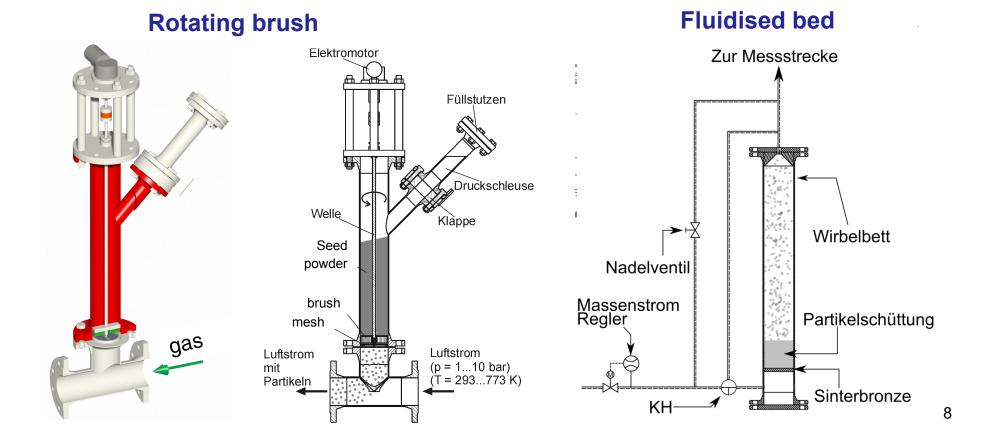


- → Smaller particles and higher viscosity (higher T) expand the range of resolvable velocity fluctuations
- $\rightarrow \underline{\text{But}}$: Mie signal decrease nonlinearly with decreasing particle size

Particle-based flow field measurements



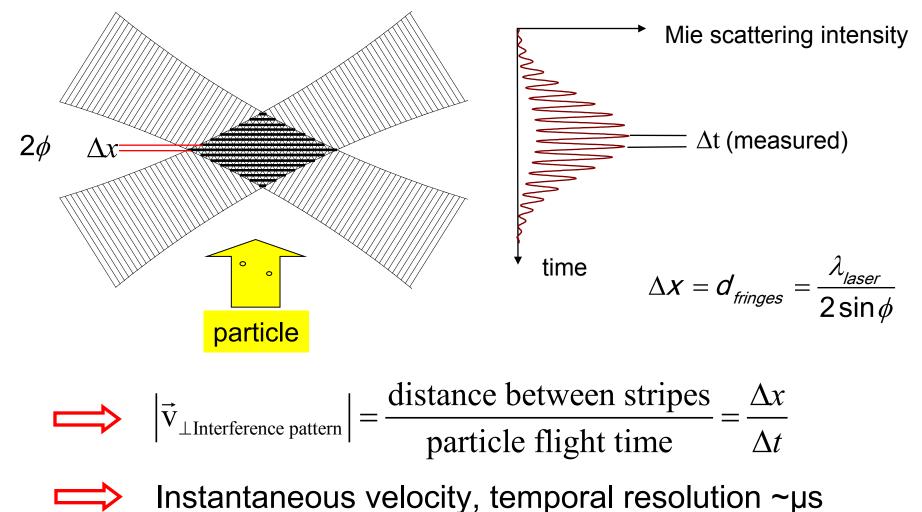
- Addition of seed material to the flow
 - All gas feeds must be seeded, otherwise results can be biased
 - Volume fraction of seed material must be variable
 - Bypass, controlled and variable mass flow
 - Appropriate assembly for addition of seed ("seeding-generator")





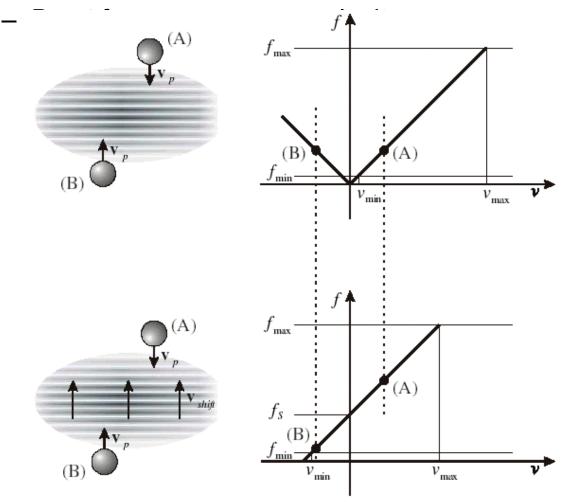
Principle



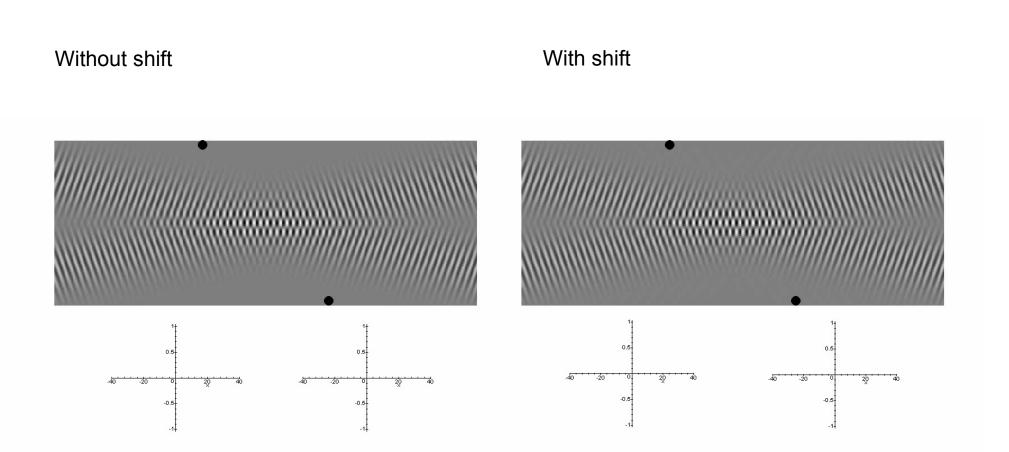




- Measurement of absolute values = ambiguity in direction
- → Use of moving interference stripes (generated by Bragg cell, phononphoton interaction, crossing laser beams slightly different frequency, difference ~ 40 MHz)





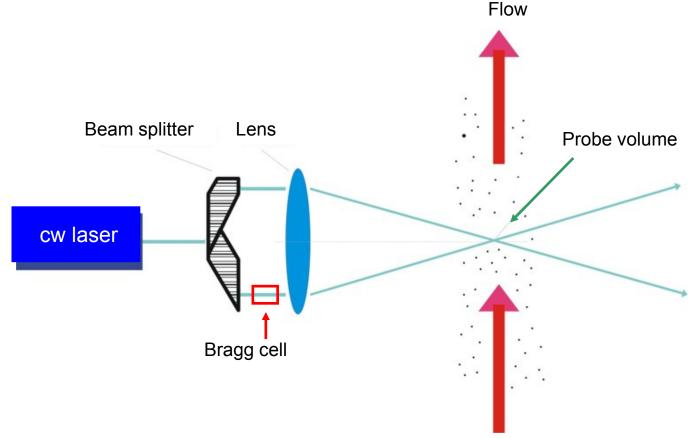


11



Practical realization

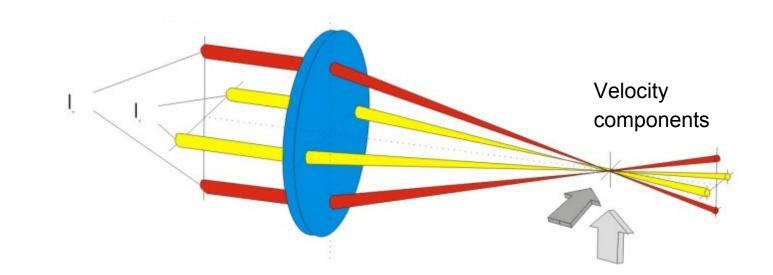
- Continuous wave (cw) laser: argon ion laser, DPSS laser



Bragg-cell: generates a moving interference pattern



- Two colors from argon ion laser
- Two photomuliplier tubes equipped with interference filters

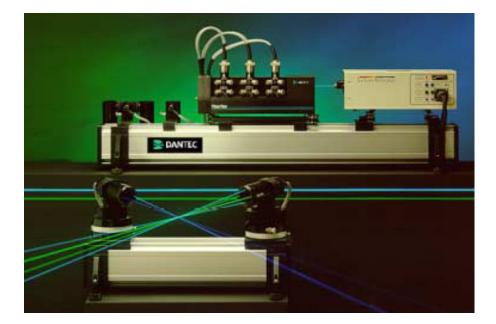


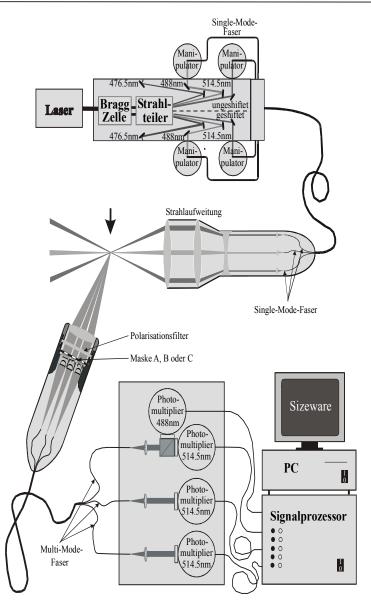
TECHNISCHE

UNIVERSITÄT DARMSTADT



- Commercial setup
 - Optical fibres
 - Simple alignment







- Single-point, 2-component LDV: measuring single point statistical moments
- Data base consisting of statistically uncorrelated data
 - Mean velocity
 - t_i: transit time, weighting by t_i to avoid bias by "fast particles"

$$\overline{u} = \frac{\sum_{i=1}^{N} u_i \cdot t_i}{\sum_{i=1}^{N} t_i}.$$

λ7

- Velocity variance

$$\left\langle u^{\prime 2} \right\rangle = \frac{\sum_{i=1}^{N} u_i^{\prime 2} \cdot t_i}{\sum_{i=1}^{N} t_i}$$

- Standard deviation, root-meansquare
- Turbulent kinetic energy (axisymmetric)
- Reynolds stresses

$$\sigma_u = \sqrt{\left\langle u_i'^2 \right\rangle}$$

$$\mathbf{k} = \frac{1}{2} \left(\frac{\sigma_{\mathrm{v}}^{2} + 2 \cdot \sigma_{\mathrm{v}}^{2}}{\sum_{i=1}^{N} u_{i} \cdot v_{i} \cdot t_{i}} \right)$$
$$\left\langle u' \mathbf{v}' \right\rangle = \frac{\sum_{i=1}^{N} u_{i} \cdot v_{i} \cdot t_{i}}{\sum_{i=1}^{N} t_{i}}$$

- Single-point, 1-component LDV (→ for higher data rates): Measuring two-point statistics
- Data base consisting of time-series (statistically correlated)

- Temporal covariance:
$$\Delta x=0$$
, i=j
 $R_{ij}(\vec{x}, \Delta x, t, \Delta t) = \overline{u'_i(\vec{x}, t)u'_j(\vec{x} + \Delta x, t + \Delta t)}$

- Integral time scale

$$T_{ij}(\vec{x},t) = \frac{1}{2u'_i(\vec{x},t)u'_j(\vec{x}+\Delta\vec{x},t+\Delta t)} \int_{-\infty}^{\infty} R_{ij}(\vec{x},t,0,\Delta t) d(\Delta t)$$

- Power spectral density

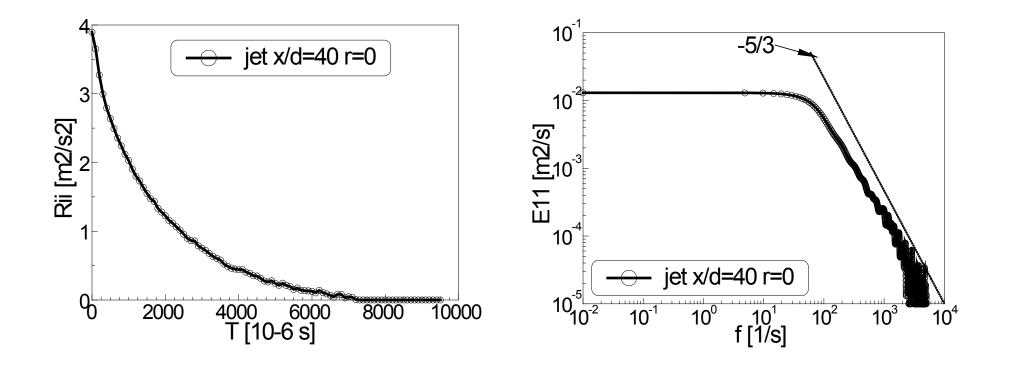
$$\Psi_{ij}(\vec{x},\kappa,t) = \frac{1}{(2\pi)^3} \int_{-\infty}^{\infty} \exp(-i\vec{\kappa}\Delta\vec{x}) R_{ij}(\vec{x},\Delta\vec{x},t) d(\Delta\vec{x})$$

TECHNISCHE

DARMSTADT



- Single-point, 1-component LDV: Measured variables
- Example isothermal jet



- Two-point, 1-component LDV: Measuring spatial two-point correlations
- Data base consisting of time-series
 - Spatial covariance: $\Delta t=0$

 $R_{ij}(\vec{x},t,\Delta\vec{x},\Delta t) = \overline{u'_i(\vec{x},t)u'_j(\vec{x}+\Delta\vec{x},t+\Delta t)}$

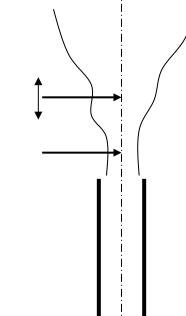
- Integral length scale

$$L_{ij}\left(\vec{x},t\right) = \frac{1}{2\overline{u'_{i}\left(\vec{x},t\right)u'_{j}\left(\vec{x}+\Delta\vec{x},t\right)}} \int_{-\infty}^{\infty} R_{ij}\left(\vec{x},t,\Delta\vec{x},0\right) d\left(\Delta x\right)$$

Moved probe volume

Fixed probe volume

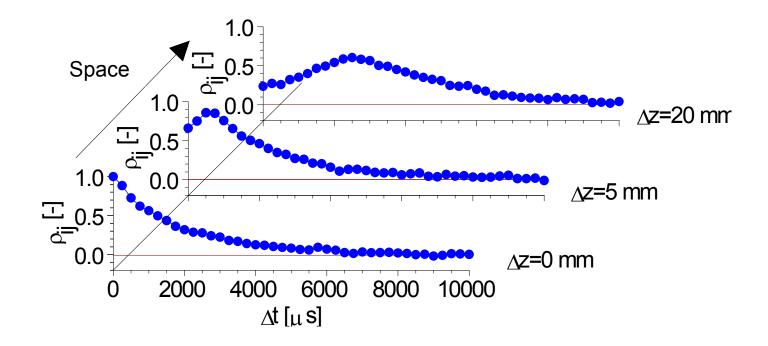






• Example: Isothermal jet, time-space correlation

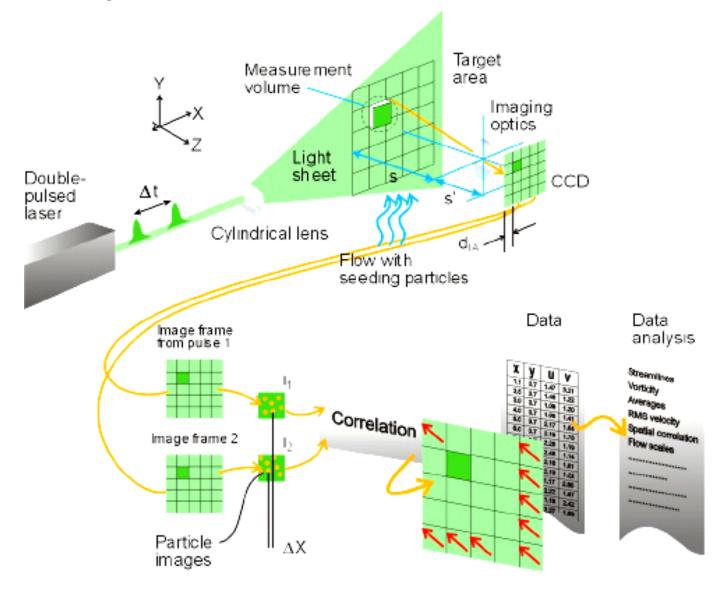
$$\rho_{ij}(\vec{x},t,\Delta z,\Delta t) = \frac{u'_i(\vec{x},t)u'_j(\vec{x}+\Delta z,t+\Delta t)}{\sqrt{u'^2_i(\vec{x},t)} \cdot \overline{u'^2_j(\vec{x}+\Delta z,t+\Delta t)}}$$







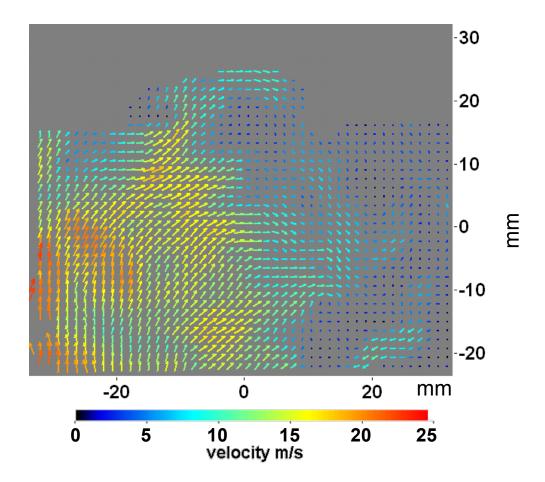
Principle



Source: LaVision

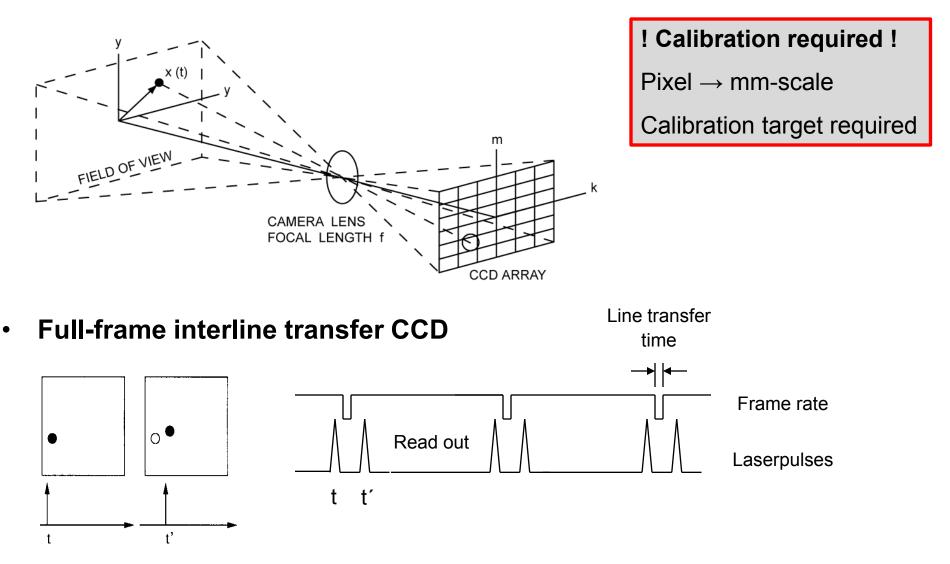


• Movie of particles in IC engine



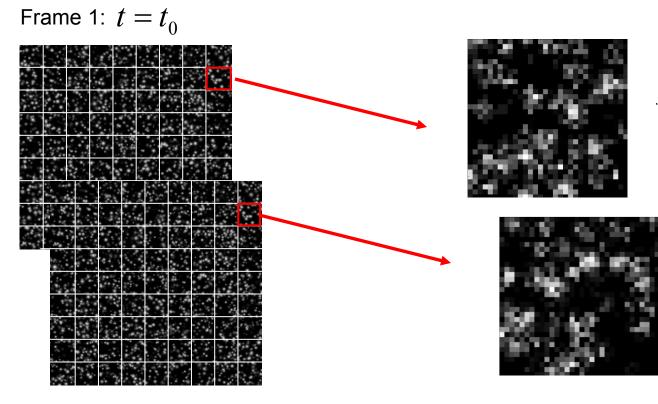


Imaging





Cross-correlation



Frame 2:
$$t = t_0 + \Delta t$$

Full frame

Interrogation windows,

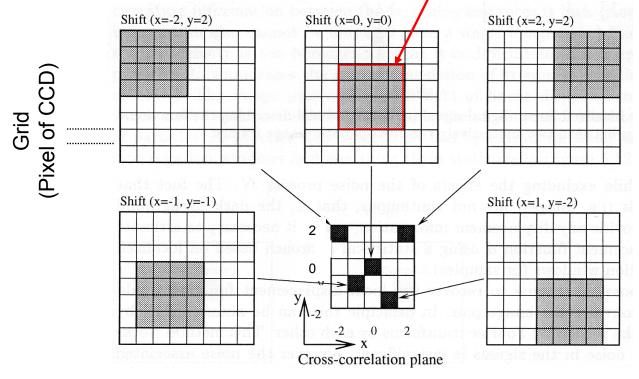
they determine spatial resolution





Cross-correlation

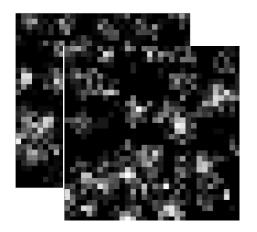
$$R_{II'}(x, y) = \sum_{i=-K}^{K} \sum_{j=-L}^{L} I(i, j) I'(i + x, j + y)$$



Interrogation window



Practical realization



FFT (real to complex)

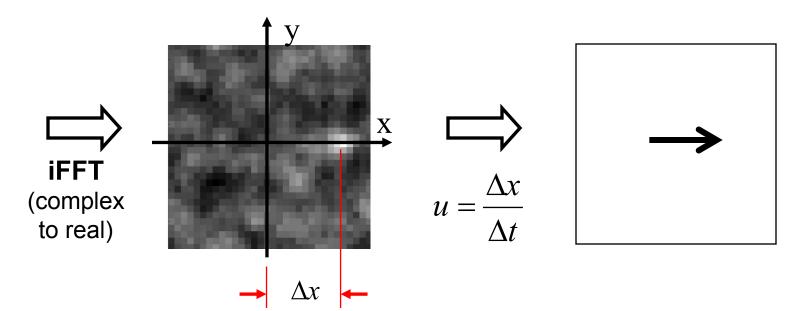
 \mathbf{k}_1 \mathbf{k}_2 \mathbf{k}_1

Interrogation volume size Here: 32 x 32 pixel

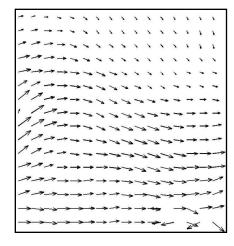
$$\hat{R}_{II}(i,j) = \hat{I}_1(i,j) \cdot \hat{I}_2(i,j)$$



Practical realization

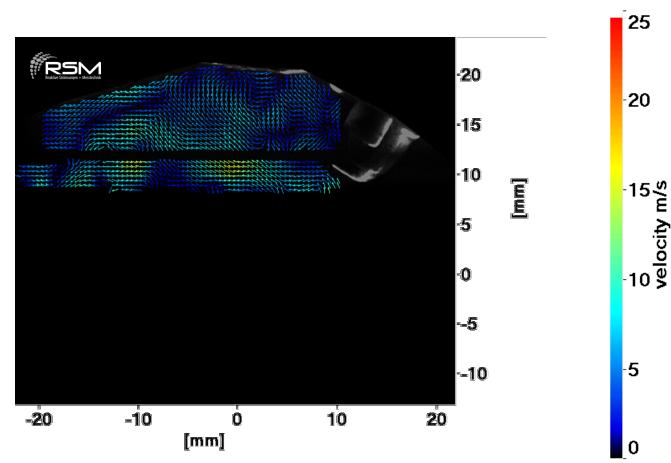


• Result: instantaneous 2-component velocity field in a plane





- Example:
 - PIV at 6 kHz repetition rate to study in-cylinder flow field





- Mean, variance and Reynolds stresses as in 2-component LDV
- Instantaneous velocity gradients (w velocity in z-direction)
 - Out-of-plane vorticity $\omega = 1/2 \left| \partial w / \partial r \partial v / \partial z \right|$
 - 2D-Dilatation $(\nabla \cdot V)_{2D} = (\partial w / \partial z + \partial v / \partial r)$
- Less suited for spatial correlation measurements

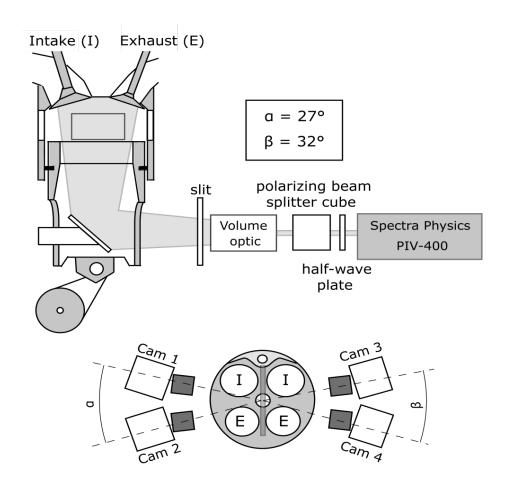


Extension to tomographic PIV: Illumination



Illumination

- Dual-cavity laser (PIV400, Spectra Physics)
- Avg. 375 mJ per single pulse
- Phase-locked acquisition during intake and compression (<5 Hz)
- Volume of: 48 x 35 x 4/8 mm

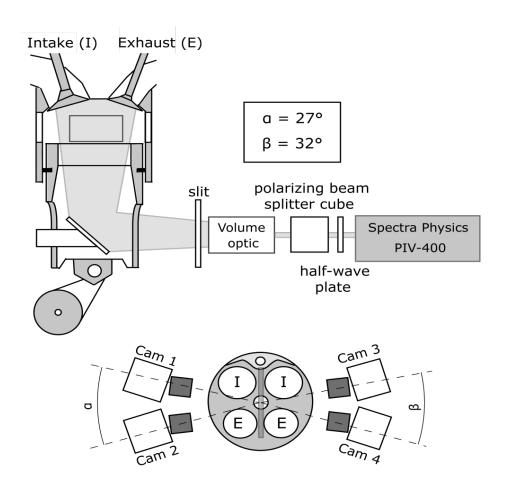


Extension to tomographic PIV: Detection



• Detection

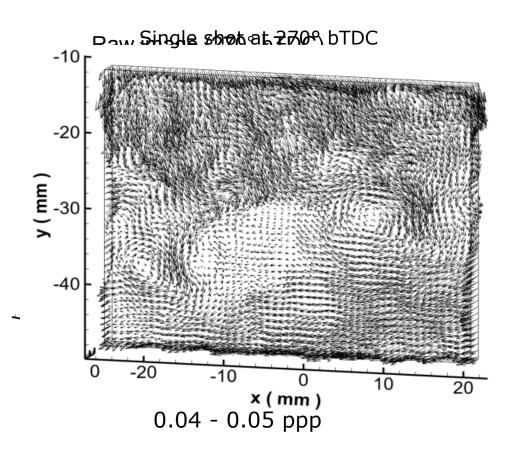
- Interline transfer CCD (ImagerIntense, LaVision, 1376x1040 pixels)
- Nikon 50 mm, 1.4 (f# 16)
- Limitation of Camera angles due to cylinder head bolts



Tomo PIV Processing

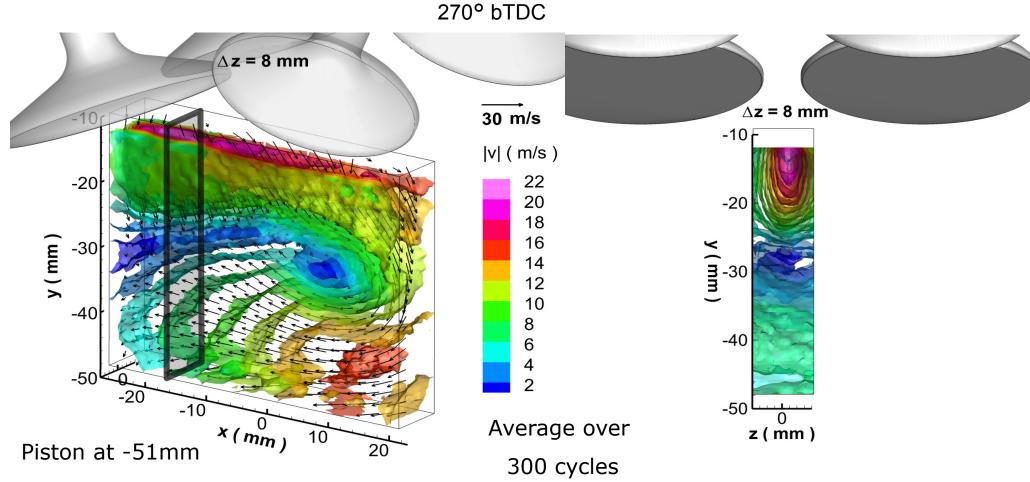


- Tomo-PIV processing using DaVis 8.1
- Image pre-processing
 - Subtract sliding average (3px)
 - Local intensity normalization
 - Gaussian smoothing
 - Sharpening filter
- **MART Reconstruction** (multiplicative algebraic reconstruction technique)
- Volume correlation (Finale size)
 - 4mm: 48x48x48 pixel (0.4mm/vector)
 - 8mm: 64x64x64 pixel (0.6mm/vector)
- Post-processing
 - Outlier detection (Neighborhood operation)
 - Gauss smoothing



Average Velocity Data – intake stroke







Particle Image Velocimetry



LDV versus PIV

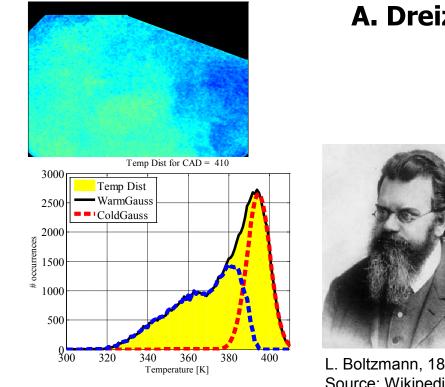
- Seeding density
 - PIV: needs at least 10 particles per interrogation volume → for a fixed spatial resolution a minimal seeding density is required
 - LDV: seeding density can be as low as required (on the expense of data acquisition time), seeding density and spatial resolution are decoupled
- Calibration/ data post processing
 - PIV: cross-correlation algorithm required, long CPU-times (→good statistics not common), "calibration" needed (pixel to millimeter)
 - LDV: fast online data processing by optimized CPUs, <u>no calibration</u> required
- Measured variables
 - LDV: reliable "point-data", investigation of local neighborhood by two-point LDV cumbersome
 - PIV: <u>instantaneous velocity fields</u> and gradients in different directions (spatial multi-point statistics accessible)
- \rightarrow LDV and PIV are complementary techniques

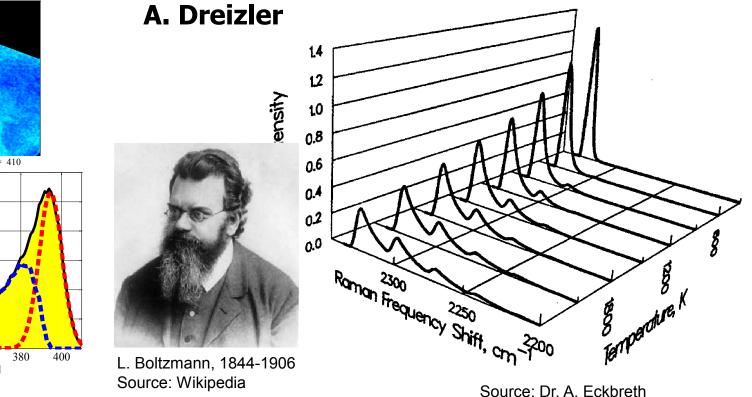
Chapter 5: Gas-Phase Thermometry

TU Darmstadt, Germany Dept. of Mechanical Engineering Institute for Reactive Flows and Diagnostics







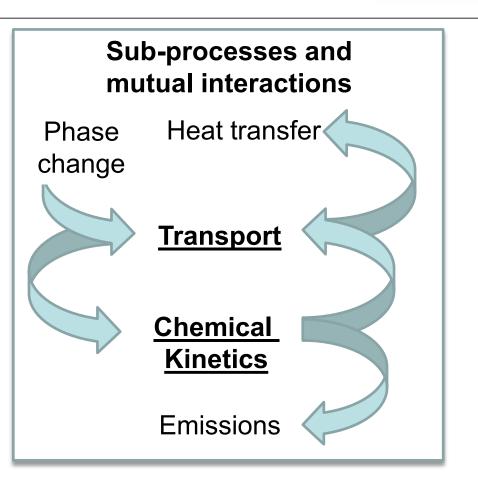


Combustion: coupled sub-processes



Combustion:

Energy conversion of chemically bound to thermal energy



→ Each of these sub-processes is significantly influenced by local gas temperatures

Need for accurate and precise temperature measurements to understand combustion



- Temperature (gas) is key quantity with impact on
 - Chemical kinetics (Arrhenius-type reaction rates)
 - Gas density (equation of state)
 - Viscosity
 - Progress variable in premixed combustion

\rightarrow Turbulence-chemistry interaction

- Understanding combustion requires knowledge of local temperatures (gas)
 - Accurately: no systematic error (ideally)
 - Precisely: low statistical error (low noise, ..)
 - Locally: due to non-linear dependency of sub-processes on temperature



Laminar vs. turbulent combustion



IVERSITÄT RMSTADT

- Laminar and stationary combustion
 - No temporal variation
 - Large spatial variation (across heat release zone)
 - \rightarrow Resolution requirements
 - Time: none
 - Space: high, depends on pressure, fuel etc., method must alow for resolving smallest scales (ideally)
- **Turbulent** (statistically stationary) combustion
 - Large temporal variation
 - Large spatial variation (heat release zone, convection, mixt. preparation)
 - \rightarrow Resolution requirements
 - Time: resolve Bachelor time-scales (ideally)
 - Space: resolve Bachelor length-scales (ideally)

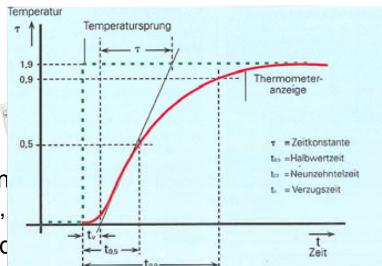




Intrusive vs. non-intrusive sensing (1)

- Intrusive sensors
 - Thermocouples
 - Resistance thermometer
 - Major disadvantages
 - Systematic errors (heat conduction flow, promoting catalytic reactions,
 - Not sustainable (melting point, oxic
 - Size: ~mm → spatial resolution too low for resolving Bachelor scales
 - Temporal response: first order system with large time-constants

\rightarrow Not well suited for many applications in combustion research

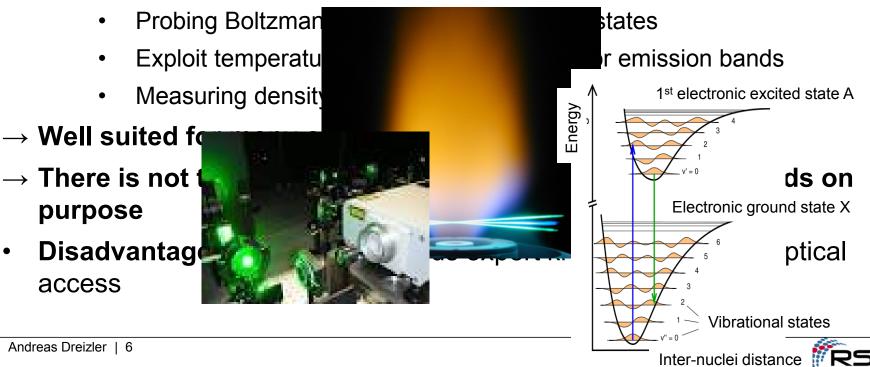




Intrusive vs. non-intrusive sensing (2)



- Non-intrusive sensors: based on spectroscopic methods
 - Thermal radiation: generally not applicable in gaseous flames, suitable for measuring particle temperatures if emissivity is known
 - Chemiluminescence (OH*, CH*,...): not in chemical equilibrium
 - Spectroscopic methods



Spectroscopic methods – classification



• Based on

Andre

• Boltzmann distribution

 $\frac{N_i}{N} = \frac{g_i \exp(-E_i / kT)}{\sum_j g_j \exp(-E_j / kT)} = \text{unique function of } T$ $g_i: \text{ degeneracy factor } E_i: \text{ energy quantum state; both from quantum mechanics}$ $\sum_{i=1}^{N_i} \sum_{j=1}^{N_i} \sum_{j=1}^$

Temperature-dependent absorption/emission

• Density (N/V) measurements

$$pV = NkT \rightarrow T = \frac{pV}{Nk}$$

$$pV = \frac{pV}{Nk}$$

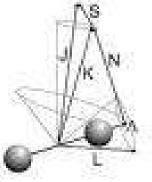
$$pV$$

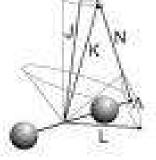


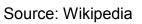
Restriction to diatomic molecules

- Two atoms, covalent bounded
- Degrees of freedom
 - 3 translation •
 - Electronic (here only valence electron considered) •
 - 1 vibrational ٠
 - 2 rotational (degenerated) •
- In combustion degrees of freedom not necessarily in equilibrium!
- \rightarrow Translational, electronic, vibrational, and rotational temperatures not always identical

Source: Wiley and Sons

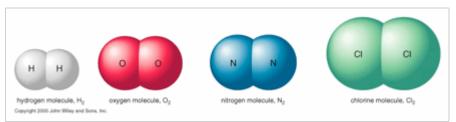








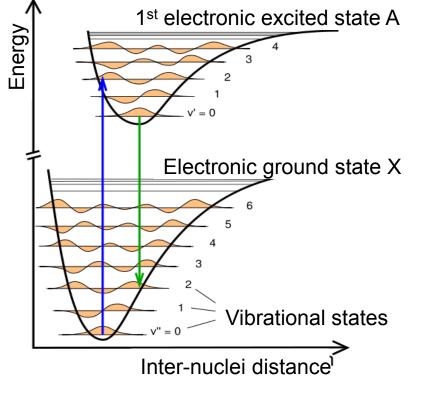




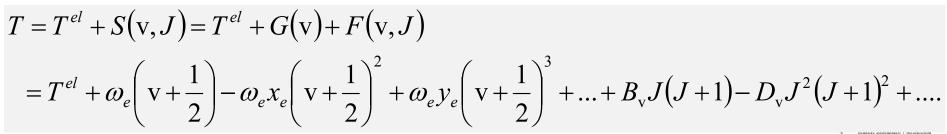
Andreas Dreizler | 8

Internal energies of diatomic molecule





Rotational sub-levels not shown



Andreas Dreizler | 10

Temperature measurement via Boltzmann (1)

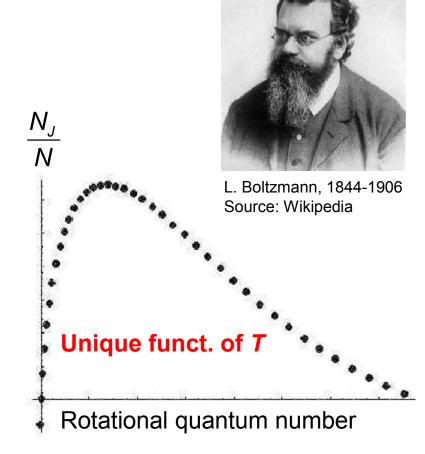
- Boltzmann distribution (diatomic molecule)
 - Rotational sub-levels

 $\frac{N_J}{N} = \frac{(2J+1)\exp(-E_J/kT)}{\sum_J (2J+1)\exp(-E_J/kT)}$

with J rotational quantum number

(fractional population)

 Already at T = 300 K many rotational sub-levels populated because energy separation between adjacent small (10 – 100 cm⁻¹)





Temperature measurement via Boltzmann (2)



- Boltzmann distribution (diatomic molecule)
 - Vibrational sub-levels

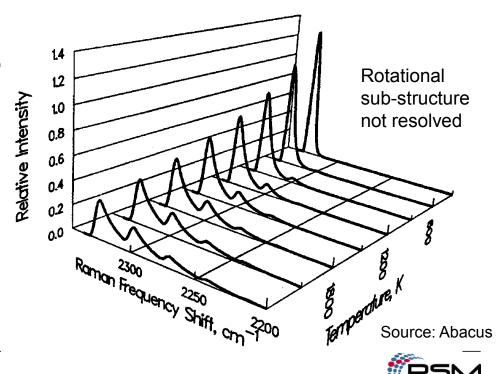
$$\frac{N_{v}}{N} = \frac{\exp(-E_{v} / kT)}{\sum_{v} \exp(-E_{v} / kT)}$$

with v vibrational quantum number

• Vibrationally excited levels n

Example N_2 :

Energy gap between
 v''=0 and v'=1 ~2300 cm⁻¹



Temperature measurement via Boltzmann (3)



- Boltzmann distribution (diatomic molecule)
 - Electronic sub-levels

 $\frac{N_{ES}}{N} = \frac{\exp(-E_{ES} / kT)}{\sum_{ES} \exp(-E_{ES} / kT)}$ with *ES* quantum number of electronic state

- Energy separation > 10000 cm⁻¹
- → In general: Not significantly populated at combustion temperatures Exception: Atomic tracer such as indium (not considered in detail during this lecture)

 \rightarrow Measure temperature via the distribution of rotational quantum states



Rotational temperatures – by microwaves



- Task: measuring Boltzmann distribution of rotational sub-levels
 - Single photon resonant processes
 - Pure rotational spectroscopy

E2: final rotational state, after absorption $|f\rangle$ Resonant absorption $E_{photon} = hv$ \longrightarrow $|i\rangle$ E1: initial rotationbal state, prior to absorption

- Energy separation: 10 100 cm⁻¹ → microwave radiation
- \rightarrow **Not common** in combustion (low spatial res., background radiation)

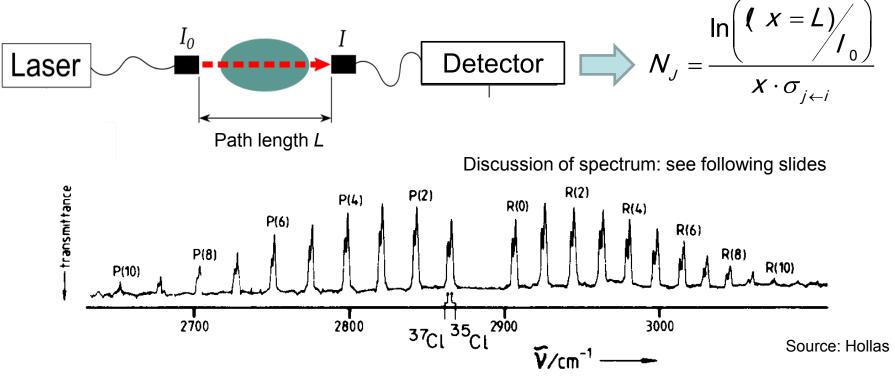


Rotational temperatures – by IR spectroscopy



Rotational-vibrational spectroscopy

- Energy separation: $\sim 1000 4160 \text{ cm}^{-1} \rightarrow \text{infrared radiation}$
- Example HCI absorption spectrum

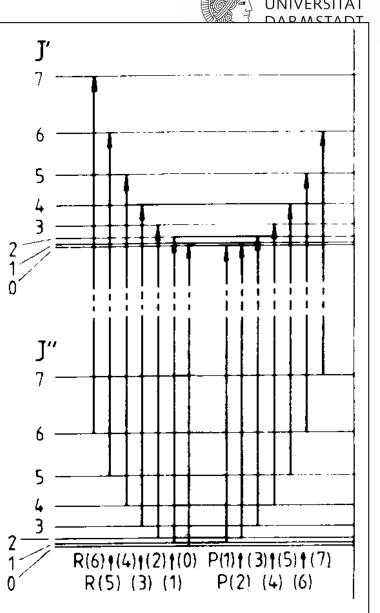




Selection rules

- Fundamental finding from quantum me
 - Change of vibrational quantum number
 - Change of rotational quantum number
 - But exceptions (for example NO)
 - Notation

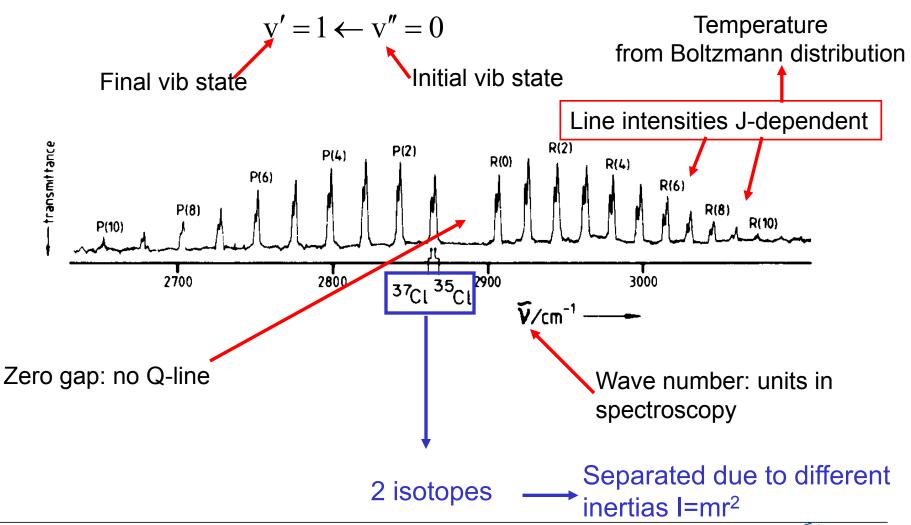
 $\Delta J = 0 \Rightarrow \text{ Q-lines}$ $\Delta J = 1 \Rightarrow \text{ R-lines}$ $\Delta J = -1 \Rightarrow \text{ P-lines}$



TECHNISCHE

Spectrum interpretation HCI







Rotational temperatures by UV/VIS spectroscopy (1)



- Electronic spectroscopy: change of electronic, vibrational and rotational states due to absorption of UV or VIS photon
 - Energy separation > 10000 cm⁻¹
 - Selection rules (extract only)

 $\Delta J = 0, \pm 1 \rightarrow Q$ -, R-, P- lines

 $\Delta v = 0, \pm 1, \pm 2, \dots \rightarrow \text{Compare "Franck-Condon principle"}$

 \rightarrow For Hund case (a) (most important rules)

- $\Delta \Lambda = 0, \pm 1 \qquad \Sigma \Sigma, \Pi \Sigma \text{ or } \Delta \Pi \text{ transitions. Not allowed for} \\ \text{example } \Delta \Sigma \text{ transitions}$
- $\Delta S = 0$ Allowed: Triplett Triplett or Singulett Singulett transitions Spin forbidden: Singulett – Triplett transitions

 Λ :Projection of orbital momentum *L* on molecule axis

S: Multiplicity

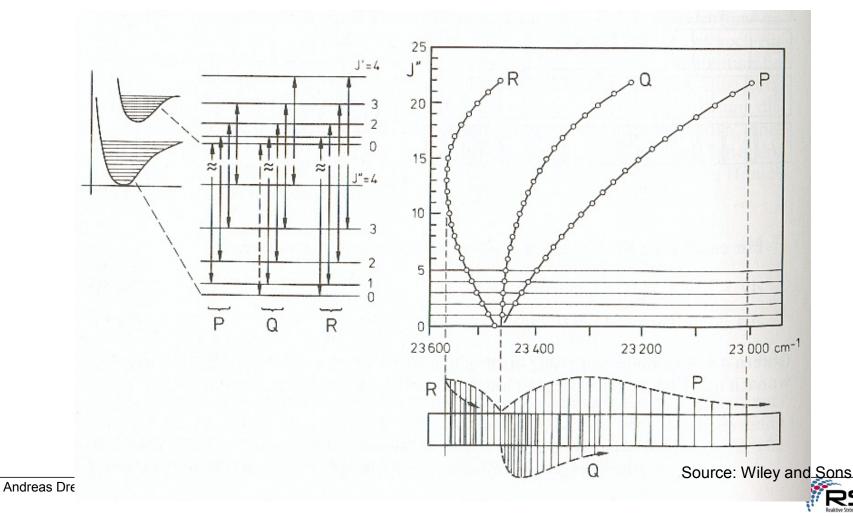
Andreas Dreizler | 17



Rotational temperatures by UV/VIS spectroscopy (2)



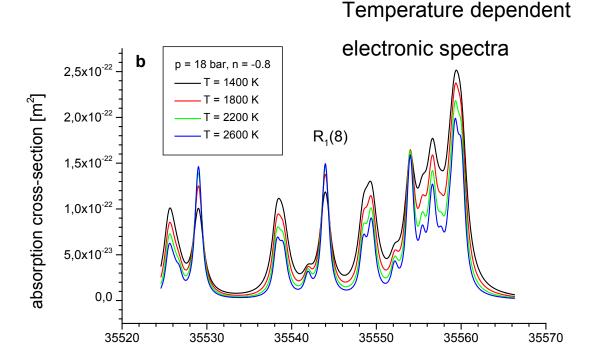
Electronic spectroscopy:



Rotational temperatures by UV/VIS spectroscopy (3)



- OH $A^2\Sigma \leftarrow X^2\Pi$ (v'=1 \leftarrow v''=0)-transition
- R-branch, band head



Methods in the IR & UV/VIS for temperature measurements via Boltzmann distribution



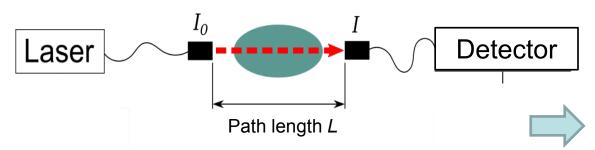
- Laser absorption spectroscopy (LAS)
- Laser-induced fluorescence (LIF)
- Raman spectroscopy (RS)
- Coherent anti-Stokes Raman spectroscopy (CARS)



Laser absorption spectroscopy (1)



• Experimental setup



Deduce number densities from Beer-Lambert's law

$$(x = L) = I_0 \exp(-x \cdot N_j \cdot \sigma_{j \leftarrow i}) \Leftrightarrow N_j = \frac{\ln((x = L)/j_0)}{x \cdot \sigma_{j \leftarrow i}}$$



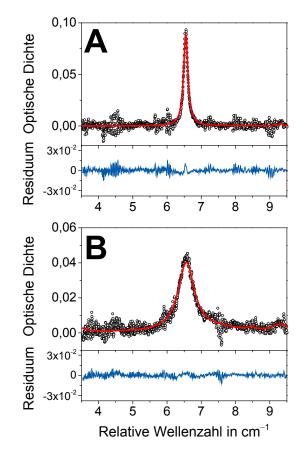
Laser absorption spectroscopy (2)



- Deduce temperature from Boltzmann distribution
 - Two-line thermometry

$$T = \frac{E_{J_2} - E_{J_1}}{k \ln\left(\frac{N_1(2J_2 + 1)}{N_2(2J_1 + 1)}\right)}$$

• Multi-line thermometry: by spectral fit





Laser absorption spectroscopy (3)



- Advantages
 - Sensitive
 - Accurate (no calibration required if spectroscopic details such as term values, line strengths, line broadening mechanisms known)
 - High accuracy, needs multi-line thermometry (for instantaneous Tmeasurements these requires rapid tuning of laser frequency and fast detection)
 - High spatial resolution perpendicularly to laser path
- Disadvantages
 - Line-of-sight (LOS): no spatial resolution along laser path, needs homogeneous distribution along laser path
 - Multi-line thermometry needs fast tuning of laser and fast detector

\rightarrow Great in laminar flames, not easily applicable in turbulent flames (LOS)



Laser Induced fluorescence (1)

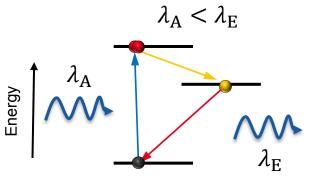
Step 1: Absorption

- Electronic excitation of molecules by laser radiation
- Wavelength λ_A

Step 2: Spontaneous emission (fluorescence)

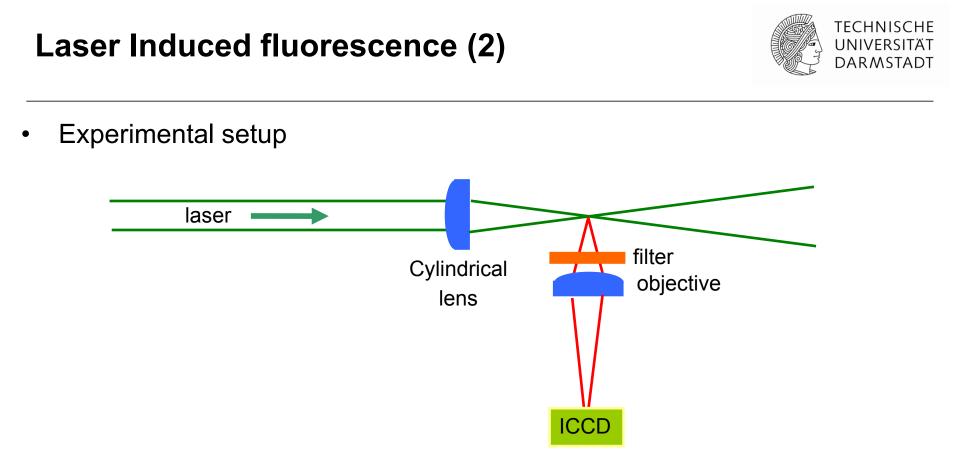
- Spectrally red-shifted $\lambda_A < \lambda_E$
- Upper state lifetime typically few ns for flame conditions
- Measure of local number density
- Linear LIF regime

$$I_{L/A}(x) = M(x)\sigma(x) \eta_{lasek}(x) \frac{\tau_{tot}}{\tau_{sp}} U \frac{\Omega}{4\pi} \varepsilon \eta$$







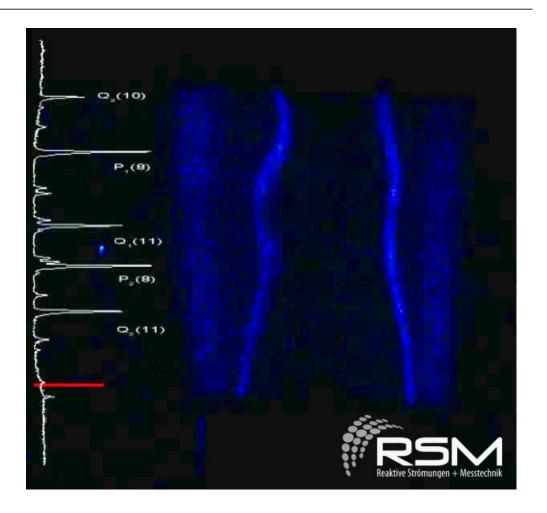




Laser Induced fluorescence (3)



- Flame front visualization in CH₄/air Bunsen flame, p = 1 bar
- Excitation by tunable KrF excimer laser at ~248 nm





Laser Induced fluorescence (4)



- **Two-line** thermometry:
 - excite two different transitions
 - Transitions selected such that ratio of number densities N_1 and N_2 vary sensitively with temperature
 - But: number density should not be too low for reasonable signal-tonoise ratio
- Calculate ratio of two LIF Signals $I_{L/F,(x)} = N(x)U\sigma I_{laser,(x)}(x)(x) = \frac{\tau_{tot}}{\tau_{sp}} \frac{\Omega}{4\pi} \varepsilon \eta$ \rightarrow Yield **ratio**

$$R_{12} = \frac{I_{L/F,1}}{I_{L/F,2}} = \frac{C_1 I_{laser,1} g_1 \exp(-E_1/kT) B_1 \gamma(p,T) \tau_{eff,1}/\tau_{sp,1}}{C_2 I_{laser,2} g_2 \exp(-E_2/kT) B_2 \gamma(p,T) \tau_{eff,2}/\tau_{sp,2}}$$

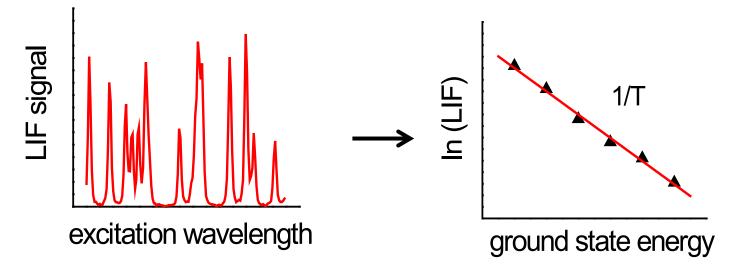
\rightarrow Issue two-line thermometry: Low precision due to experimental noise



Laser Induced fluorescence (5)



- Multi-line thermometry: measure entire excitation-fluorescence spectrum
- Method 1: Spectral fit of entire spectrum by variation of temperature
- Method 2: Plot In(I_{LIF}) vs ground state energy and deduce temperature from slope



→ Great in laminar flames, not applicable in turbulent flames as wavelength scan takes too long



Laser Induced fluorescence (6)



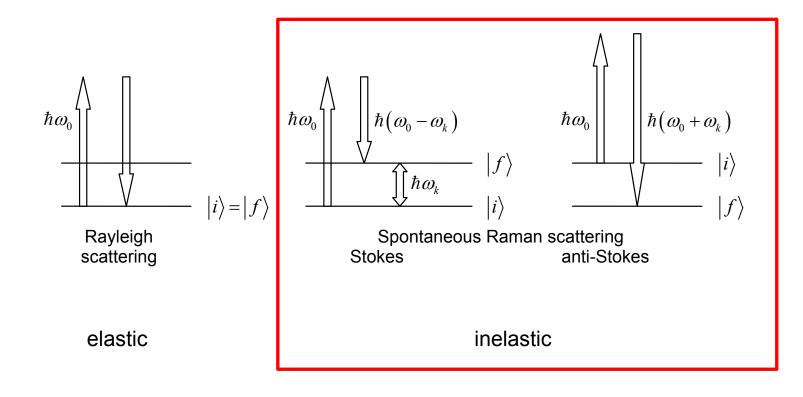
- Choice of species for LIF thermometry based on Boltzmann distribution
 - Naturally occurring molecules: OH radical, concentration level in typical flames sufficiently high only for T > 1500 K
 - Seeded species:
 - NO, chemically more or less inert, but may not be a good choice for cases studying auto-ignition (NO promotes auto-ignition), caution: NO is toxic
 - Indium, typically via InCI, for example dissolved in liquid fuel such as iso-octane, seeding is difficult in general (compare papers from Hult et al. or Nathan et al.)



Raman spectroscopy (1)



• Elastic and inelastic light scattering of photons off molecules





Raman spectroscopy (2)



• Selection rules

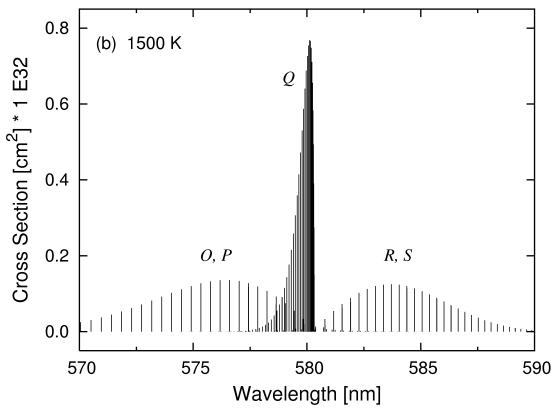
 $\Delta J = 0, \pm 2$ $\Delta J = 0 \rightarrow \text{Q-branch}$ $\Delta J = +2 \rightarrow \text{O-branch}$ $\Delta J = -2 \rightarrow S\text{-branch}$

Oxygen molecule O_2 , T = 1500 K

Simulated "stick spectrum" – infinite resolution

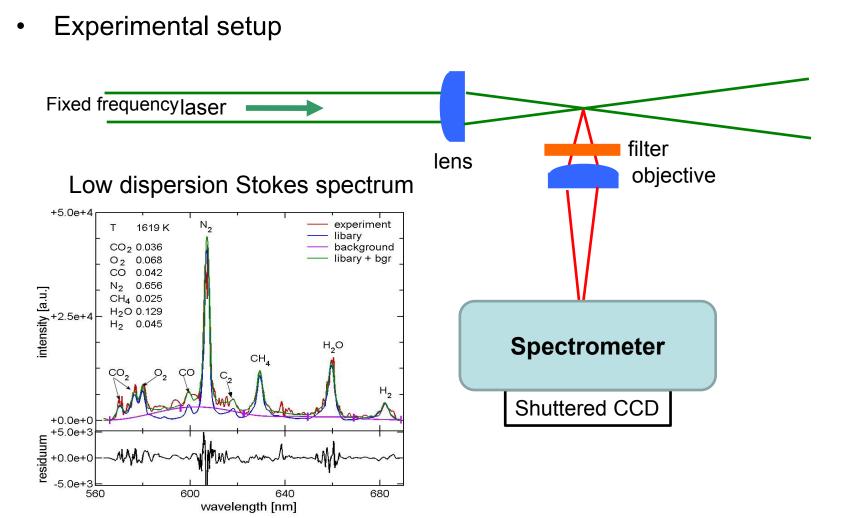
Ro-vibronic Stokes-Raman

Exception: very weak R and P-lines



Raman spectroscopy (3)



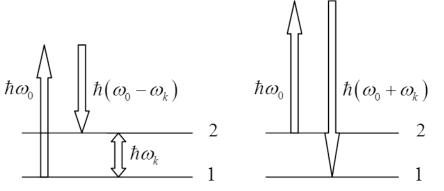




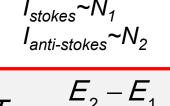
Raman thermometry (1)

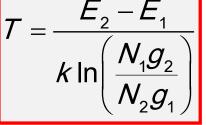


• Ratio of I_{Stokes} to $I_{anti-Stokes}$



Spontaneous Raman scattering Stokes anti-Stokes





- Typically applied for vibrational levels
- \rightarrow Example N₂: Temperature sensitivity starting from ~ 500K (otherwise too low fractional population)
- \rightarrow Not very common in combustion community



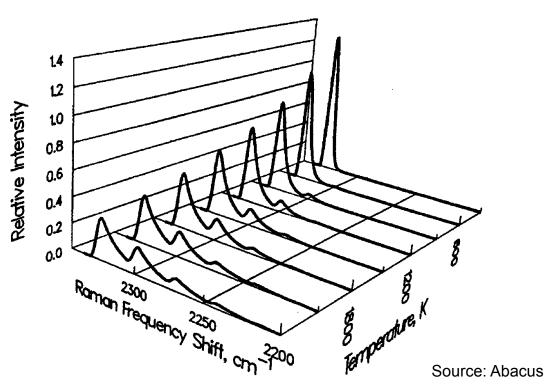
Raman thermometry (2)



- Measure entire Raman Stokes spectrum
- Combustion: Typically ro-vibronic spectrum of N₂
- **High** dispersion \rightarrow resolve only N₂, no other molecules

Not very common in combustion research (high dispersion comes along with low signal)

Pure Raman thermometry not common in combustion community



Coherent anti-Stokes Raman spectroscopy (1)



- Non-linear polarization $P_{i} = \mathcal{E}\left(\chi_{ij}^{(1)}E_{j} + \chi_{ijk}^{(2)}E_{j}E_{k} + \chi_{ijkl}^{(3)}E_{j}E_{k}E_{l} + \ldots\right)$
 - P_i : Polarization
 - E_i : Electrical field
 - $\chi^{(n)}$: Susceptibility of n-th order
 - Non-linear effects are observable only at high electrical field strength

 $\approx 10^{0} \approx 10^{-12} \approx 10^{-23}$

➡ Pulsed LASER is prerequisite

In Gases :

$$\chi^{(2)}=0$$



CARS: theoretical background



• Wave equation describes light emission due to non-linear polarization

$$\nabla^2 \vec{E} - \frac{1}{c^2} \frac{\partial^2 \vec{E}}{\partial t^2} = \mu_0 \frac{\partial^2 \vec{P}}{\partial t^2} \quad \text{Here:} \quad P_i = \varepsilon_0 (\chi_{ij}^{(1)} E_j + \chi_{ijkl}^{(3)} E_j E_k E_l)$$

Common practice in CARS: $\omega_1 = \omega_3$

$$I_{CARS} \propto I_1^2 I_2 \left| \chi_{CARS_{(\omega_1,\omega_2)}} \right|^2 l^2 \left(\frac{\frac{\sin \frac{\Delta kl}{2}}{2}}{\frac{\Delta kl}{2}} \right)^2$$



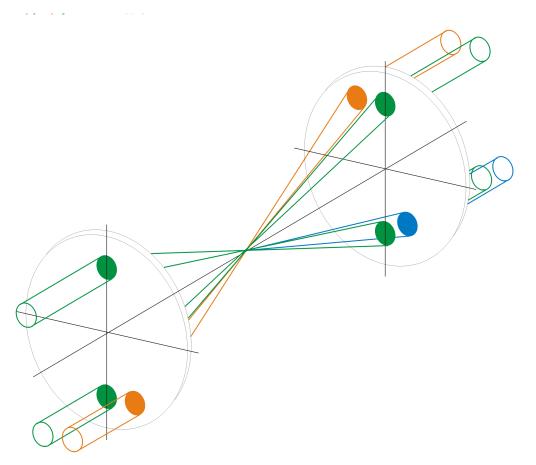
TECHNISCHE CARS: energy and momentum conservation UNIVERSITÄT DARMSTADT Pump laser Pictorial view of CARS Stokes laser Energy balance: $\omega_3 = 2\omega_1 - \omega_2$ CARS signal (anti-Stokes) Selection rules ω \mathcal{O}_1 ω_{2} \mathcal{O}_{2} \mathcal{W}_1 (\mathcal{D}_1) ω_3 ω_{2} $\Delta J = 0, \pm 2$ $\Delta v = 1$ \mathcal{O}_{R} Momentum balance: $k_3 = k_1 + k_1 - k_2$ Termed phase matching k_1 k_1 \vec{k}_{2} \vec{k}_3 k_{3} **Co-linear CARS** BOX CARS: preferred, higher spatial resolution



CARS: phase matching



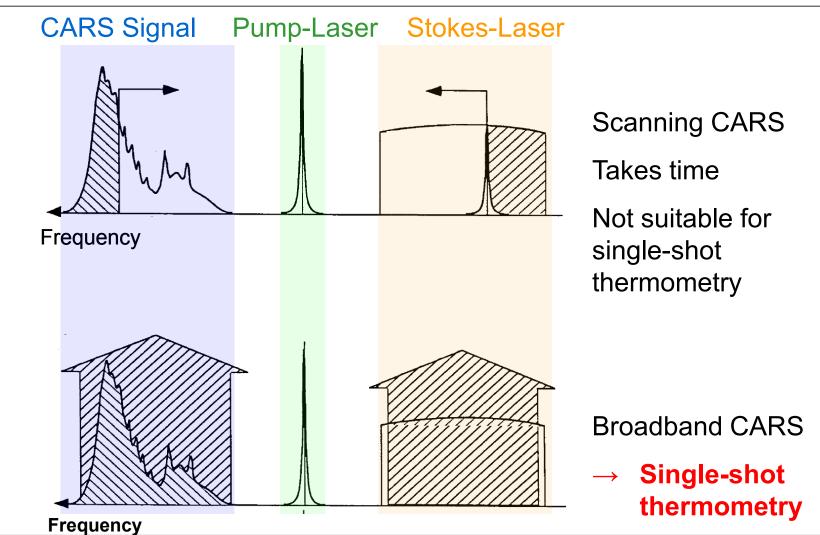
- Realization of phase matching
 - Pump laser: 532 nm (frequency-doubled Nd:YAG)
 - Stokes laser: 607 nm (broadband dye laser)
 - CARS signal: 473 nm





CARS: broad band and scanning





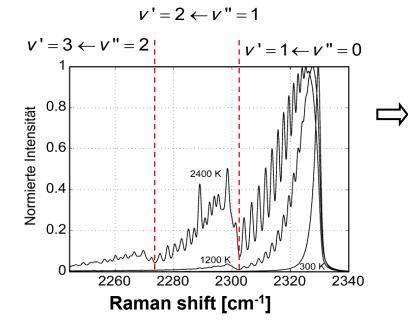
Andreas Dreizler | 39



CARS: thermometry



• Typical application in turbulent flames: ro-vibronic N₂-broad band CARS



Temperature obtained by fitting CARS spectrum to experimental spectrum

Temperature information is contained in line-strength~ N_i^2 (in χ^3 -tensor)

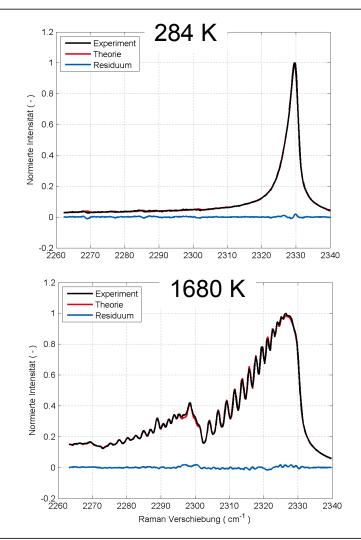
Based on Boltzmann distribution

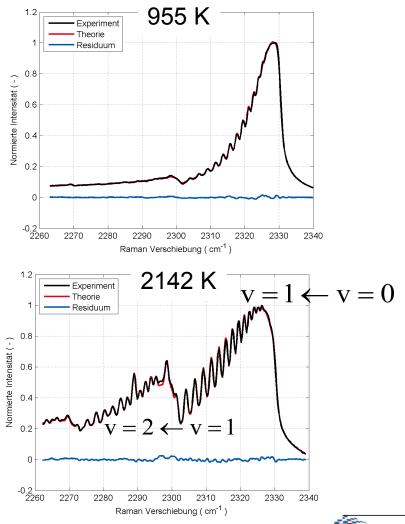
$$\frac{N_i}{\sum_i N_i} = \frac{g_i e^{-E_i/kT}}{\sum_i g_i e^{-E_i/kT}}$$



CARS: single shot spectra and spectral fit



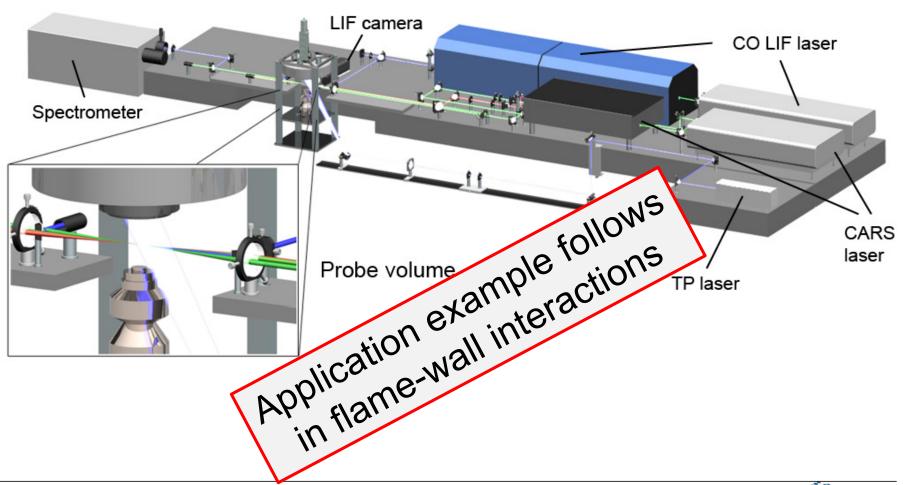






CARS: experimental setup, combined with CO-LIF







CARS: pro and con



Advantages:

- precise single-shot temperature measurement of gas phase
- coherent signal allows detector placed far away from combustor
- No calibration required

Disadvantages:

- complicated optical setup
- spatial resolution in mean beam propagation direction only ~0.5mm, often worse
- mostly point-measurements (new fs/ps CARS allows for 1D and 2D CARS!!)



Spectroscopic methods – classification



- Based on
 - Boltzmann distribution

$$\frac{N_i}{N} = \frac{g_i \exp(-E_i / kT)}{\sum_j g_j \exp(-E_j / kT)} = \text{unique function of } T$$

 g_i : degeneracy factor E_i : energy quantum state; both from quantum mechanics

- Temperature-dependent absorption/emission
- Density measurements via equation of state

$$pV = NkT \rightarrow T = \frac{pV}{Nk}$$



Temperature dependent emission/absorption



- Fluorescence tracer added to gas
 - Typical tracers
 - Hydrocarbons: aromates, ketones or aldehydes
 - Atoms
- Pro
 - Tracer and its spectroscopic characteristics can be chosen in dependence of measuring task
- Con
 - Hydrocarbon tracer is thermally decomposed for T > ~700 K, not applicable in flames, but for example compression stroke in IC engine
 - Tracer may influence chemical and physical properties of the fluid
 - Spectroscopic properties of tracer often not independent of surrounding gas phase



Typical tracers for LIF thermometry



- Ketones:
 - acetone
 - 3-pentanone _{H₃C, CH₃}
- Aromates: toluene

- Aldehydes: acetaldehyde $_{H_3C} \downarrow_H$
- List is not complete: search for LIF-tracers with higher quantum yield, less O₂-quenching, etc. goes on

CH₃



Classification of LIF-thermometry



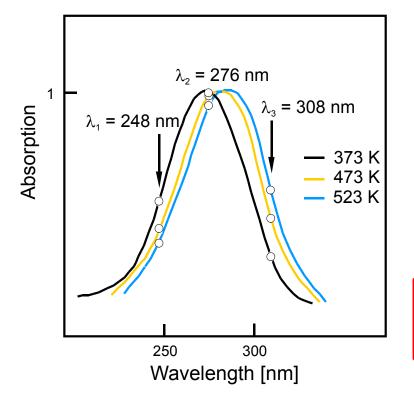
- Two options
 - Two line excitation one color detection: excite tracer at two different wavelengths (two lines) and measure fluorescence broadband (one color)
 - \rightarrow Exploit temperature dependent **absorption** band
 - Single line excitation two color detection: excite tracer at one wavelength (single line) and measure fluorescence at two spectrally separated bands (two color)
 - \rightarrow Exploit temperature dependent emission band



3-pentanone LIF thermometry



• 3-pentanone: Example for **two line – one color** thermometry



- Spectra are normalized
- total integral increases with temperature
- Two lasers/two cameras needed
- For more information see Schulz, Dreizler, Ebert, Wolfrum Combustion Diagnostics, Springer Verlag 2007

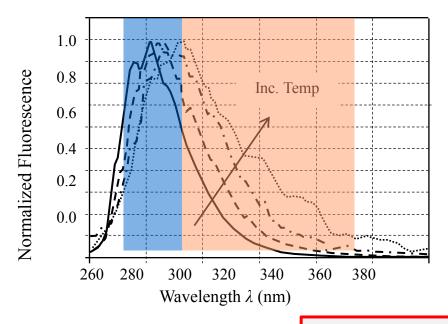
$$\frac{S_1(\lambda_1, \boldsymbol{p}, \boldsymbol{T})/I_{Laser_1}(\lambda_1)}{S_2(\lambda_2, \boldsymbol{p}, \boldsymbol{T})/I_{Laser_2}(\lambda_2)} \frac{\pi_2}{\pi_1} = \frac{\sigma_1(\lambda_1, \boldsymbol{T})}{\sigma_2(\lambda_2, \boldsymbol{T})} \frac{\phi_1(\lambda_1, \boldsymbol{T})}{\phi_2(\lambda_2, \boldsymbol{T})} = \boldsymbol{F}(\boldsymbol{T})$$



Toluene LIF thermometry



• Toluene: Example for **single line – two color** thermometry



- Spectra are normalized
- Strong quenching by O₂ → reducing high quantum yield compared to oxygen-free atmosphere
- For more information see Peterson, Baum, Böhm, Dreizler, Appl. Phys. B 2014

Application example follows at end of this chapter



Spectroscopic methods – classification



- Based on
 - Boltzmann distribution

$$\frac{N_i}{N} = \frac{g_i \exp(-E_i / kT)}{\sum_j g_j \exp(-E_j / kT)} = \text{unique function of } T$$

 g_i : degeneracy factor E_i : energy quantum state; both from quantum mechanics

- Temperature-dependent absorption/emission
- Density measurements via equation of state

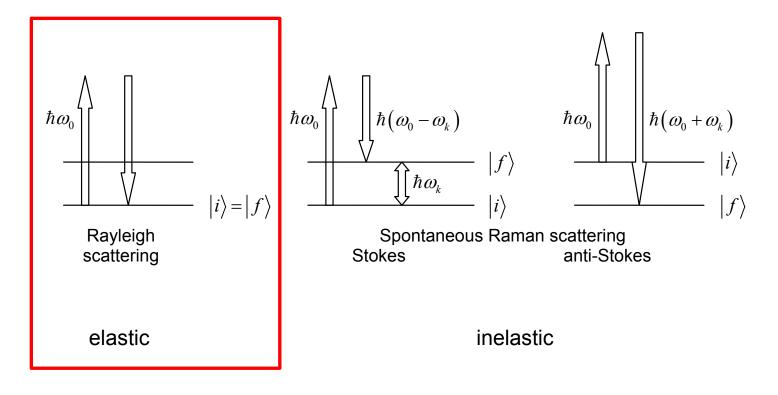
$$pV = NkT \rightarrow T = \frac{pV}{Nk}$$



Rayleigh spectroscopy – in combination with Raman if gas composition unknown



• Elastic and inelastic light scattering of photons off molecules





Rayleigh thermometry: known gas comp.



Rayleigh signal intensity
$$F_{ray}(x) = C_{calib} \sigma_{ray} I_{lase}(x) \frac{N}{V}$$

- With known Rayleigh cross-section σ_{ray}(known gas mixture, no reactions), measured laser intensity, and calibration Ray-signal proportional to local gas density
- Deduce temperature in combination with equation-of-state
- Example: ideal gas law pV = NkT

$$\rightarrow T = \frac{pV}{Nk} = \frac{p \cdot C_{calib} \cdot \sigma_{Ray} \cdot I_{laser}(x)}{k \cdot F_{Ray}(x)}$$

• Wavelength-dependent Ray cross section of gas *i* can be calculated from index of refraction $4\pi^2(n-1)^2$

$$\sigma_{ray,i} \cong \frac{4\pi^2 \left(n_i - 1\right)^2}{\left(N_A / V\right)^2 \lambda^4}$$



Rayleigh thermometry: <u>unknown</u> gas comp.



- Rayleigh signal intensity $F_{ray}(x) = C_{calib} \sigma_{ray} I_{lase}(x) \frac{N}{V}$
- Measure laser intensity and perform calibration Ray-signal proportional to local gas density
- Gas mixture unknown (for example due to chem. reactions or mixing)
 - \rightarrow gas composition must be measured
 - \rightarrow simultaneous Raman scattering
- Once gas composition is known, effective Rayleigh cross-section can be calculated by:

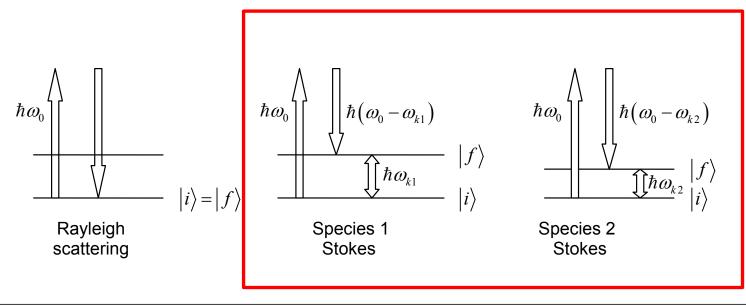
$$\sigma_{ray} = \sum_{i} X_{i} \sigma_{ray,i}$$



Raman/Rayleigh spectroscopy (1)



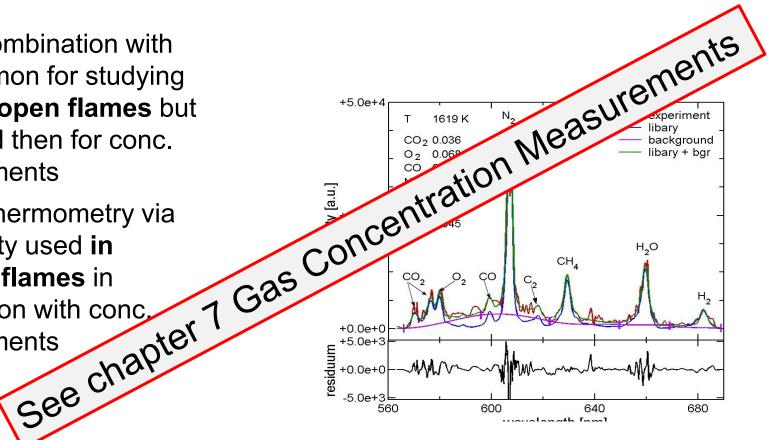
- Measure entire Raman Stokes spectrum
- Low dispersion → measure multi-scalars and deduce temperature either from Rayleigh scattering (see below) or from absolute gas density
- Multi-scalar: exploit different energy separation between quantum states for different molecules





Raman/Rayleigh spectroscopy (2)

- Measure entire Raman Stokes spectrum with **low** dispersion
- Ram in combination with Ray common for studying details of open flames but Ram used then for conc. measurements
- Ram for thermometry via gas density used in confined flames in combination with conc. measurements







Simultaneous Raman/Rayleigh spectroscopy



• Raman scattering \rightarrow species concentrations $N_i(r)$

$$S_{ram,i}(\vec{r}) \propto \sigma_{ram,i}(\vec{r}) \Lambda_{Laser} \Lambda(\vec{r})$$

• Rayleigh scattering \rightarrow density, with EOS \rightarrow temperature (r)

$$S_{ray}\left(\vec{r}\right) \propto \sigma_{ray}\left(N_{i}\left(\vec{r}\right)\right) I_{Laser} \sum N_{i}\left(\vec{r}\right)$$

$$\sigma_{ray} = \sum_{i} \left(\frac{N_{i}\left(\vec{r}\right)}{\sum_{j} N_{j}\left(\vec{r}\right)}\right) \sigma_{ray,i} \quad \overrightarrow{\text{Ideal gas law}} \quad \overrightarrow{T\left(\vec{r}\right)} \propto \frac{1}{\sum N_{i}\left(\vec{r}\right)}$$
(EOS)

Iterative procedure to determine temperature and species

See chapter 7 Gas Concentration Measurements



Motivation



- Gas temperature is a leading parameter in combustion
- Internal combustion engines
 - Temperature dependencies
 - Mixture preparation
 - Ignition, auto-ignition
 - Combustion
 - Pollutant formation
 - Heat loss



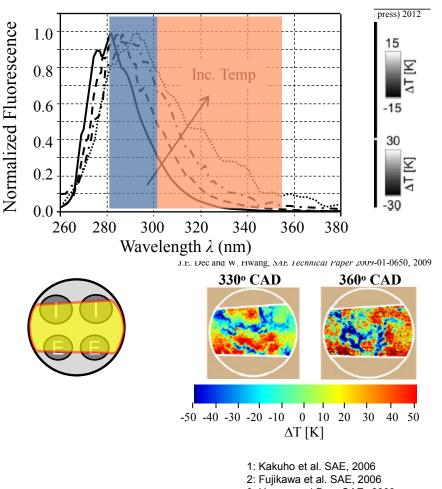
- Measure and understand spatial and temporal evolution of unburned gas temperature in IC engine
- For details see: Peterson et al. PCI 2013



Temperature Fields in IC Engines



- Laser Induced Fluorescence (LIF) Thermometry
- Toluene LIF Thermometry
 - Single line excitation
 - 248 or 266 nm
 - Single or two color detection
- IC Engines
 - Temperature stratification^{1,2,3,4}
 - Low repetition rates
- Focus here
 - High-speed toluene LIF and PIV measurements
 - Temporal evolution of 2D temperature field



- 3: Hwang and Dec, SAE, 2009
- 4: Kaiser et al., ProCl In Press, 2012
- 5: Dronniou and Dec, SAE, 2012



Experimental Setup

TECHNISCHE UNIVERSITÄT DARMSTADT

Exhaust

30 mm

Intake

25 mm

Optical Engine

Red

Inc. Temp

30 mm

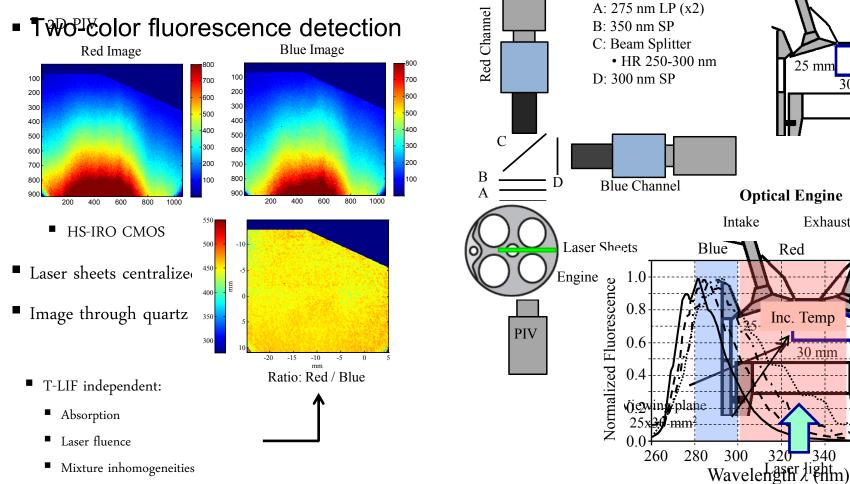
340

320

Exhaust

Bandpass filters

Highureneintageng





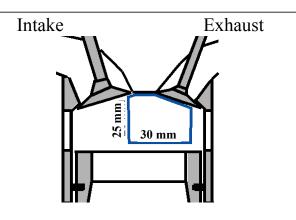
360

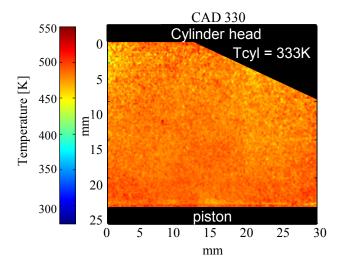
380

Experimental Setup

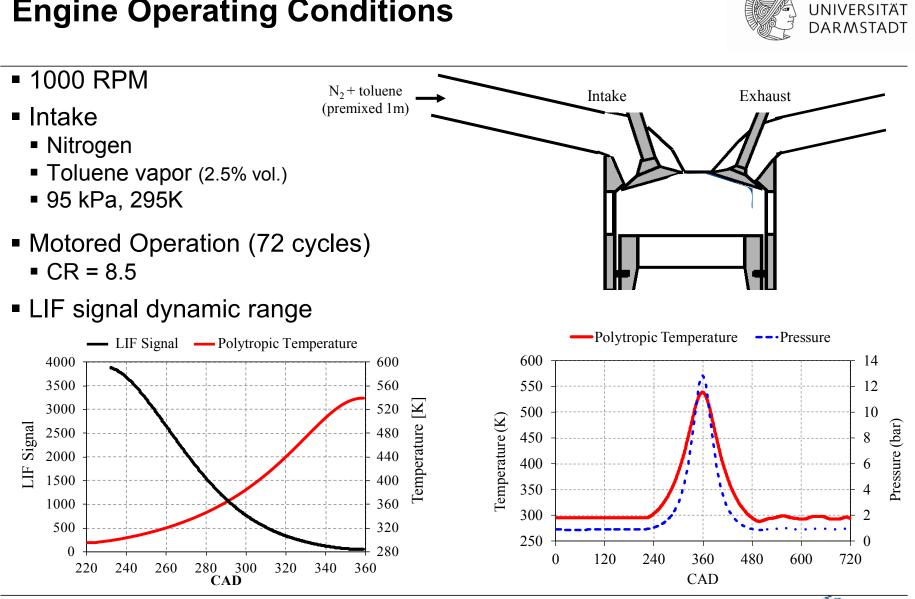
- Field-of-view
 - 25x30 mm² region
 - Offset from cylinder axis
 - Near cylinder head
 - Cylinder head
 - Set temperature: 333K
 - Expected thermal gradients near colder surfaces
- Images
 - 3x3 median filter
 - 3x3 pixel binning
 - Spatial resolution
 - 0.08 mm/pixel











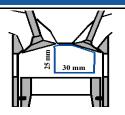
Engine Operating Conditions

TECHNISCHE

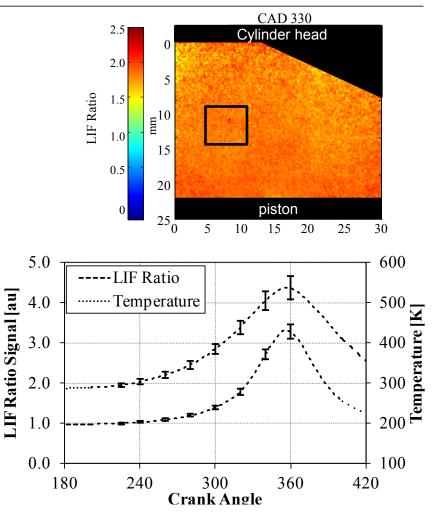


LIF Signal

- Calibration (LIF \rightarrow Temp)
 - LIF ratio (72 cycles)
 - 5x5 mm² region
 - Calibrate to polytropic temperature
- Precision Uncertainty
 - LIF_{ratio, stdev} / LIF_{ratio}
 - Pixel-wise (0.08 x 0.08 mm² region)
 - LIF precision uncertainty
 - T = 295 ± 5 K (2%)
 - T = 540 ± 29 K (5.2%)
 - 10x10 pixel region
 - T = 540 ± 19K (3.5%)









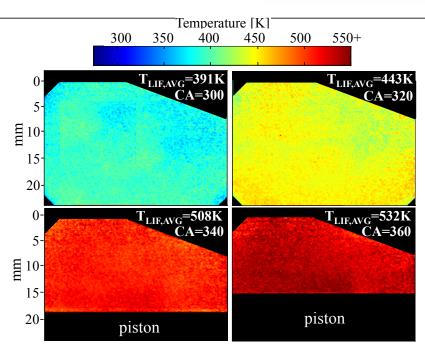
Temperature Images for fired operation



- Compression
 - Homogeneous temperature distribution
 - Temperature "structures" not present



- Cold temperatures emerge from cylinder head
- Out-gassing of crevice gases
- Cold gas entrainment from right side
 - 50 K colder

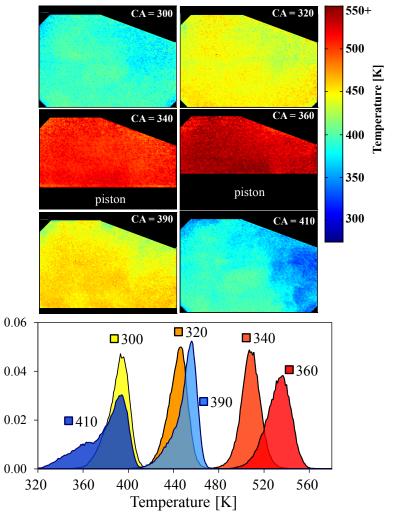




Temperature distributions



- Compression
 - Homogeneous temperature distribution
 - Gaussian-like distribution
- Expansion
 - Temperature inhomogeneities
 - Skew / bimodal distributions

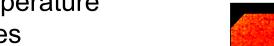


PDF

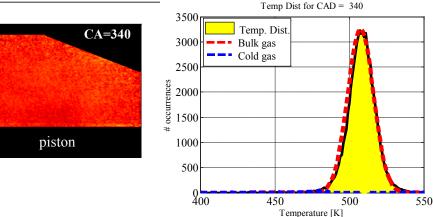


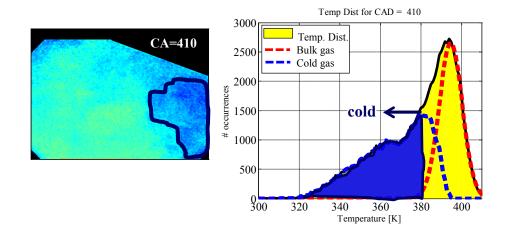
Temperature Distribution

- Identifying temperature inhomogeneities
 - Cold gas
- Gaussian fit to bulk gas temperature
- Subtract from temperature distribution
 - Cold gas distribution
- Cold temperature inhomogeneities
 - < peak of cold gas distribution</pre>





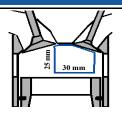




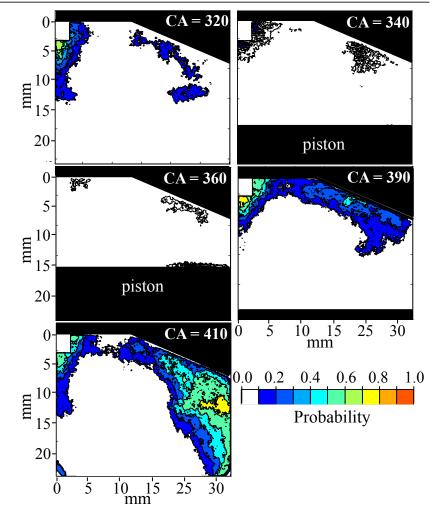


2D PDF Cold Temperature

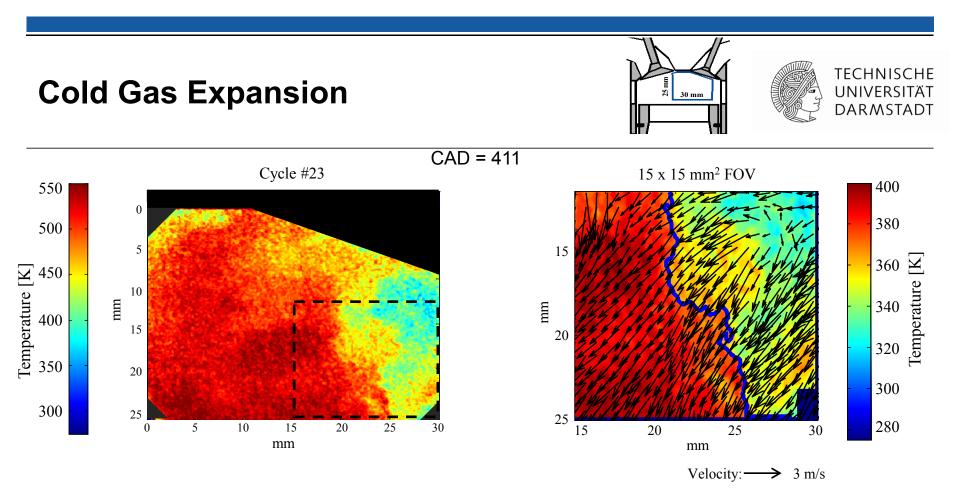
- 72 motored cycles
- Location, occurrence of cold temperature
- Compression
 - Colder temperatures near cylinder head
 - Low probability (< 30%)
 - Temperature boundary layer not visible
- Expansion
 - Cold regions near cylinder head
 - Cold gas enters viewing plane from crevices



TECHNISCHE UNIVERSITÄT DARMSTADT







Temperature and velocity field

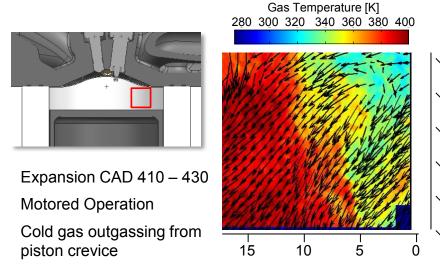
---- cold temperature threshold



High speed toluene PLIF combined with PIV



Visualization of outgassing from crevices



Peterson et al. Proc. Combust. Inst. 34, 3653-3660 (2013)



Conclusions temperature/velocity measurements in IC engine



- High-speed Toluene-LIF and PIV to assess thermal transport in IC engine
- 2-color detection
 - LIF independent from absorption and local mixing
 - Precision uncertainty limited to 3-6% (dependent on temperature)
- Compression
 - Quasi-homogeneous temperature distribution
- Expansion
 - Evident colder gas evolution
 - Thermal stratification
- Cold front tracking
 - LIF vs. PIV
 - Transport of cold gas
 - Discrepancies
 - Out-of-plane motion



Overall summary



- Spectroscopic methods well suited for minimal invasive thermometry
- High resolution in time and reasonable resolution in space
- There is not the single method best suited for all tasks choice depends on measurement task
- Optical access required can be a problem
- High instrumental effort and expert knowledge needed

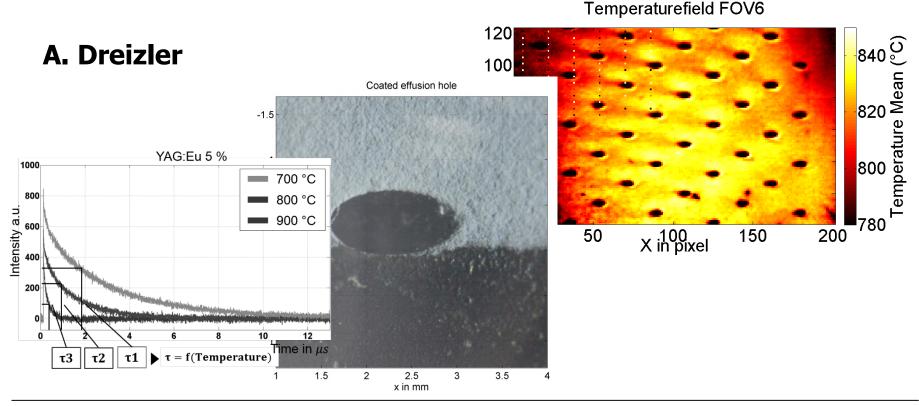


Chapter 6: Surface Thermometry – Thermographic Phosphors

TU Darmstadt, Germany Dept. of Mechanical Engineering Institute for Reactive Flows and Diagnostics







Andreas Dreizler | 1

Outline phosphor thermometry



- Introduction & Motivation
- "Decay-Time Method" versus "Ratio Method": comparing precision and accuracy
- Error treatment for decay-time method
- Application examples



Surface temperature: diagnostics



Thermocouples

- Invasive, limited spatial and temporal resolution, only point measurements
- Pyrometry (Infrared thermometry)
- Emission coefficient generally unknown
- Sensitive against chemiluminescence and stray light

Temperature sensitive paints (TSP - coated), thermoliquid crystals (TLC)

- Temperature range < 380 K

Heat sensitive paints (HSP - coated)

- No temporal resolution

Thermographic phosphors (TGP – coated)

- + Broad temperature sensitive range (7 K -1870 K)
- + Insensitive against blackbody radiation, stray light and chemiluminescence
- + High spatial and temporal resolution, 2D diagnostics



Thermographic Phosphors



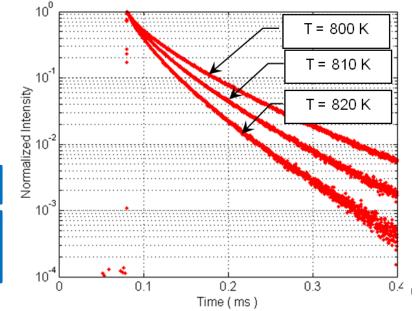
Thermographic phosphors:
Rare-earth or transition metal doped ceramic materials
Exploit temperature dependent spectroscopic properties following electronic excitation



Introduction & Motivation I

Principle of Phosphor Thermometry:

- Coat surface with thermographic phosphor
- Excite coating with UV-light source
- Detect emission with appropriate device either
 - time-resolved (fixed spectral range) or
 - Time-integrated and spectrally resolved (fixed temporal range)





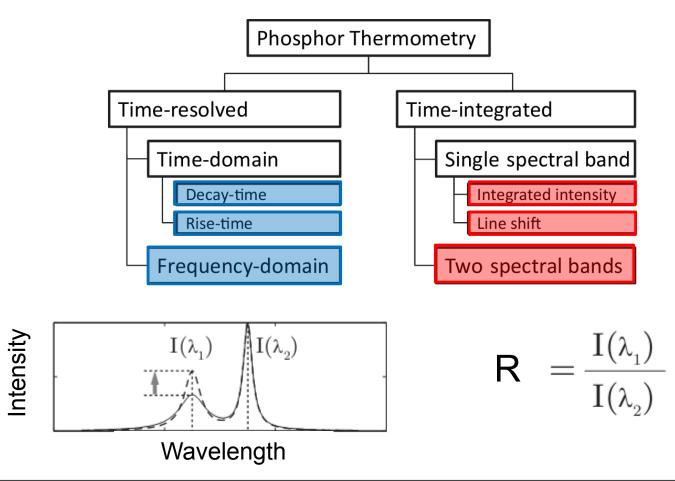


Introduction & Motivation II



TECHNISCHE UNIVERSITÄT DARMSTADT

Approaches of Phosphor Thermometry

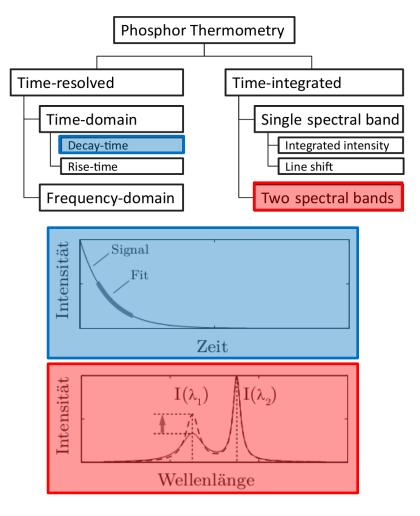




Introduction & Motivation III



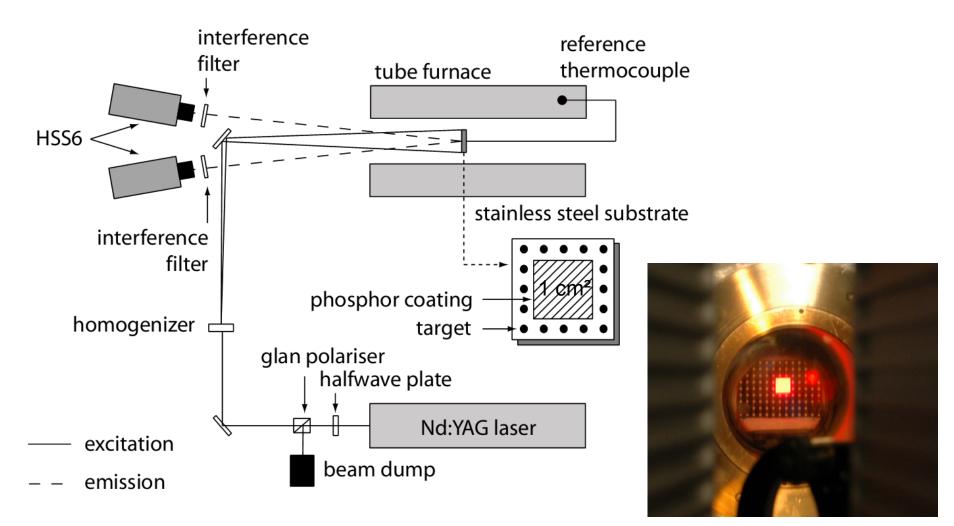
- Comparison of the two most popular approaches:
 - Luminescence Lifetime (Decay-time)
 - Intensity Ratio (Two-line)
- Motivation:
 - Decision support required for users
 - Comparison to highlight pros vs cons
 - Investigation of sensitivities, precision, accuracy and application
- Procedure
 - Use two CMOS high-speed cameras (same data-set)
 - Exemplified for phosphor which exhibits sensitivities in both approaches: Mg₄FGeO₆: Mn





Experimental Setup

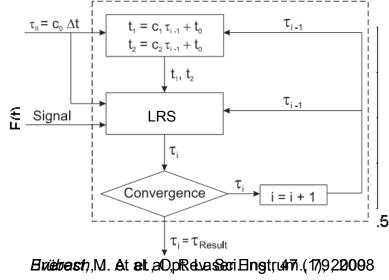






Data evaluation

- Nonlinearity intensity-correction of the CMOS Chip
- Image matching by pinhole model (Software: Davis 7) Lifetime
- Pixelwise fitting of waveforms
- Brübach Algorithm + Linear Regression of the Sum (LRS)

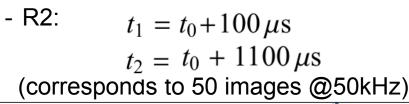


Intensity ratio

- Pixelwise temporal integration:

$$R = \frac{\int_{t_1}^{t_2} I_{633\,\mathrm{nm}}(t) \, dt}{\int_{t_1}^{t_2} I_{660\,\mathrm{nm}}(t) \, dt}$$

- Two ratios R1 and R2 used:
 - R1: $t_1 = t_0 + 100 \,\mu s$ $t_2 = t_0 + 120\,\mu s$ (corresponds to 1 image @50kHz)



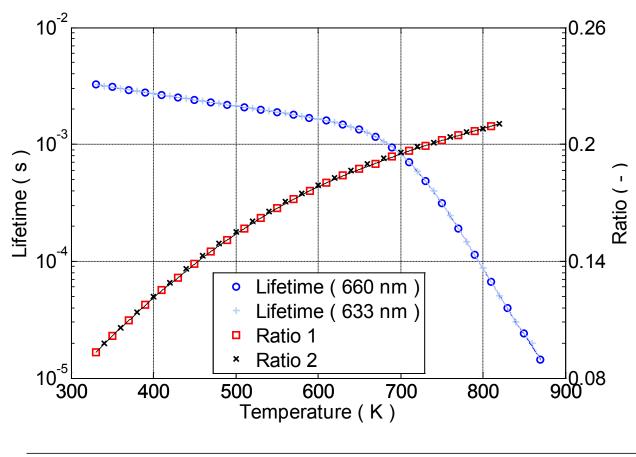




Results: Temperature dependent characteristics



• Temperature-Lifetime / Temperature-Ratio characteristics



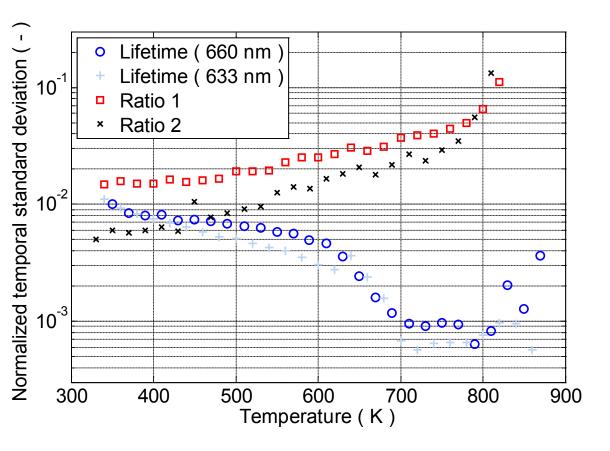
- Temperature-Lifetime characteristics of both spectral bands similar
- Temperature-Ratio characteristics for both ratios similar as well
- Very different sensitivities for lifetime approach and only slightly differing sensitivities for ratio approach



Results: Precision I



• Shot-to-Shot (temporal) standard deviations



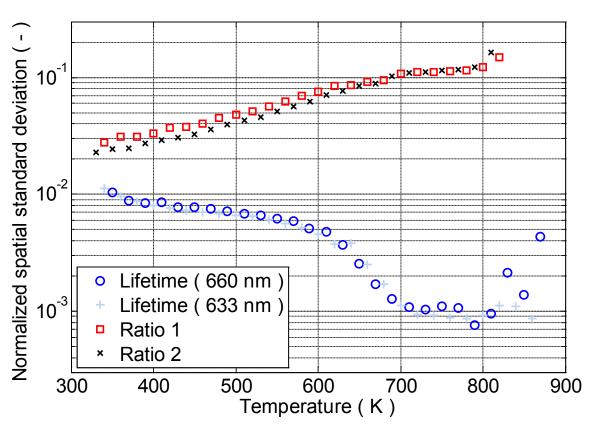
- Comparable precision of both techniques at lower temperatures
- Lifetime method ~2 orders of magnitude better at higher temperatures



Results: Precision II



• Pixel-to-pixel (spatial) standard deviations



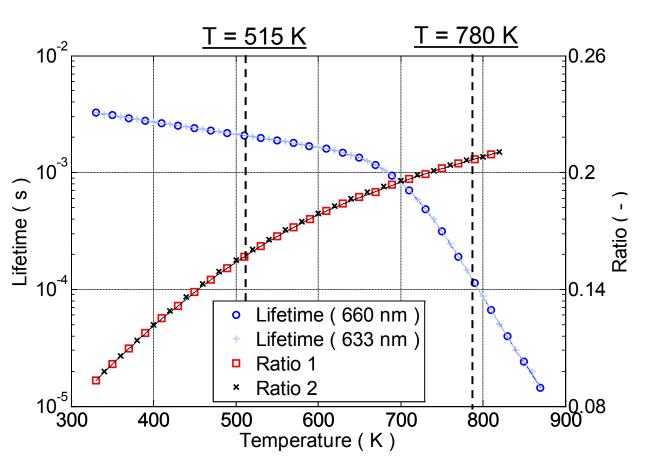
- Huge difference in spatial precision between the two techniques
- Spatial precision of lifetime method superior over the entire temperature range



Results: Accuracy I



• Evaluation of systematic errors



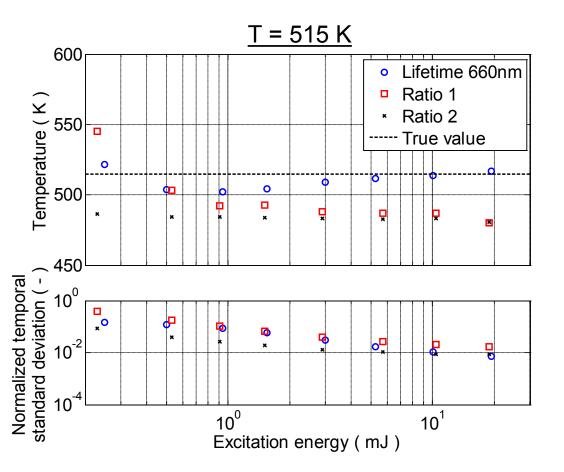
- Evaluated at two different temperatures corresponding to two different sensitivities in the temperature lifetime characteristic
- Calibration at fixed conditions and then parametric variation:
 - Energy variation
 - Changing settings in optical setup



Results: Accuracy II



• Dependency on excitation energy at T = 515K



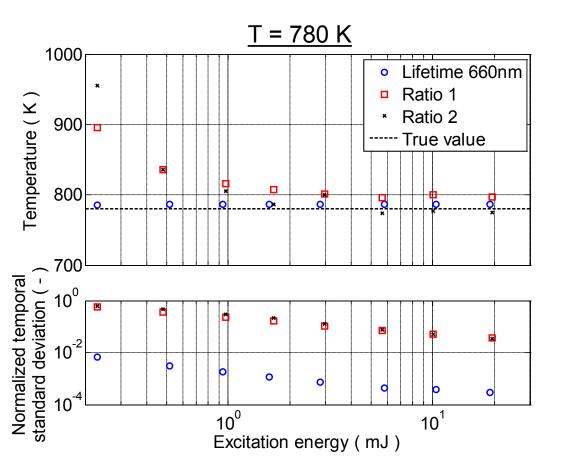
- Inaccuracy for too low excitations energies of lifetime approach well known (i.e. Brübach et al. 2008)
- Ratio 2 rather robust against energy variations, but inaccuracy over whole energy range



Results: Accuracy III



• Dependency on excitation energy at T = 780K



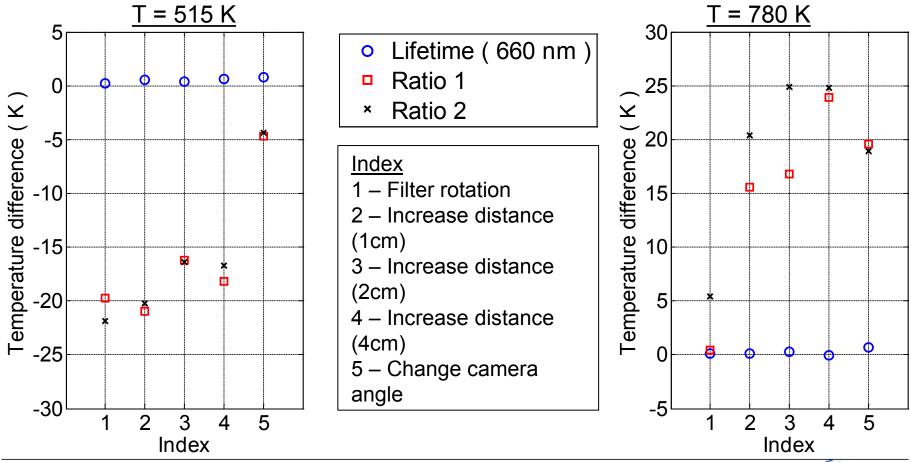
- Lifetime approach very accurate due to high sensitivity
- Ratio 1 & 2 show overestimation of more than 100 K at lower energies



Results: Accuracy IV



• Accuracy due to changes of settings in the optical setup







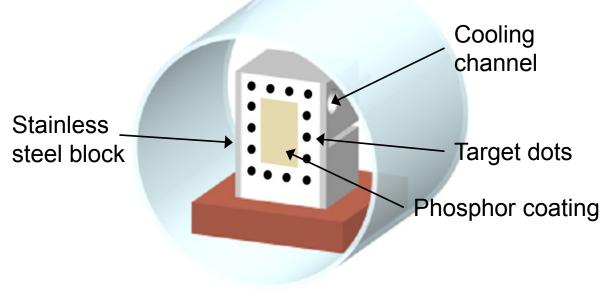
Results: Cooling device I



• Stainless steel block with cooling channel placed inside oven

Tube furnace

- When block is at designated temperature, cold water is pumped through cooling channel
- For image mapping purposes target dots have been transferred to device



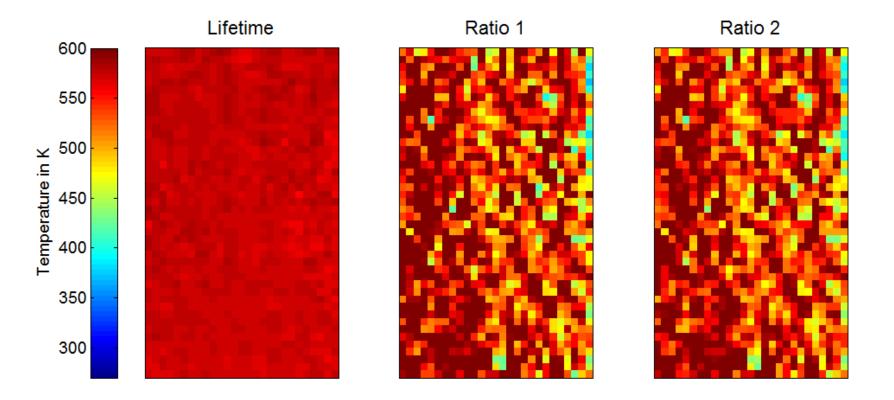
Kissel, T., PhD Thesis, TU Darmstadt, 2011



Results: Cooling device II

TECHNISCHE UNIVERSITÄT DARMSTADT

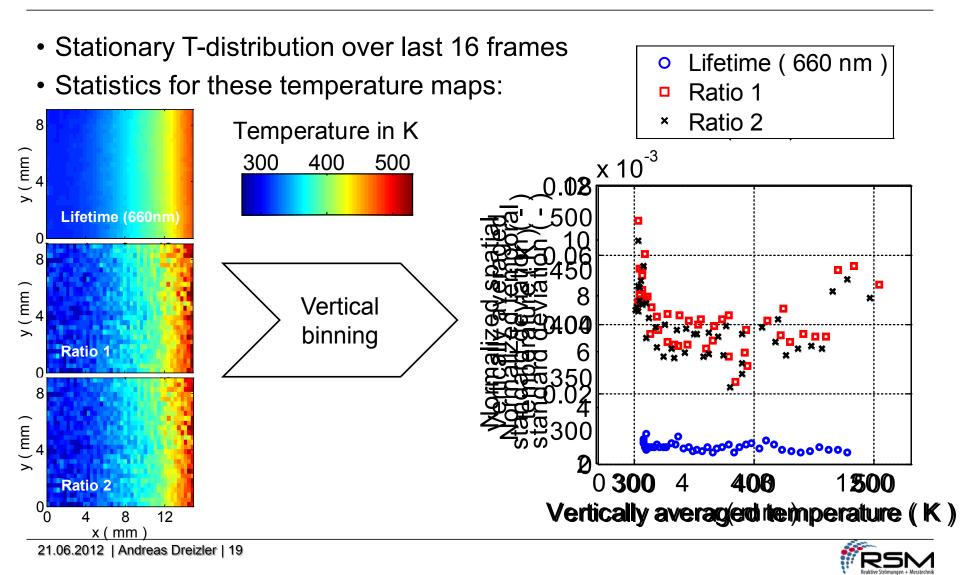
- Transient Experiment
- Same set of data for all three methods





Results: Cooling device III





Summary & Conclusions



Comparison of Mg₄FGeO₆: Mn for the lifetime and the intensity ratio method in terms of

- Precision
- Accuracy
- Application (cooling device)

Main results

- High temperature range (>650K): Lifetime method is superior in all aspects
- Low temperature range: Lifetime method superior for spatial standard deviation and for accuracy, similar temporal standard deviations
- Only valid for the phosphor under consideration
- For other phosphors similar investigations required

Fuhrmann PCI 34, 2013, Fuhrmann et al.





- 1. Introduction
- 2. Measurement chain / Error sources
- 3. Applications
- 4. Summary

For details see PECS 2013, Brübach et al.







1. Introduction

2. Measurement chain / Error sources

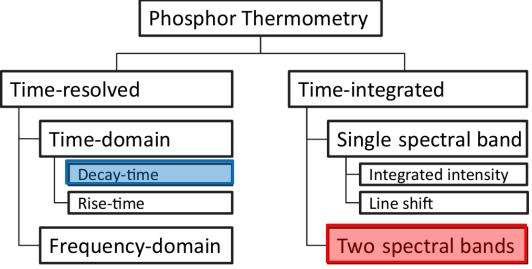
- 3. Applications
- 4. Summary



Combustion applications: mostly used approaches



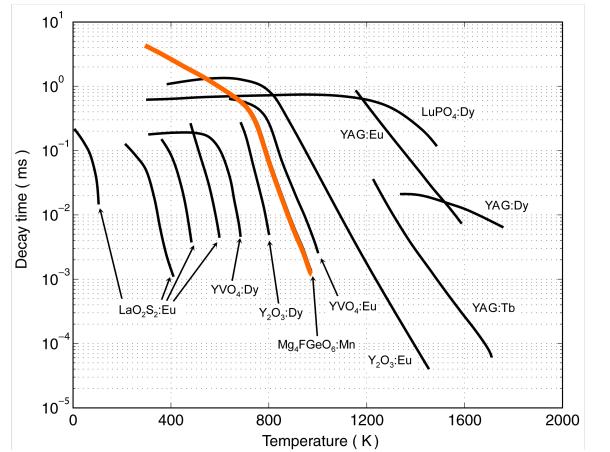
- Most often used approaches are <u>decay-time</u> and two-spectral-bandmethod
- As discussed: Decay-time method does have the potential for superior precision and accuracy (especially in 2D application); see Fuhrmann, Brübach and Dreizler, PCI 33, 2013
- Decay-time varies with temperature due to varying energy transfer processes





Thermographic Phosphors: materials showing temperature dependent decay times





Approx. 100 different phosphors documented in literature See Brübach et al. PECS 2013

Magnesium-Fluorogermanate doped with manganese:

Mg₄FGeO₆:Mn

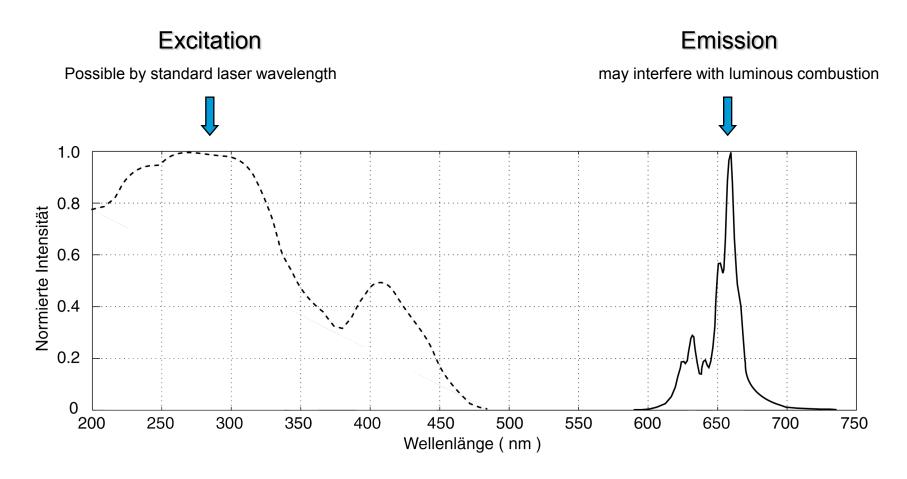
Allison and Gillies, Rev. Sci. Instr., 68:2615-2650, 1997.



Spectra







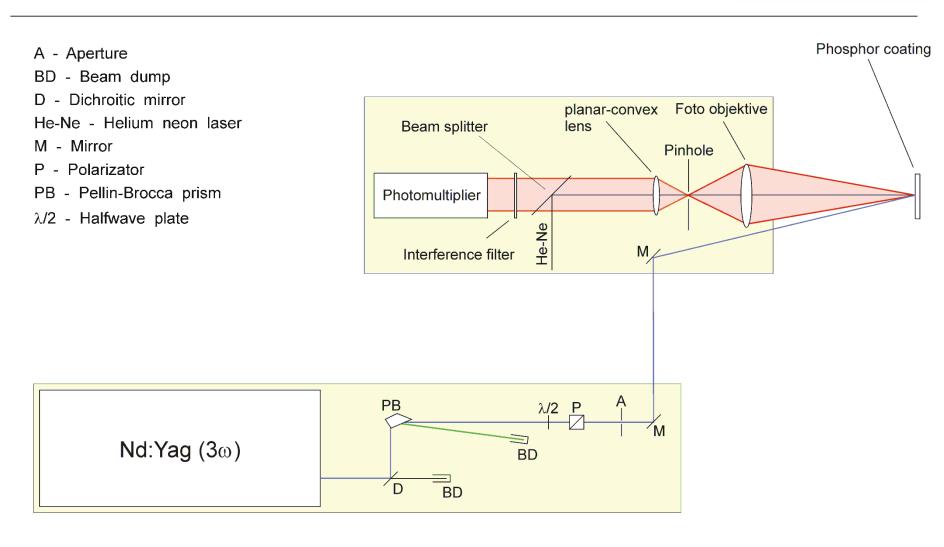




Experimental Setup – 0D









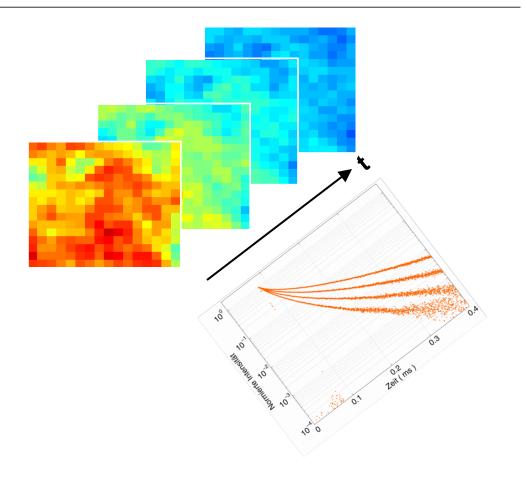
Experimental Setup – 2D

CMOS Kamera LaVision HSS6:

- Dynamic Range: 12 bit
- max. frame rate of 675 kHz at a resolution of 64 x 16 Pixels



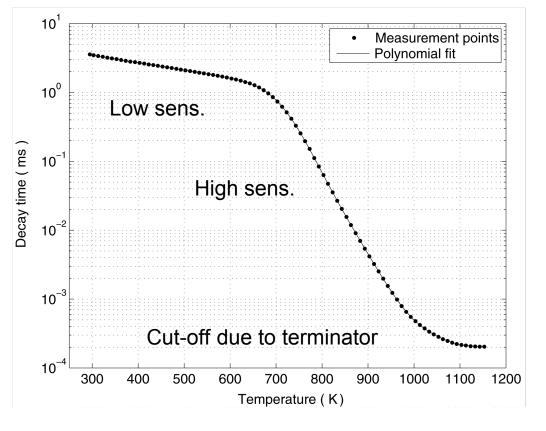




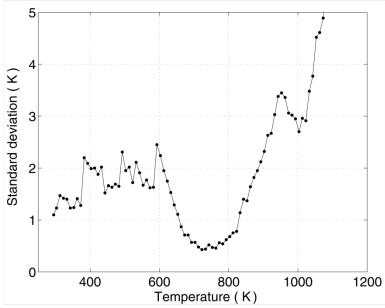


Calibration in well-controlled environments (oven)





- Phosphor: Mg₄FGeO₆:Mn
- Substrate: Stainless Steel (1.4301)
- Gas phase pressure: 1 bar (air)
- Detection: PMT at 500 Ω







1. Introduction

2. Measurement chain / Error sources

- 3. Applications
- 4. Summary

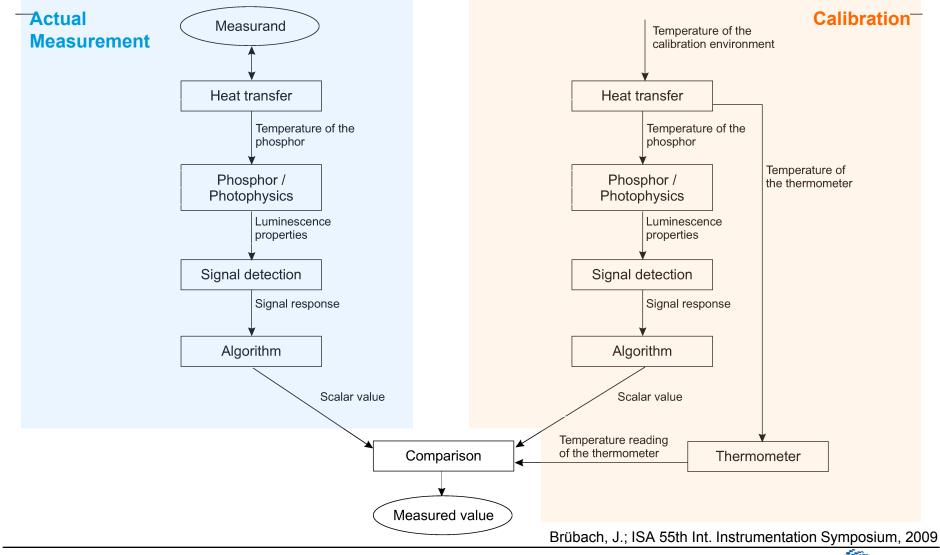


Measurement chain





RSM



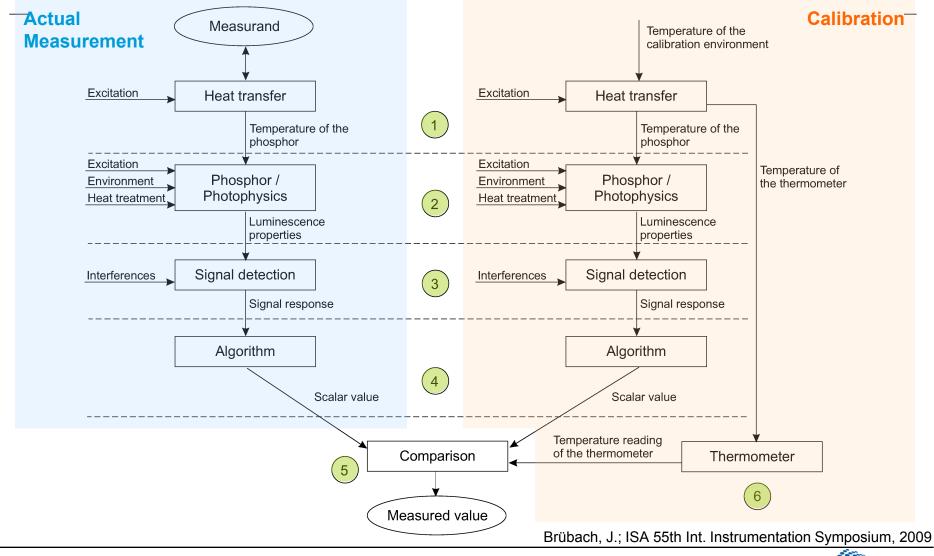
32

Measurement chain



TECHNISCHE UNIVERSITÄT DARMSTADT

RSM

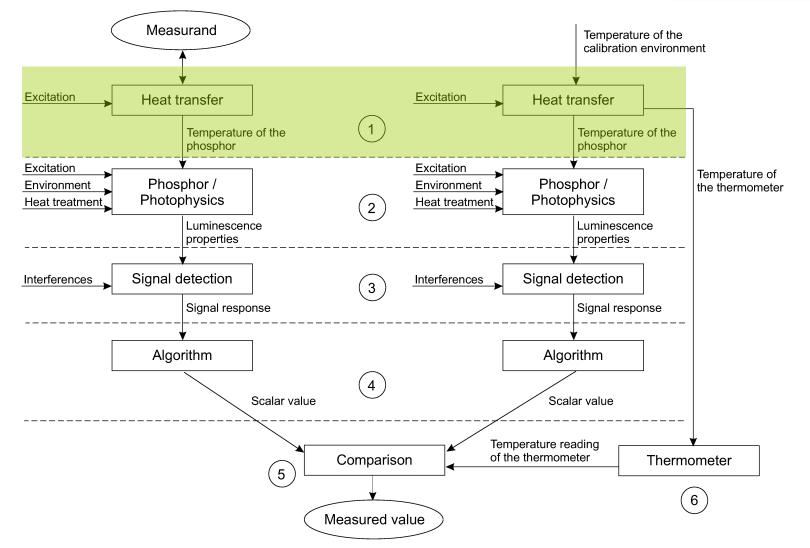


Andreas Dreizler / TU Darmstadt

33

Error class 1: Thermal interactions





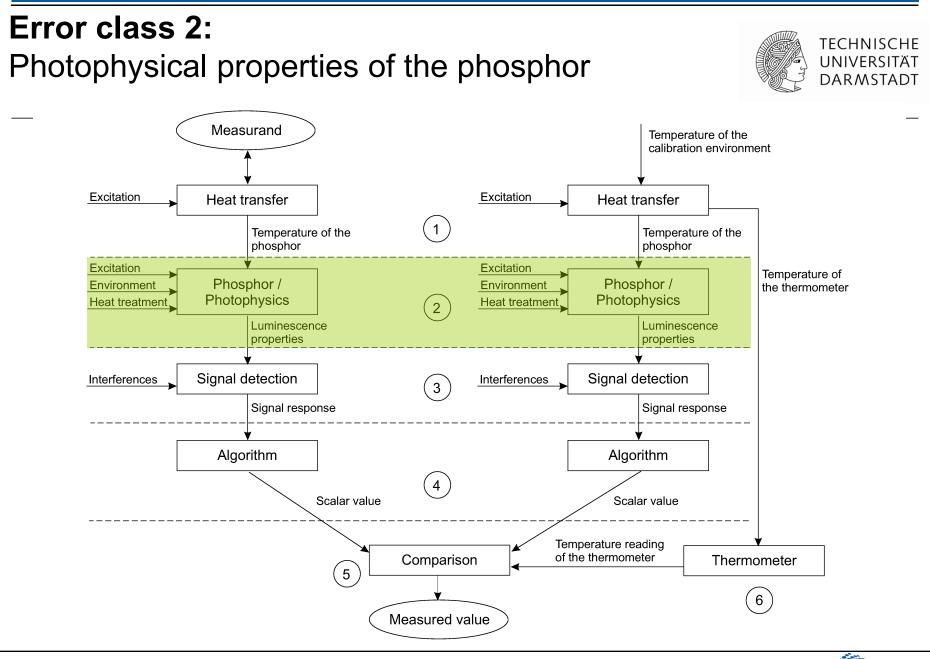


Error class 1: Thermal interactions



- Device under test (DUT) and phosphor or phosphor and calibration thermometer are not in thermal equilibrium
- Impact of the presence of the phosphor on the thermal state of the DUT (e.g. heat insulation) → "semi-invasive" method
- Excitation induced heating of the phosphor \rightarrow check by power scan





RSN

36

Error class 2:

Photophysical properties of the phosphor

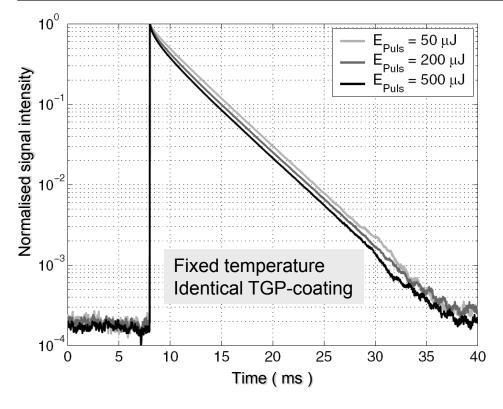


- Impact of the transfer function of the phosphor
 - → Temperature sensitivity, varies with temperature
 - → Temporal low pass character due to finite decay time (thermal inertia versus decy time)
- Parameters that manipulate the transfer function of the phosphor
 - Diffusion processes between the phosphor material and the substrate due to heat treatments
 - \rightarrow Chemical and physical environment (oxygen quenching)
 - \rightarrow Laser excitation (variations with intensity)



Error class 2: Excitation irradiance





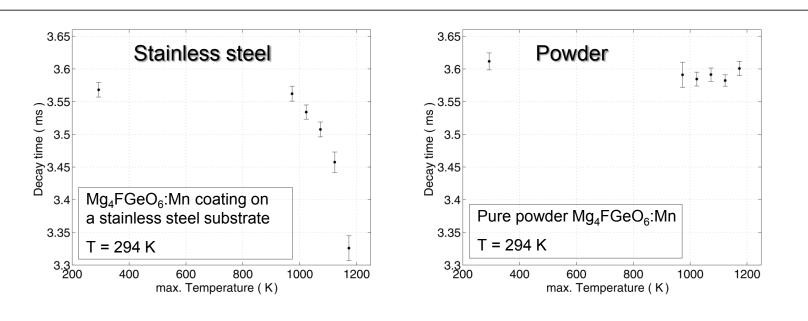
- Decay behaviour "more multi-exponential" at higher laser intensities
- Significant influence of the position of the fitting window

Brübach, J.; Feist, J. P.; Dreizler, A.: Meas. Sci. Technol., 19(2):025602, 2008.



Error class 2: Decay time @ 294 K after heat treatment



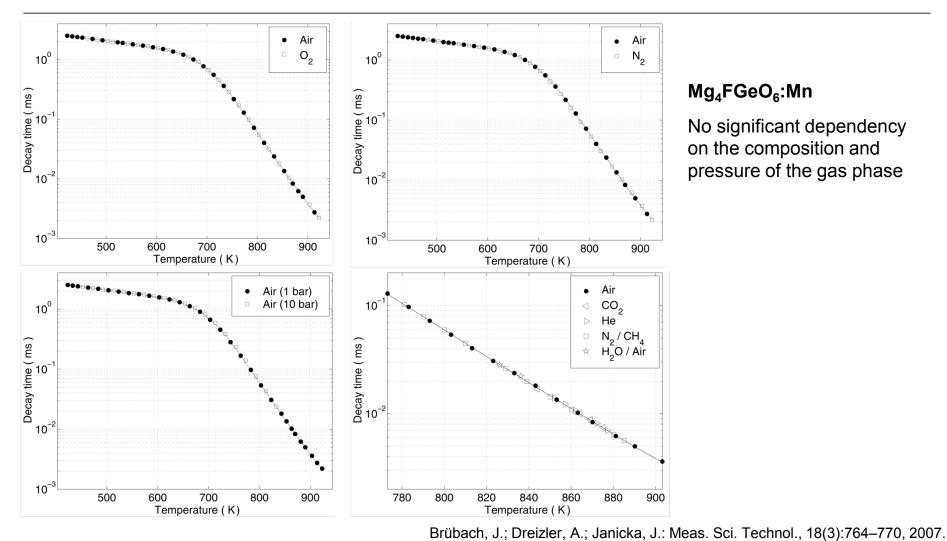


- Dependency on: Substrate material
 - Duration of the heat treatment
 - Heat treatment temperature

Diffusion process between phosphor und substrate

Brübach, J.; Feist, J. P.; Dreizler, A.: Meas. Sci. Technol., 19(2):025602, 2008.

Error class 2: Surrounding gas phase





Mg₄FGeO₆:Mn

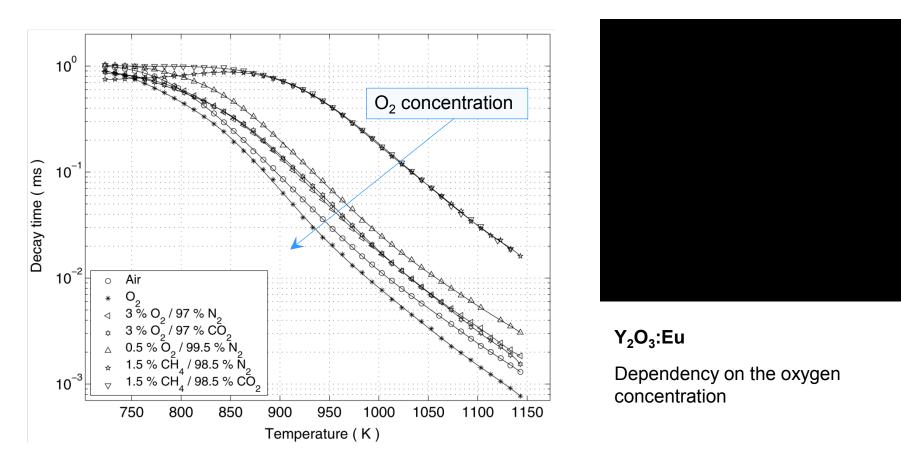
No significant dependency on the composition and pressure of the gas phase

Andreas Dreizler / TU Darmstadt



Error class 2: Surrounding gas phase



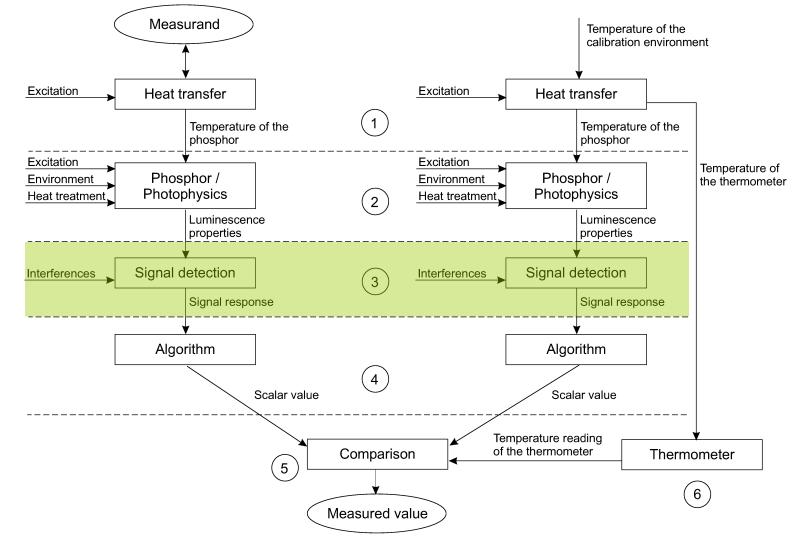


Brübach, J.; Dreizler, A.; Janicka, J.: Meas. Sci. Technol., 18(3):764–770, 2007.



Error class 3: Signal detection





42



Error class 3: Signal detection – overview



TECHNISCHE UNIVERSITÄT DARMSTADT

- Impact of the transfer function of the detection system
 - → limited spatial, temporal and spectral resolution
 - ➔ nonlinear behaviour of the detector (CMOS camera)
- Parameters that manipulate the transfer function of the detection system
 - → small changes in the alignment (intensity ratio, see PCI 33-paper 2013)
 - → terminating resistor, BNC length, amplifier (PMT, decay time)
- Optical and electrical interferences
 - ➔ optical interf. (e.g. background radiation, CL, fluorescence of substrate,...) most often temporally not correlated (worse precision)
 - ➔ electrical interf. (e.g. high voltage Q-switch electronics) might be temporally correlated (worse accuracy)
- Dynamic DUTs (e.g. moving surfaces)
 - ➔ signal decay might be superimposed by spatial variations of the absolute luminescence intensity; depending on the homogeneity of the excitation irradiance and the phosphor coating as well as on spatial temperature variation

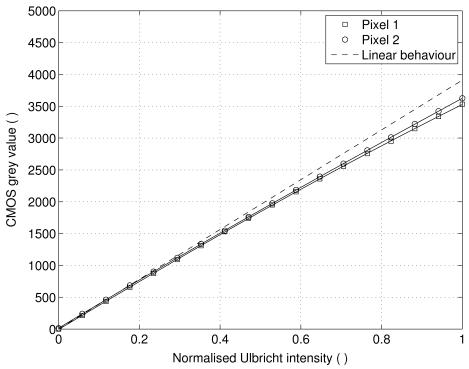




Error class 3: Signal detection – PMT versus CMOS



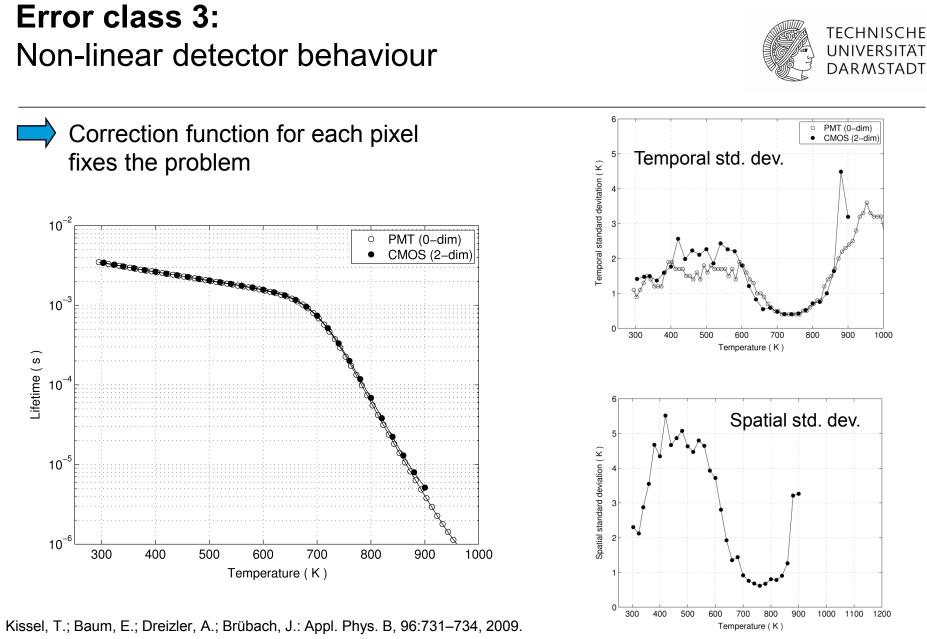
- Photomultiplier unproblematic
- CMOS camera shows problems regarding
 - → Linearity
 - ➔ Pixel-to-pixel homogeneity
 - ➔ Offset stability



Kissel, T.; Baum, E.; Dreizler, A.; Brübach, J.: Appl. Phys. B, 96:731–734, 2009.

44

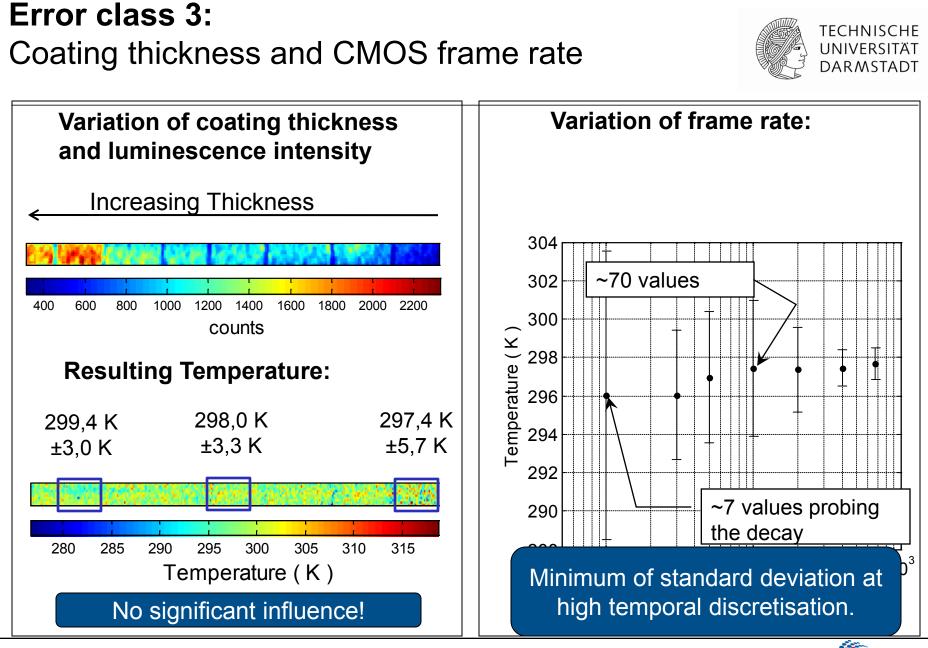




Andreas Dreizler / TU Darmstadt

45



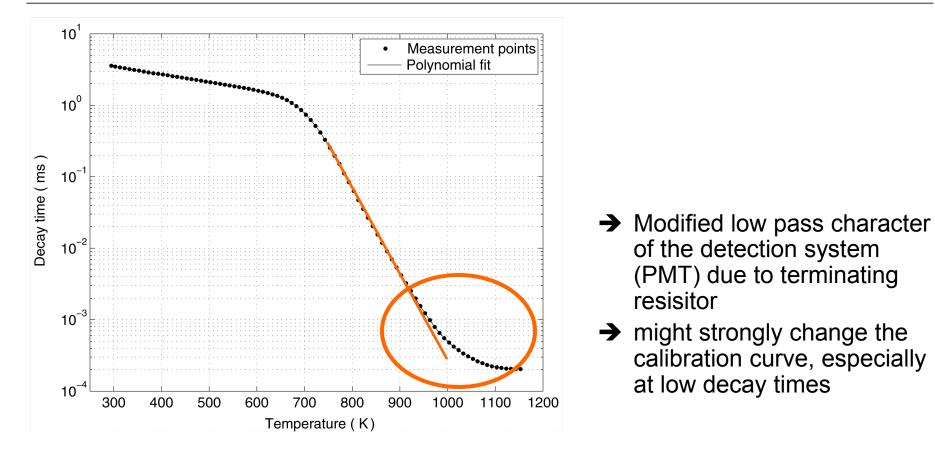




Error Class 3:

Parameters impacting the transfer function



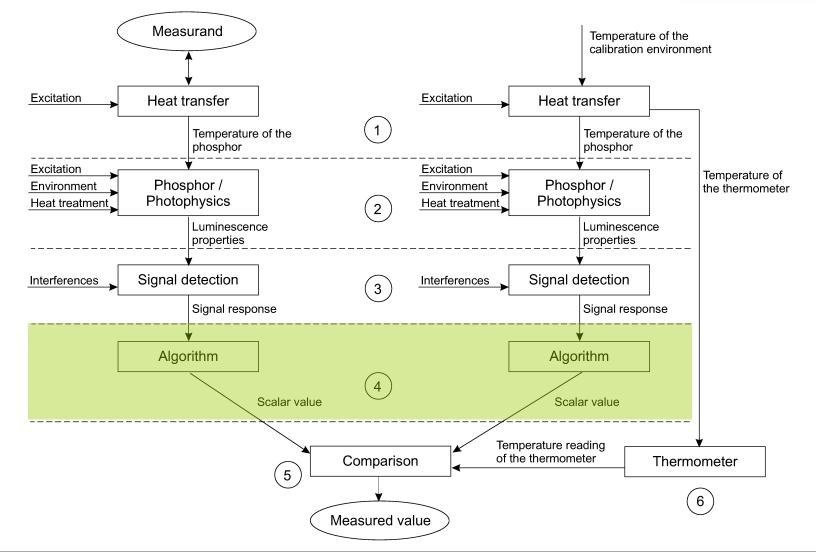




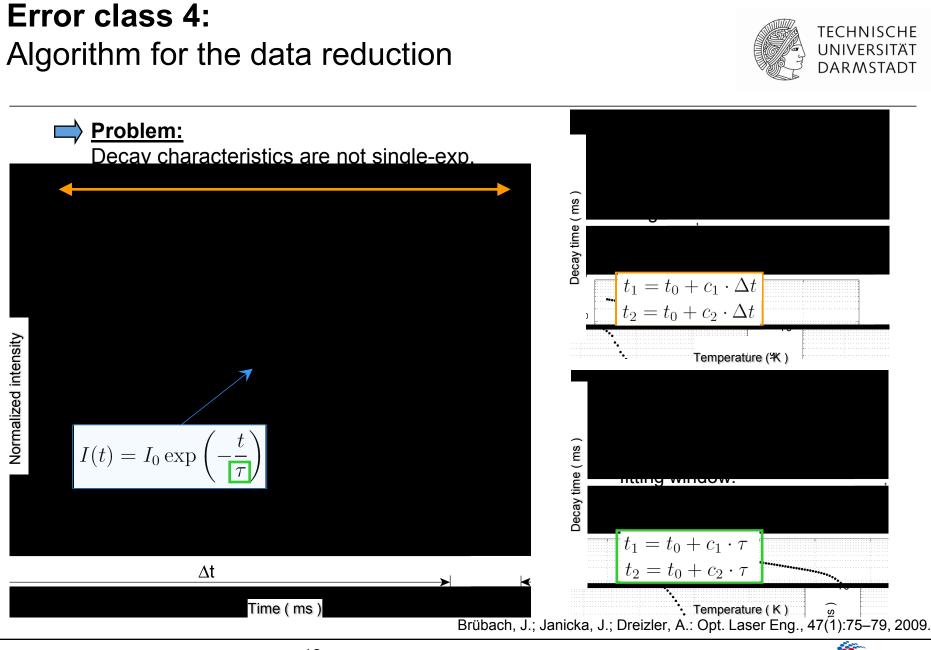
Error class 4: Algorithm for the data reduction











Andreas Dreizler / TU Darmstadt

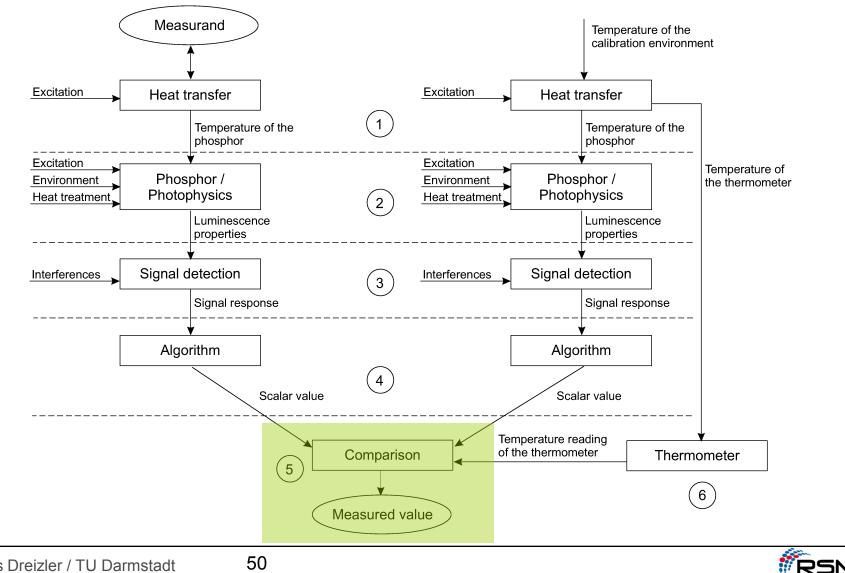
49

RSM

Error class 5: Comparison of the scalar values



TECHNISCHE UNIVERSITÄT DARMSTADT



Andreas Dreizler / TU Darmstadt

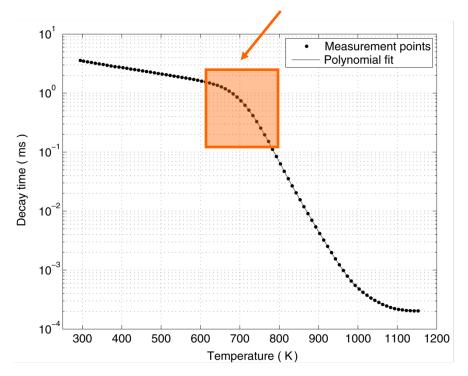
50

Error class 5:

Comparison of the scalar values

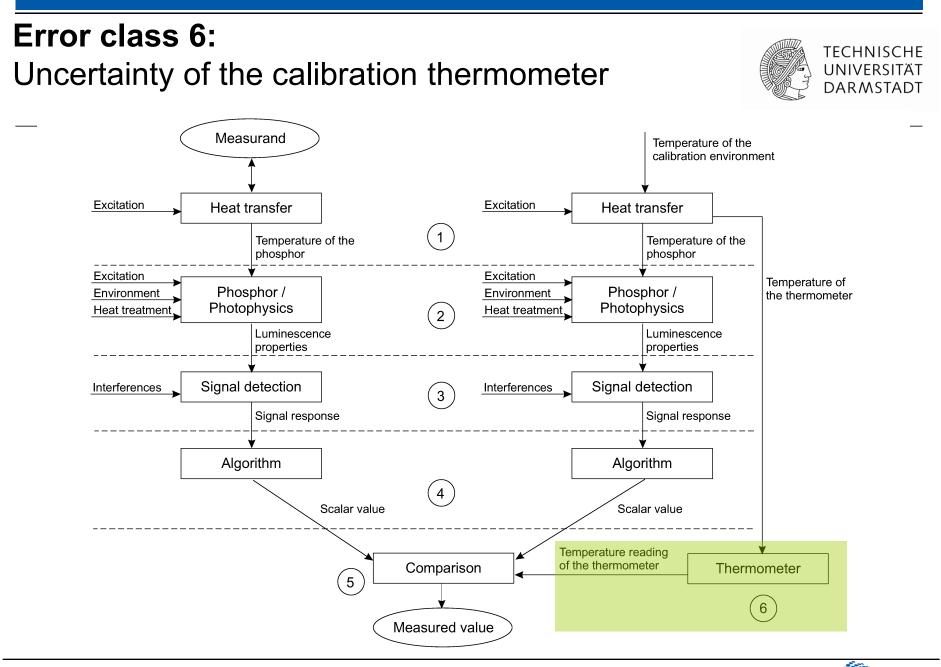


- Error depending on the calibration temperature intervals and the quality of the interpolation in between the calibration points.
- High error potential in strongly curved regimes of the calibration curve



• Calibration intervals of at least $\Delta T = 20$ K or even $\Delta T = 10$ K are recommended.





RSN

Error class 6: Uncertainty of the calibration thermometer



- Most often, thermocouples are employed
- High quality thermocouples offer an accuracy of better than 0.4 % of the absolute temperature.





Systematic Error:	Provided a careful practice: → Systematic Error < 1 %	
Error class		max. error
1. Heat transfer		?
2. Photophysics	Excitation	<i>O</i> (10 ¹ K)
	Dopant concentration	<i>O</i> (10 ² K)
	Heat treatments	<i>O</i> (10 ¹ K)
	Surrounding gas phase	<i>O</i> (10 ² K)
3. Detection system		<i>O</i> (10 ² K)
4. Algorithm for data reduction		<i>O</i> (10 ¹ K)
5. Comparison of calibration and measurement		<i>O</i> (10 ¹ K)
6. Accuracy of the calibration thermocouple		<i>O</i> (10 ⁰ K)

54

Brübach, J.; ISA 55th Int. Instrumentation Symposium, 2009





1. Introduction

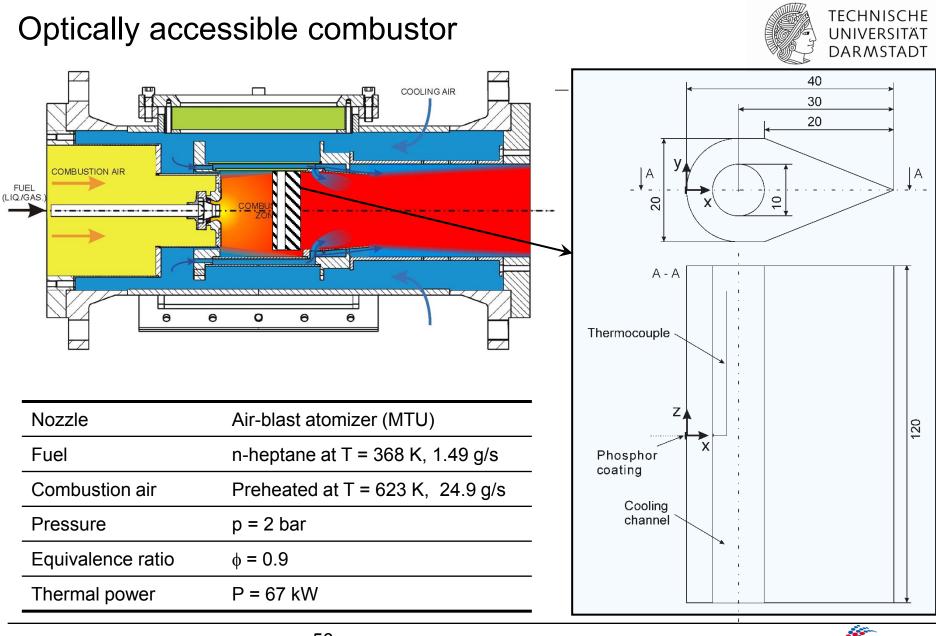
2. Measurement chain / Error sources

3. Applications

55

4. Summary

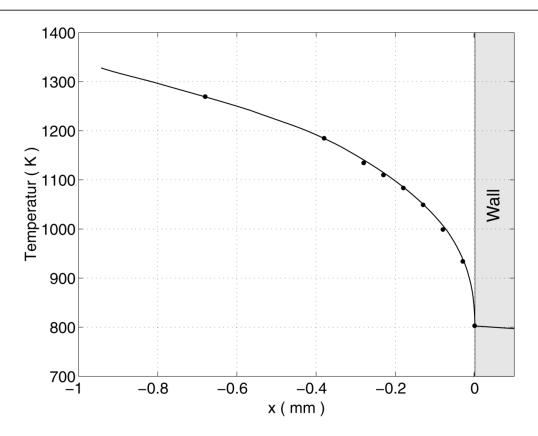






Optically accessible combustor

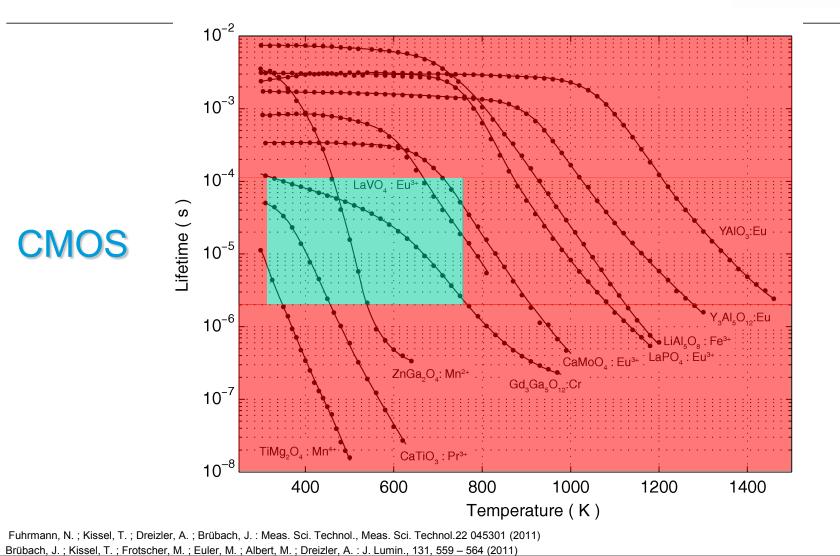




- Distance of the probe volume next to the wall: 30 µm
- Temperature progression of the gas phase can be extrapolated very well to the wall

Brübach, J.; Hage, M.; Janicka, J.; Dreizler, A.: Proc. Comb. Inst., 32(1):855-861, 2009.





Optically accessible combustion engine

Andreas Dreizler / TU Darmstadt

58



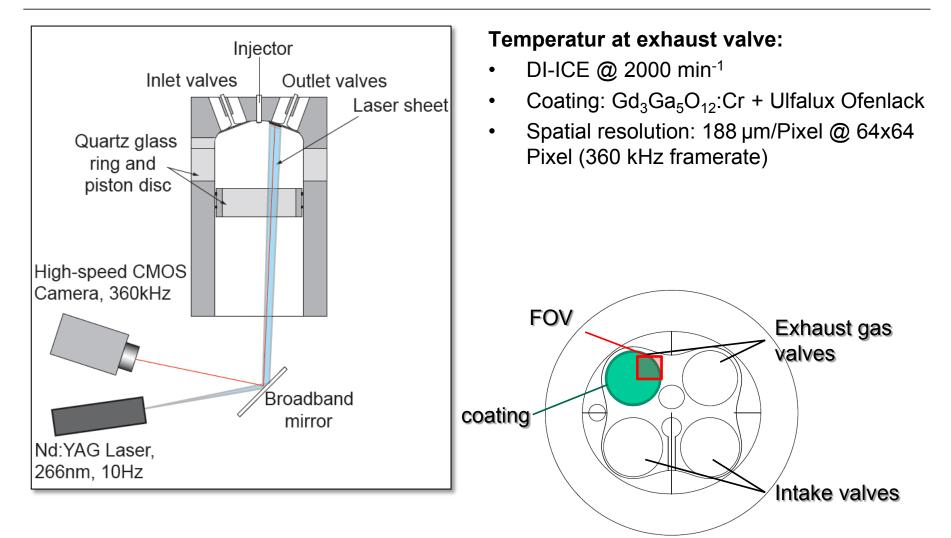
TECHNISCHE

UNIVERSITÄT DARMSTADT

Optically accessible combustion engine

TECHNISCHE UNIVERSITÄT DARMSTADT

See Appl. Phys. B 2011, Fuhramnn et al.



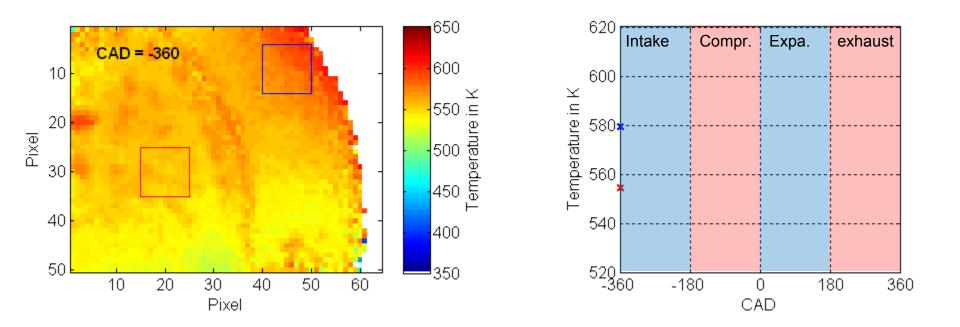


Optically accessible combustion engine

TECHNISCHE UNIVERSITÄT DARMSTADT

Fired engine operation:

Temperature measurement at selected CAD



N. Fuhrmann, M. Schild, D. Bensing, S.A. Kaiser, C. Schulz, J. Brübach, A. Dreizler: *Two-dimensional cycle-resolved exhaust valve temperature measurements in an optically accessible internal combustion engine using thermographic phosphors;* Applied Physics B, DOI 10.1007/s00340-011-4819-2.

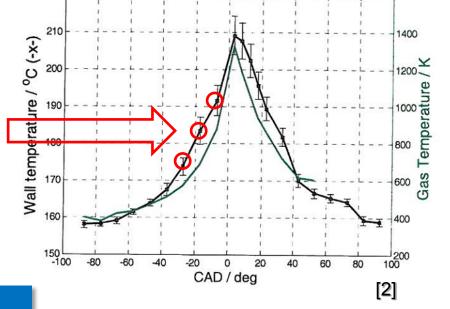
60



Extension to high speed phosphor thermometry in ICE

- Former measurements use 10Hz laser-systems for phosphor thermometry
- Temperatures originate from different cycles → averaging of uncorrelated single shots

High speed phosphor thermometry Use laser at high repetition rate to resolve temperatures within cycles



Mean temperature with std for wall and gas / °C



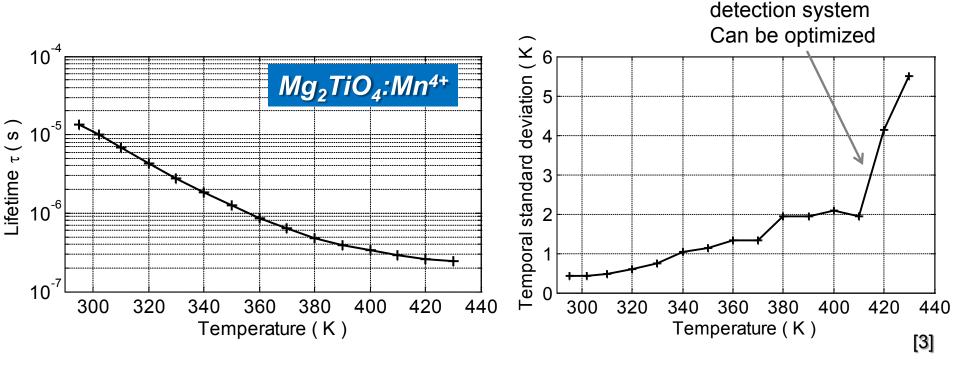


Resolving singly cycles by high speed TGP

TECHNISCHE UNIVERSITÄT DARMSTADT

Steep increase due to

- High speed phosphor thermometry
- Very fast decaying phosphors
- Well below 167µs (1°CA at 1000 rpm)





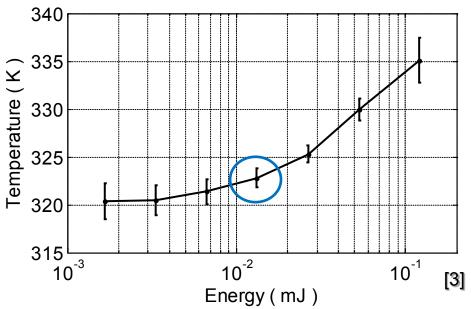
Influence of laser-induced heating



- Challenges when using High Speed Phosphor Thermometry:
- → Laser-induced heating effects
- Due to high power delivered by laser
- Quantify by energy-scan
- Trade-off between precision and accuracy

Optimum at $E = 13\mu J$:

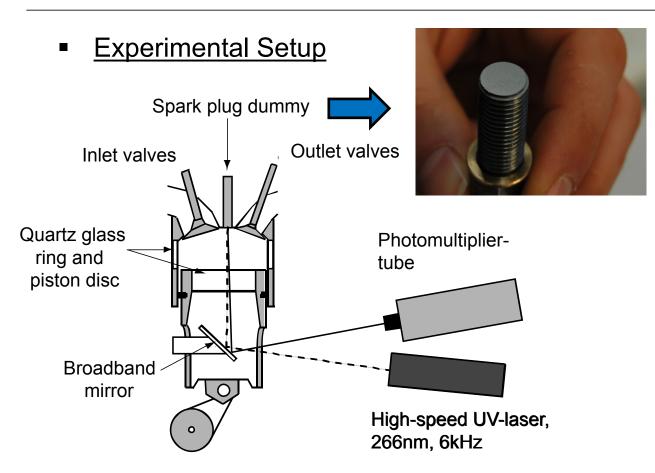
- Standard deviation below 1K
- Systematic error of 2.5K





Set-up and realization





<u>Coating</u>

- Coated via airbrush
- Dispersion of binder and phosphor

<u>Engine</u>

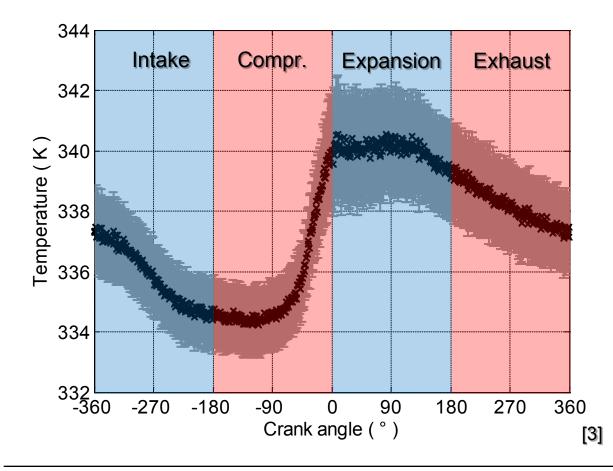
- Motored at 1000rpm
- No injection and ignition
- Compression ratio 8.5:1



Results for motored engine (no combustion)



Temperature progression of the spark plug dummy

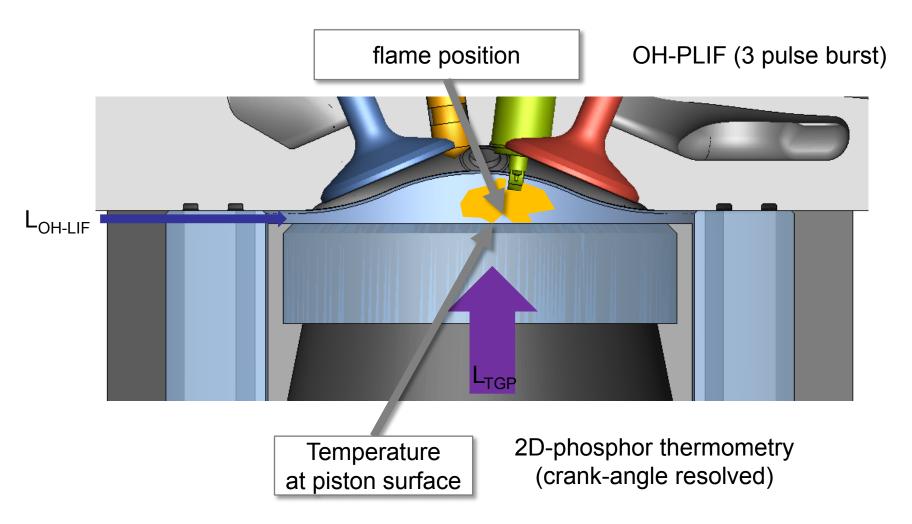


- Mean values and temporal standard deviations of 100 cylces
- Resolution of 1 ° CA
- Precision of about

1-2 K



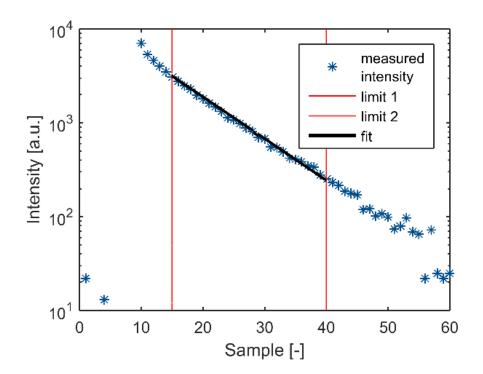
Wall temperature measurements during flame wall interactions in IC engine





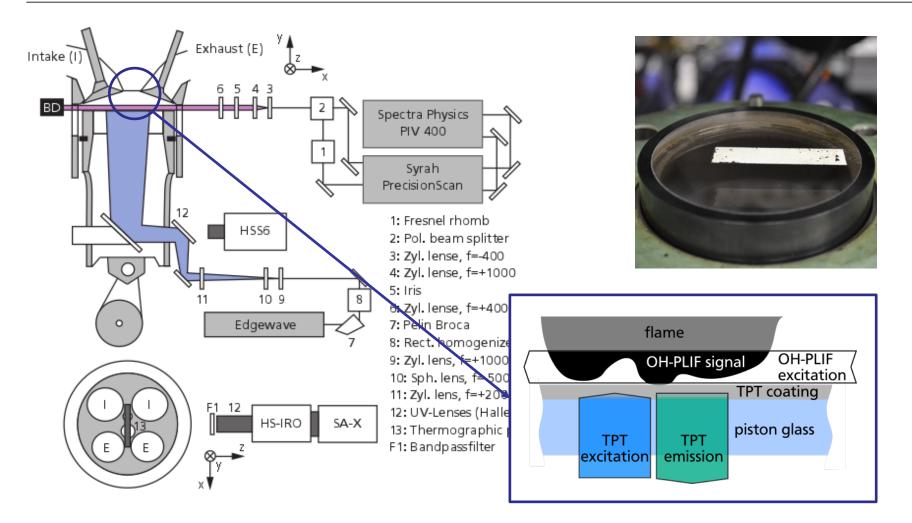
Phosphor thermometry

- Decay-time method
 - Ex-situ calibration
- Engine requirements
 - Fast temperature measurements (~ 10µs)
 - High sensitivity, high SNR (~ 5K)
- Suitable thermographic phosphor: Gd₃Ga₅O₁₂:Cr,Cer





Experimental setup for studying flame-induced heating

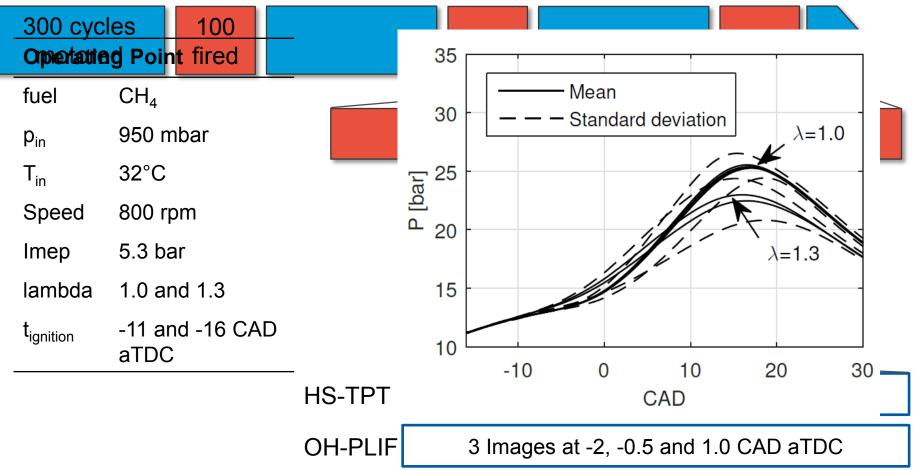




Engine operational conditions

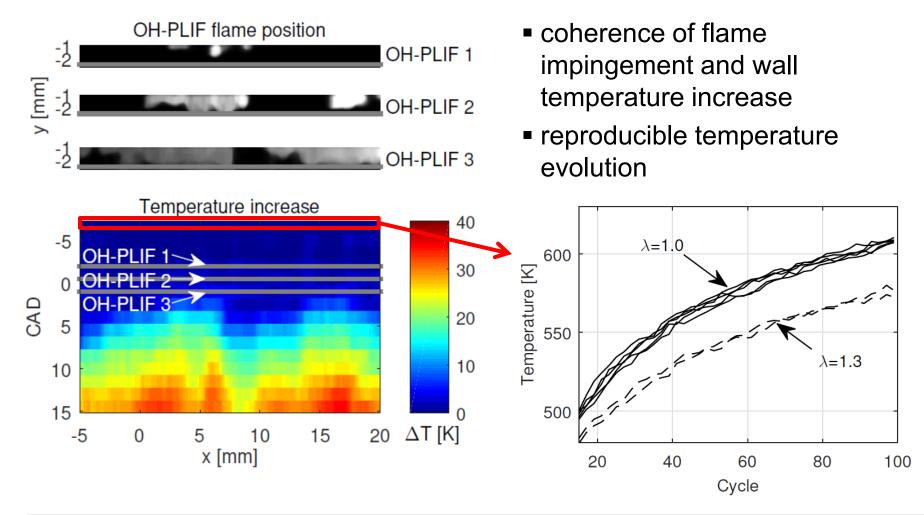
Heating up the engine for several runs

multiple runs recorded



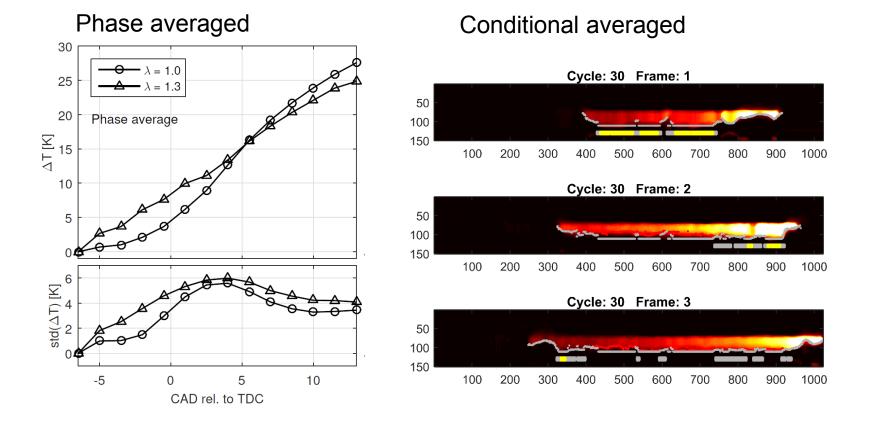
 \rightarrow

Flame position and wall temperature





Temperature rise during flame-wall interaction



Maximum heating rates of up to 20,000 K/s





1. Introduction

2. Measurement chain / Error sources

3. Applications

4. Summary







- Systems for 0D und 2D phosphor thermometry
- Decay-time method superior compared to ratio method with respect to precision and accuracy
- Quantification of systematic and statistic error
- Application (relatively) straight forward, even to complex systems
- High potential for further applications

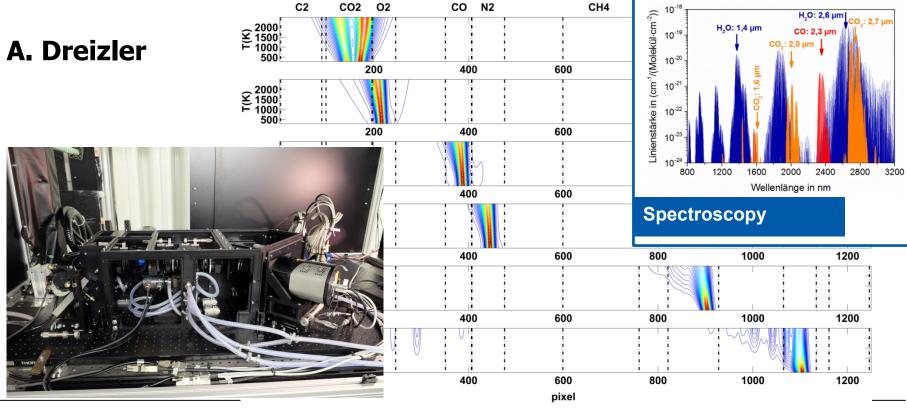


Chapter 7: Gas-Phase Concentration measurement

TU Darmstadt, Germany Dept. of Mechanical Engineering Institute for Reactive Flows and Diagnostics







Andreas Dreizler | 1

Motivation for quantitative species concentration measurement



- Quantitative concentration measurements are motivated by various scientific and technological issues
- Target species depends on the combustion process
 - Mixture fraction
 - Reaction progress and intermediate species concentration
 - Pollutants
 - ...
- A quantitative species measurement in combustion application requires information of local gas temperature (density correction and methodrelated correction such as quenching correction in LIF)
 - Best option: measure simultaneously local temperature



Methods in the NIR/UV/VIS for temperature measurements via Boltzmann distribution



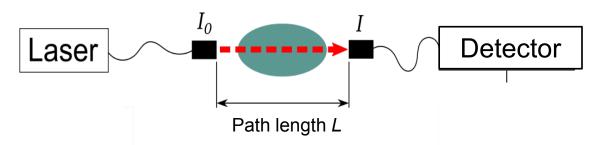
- Laser absorption spectroscopy (LAS)
- Laser-induced fluorescence (LIF)
- Raman spectroscopy (RS)



Laser absorption spectroscopy (1)



• Experimental setup



 Deduce number densities from Beer-Lambert's law (shown in its simplest form)

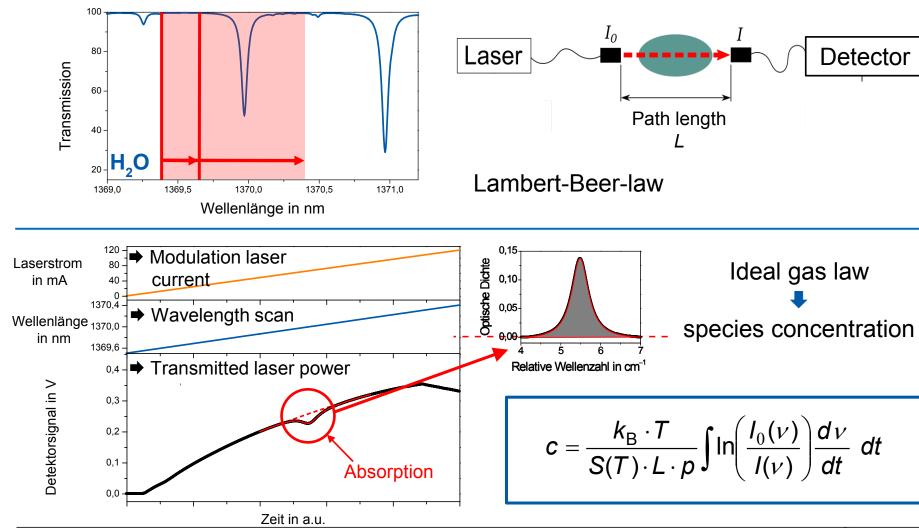
$$(L) = I_0 \exp(-L \cdot N_j \cdot \sigma_{j \leftarrow i}) \Leftrightarrow N_j = \frac{\ln(L)/I_0}{L \cdot \sigma_{j \leftarrow i}}$$

Calibration free (once the path length and absorption cross-section is known) Line-of-sight: no resolution along laser beam path

 \rightarrow restrictions for application in turbulent flames



Tuneable diode laser absorption spectroscopy TDLAS



TECHNISCHE UNIVERSITÄT

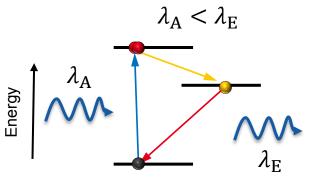
DARMSTADT

Laser Induced fluorescence: Principle

Step 1: Absorption

- Electronic excitation of molecules by laser radiation
- Wavelength λ_A
- Step 2: Spontaneous emission (fluorescence)
- Spectrally red-shifted $\lambda_A < \lambda_E$
- Upper state lifetime few ns
- Measure of local number density
- Linear LIF regime

$$I_{L/A}(x) = N(x)\sigma(x)\sigma(x)I_{lase}(x)\frac{\tau_{tot}}{\tau_{sp}}U\frac{\Omega}{4\pi}\varepsilon\eta$$



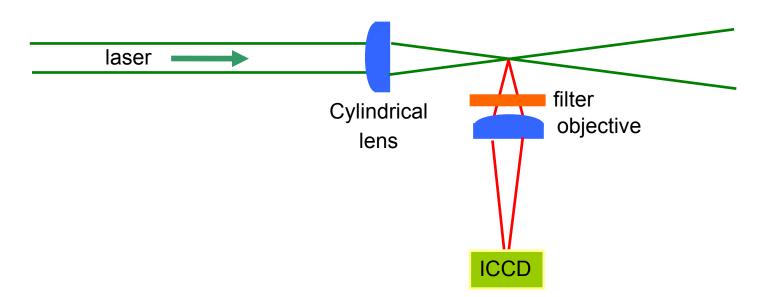




Laser Induced fluorescence: Experimental setup



• Experimental setup





Laser Induced fluorescence: pros and cons

- Good spatial resolution (90° detection angle) $I_{L/A}(x) = N(x)\sigma(x)I_{lase}(x)\frac{\tau_{tot}}{\tau_{sp}}U\frac{Q}{4}$
- Sensitive
- Calibration required to determine $U \frac{\Omega}{4\pi} \varepsilon \eta$
- Total lifetime τ_{tot} needed but often not known!

$$\tau_{tot} = \frac{1}{A + P + Q}$$

- A: Einstein A-coefficient, molecular property, often known
- P: Predissociation rate, molecular property, often known
- *Q* : Quenching rate, depends on gas matrix, pressure, temperature \rightarrow PROBLEM

Total lifetime τ_{tot} makes quantitative LIF challenging!



TECHNISCHE

DARMSTADT

How to make LIF quantitative – options



- 1. Quantification of τ_{tot} : Measure τ_{tot} = fct(T, species), once τ_{tot} (T, species) is known measure LIF simultaneously with T and species (via Raman/Rayleigh)
- 2. Calibration: determine C = C(T) in $I_{LI}(x) = C(T)[N(x)]$ \rightarrow Example CO-LIF in application example flame-wall interaction
- 3. Saturated LIF: does not really work, not detailed here
- 4. Combine 1D-LIF with absorption spectroscopy (see CST 158, 2000, Pixner et al.)

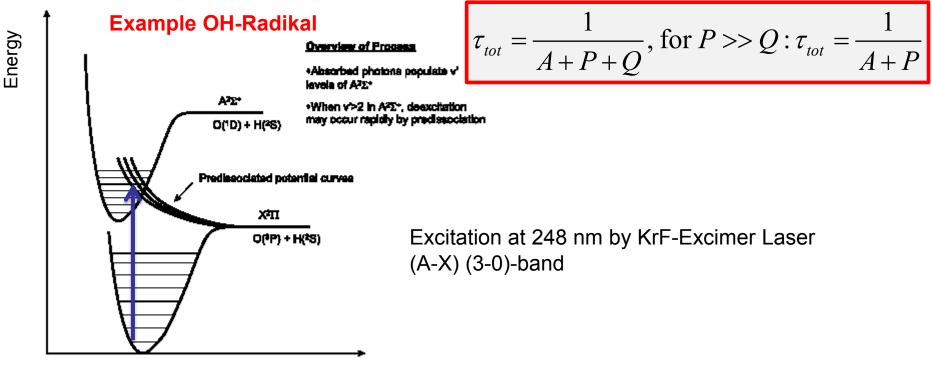
$$N_{1}(x) = -\frac{1}{\sigma} \cdot \frac{(T-1)\frac{dV(x)}{dx}}{(T-1)V(x)+1} \qquad V(x) = \frac{\int_{0}^{x} F(x')dx'}{\int_{0}^{L} F(x')dx'} = \frac{\exp\left(-\sigma\int_{0}^{x} N_{1}(x')dx'\right) - 1}{\exp\left(-\sigma\int_{0}^{L} N_{1}(x')dx'\right) - 1} \\ T = \frac{I(L)}{I(0)} = \exp\left(-\sigma\int_{0}^{L} N_{1}(x')dx'\right)$$



How to make LIF quantitative – options



5. Predissociative LIF: Independent of Q; low SNR, works for few molecules at low pressure



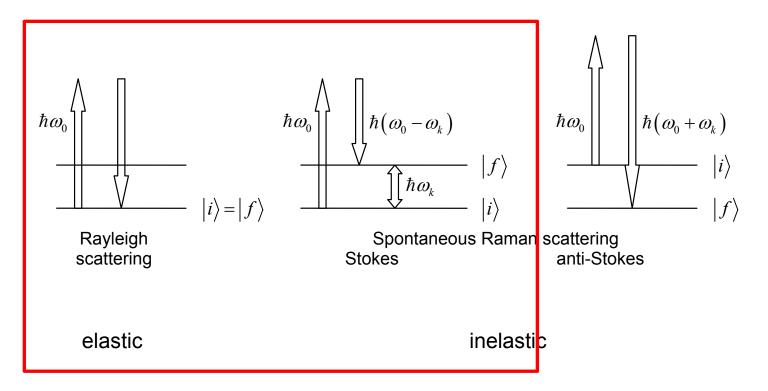
Inter nuclear distance



Raman spectroscopy



• Elastic and inelastic light scattering of photons off molecules

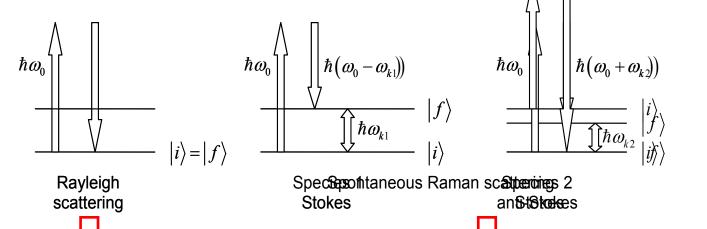




Combined Raman/Rayleigh spectroscopy



 Multi-scalar method: instantaneous measurement of main species (Raman) and temperature (Rayleigh)



- Spectral dispersion and simultaneous meas. of: CO₂, O₂, CO, N₂, CH₄, H₂O, H₂, equivalence ratio (phi), Temp.
 Density/ Temperature
- Challenges:
 - Low Raman scattering cross-sections and single-shot requirement
 - Data evaluation of noisy data
 - 1D application, high spatial resolution

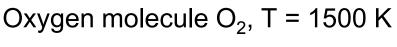


Raman spectroscopy: selection rules and spectra



• Selection rules

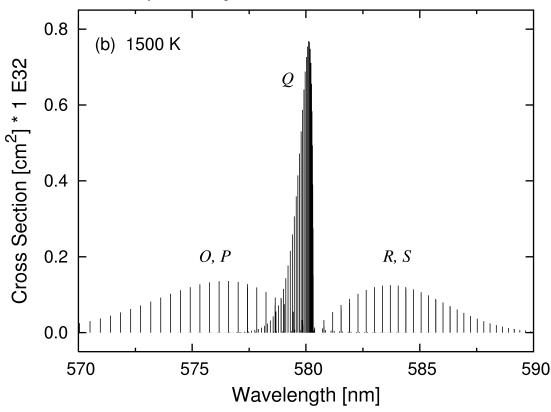
 $\Delta J = 0, \pm 2$ $\Delta J = 0 \rightarrow \text{Q-branch}$ $\Delta J = +2 \rightarrow \text{O-branch}$ $\Delta J = -2 \rightarrow S$ -branch



Simulated "stick spectrum" – infinite resolution

Ro-vibronic Stokes Raman

Exception: very weak R and P-lines



TECHNISCHE Raman spectroscopy: setup UNIVERSITÄT DARMSTADT **Experimental setup** Fixed frequencylaser filter lens objective Low dispersion spectrum +5.0e+4 N₂ experiment 1619 K Т libary CO2 0.036 background libary + bgr O₂ 0.068 CO 0.042 intensity [a.u.] +5.26+4 0.656 N₂ CH₄ 0.025 H₂O 0.129 H₂ 0.045 **Spectrometer** н,0 CH н, Shuttered CCD +0.0e+0 +5.0e+0 +5.0e+3 +0.0e+0 -5.0e+3 -5.0e+3∟ 560 600 640 680 wavelength [nm]

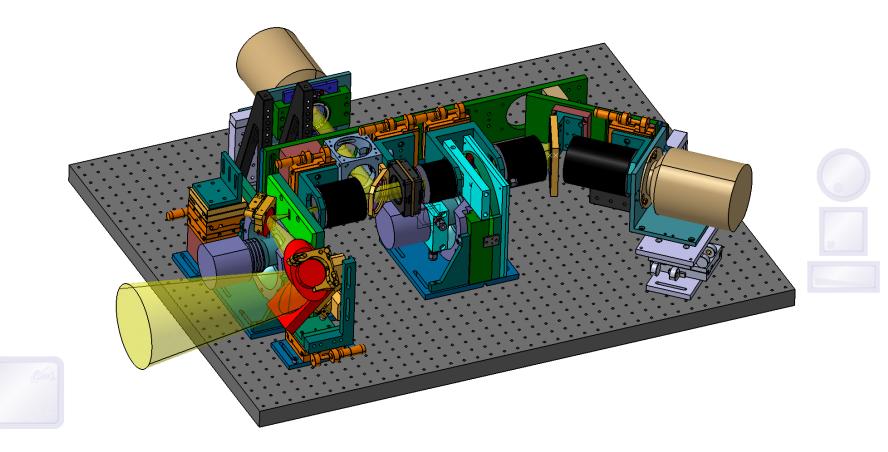


1D Raman/Rayleigh: spectrometer



TECHNISCHE UNIVERSITÄT DARMSTADT

• New TU Darmstadt design

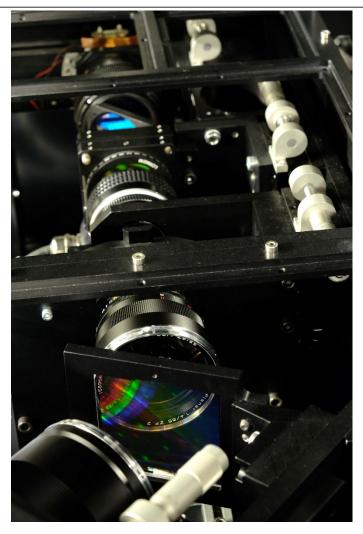




1D Raman/Rayleigh: spectrometer









1D Raman/Rayleigh spectroscopy: iterative post-processing procedure



• Raman (inelastic) scattering \rightarrow concentrations $N_i(r)$

$$S_{ram,i}\left(\vec{r}\right) \propto \sigma_{ram,i}\left(\frac{T(\vec{r})}{I_{Laser}} \quad N_{i}(\vec{r})\right)$$
Rayleigh (elastic) scattering \rightarrow temperature T(r)
$$S_{ray}\left(\vec{r}\right) \propto \sigma_{ray}\left(N_{i}(\vec{r})\right) I_{Laser} \sum N_{i}\left(\vec{r}\right)$$

$$\sigma_{ray} = \sum_{i} \left(\frac{N_{i}(\vec{r})}{\sum_{j} N_{j}(\vec{r})}\right) \sigma_{ray,i} \xrightarrow{\text{Ideal gas law}} T(\vec{r}) \propto \frac{1}{\sum N_{i}(\vec{r})}$$

 Determination of N_i, T by iterative procedure: Need σ_{ram,i} of each species *i*



Different options for data evaluation DARMSTADT Spectral fit experiment 1619 K libary CO2 0.036 background libary + bgr 02 0.068 CO 0.042 N₂ 0.656 intensity [a.u.] CH₄ 0.025 H₂O 0.129 H₂ 0.045 CH +0.0e+. +5.0e+' unnp+0.' -5.0e+3 680 560 600 640 Combining the strength of both wavelength [nm] Matrix inversion (MI) method →The Hybrid MI-method $\vec{S} = \underline{M} \cdot \vec{N}$ $\Rightarrow \overrightarrow{N} = \underline{\underline{M}}^{-1} \cdot \overrightarrow{S}$



TECHNISCHE

UNIVERSITÄT



A Hybrid Method for Data Evaluation in 1D Raman Spectroscopy

F. Fuest¹, R.S. Barlow², D. Geyer³, F. Seffrin¹, A. Dreizler¹

¹ FG Reactive Flows and Diagnostics, Center of Smart Interfaces TU Darmstadt, 64287 Darmstadt, Germany

² Sandia National Laboratories, Livermore, CA 94551-0969, USA

³ Hochschule Darmstadt - University of Applied Sciences, 64295 Darmstadt, Germany

Supported by: Deutsche Forschungsgemeinschaft (SFB 568 B1, EXC 259) and the US Department of Energy, Office of Basic Energy Sciences







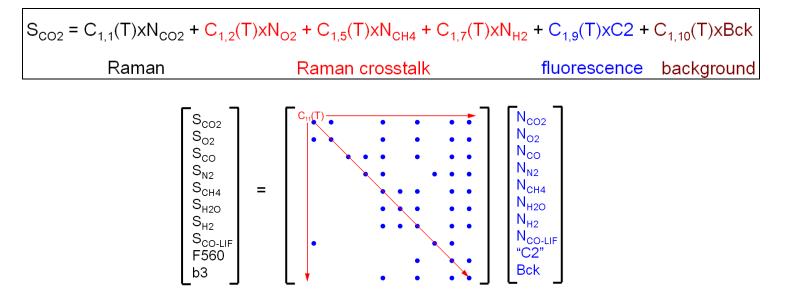


- Spontaneous Raman scattering
 - important technique in combustion research
 - major species, scalar gradients, scalar dissipation
 - need best possible accuracy, precision, and spatial resolution
 - improvements in detection hardware and methods of analysis
- Two approaches to data analysis for hydrocarbon flames; both are complicated
- "Hybrid" method of Raman data analysis
 - combine strengths of methods used by Sandia and TU Darmstadt
 - reduce level of expertise needed to interpret Raman data
- Demonstrate using laminar flame measurements from Sandia system
 - Premixed CH₄/air flat flames
 - Laminar H₂ jet flame (no hc fluorescence interference)





- On-chip binning of Raman bands to reduce camera readout noise
- Matrix equation relating signals and sources



- Extensive calibrations to determine temperature dependence of matrix elements for Raman response and crosstalk (represented as polynomials)
- Solve inverse problem to get species concentrations and temperature
- Iterate on Rayleigh temperature (1K conversion, 3-4 iterations)



Spectral Fitting (TU Darmstadt)



- Individual rovibrational Raman transitions calculated for each species, based on Placzek's theory of polarizability (TUD Ramses code)
- Each Raman transition convolved with experimentally determined apparatus function, then all convolved Raman transitions superposed
 - Rayleigh scattering image \rightarrow apparatus function in this work
 - Raman bands broaden with increasing temperature due to the population of higher quantum states
 - Spectral library composed of temperature-dependent Raman bands
- The spectral library for each molecule is calibrated to an experimental spectrum measured in a gas sample with known mole fraction and temperature.
- Details of fitting procedure (Dirk Geyer thesis)



Pro's and Con's



Matrix Inversion (old version)

- Pro's
 - Lower noise
 - Faster acquisition & processing
- Con's
 - Extensive calibrations required
 - Cannot calibrate accurately at some conditions
 - Spectral information lost
 - Impractical to account for beam steering or spatial dependence of response function

Spectral Fitting

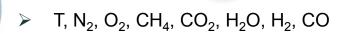
- Pro's
 - Based on quantum mechanical theory
 - One calibration per species
 - Beam steering handle automatically
 - Background corrected more rigorous
- Con's
 - Higher readout noise
 - Slower data acquisition rate
 - Significant time/effort in fitting





Turbulent Combustion Laboratory: Raman/Rayleigh/CO-LIF & Crossed OH PLIF





- 6-mm segment
- Mixture fraction, reaction progress \succ
- 3D flame orientation \triangleright
- 1D, 3D scalar gradients, dissipation





Finite Sandia National Laboratories

LSF 40-60 µm

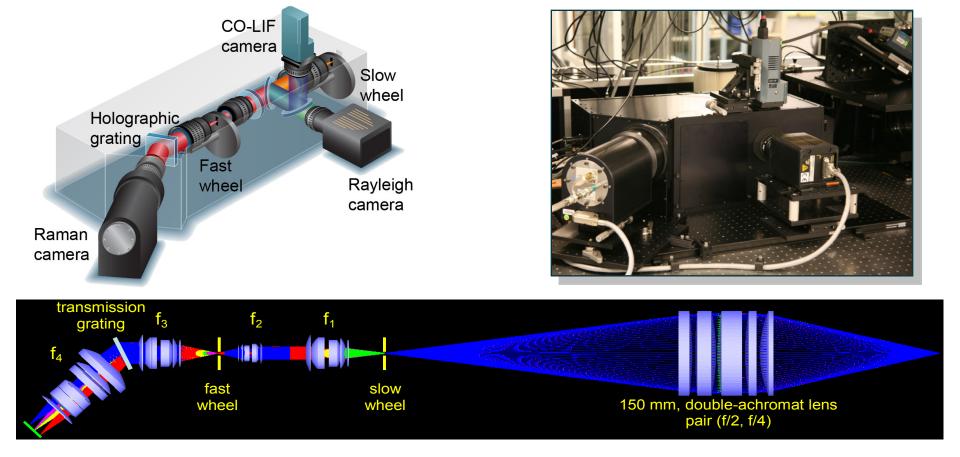
Transmission grating

33rd International Symposium on Combustion, Beijing 2010

Mechanical gate: 3.9 µs gate (FWHM)

103 µm data spacing

Detection System



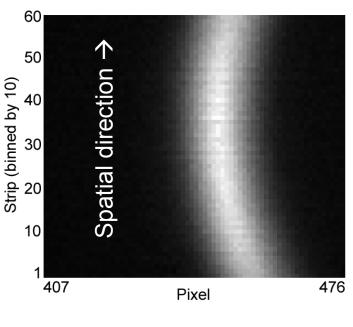
TECHNISCHE UNIVERSITÄT DARMSTADT



CRE

Optical Bowing Effect





Wavelength \rightarrow

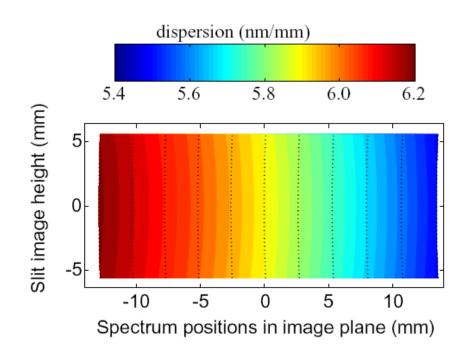
- Image of N₂ Raman scattering in air
- Low f-number spectrograph
 - bowed image of slit
 - Jun Zhao, Appl. Spectr. 57, 11 (2003)
 1368-1375
- Calculated (Zemax) and measured
 - Map CCD for wavelength at each pixel
- Must account for this optical effect



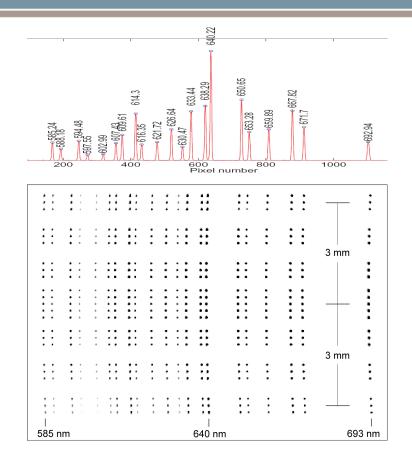
Spectrometer Characteristics







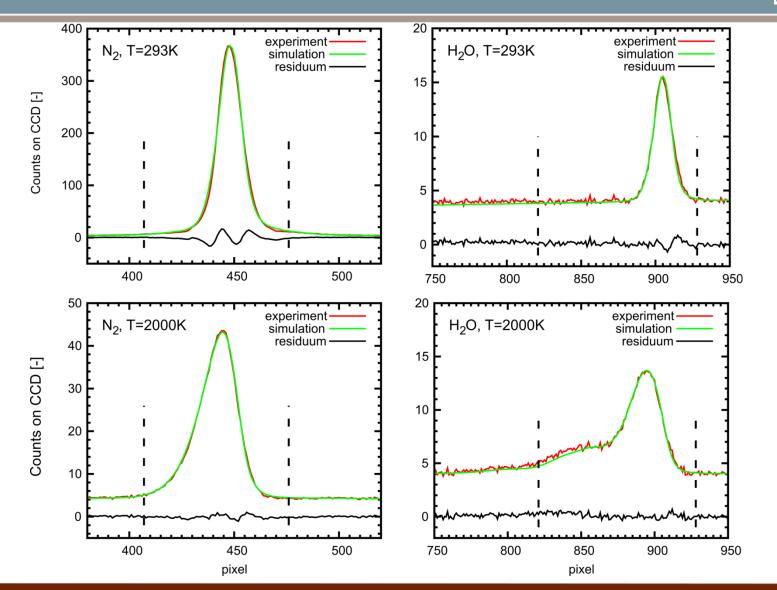
 Calculated (Zemax) dispersion is not linear across the image plane



 Spectral/spatial calibration using neon lamp and target with 50-µm holes on 200-µm centers



Spectral Library vs. Measurement



TECHNISCHE UNIVERSITÄT DARMSTADT

CRE



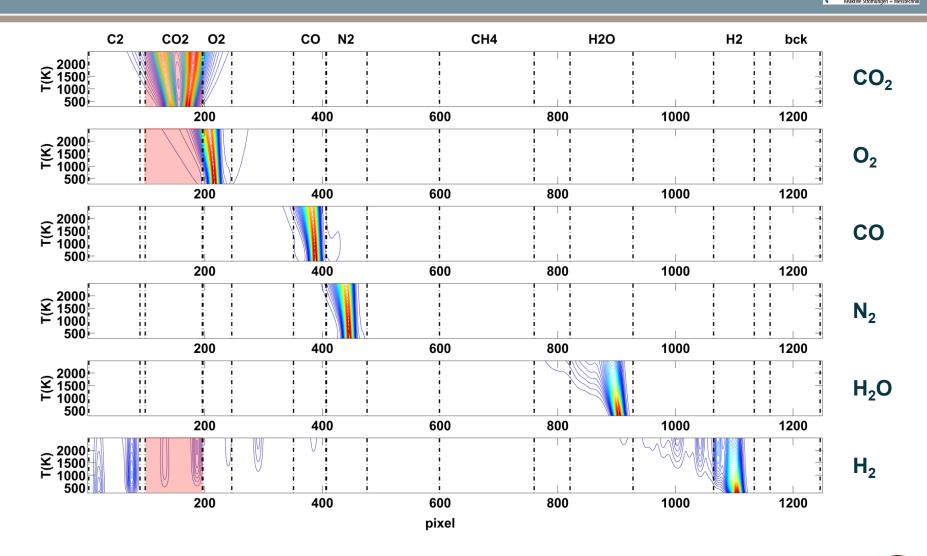


33rd International Symposium on Combustion, Beijing 2010



CRE

Calculated Spectral Libraries (Ramses code)

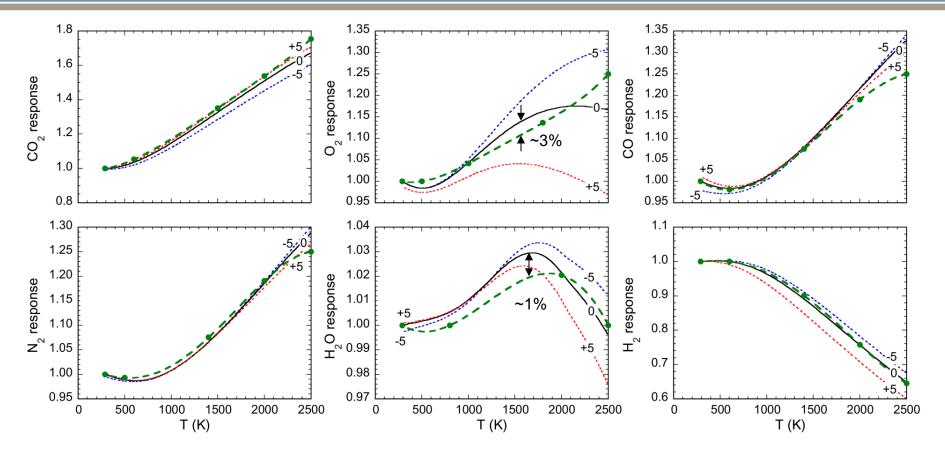




Major Species Response Curves



CRE

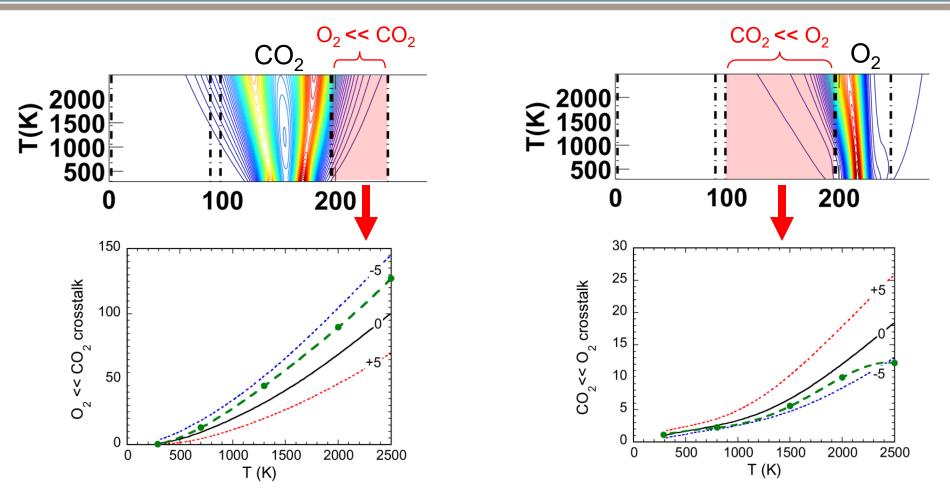


- Good agreement, except for O₂ curve shape at high T
- O₂ response sensitive to bowing effect and beam steering

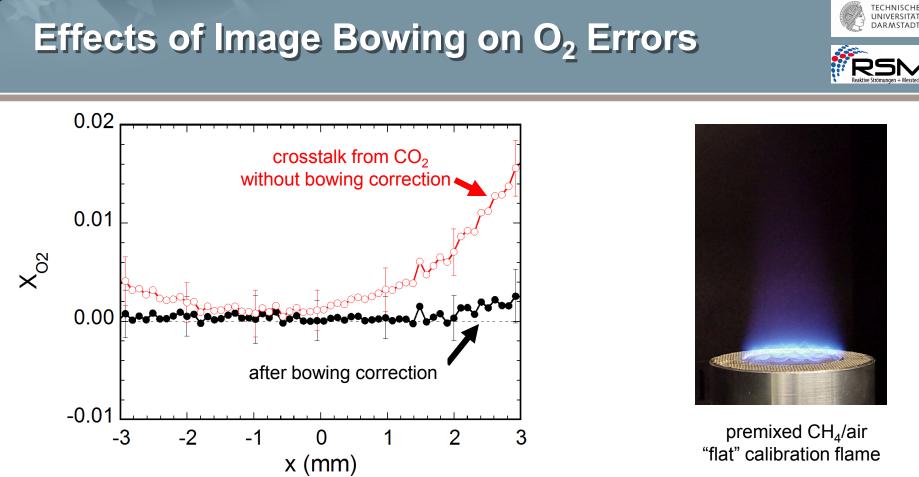
Crosstalk between CO₂ and O₂



CRE



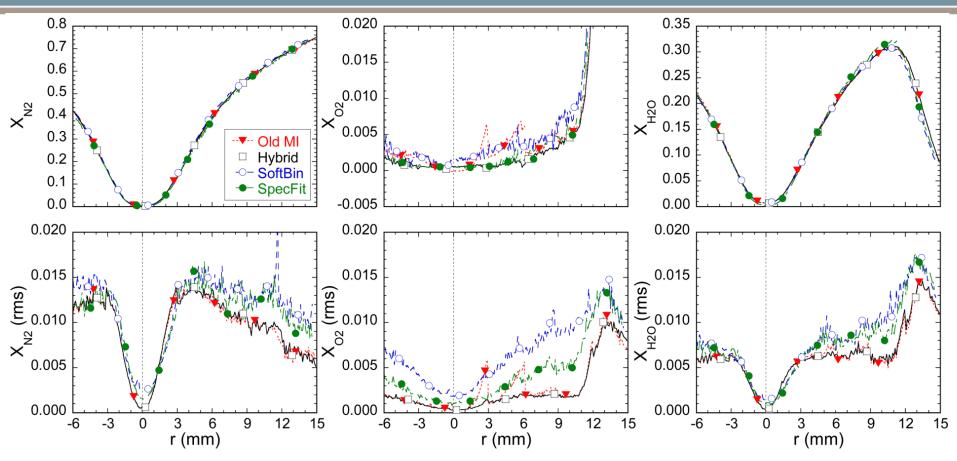
- Greater uncertainty in calibration polynomials
- Sensitive to bowing effect and beam steering



- O_2 mole fraction should be zero in the rich flame products (ϕ =1.3)
- Bowing effect leads to error of $X_{O2} \sim 1.6\%$ due to uncorrected CO_2 crosstalk







JNIVERSITÄT

CRE

- Close agreement on mean values from hybrid-MI and spectral fitting
- Hybrid method yields better precision (on chip binning)
- Spectral fitting yields lower noise than MI with software binning





- Hybrid method of Raman data analysis has been developed
 - Calculated Raman libraries are integrated to determine temperature-dependent terms for matrix inversion
 - Response and cross talk for N_2 , O_2 , H_2 , CO, CO₂, H_2O
- Combines advantages from both previous methods
 - Low noise from on-chip binning
 - Fast data acquisition and processing
 - Temperature dependence based on QM theory
 - Automatic correction for image bowing and beam steering
- Relatively easy to adapt to other Raman/Rayleigh systems





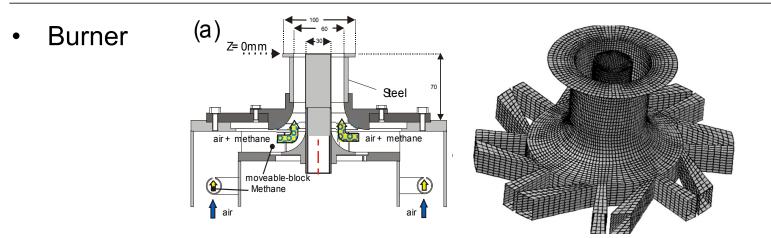
Application example



 Thermo-chemical state in swirling premixed flame: PCI 32 2009, Gregor et al.



Thermo-chemical state in swirling premixed flame



• Operational conditions

		PSF-30	PSF-90	PSF-150
S _{0,th}	[-]	0.75	0.75	0.75
Ρ	[kW]	30	90	150
ϕ	[-]	0.833	0.833	1.0
Re _{tot.}	[-]	10000	29900	42300



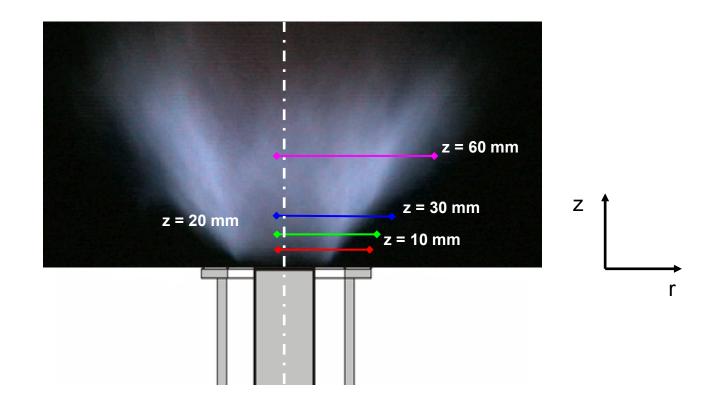
TECHNISCHE UNIVERSITÄT

DARMSTADT

Measurement locations



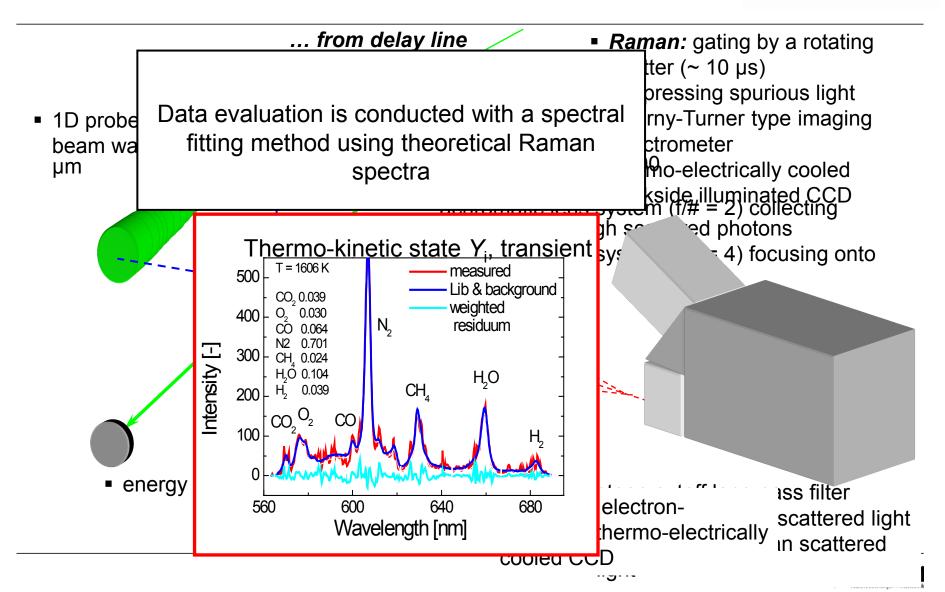
Radial profiles at 4 axial heights





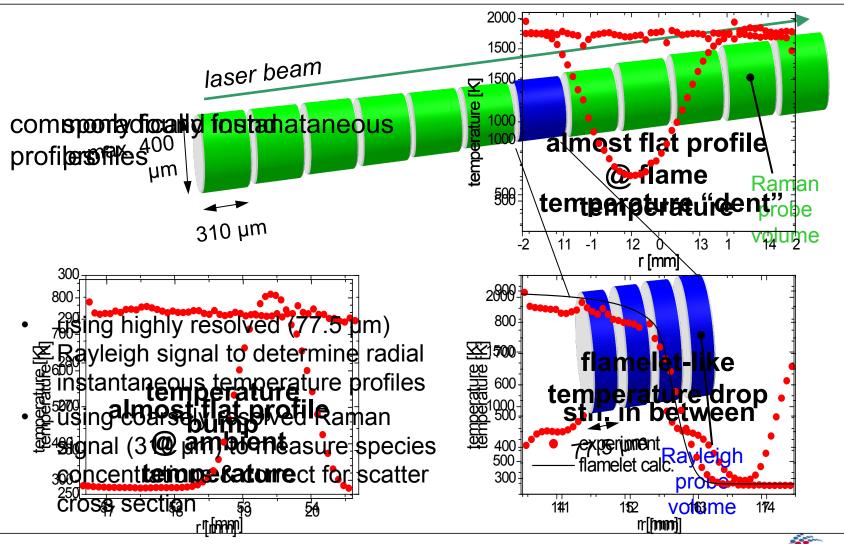
Raman scattering – exp. setup





Raman scattering – spatial resolution

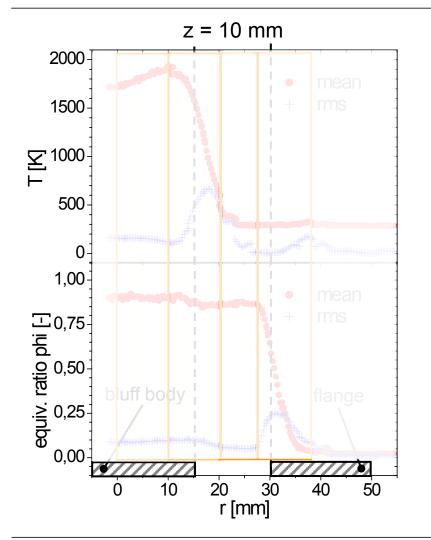






Radial Profiles (mean and rms)



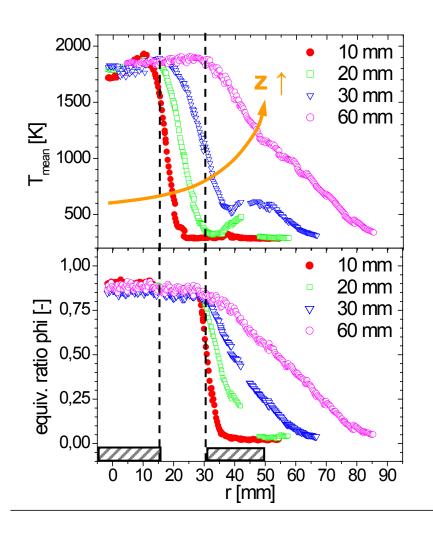


- inner recirculation zone (~0-10mm):
 - fully burnt exhaust
 - heat loss to bluff body
- inner mixing layer (~10-20mm):
 - strong intermittency hence high fluctuation levels
 - r ~ 17 mm: mean premixed flame front position as deduced from max. T & c gradients / max. CO concentration
- centras annular jet (~20-27mm):
 - amost unreacted uel without atto
- outer mixing layer ~27-38mm).
 - is a second sec
 - Econd temperature naximum due to outer



Mean Radial Profiles - z Dependency





- for increasing height z:
- mean flame front position at larger radii
- wider flame brush & broader mixing layer hence flatter radial T & phi profiles
- distinct 2nd T maximum (up to z = 30mm) due to outer recirculation of exhaust
- premixed flame front is located in regions with very low stratification of nearly constant phi (up to z = 30mm)





Single Shot Correlations - Scatter Plots

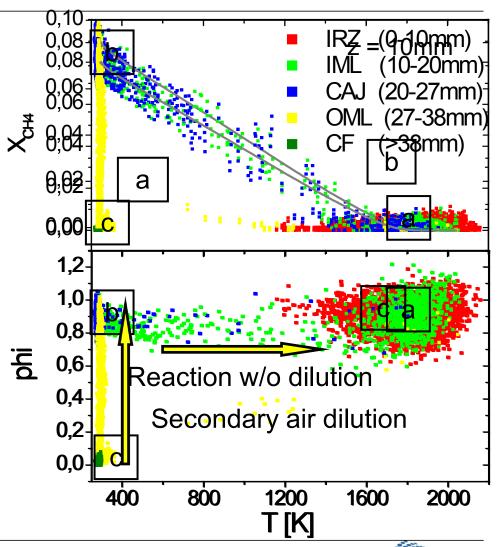
■ Sample S For dor an a signed to the series of the serie

- inner recirculation zone (0-10mm):
 each scatter corresponds to one fully burnt samples @ max T, no single shot secondary air
- samples spanned between 3 thermorking layer & central annular thermorking ticnstates:

 - b) People Canden Maifuel
 - c) Cold Secondary (27 38 mm): mostly unburnt fuel and / or secondary air

rarely mixing between burnt samples and secondary air

coflow / flange (>38 mm):
 exclusively ambient air





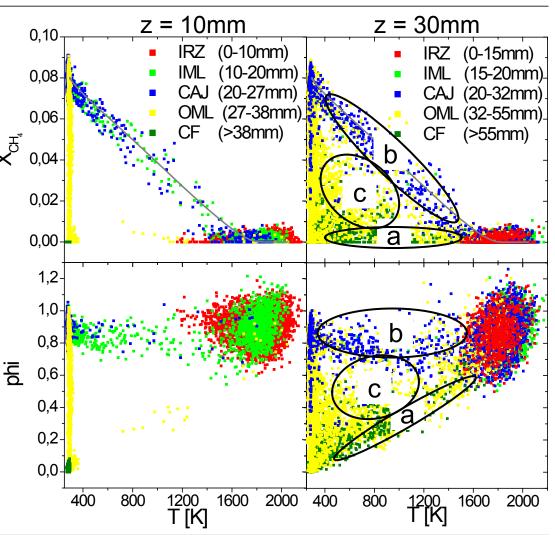
Scatter Plots - z Dependency



- at z = 30 mm:
- significantly increased probability to measure intermediate samples due to:
 - a) secondary air entrainment > into burnt exhaust (OML, CF)
 - b) mixing between burnt / unburnt fuel (CAJ) and reaction without dilution
 - c) mixing of air with reacted AND unreacted fuel

or

 slowed or extinguished reactions (CAJ, OML, CF)





Conclusions Raman/Rayleigh scattering in swirling premixed flame



- Temperature is key-quantity (reaction progress)
- Thermo-kinetic state precisely measured
- Thermo-kinetic state is a prerequisite for understanding pollutant formation and finite rate chemistry effects
- Main findings are
 - In region of flame stabilization (z < 30 mm) premixed flame front is not located in areas of stratification but in areas of almost constant phi
 - typical reaction and / or mixing behavior can be assigned to different flame regions
 - intermediate reaction states are promoted by dilution with air
 - distinction between pure mixing and local flame quenching needs additional diagnostics monitoring intermediate species

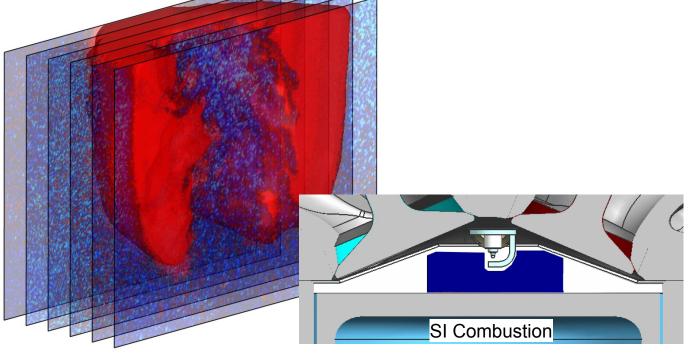


Chapter 8: High-speed Laser Combustion Diagnostics – General Aspects

TU Darmstadt, Germany Mechanical Engineering – Reactive Flows and Diagnostics







Photron.com





Contents



- Why high-speed laser diagnostics?
- Instrumentation
 - High-speed lasers
 - High-speed cameras



State-of-the-art laser combustion diagnostics

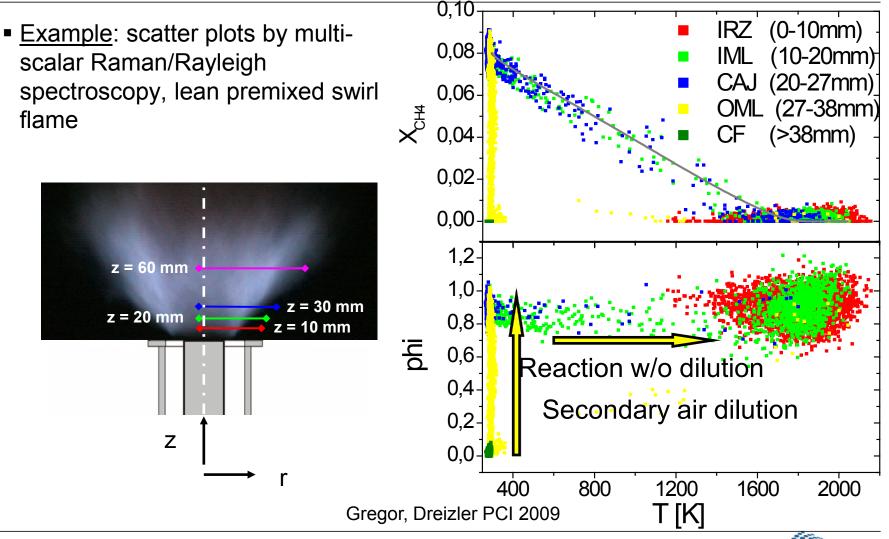


- Flow and multi-scalar measurements
 - Low sampling rates (<100 Hz)
 - High precision and accuracy
 - Good for measuring statistical moments (single-point, two-point statistics)
 - Example: scatter plots by multi-scalar Raman/Rayleigh spectroscopy



State-of-the-art laser combustion diagnostics



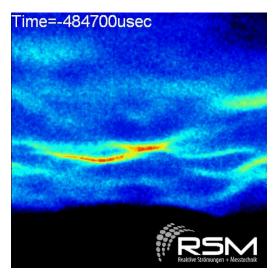




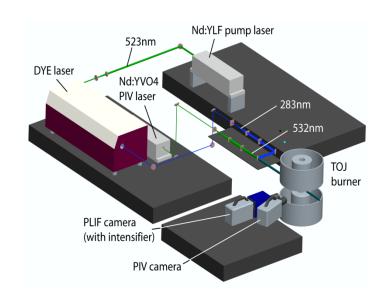
Motivation for high speed diagnostics



- Example flame extinction (w/o subsequent re-ignition)
 - Here turbulent opposed jet flows, partially premixed flame
 - Bulk flow rates close to global extinction



Böhm, Dreizler PCI 2009

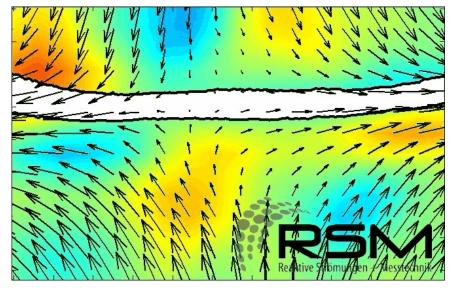


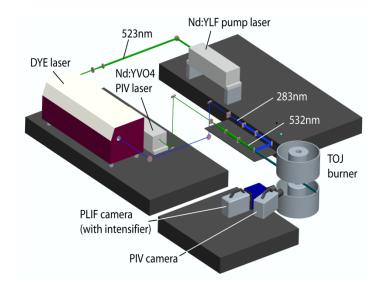


Motivation for high speed diagnostics



- Example flame extinction (w/o subsequent re-ignition)
 - Here turbulent opposed jet flows, partially premixed flame
 - Bulk flow rates close to global extinction





Böhm, Dreizler PCI 2009

→ Tracking extinction needs high sampling rates, post eventtriggering and sequence lengths over 10 – 100ms



Individual extinction events

-6

0

-4 -2

0

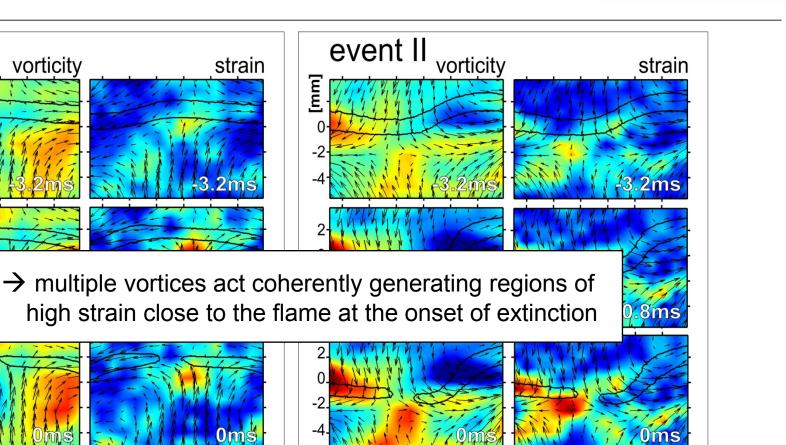
1500

2

[mm]

strain[1/s]





-2

0

-4

-1500

0

1500

2 4

ω[1/s]

-6

0

-2

0

1500

2

-4



[mm]

strain[1/s]

-4 -2

0

-6

-1500

0

1500

2 4

ω[1/s]

event I

[mm]

Conditional averages

- → Maximum of axial strain surrounded by maxima of radial strain
- → Imposed strain requires time to cause extinction
- \rightarrow Time history is important

-0.4ms

2

800

[1/s]

MP1

0

→ Diffusion requires time to reduce scalar gradients

-2

0

2d strain

2

800

[1/s]

-2

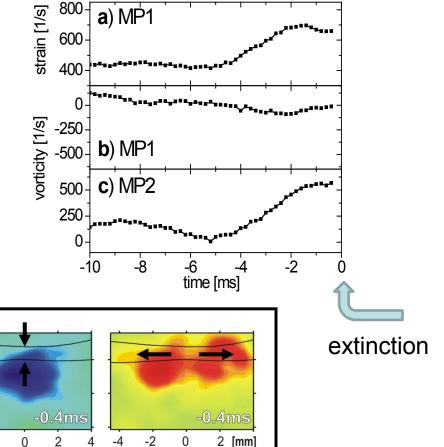
axial strain

-1200

[1/s]

0

0



[1/s]

1200

radial strain



TECHNISCHE

UNIVERSITÄT DARMSTADT

-800

[mm]

0

-2-

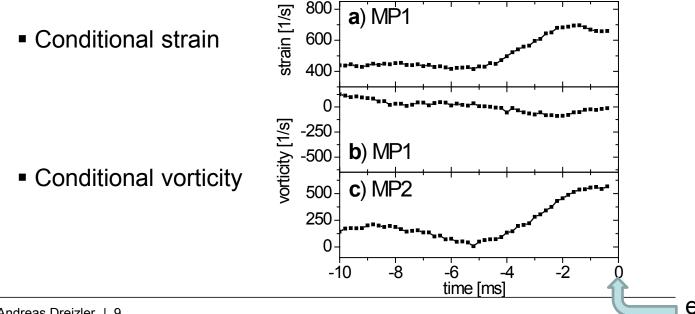
MP2

-2

Multi-parameter diagnostics at high speed



- Simultaneous measurement of velocity fields and qualitative scalar fields that mark features of flames (such as flame fronts) allows determination of conditional velocities:
 - Switch from lab-coordinates to flame-fixed coordinates
 - De-convolute effects from intermittency
 - Better observation of interaction between flow and scalar fields





Transient phenomena in combustion research



- Phenomena requiring high speed diagnostics for better understanding
 - Extinction and re-ignition
 - Flame stabilization of lifted flames and flame propagation
 - Flashback in nozzles
 - Auto- and spark-ignition
 - Cycle-to-cycle variations in IC engines
 - 4D-imaging
- What repetition rate is needed?

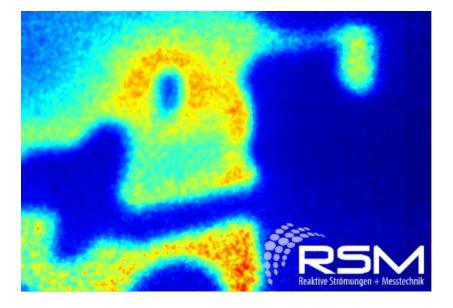


Typical time scales – lab-scale turbulent premixed flame

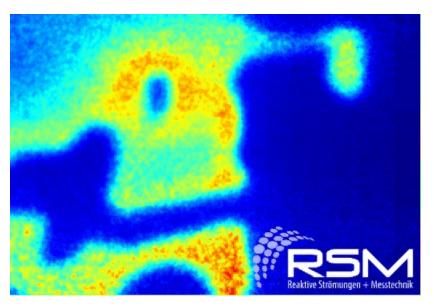


• $T_{int} \sim 1.0 ms \rightarrow Sampling rate (0.1 x T_{int}) \sim 100 \mu s \rightarrow 10 kHz$

OH PLIF @ 5 kHz



@ 10 kHz



sequence runs "smoothly"

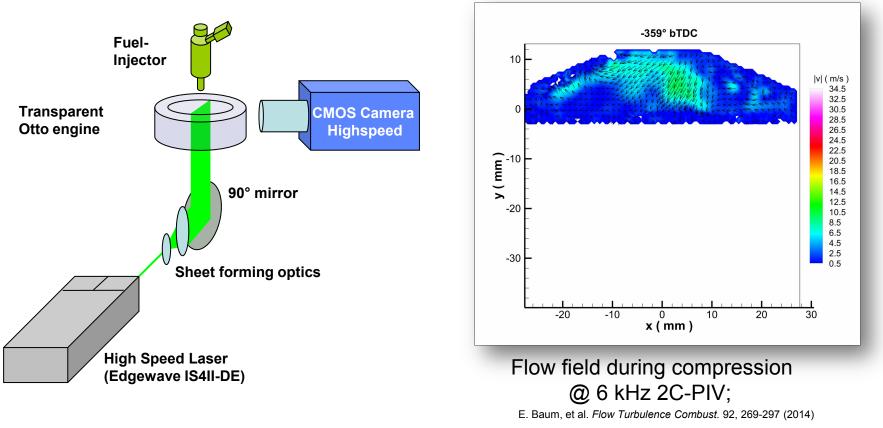


sequence "judders"

Typical time scales – IC engine



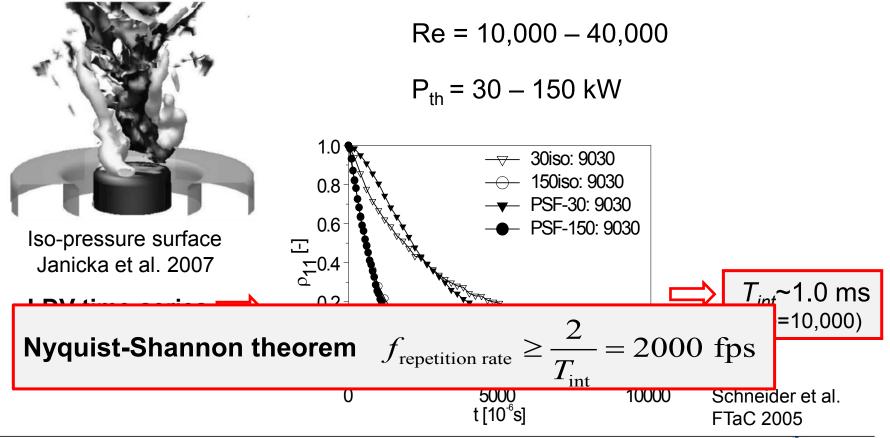
• IC engine operating at 1000 rpm \rightarrow resolving 1 °CA corresponds to 166 $\mu s \rightarrow 6 \ kHz$





Statistically correlated measurements: Scales to be resolved – integral time scale (T_{int})

- TECHNISCHE UNIVERSITÄT DARMSTADT
- Swirling annular flow: non-reacting and premixed flame (lab scale)





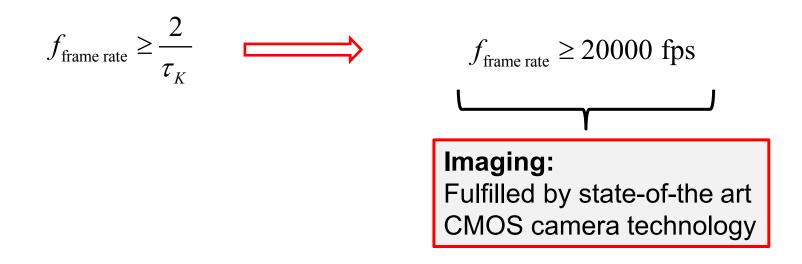


• Kolmogorov time scale τ_{K} (integral length scale L_{int} from 2-point correlations)

$$\tau_{K} = \left(\frac{\nu}{\varepsilon}\right)^{0.5}; \quad \varepsilon = \frac{k^{1.5}}{L_{\text{int}}} \quad \begin{array}{c} \text{Example} \\ \text{Swirl flame} \\ \text{Re} = 40,000/10,000 \end{array}$$

 τ_{K} ~ 100 µs (representative estimate)

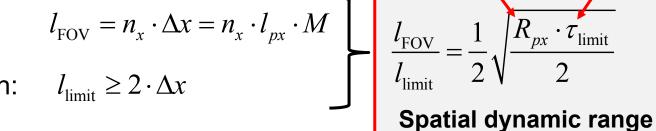
• Nyquist-Shannon theorem





Interdependency of time and length scales Field of View: $l_{FOV} = n_x \cdot \Delta x = n_x \cdot l_{px} \cdot M$ $l_{FOV} = 1$ $R_{px} \cdot \tau_{limit}$

• Nyquist-Shannon:



Spatial and temporal resolution are interconnected via the maximum pixel rate R_{px} (read-out-rate of CMOS)

Measurement volume

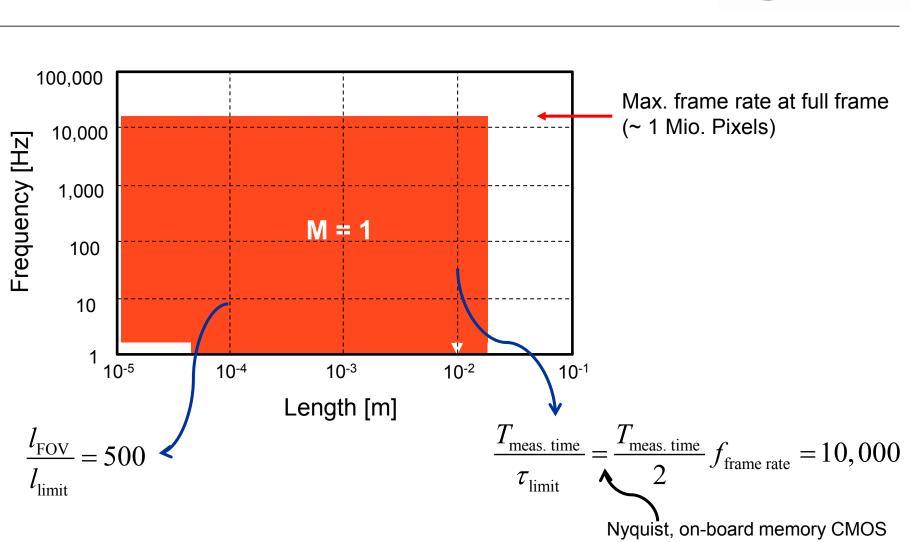
Pixel array



Interdependency of time and length scales







Dynamic ranges – spatial and temporal



TECHNISCHE

UNIVERSITÄT DARMSTADT



Application high speed diagnostics – examples



- Field of application
 - Experiments where only few realizations or short measurement periods are available (shock tubes, IC engines, ...)
 - Transients in combustion
 - ignition, extinction
 - blow off, flashback
 - flame propagation, cyclic variations ... _
- Instrumentation specific to spectral range and diagnostic method
 - Towards 4D imaging (3D in space + time) → new high speed lasers and CMOS cameras

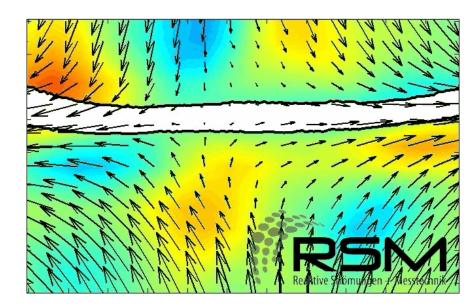
- (conditional) statistics



Ex2: High speed imaging



- Rapid progress of laser and camera technology over the last 6-8 years
- Recent reviews on high speed imaging
 - Böhm et al. (FTaC 2011)
 - Thurow et al. (MST 2013)
 - Sick (PCI 2013)
- Requirements
 - High power lasers
 - High frame rate cameras

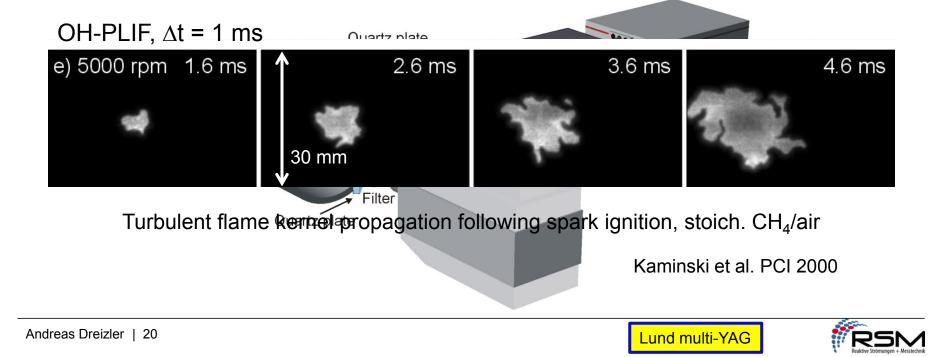


Extinction in turbulent opposed jet flame B. Böhm et al. PCI 2009



Burst lasers for high speed imaging

- Low duty cycle, high pulse energies
 - Aldén group (Lund)
 - Cluster of 4 Nd:YAG lasers, frequency doubled
 - 4 8 pulses/burst, <500mJ/pulse</p>
 - Use of harmonics directly or for pumping a dye laser/dye laser cluster

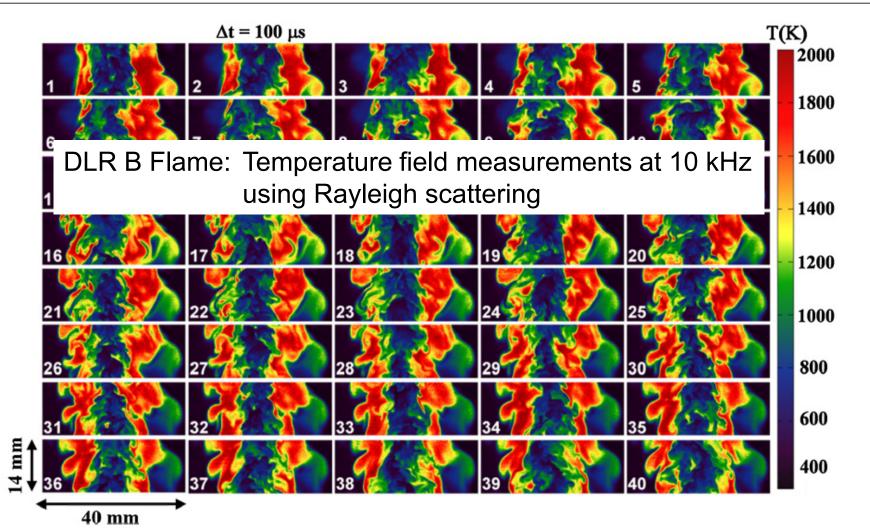






Burst lasers for high speed imaging





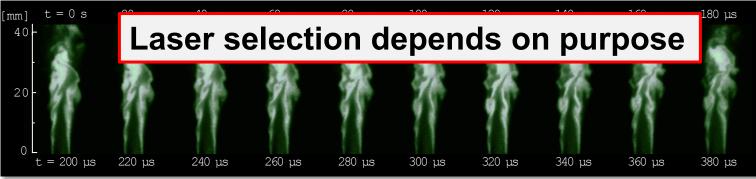


Continuously pulsed high speed lasers



- High duty cycle, low pulse energies
 - Long pulse-lasers: $\Delta t_{laser} > 100$ ns \rightarrow intra-cavity conversion for VIS, UV generation
 - Short pulse-lasers: ${\Delta t}_{\text{laser}}$ < 20ns \rightarrow extra-cavity conversion for VIS, UV generation
 - Suitable to pump dye lasers
 - Most recent specifications:
 - 50 kHz, 200 W pump power @ 532 nm \rightarrow 7 W @ 283nm (2-step SHG)
 - S. Hammack, C. Carter, C. Wünsche, T. Lee: Appl. Optics (2014)

plasma-torch stabilized CH₄/air flame



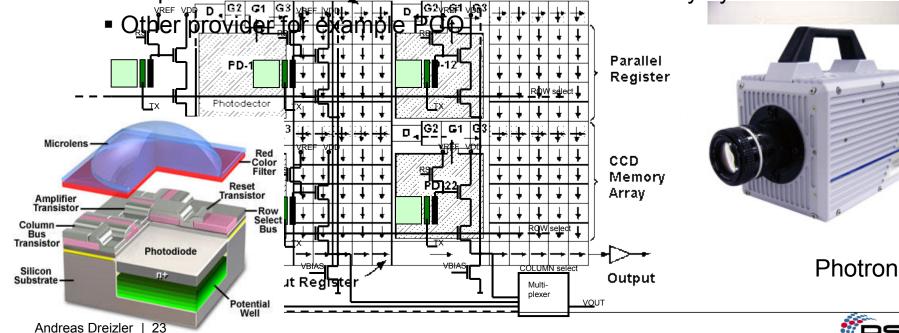


Instrumentation – cameras





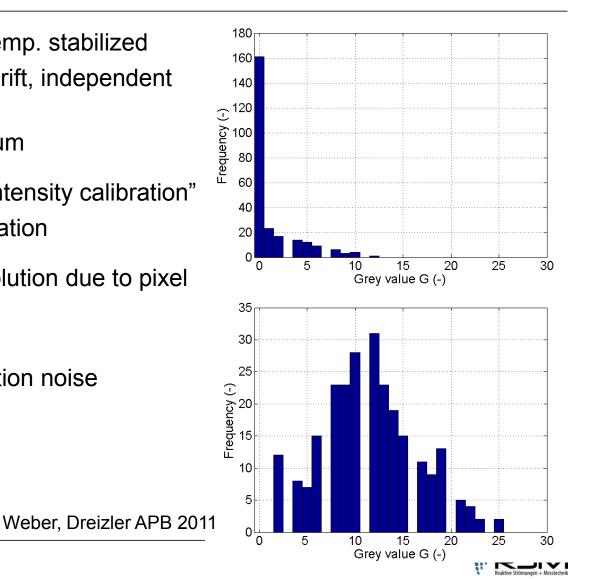
- High speed cameras
 - Multi-frame CCD's cameras
 - € El Cesn chementis ceton Scientific Instruments PSI 4
 - Example 28Pinantes, 3/2/5/H2, 80x160 pixels, 14 bit)
 - (1280 x 800@ 25,000 fps, 128 x 16 pixels @ 1,000,000 fps)
 - Sequences consist of thousands of frames limited only by onboard memory





CMOS – basic sensor checks

- High speed CMOS not yet temp. stabilized
 - → Significant temperature drift, independent on illumination
 - \rightarrow Wait for thermal equilibrium
- Truncated dark noise with "intensity calibration"
 → Switch off intensity calibration
- Vacancies in grey value resolution due to pixel gain
 - \rightarrow Reduces dynamic range
 - \rightarrow Introduces larger digitization noise





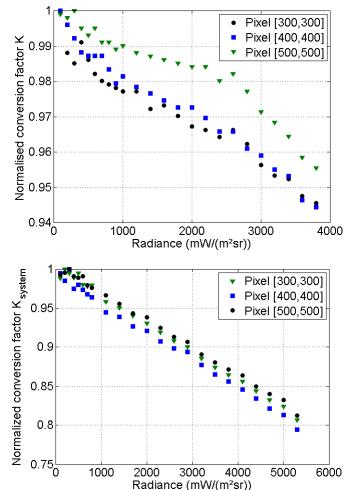
CMOS – Non-linearity

- Checking camera response (pixelwise)
 → Homogenous calibrated light source (Ulbricht sphere)
- Model for pixel response as

 $G_i = G_{0,i} + K_{i,N_{e,i}} N_{e,i}$

- \rightarrow Inherent non-linear response
- \rightarrow Deviations from linearity < 6%
- Inclusion of image 2-stage-intensifier (MCP + booster)

 \rightarrow Significantly increased non-linearity



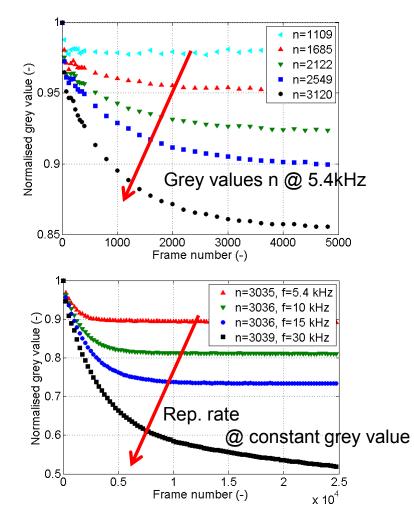




CMOS – image intensifier signal depletion



- Intensified systems suffer from signal depletion
- Full sensor illumination: Depletion increases with signal intensity (grey value n) and repetition rate
- → Without correction: device is unable to reproduce a constant signal within the first few 2000 frames
- Dependent on
 - Signal intensity
 - Frame rate
 - Exposure time
 - Illuminated area
 - \rightarrow In-situ calibration required





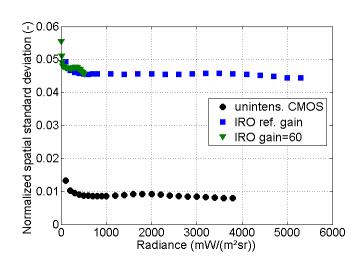
CMOS – quantitative measurements

Unintensified CMOS camera (preferred)

- Resolve dark signal (disable IC)
- (Pixelwise) correction of nonlinearity

Intensified CMOS

- Pixelwise correction of nonlinearity
- Signal depletion. No best practice advice available
- \rightarrow Solution: monitor depletion with spot of known illumination?
- "Halos" (steep intensity gradients cause cross-talk to neighboring pixels)?
- \rightarrow Each CMOS camera/ intensifier has unique characteristics
- \rightarrow Need for common calibration procedure
- \rightarrow EMVA 3.0 not suitable for our needs

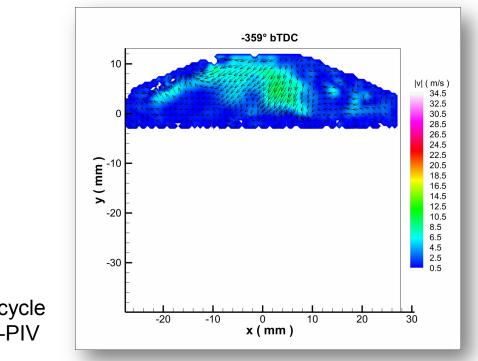






Chapter 8: Towards 4D-imaging

TU Darmstadt, Germany Mechanical Engineering – Reactive Flows and Diagnostics



A. Dreizler

Flow field of full IC engine cycle @ 6 kHz 2C-PIV





Contents



- Motivation for 4D-imaging
- Scanners
- Fixed multiple sheets
- Tomographic LIF



Motivation for 4D-imaging

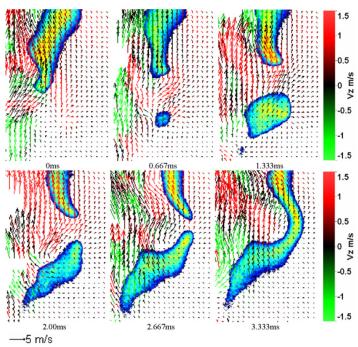


- Turbulent flame are 3D in space and time-dependent
 → 4D diagnostics is a "natural" aim
- Interpretation of 2D-data often ambiguous
- 2D-plane not necessarily representative for observations

Lifted jet flame investigated by planar diagnostics:

Isolated flame islands or connected flame??

PCI 32, 2009, Gordon et al.

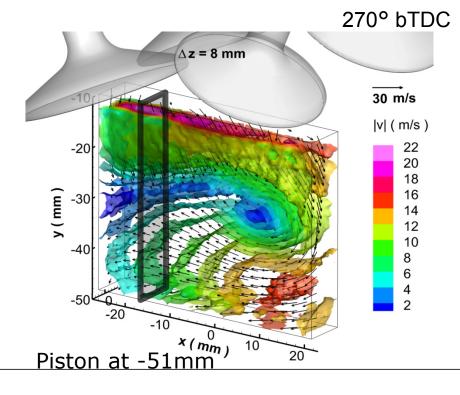




Towards 4D-diagnostics – previous work



- Flow field (3D-3C) not discussed here
 - Tomo PIV: volumetric reconstruction of seeding particles (Elsinga, Scarano et al.)
 - Holographic PIV: holographic reconstruction of time-dependent particle positions
 - Shake-the-box: DLR/LaVision-cinematographic volumetric particle tracking



Tomo PIV in IC engine PCI34, 2013, Baum et al.

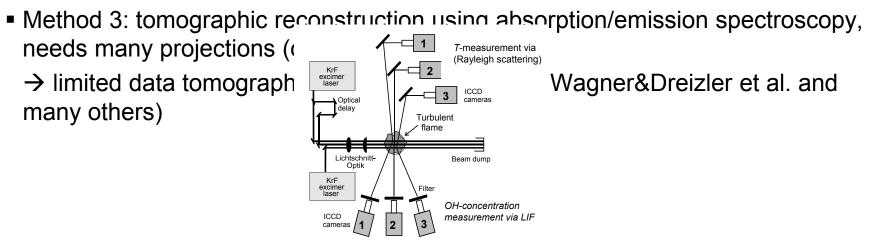


Towards 4D-diagnostics – previous work



Scalar field

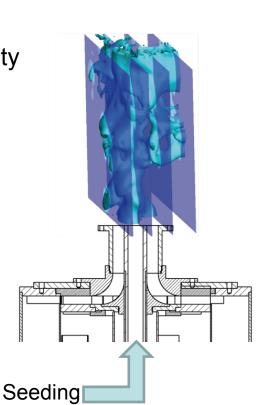
- Challenge: Continuous spatial distribution instead of disperse particle locations in particle-based velocimetry
- Method 1: crossed PLIF sheets \rightarrow 3D information along a line (Barlow et al.)
- Method 2: quasi-3D by parallel PLIF sheets
 - Scanning of a pulse sequence (Hanson et al., Long et al., Alden et al., Dreizler et al.)
 - Use of different lasers w/o scanning (Wolfrum et al., Dreizler et al.)





Quasi-4D-diagnostics – flow visualization

- Mie-Scattering Experiments with modified swirl burner
 - Bluff-body replaced by seeding tube
 - \rightarrow Central jet surrounded by swirled unseeded coflow
 - Isothermal flow
 - Parameters varied: Swirl No., Re No., seeding density
- Sweeping of light sheet by Galvo scan mirror
 - Scan Rate up to 2.5 kHz \rightarrow suitable for low Re-No.
 - Scanning volume approx. 50x50x50 mm (max)





TECHNISCHF

DARMSTADT

Experimental setup



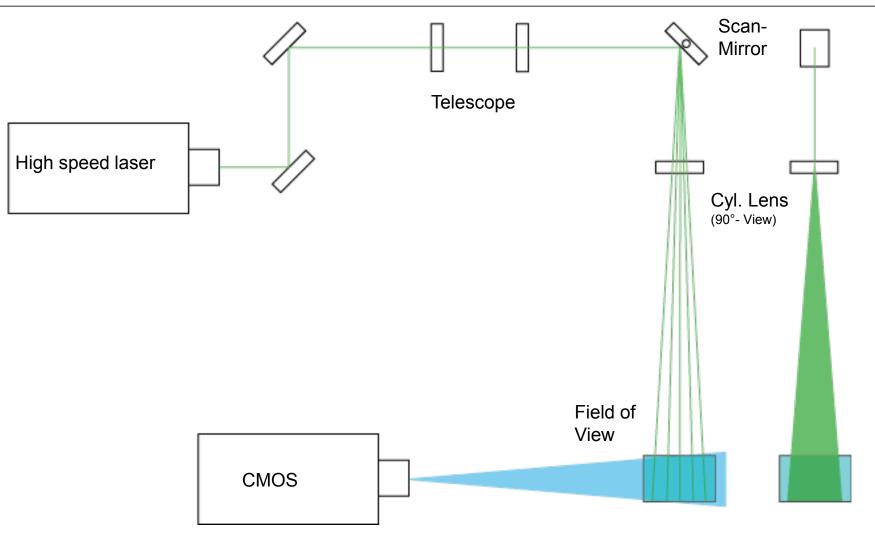
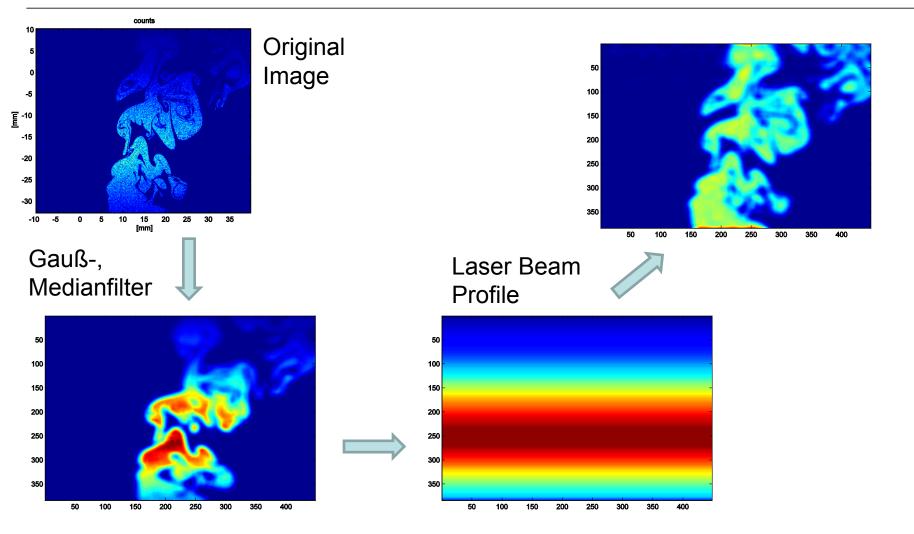




Image post-processing







Results for low Reynolds numbers

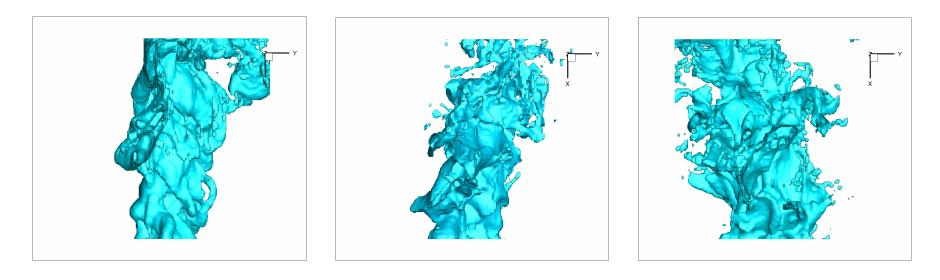


Low speed scanning: 250 Hz Laser repetition rate: 30 kHz \rightarrow 60 planes/"instant (2ms)"

 Field of view ~ 50x50x50mm

 Jet: 3800 l/h
 Re ~ 1000

 Annulus: 800 l/h
 Re ~ 800



0% Swirl (S_{geo} = 0) 50% Swirl (S_{geo} ≈ 1) 100% Swirl (S_{geo} ≈ 2)

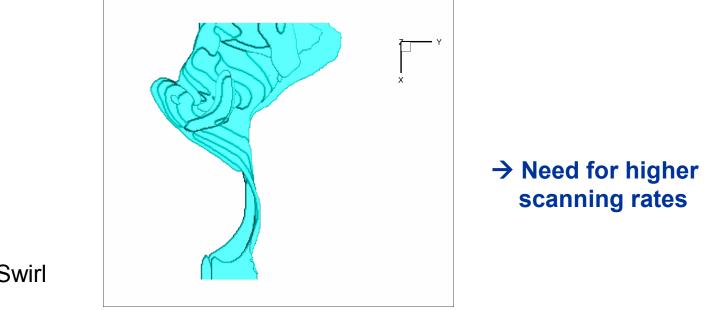
Increasing swirl breaks up core flow faster



Results for intermediate Reynolds numbers



High speed scanning: 2500Hz Laser repetition rate: 60 kHz \rightarrow 12 planes/"instant (0.2ms)" Field of view ~ 40x40x20mmJet: 17000 l/hRe ~ 4700Annulus: 1700 l/hRe ~ 1700



0% Swirl

Spatial resolution too low due to "low" repetition rate Better reconstruction algorithms required

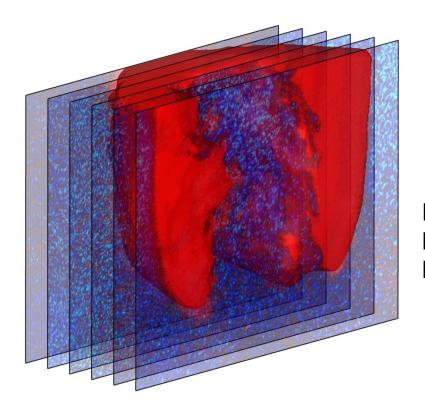


Laser Scanning Multiplane Flamefront Imaging

Master Thesis Max Greifenstein







For more details see: M. Greifenstein et al. MST 26 (2015)105201

Polygon-Scanning: achieving higher scan rates



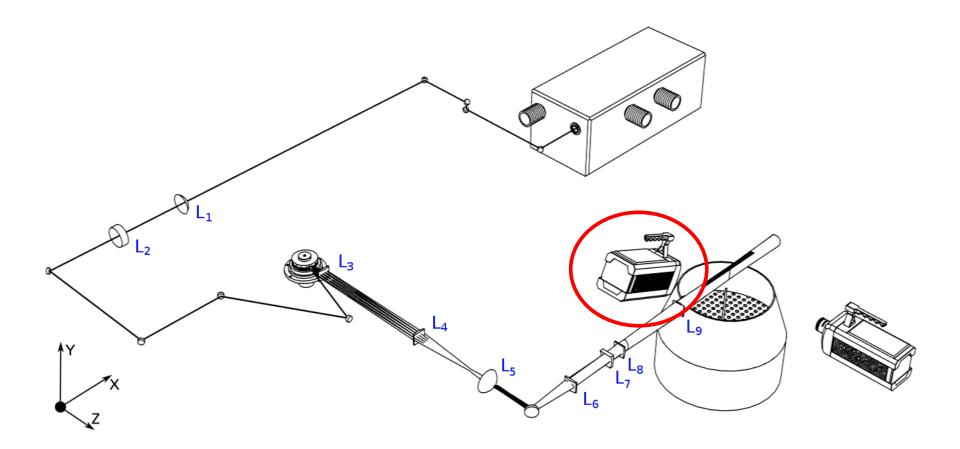






Measuring the Spatial Jitter

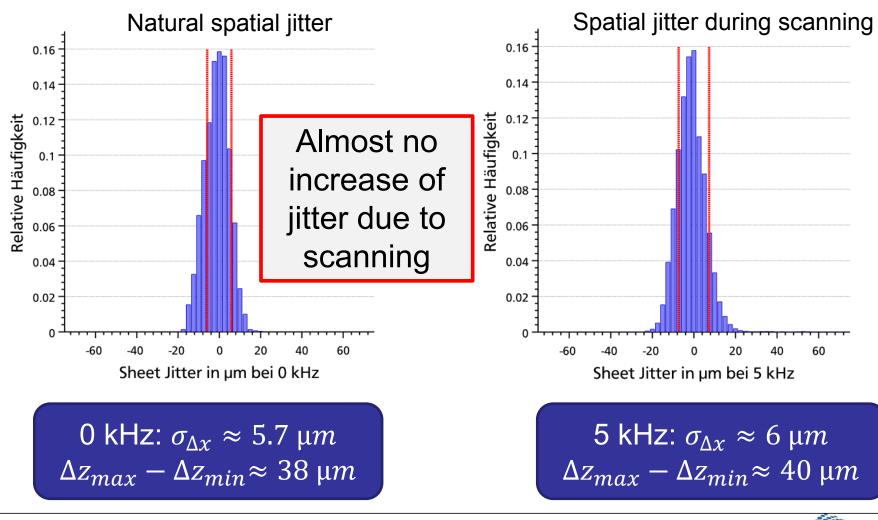






Spatial Jitter, air atmosphere limits speed to 5 kHz



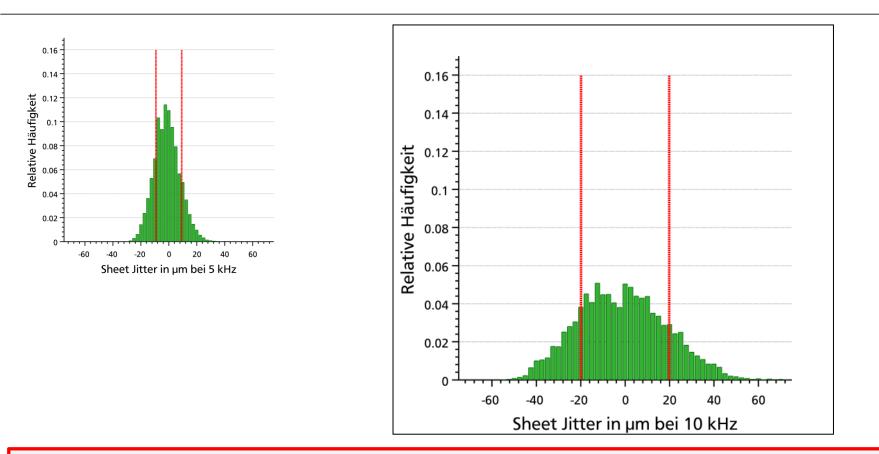


Andreas Dreizler | 17



Higher scan rates needs helium atmosphere → reduce frictional losses





→ At 10 kHz increased jitter to $\sigma_{\Delta x} \approx 20 \ \mu m$ For optimal performance control parameters need to be adjusted for scan speed



Demonstrating the performance **Target**



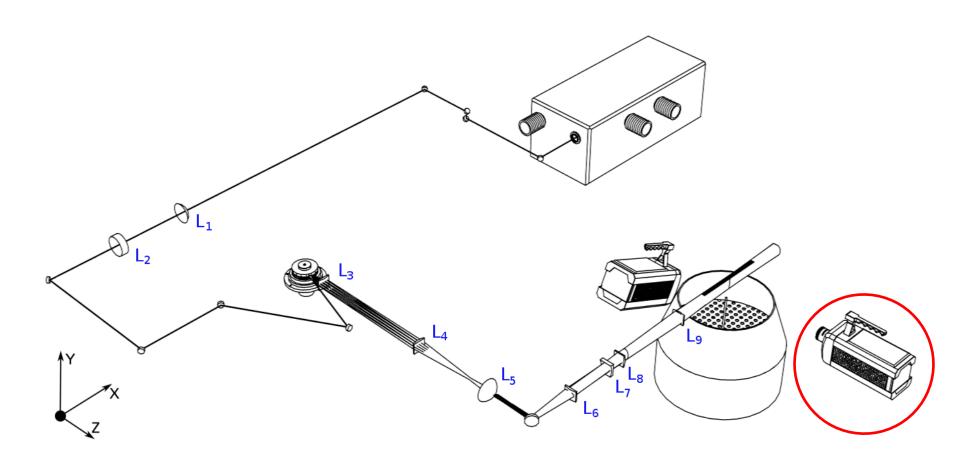
- Explore limits of polygon scanning
- Measurements at 2, 5 and 10 kHz scan frequency
- Laser repetition rate (@532 nm): 50 kHz

→ Time-resolved volumetric reconstruction of a turbulent flame front by using Mie scattering off µm-sized particles



Demonstrating the performance **Beam path**



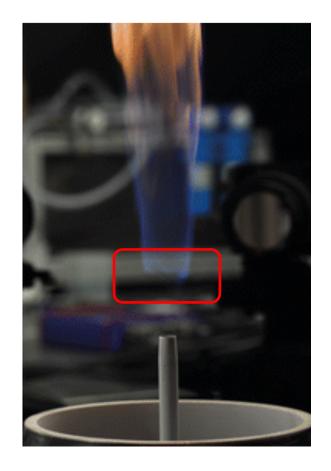




Demonstrating the performance Lifted turbulent flame

- Lifted jet-flame
- Methane-jet: Re = 5000
- Co-Flow air: Re = 1625
- Seeding: variation used for flame front tracking
 - 1 µm-sized oil droplets
 - Al₂O₃ solid seeding



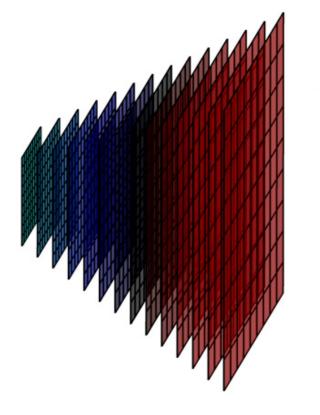




Demosntrsting the performance Calibration

- Type 058-5
 - Point-to-point distance: 5 mm
- Each plane calibrated by traversing

\rightarrow account for different magnification







Demonstrating the performance **2D flame front detection**

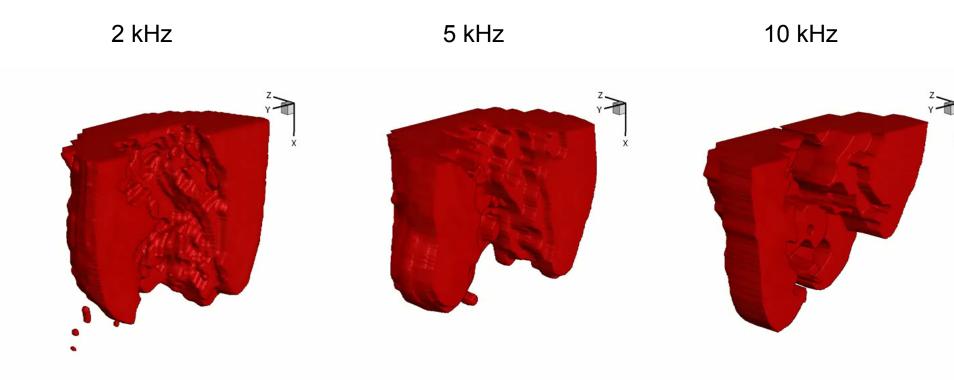
- 1. Raw image
- 2. Normalization
- 3. Low pass filter
- 4. Normalization
- 5. Median filter
- 6. Low pass filter
- 7. Normalization
- 8. Gradient
- 9. superposition





Demonstrating the performance Cinematographic and volumetric flame front







Demonstrating the performance temporal resolution and spatial discretization



In-Plane correlation:

How well correlates one image with following one from next sweep at the same spatial position?

 \rightarrow Measure for temporal resolution of the scan

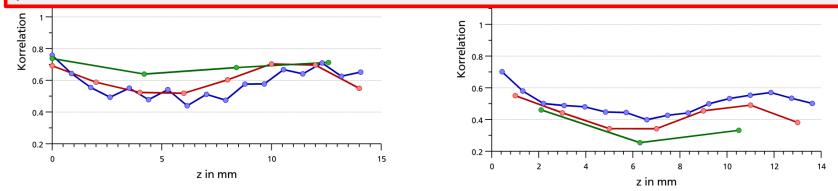
Out-of-Plane correlation:

How well correlates one image with the neighbouring ones during one sweep?

→ Measure for the spatial discretisation in scan direction

Raw data!

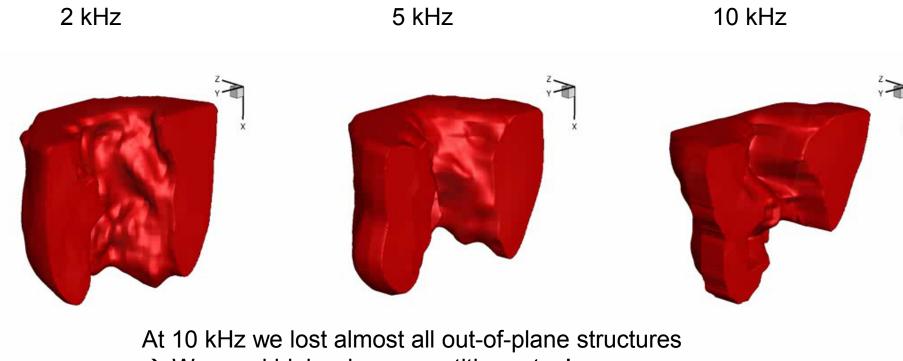
High scan rate with good temporal resolution comes along with bad out-ofplane discretization





Demonstrating the performance Smoothing





 \rightarrow We need higher laser repetition rates! t = 0 ms



Demonstrating the perfromance Results of spatial smoothing



In-Plane correlation:

How well correlates one image with following one from next sweep at the same spatial position?

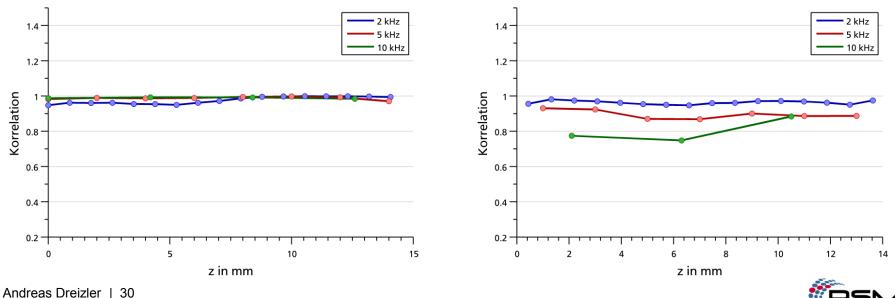
 \rightarrow Measure for temporal resolution of the scan

Out-of-Plane correlation:

How well correlates one image with the neighbouring ones during one sweep?

 \rightarrow Measure for the spatial discretisation in scan direction

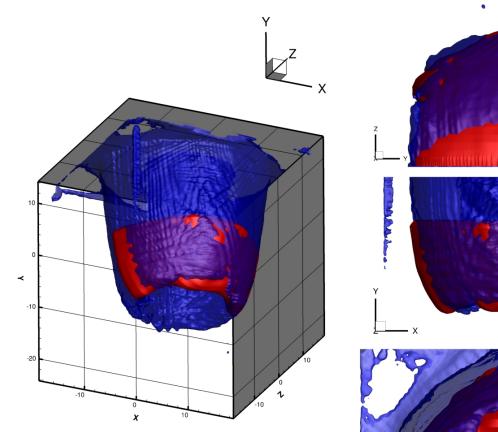
Filtered data!

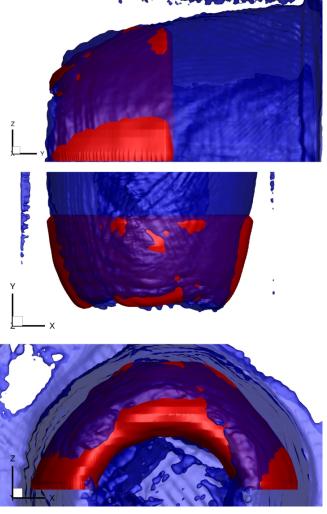




Demonstrating the performance Mean flame front and mean tomographic chemiluminescence results









Summary polygon scanner performance



- Sheet-Jitters < 8 µm for 2-5 kHz scan frequency in air</p>
- In helium-atmosphere at 10 kHz scan frequency: ~20 µm
- →Compared to commercial galvo-scanners 2-10 times higher scan frequency with lower sheet-jitter
- →Find compromise between temporal resolution and spatial discretization
 →Need for lasers with higher pulse repetition rate
- Data post-processing of high importance
- Need for proper documentation of procedure used for data postprocessing

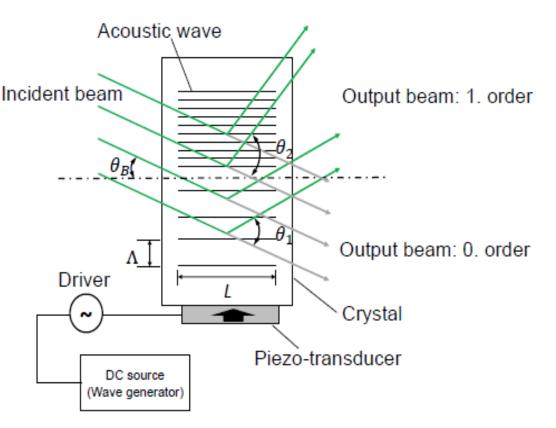


Most recent development: Acousto-optic deflector



- Faster than any mechanical device
- No moving parts
- Use of Bragg reflection
- Changing acoustic wavelength (frequency)
 → change of Bragg angle

$$sin\theta_B = \frac{\lambda}{2\Lambda}$$



Dual plane imaging



Example turbulent flame speed measurements

- Atmospheric pressure: freely propagating flame
- SI IC Engine: early flame propagation

Method developed in collaboration with I. Boxx and W. Meier (DLR-Stuttgart)

PCI 34, 2013, Trunk et al.





Premixed flame propagation – background



- Turbulent flame speed ($\vec{n} \cdot s_{\tau}$) is a key-quantity: determines rate of fuel consumption
- 3D in nature → needs multi-parameter + temporally resolved quasi-3D measurement techniques
- Background:

$$\vec{u}_{flame} = \vec{u}_{displacement} + \vec{u}_{convection}$$

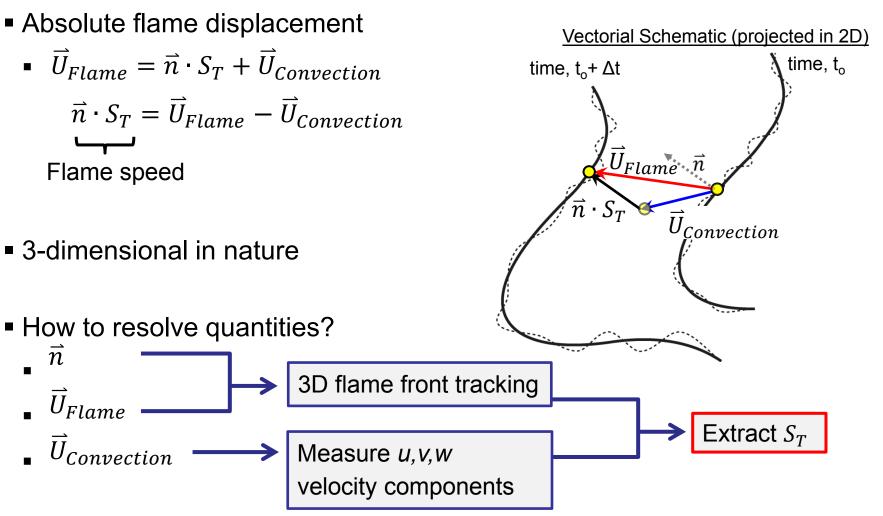
$$= \vec{n} \cdot \mathbf{S}_{T} + \vec{u}_{convection} \qquad \vec{n} \cdot \mathbf{s}_{d} \qquad \vec{u}_{Flamme}$$

$$\vec{n} \cdot \mathbf{S}_{T} = \vec{u}_{flame} - \vec{u}_{convection} \qquad \vec{u}_{Konvektion}$$



Turbulent displacement speed

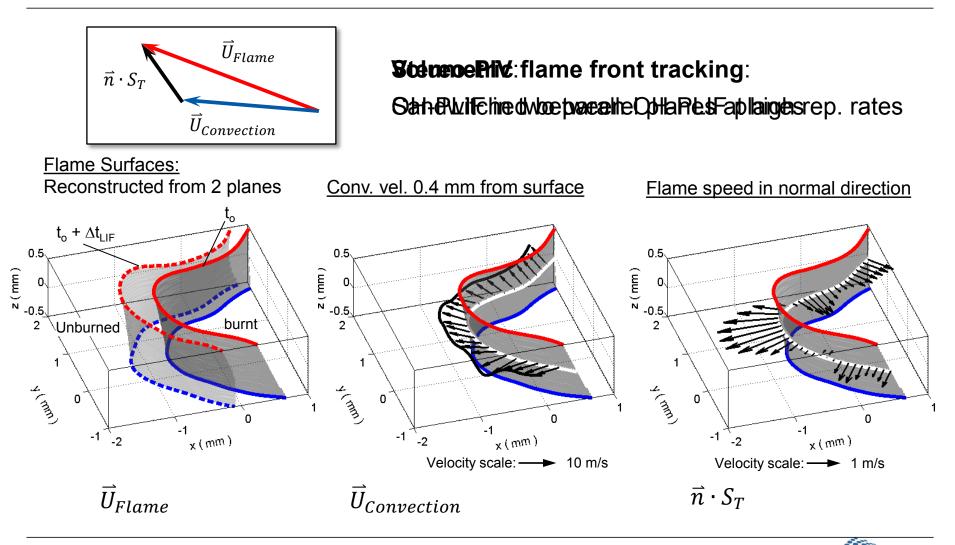






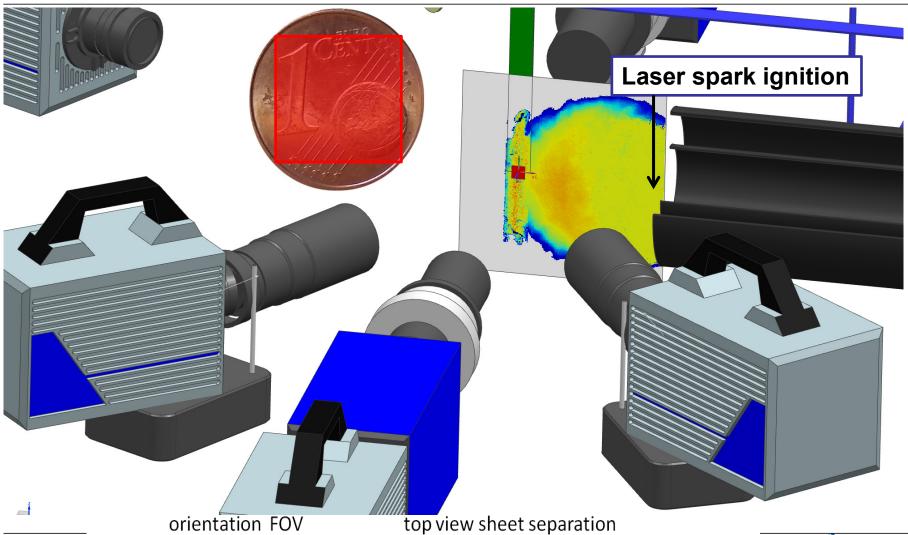
Turbulent flame speed during early flame dev.





Premixed flame propagation – exp. setup



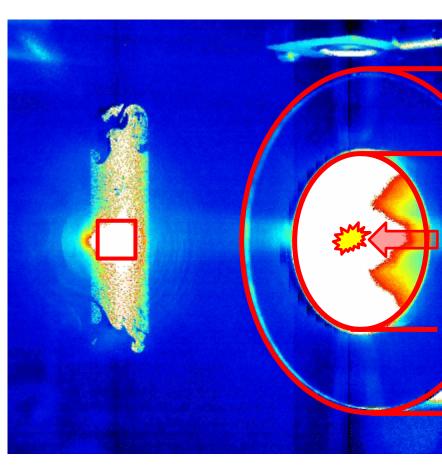


Method – Configuration



Flow Facility and Flame Configuration

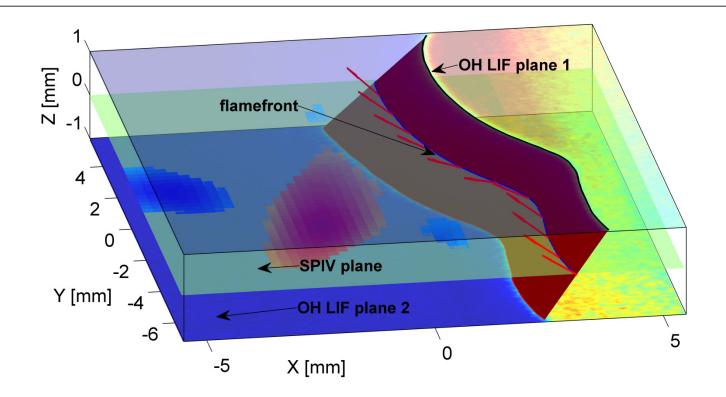
fuel	methane - air
Re	10000
Φ	1
d	85 mm
U ₀	1.81 m/s
Integral length scale	ca. 40 mm
Kolmogorov scale	0.26 mm
coflow	no shear
measurment location	160 mm (2d)upstream
Re _t	90
FOV	12 x 12 mm





Visualization of flame surface in 3D space



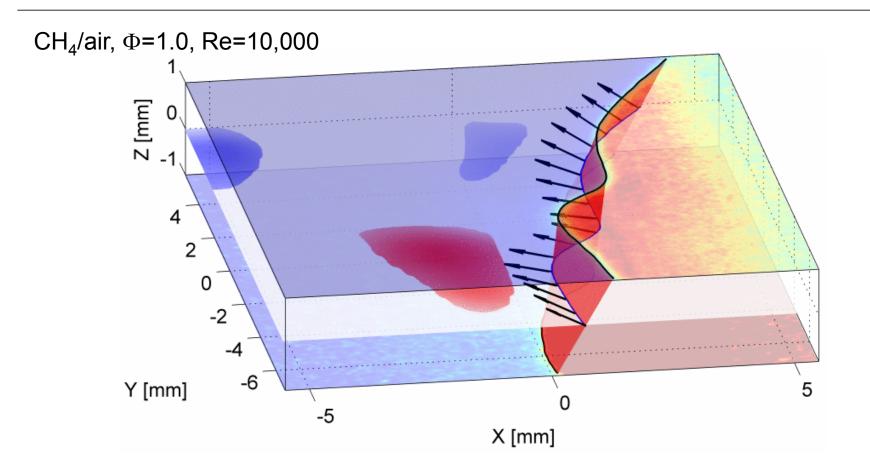


+ information on temporal development \rightarrow displacement speed

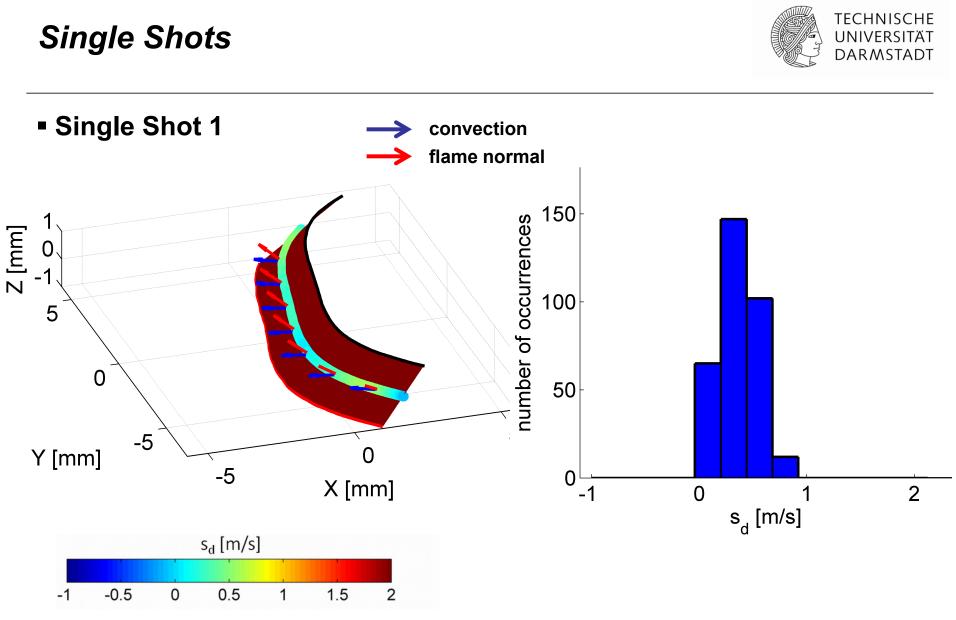


Temporal sequence of flame sequence

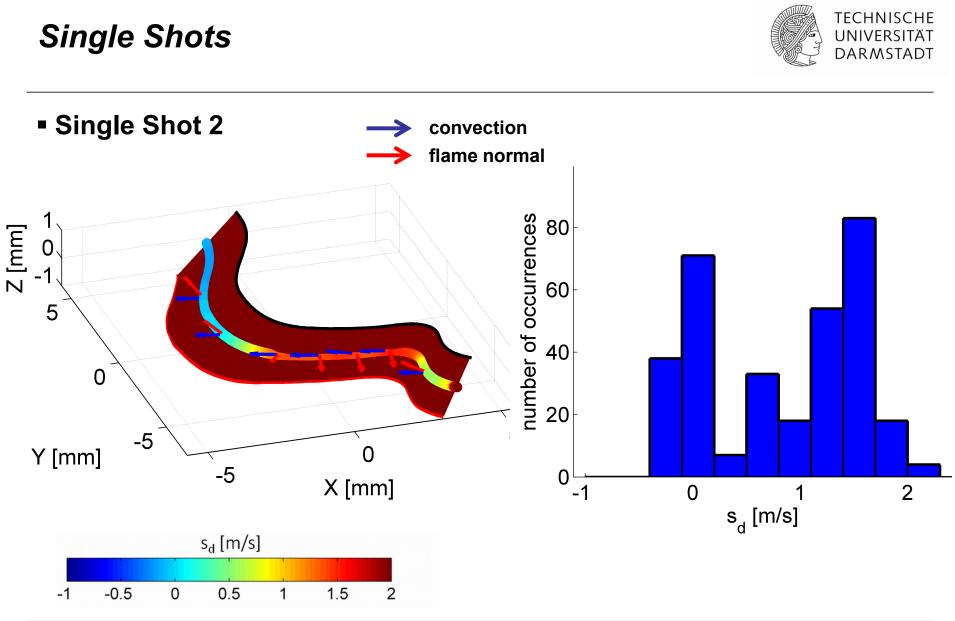




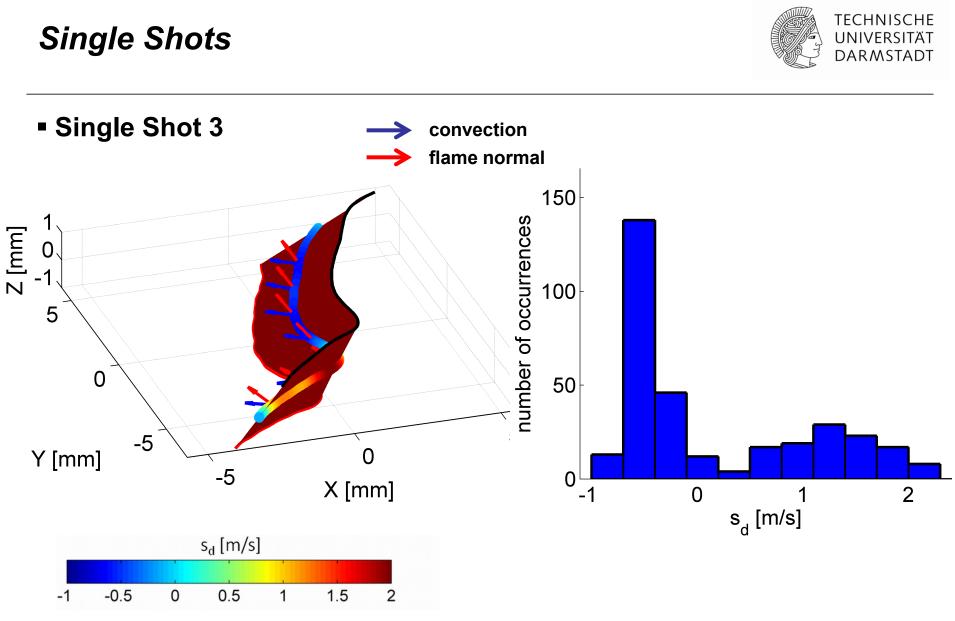










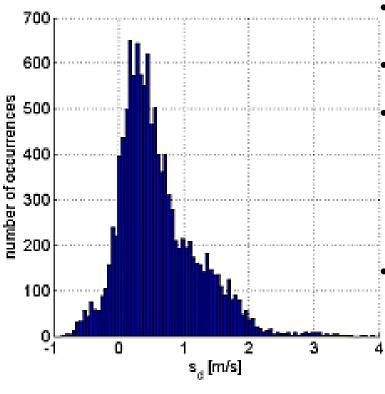




Displacement speed statistics



Displacement speed statistics (CH₄/air; φ = 1.0)



- Histogram centered around 0.35 m/s
- also higher displacement velocities up to 8 x s_L

small parts show negative displacement velocity

- \rightarrow thermo-diffusive effects
- → changes in flame structure not accounted for in turbulent combustion models

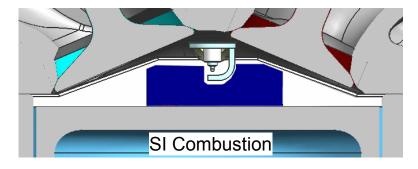
can also be found in numerical work:

- ➢ Gran & Chen 1996
- Bilger & Kim 2005

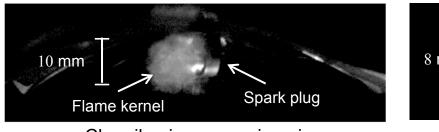


Transfer to IC engine: Early flame propagation in SI-IC-engine

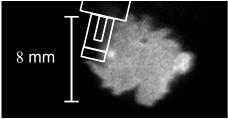
- Early flame development, less than 5% burned mass
- Issue here:
 - 1. Influence of turbulence on local flame displacement speed
 - 2. Cyclic variations



Mie scattering, evaporating oil drops



Chemiluminescence imaging



OH-LIF imaging



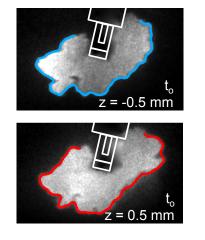


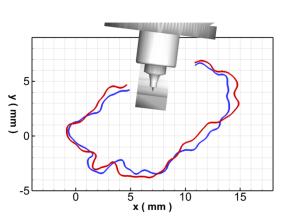
Experimental setup

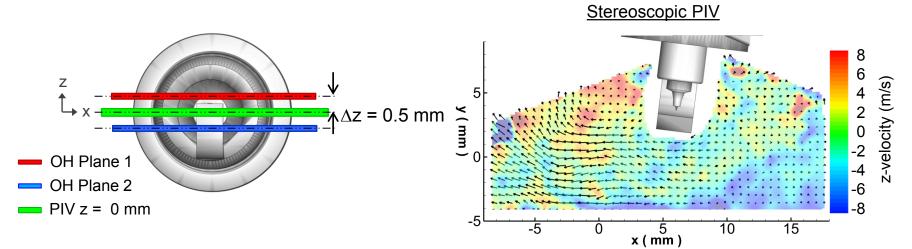


- Dual-plane OH-LIF
 - Two independent UV laser systems (double-pulsed)
 - OH LIF images in parallel planes
- SPIV
 - Central tumble plane

Dual-plane OH-LIF



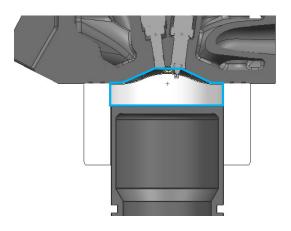






Operating conditions

- 800 RPM
- Iso-octane, air, λ= 1
 - Port-fuel, homogeneous
- Intake: P = 0.95 bar, T = 295 K
- Spark 19° bTDC
- HS-PIV, Chemiluminescence
- 4 shot OH-LIF (2 shots each plane, ∆t = 50µs) @ 14°bTDC
- Spray-guided cylinder head

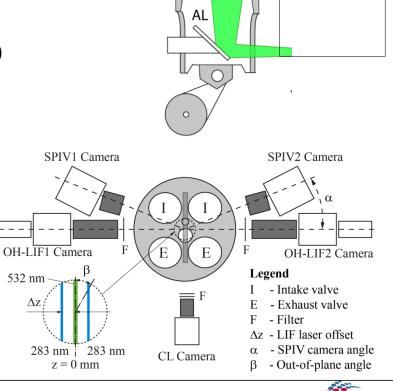




Viewing planes

15x25 mm²

Optical Engine

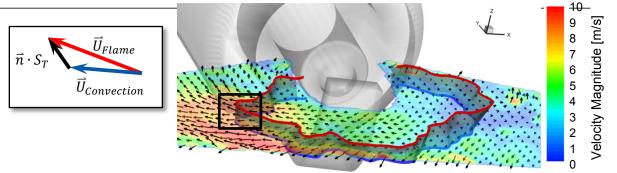


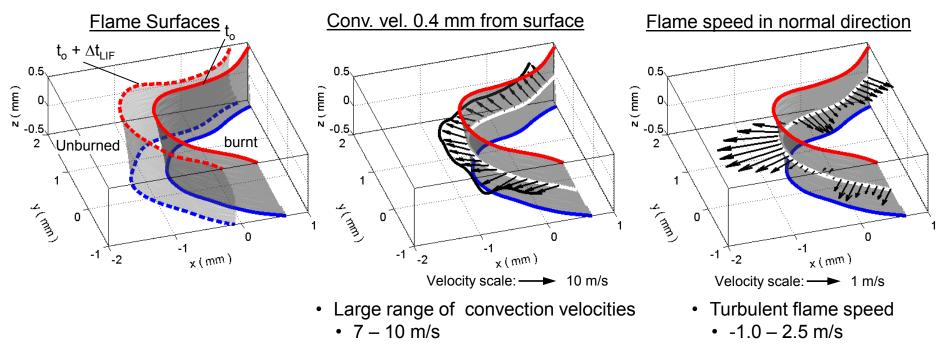
Intake

Turbulent flame speed during early flame dev.



- Local flame speed
 - Absolute velocity: \vec{U}_{Flame}
 - Convection: $\overline{U}_{Convection}$
 - Flame speed: $\vec{n} \cdot S_T$





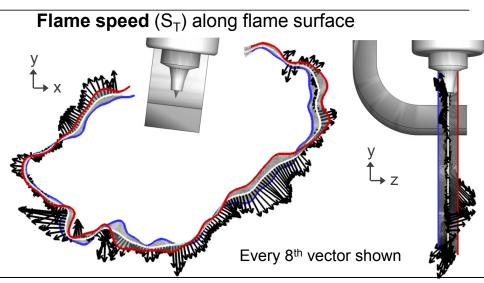
Turbulent flame speed during early flame dev.



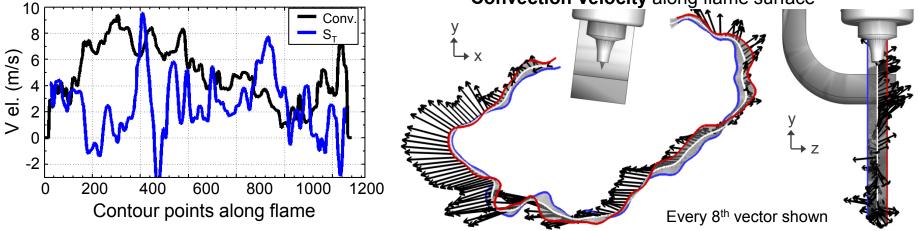
UNIVERSITÄT DARMSTADT

- S_T and convection along flame surface
 - Non-uniform
 - S_T: -2 10 m/s
 - Conv.: 0 10 m/s
 - 3D dependent

Velocity Scale: ----> 8 m/s



Convection Velocity along flame surface

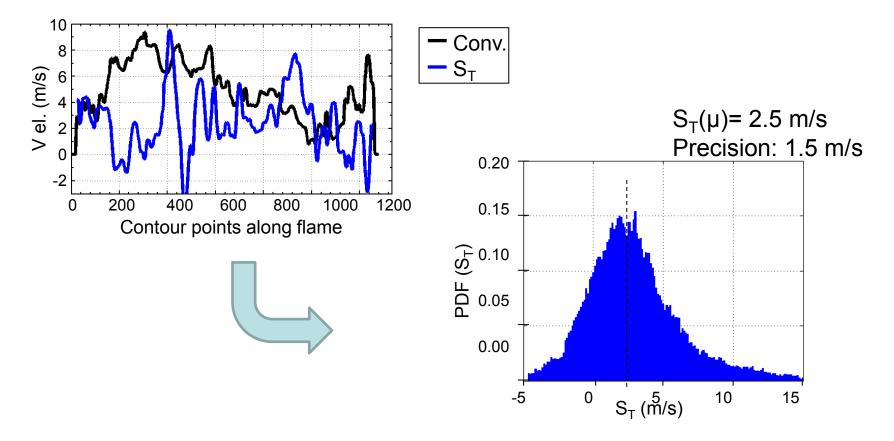




Flame displacement speed during early flame development



- Statistical Quantities
 - Distribution of S_T (80 cycles)

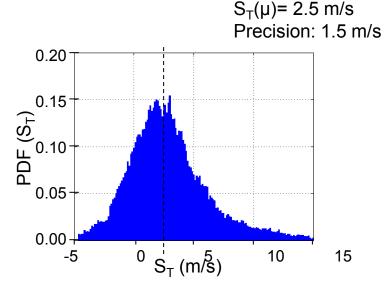




Statistics of turbulent flame speed



- Local flame speed: S_T: -5 15 m/s
- Avg. S_T = 7.2 x S_L
 - S_L = 0.36 m/s (P = 12 bar, T = 550K)
- Strong flame wrinkling due to
 - High turbulence levels
 - Thermal-diffusive /hydrodynamic instabilities (promoted by thin flames at high pressure)



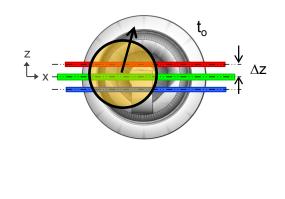


Negative end of the PDF

- Negative flame speeds
 - Flame displacement relative to flow
 - Not rate of consumption!

Planar imaging

- Out-of-plane transport
- Conditional analysis
 - Exclude strong w, convection angles



Precision

0.20

0.15

0.05

0.00

-5

0

15

20

10

s_T (m/s)

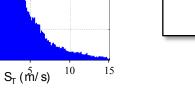
(^LS) <u>10</u>

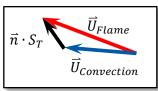
- LIF Resolution: 0.08 mm
 - ∆S_T = 1.5 m/s

0.04

0.02

■ ∆S_{T , MAX} = 3.0 m/s





<u>Physical</u>

- Mechanisms (DNS*)
 - High positive curvature
 - High comp. & tang. Strain
 - Sensitivity of iso-level
- No experimental correlations found
 (Trunk 2013, Kerl 2013)
- Change of flame structure
 - Transport effects

* Gran 1996, Chen 1998, Chen 2002, Kim 2005



Andreas Dreizler | Baetjer-Seminar Princeton | 57



Tomographic OH-LIF Work-in-Progress Poster, 36th Intl. Symp. On Combustion 2016, South Korea



- Turbulent flow phenomena are three-dimensional in nature
- Planar OH-LIF is a common tool to investigate turbulent flame characteristics
- Information in 3rd dimension, however, is lost in planar techniques
- Turbulent flame features such as flame holes can only be characterized by fully three-dimensional measurements
- Tomographic OH-LIF imaging as an approach to yield the full threedimensional OH concentration field



Setup Tomo LIF

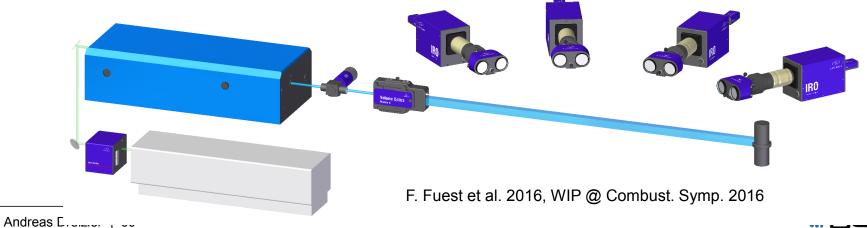


Detection

- Four intensified CCD cameras in one plane at 45° angle separation
- Image doubler
- 8 simultaneous views

Excitation

- Frequency-doubled output of a dye laser tuned to excite the Q₁(8) transition (λ = 283.55 nm) of the A²∑ ← X²∏ (v'=1, v"=0) band of hydroxyl radicals
- 20 mJ at probe volume of 3x3x3 cm³



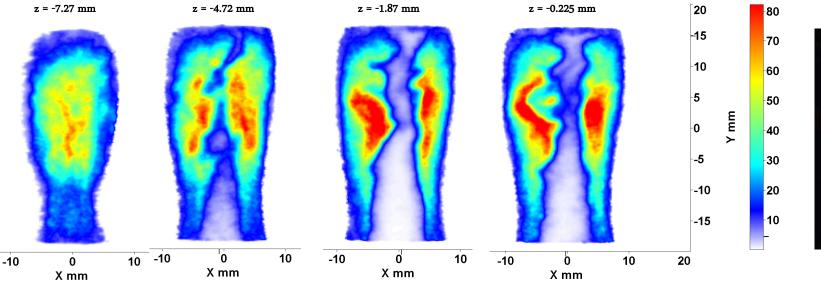


Tomographic reconstruction Example turbulent Bunsen flame



- Simultaneous Multiplicative Algebraic Reconstruction Technique (SMART)
- 100 iterations
- Computational time for 8 views @ 16 cores (3.10 GHz, 128 GB RAM):
 - > 5 min for 100M voxel of $75^3 \mu m^3$, no binning,
 - ➤ 45 s for 12M voxel of 150³ µm³, 2x2 binning

Reconstructed z-planes of turbulent Bunsen flame



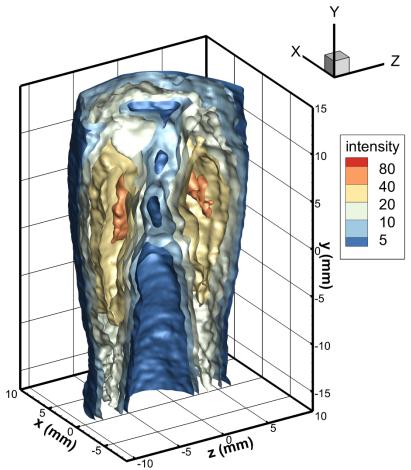




Tomographic reconstruction Example turbulent Bunsen flame



Reconstructed 3D iso surface of LIF intensity



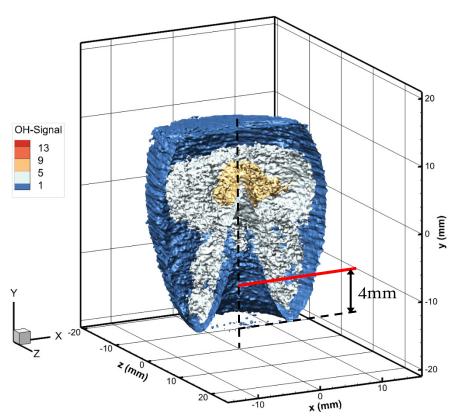
F. Fuest et al. 2016, WIP @ Combust. Symp. 2016

Comparison with 2D PLIF measurements Laminar Bunsen flame

- Tomographic LIF and PLIF at same location
- Laminar premixed methane flame, d = 13 mm
- Center plane
- One side of OH-LIF profile
- 4 mm above the nozzle exit



Reconstructed single-shot laminar flame and location of extracted intensity profiles.



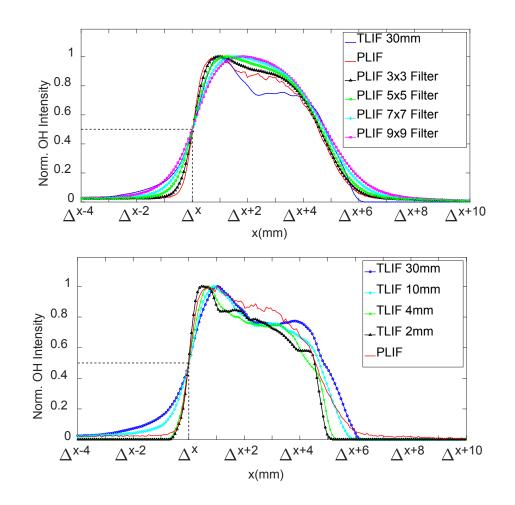






Comparison with 2D PLIF measurements

- Different filter sizes for PLIF and different volume-sheet thicknesses for tomographic LIF
- →PLIF using 5x5 filter shows similar gradient at large OH intensity
- → Steeper gradient with decrease of sheet thickness



F. Fuest et al. 2016, WIP @ Combust. Symp. 2016



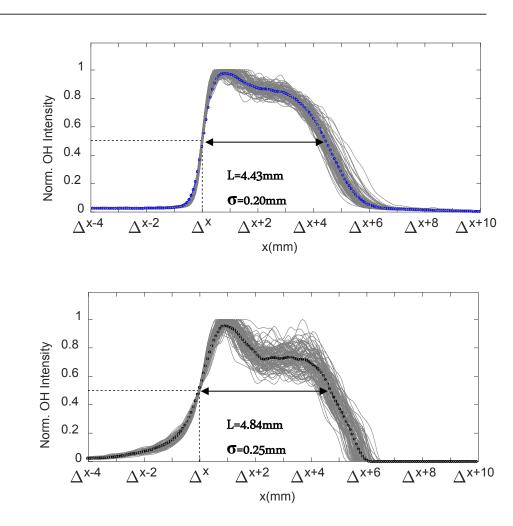
Comparison with 2D PLIF measurements



 PLIF: Single-shot and average profile

 TLIF: Single-shot and average profile

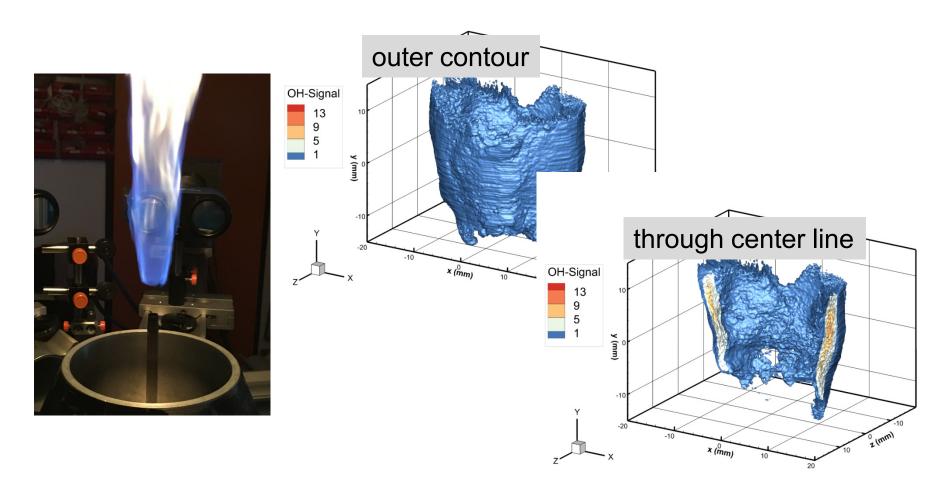
Length L at 50% intensity and its standard deviation $\boldsymbol{\sigma}$





Turbulent lifted flame Re 5000, voxel of 75³ µm³, no binning

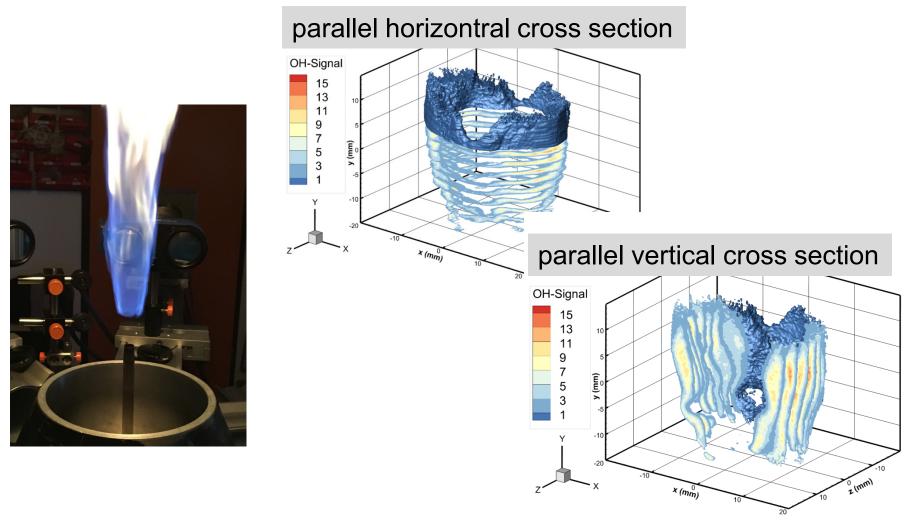






Turbulent lifted flame Re 5000, voxel of 75³ µm³, no binning







Chapter 9: Flame wall interactions in canonical configurations

TU Darmstadt, Germany Dept. of Mechanical Engineering Institute for Reactive Flows and Diagnostics





A. Dreizler

Sponsored by Deutsche Forschungsgemeinschaft Center of Smart Interfaces Technische Universität Darmstadt

Co-authors

- C. Jainski
- M. Rißmann
- H.Kosaka
 - B. Böhm

Outline

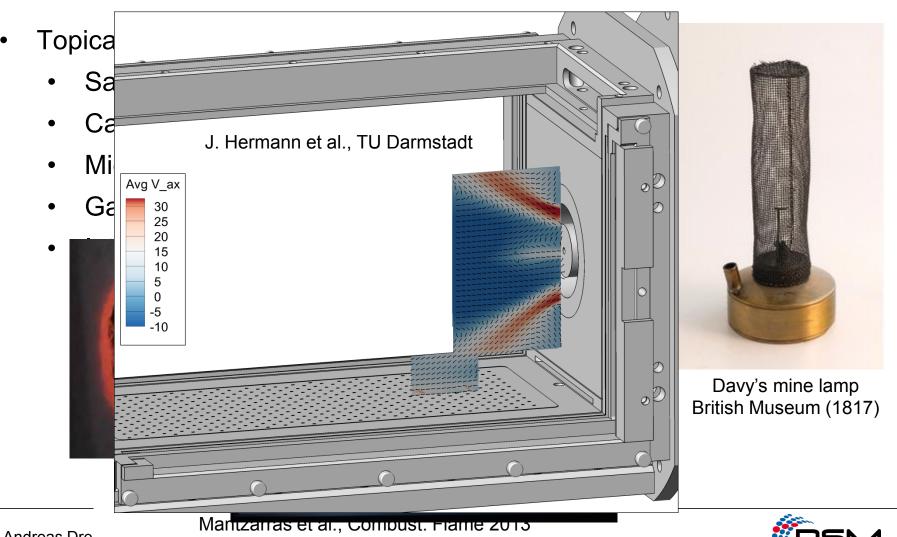


- Motivation of Flame-Wall Interaction (FWI) Research
- Experimental Approach at RSM/TU Darmstadt
- Head-on Quenching
 - Flame dynamics of turbulent flames
 - Thermo-chemical states
- Side Wall Quenching
 - Flame dynamics of turbulent flames
 - Flame surface density
 - Mean reaction rate modelling
 - Thermo-chemical states
 - Laminar flames
 - Turbulent flames



Flame-wall interaction (FWI)





Andreas Dre._...

General properties of FWI



- When flame approaches closer than a few flame thicknesses to the wall (for premixed combustion)
- \rightarrow Intense coupling between flame and wall
 - Large heat fluxes (exceeding 1 MW/m² for HC-fuels at 1 bar)
 - Flame quenching causing incomplete combustion
 - Emission of unburned hydrocarbons and CO
 - Relevant especially for cold-start engine conditions



Flame-Wall Interaction in IC engines

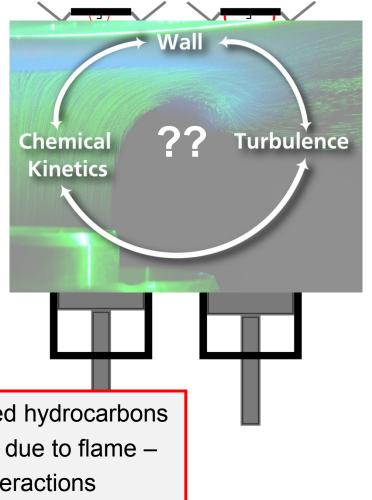
 Turbulent flame (1500-2500 K) surrounded by cold walls (≤700 K)

- Heat losses and radical recombination leads to flame quenching
- Incomplete combustion generates UHC, CO and soot
- Flame wall interactions affect **efficiency** and **pollutant formation** [Alkidas, PECS 1999]

30% combustion energy in an engine is lost by heat transfer trough the wall **40%** of unburned hydrocarbons in engines is due to flame – wall interactions

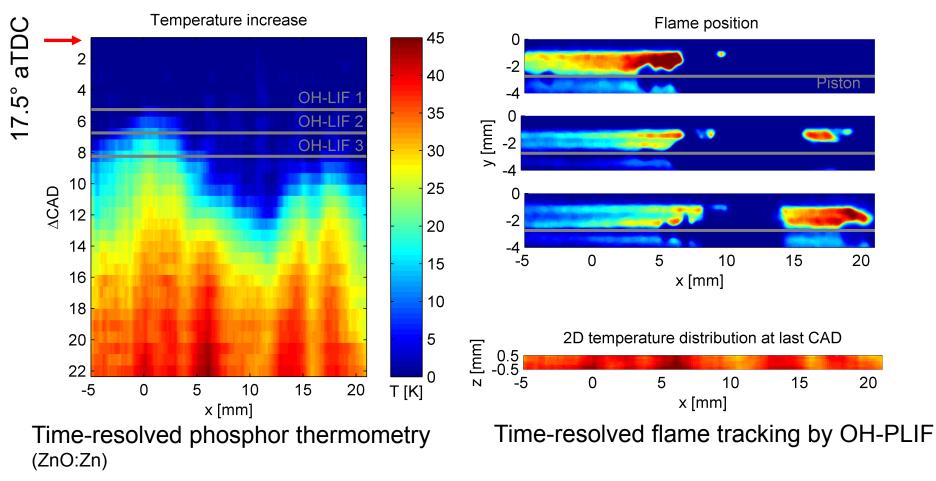






Flame-Wall Interaction in IC engines: Temperature rise due to flame impact at piston





C.-P. Ding et al., Appl. Phys. B 2017

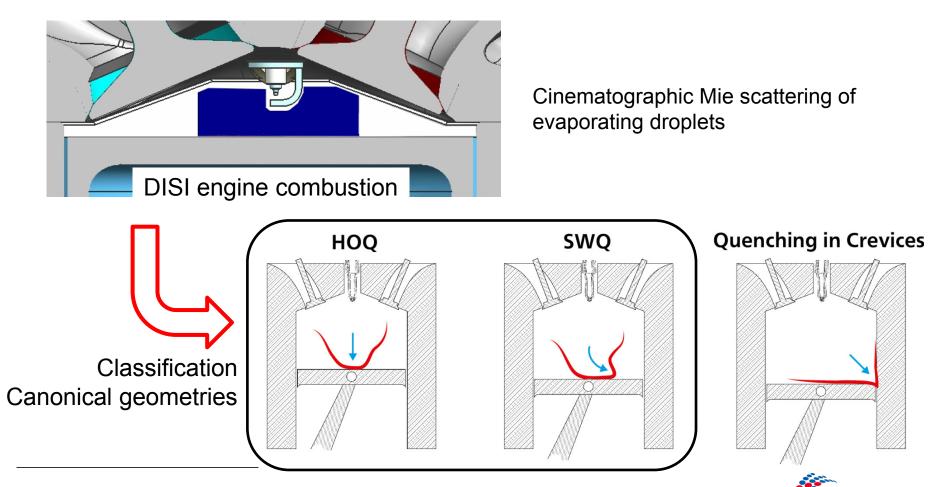


Flame-Wall Interaction in IC engines



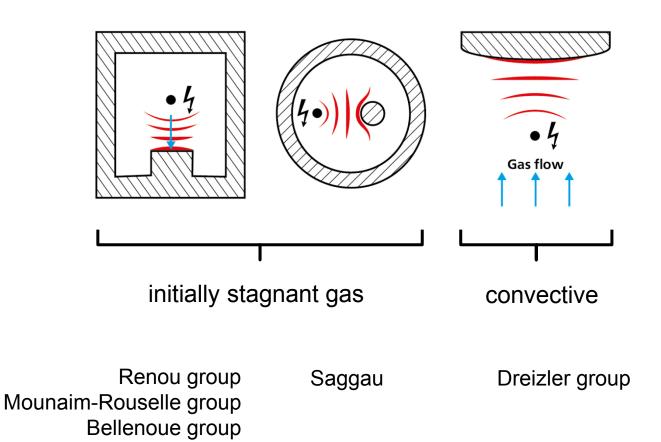
TECHNISCHE UNIVERSITÄT DARMSTADT

Focus here: premixed flames



Head-on quenching – canonical geometries



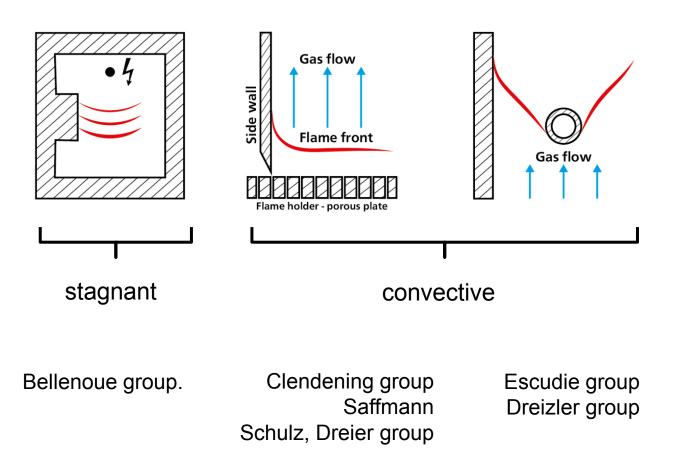




Andreas Dreizler | 8

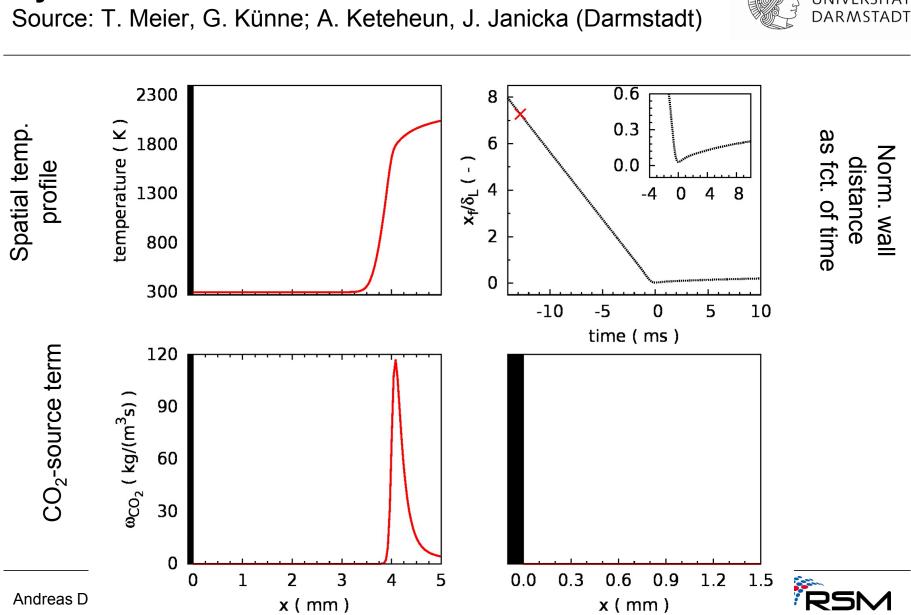
Sidewall quenching – canonical geometries







Andreas Dreizler | 9

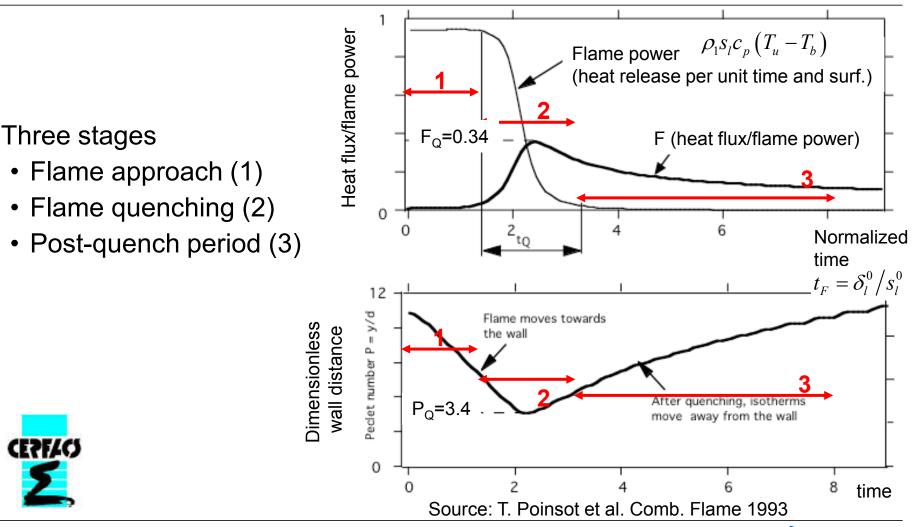


Dynamics of HOQ: 1D-simulation

TECHNISCHE UNIVERSITÄT DARMSTADT

Results of 1D-DNS



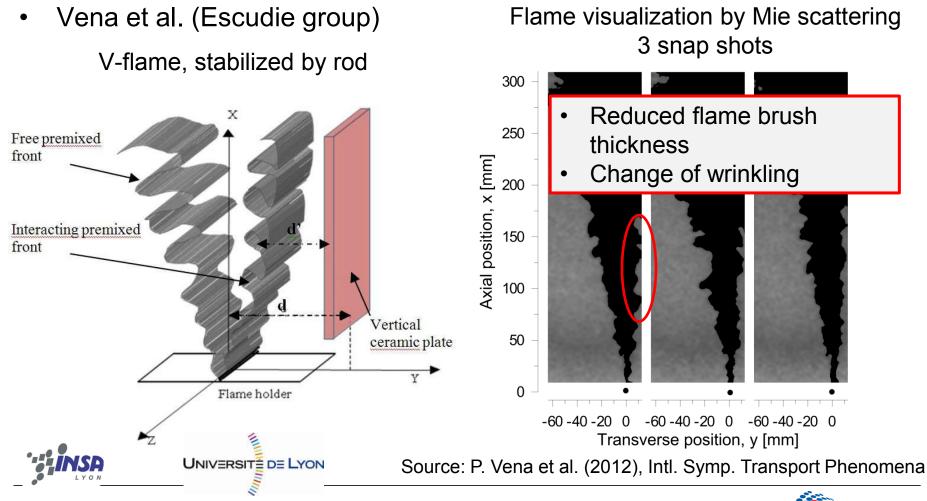


•



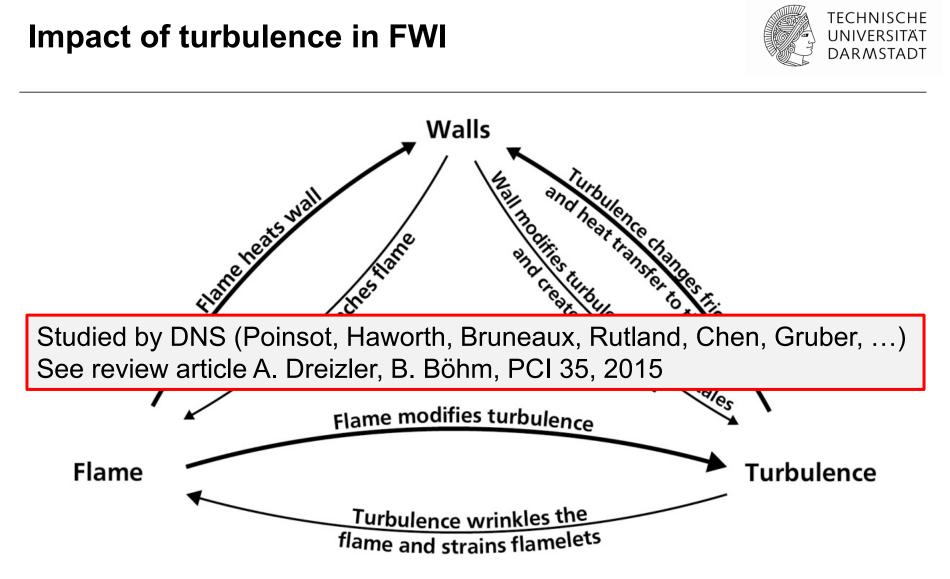
Impact of turbulence





Andreas Dreizler | 12





Source: T. Poinsot and D. Veynante, Theoretical and Numerical Combustion 2005

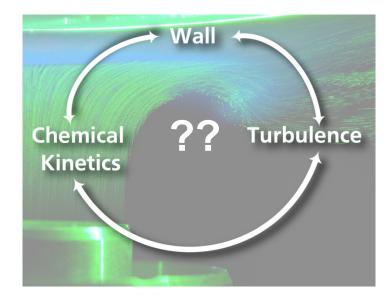


Andreas Dreizler | 13

Conclusions from previous studies



- Lack of detailed experimental studies providing quantitative data
- The focus was primarily on quenching distances and heat transfer
- Analysis of boundary layers, flame structure and thermo-chemical states during flame-wall interaction is limited





Outline

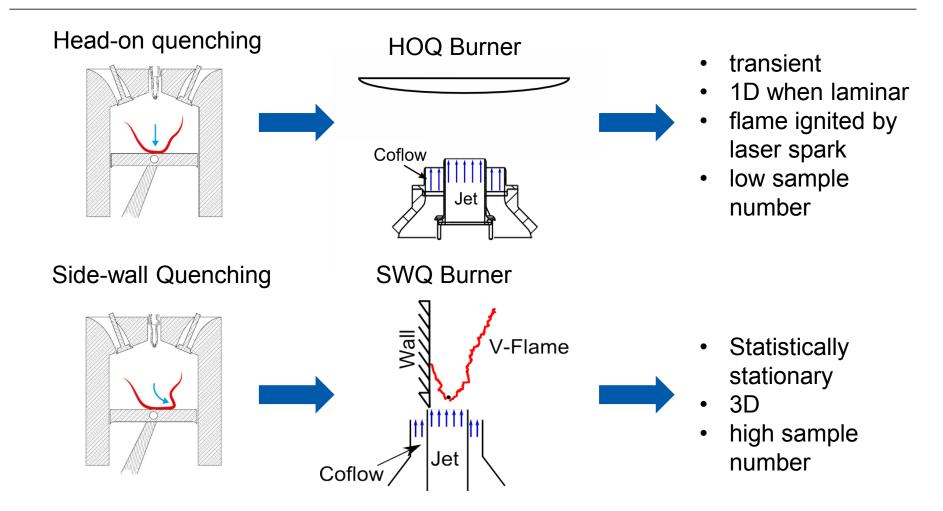


- Motivation of Flame-Wall Interaction (FWI) Research
- Experimental Approach at RSM/TU Darmstadt
- Head-on Quenching
 - Flame dynamics of turbulent flames
 - Thermo-chemical states
- Side Wall Quenching
 - Flame dynamics of turbulent flames
 - Flame surface density
 - Mean reaction rate modelling
 - Thermo-chemical states
 - Laminar flames
 - Turbulent flames



Fundamental Flame-Wall Interaction



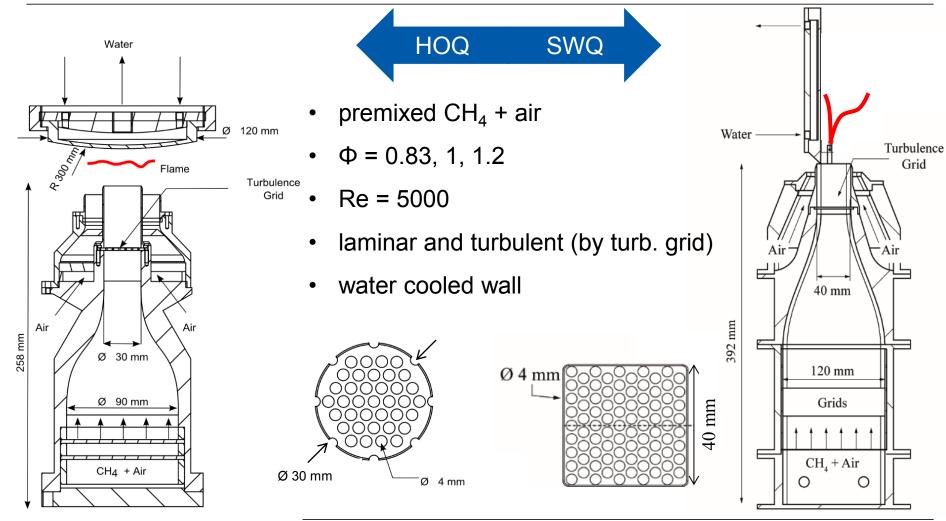




Experimental conditions



TECHNISCHE UNIVERSITÄT DARMSTADT

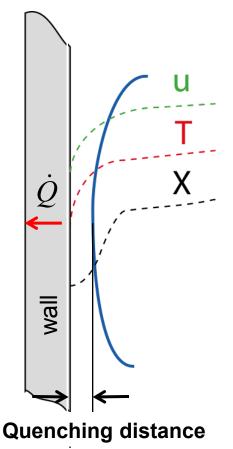




Experiments in FWI: parameters of interest

- Quenching distances, visualization of flames near walls
- Wall temperature and heat flux \dot{Q}
- Flow field studies near walls
 - Velocity boundary layers u
- Reaction rates near walls
- Thermo-chemical states during FWI
 - Thermal boundary layers T
 - Concentration boundary layers X

Focus today







Measurement techniques

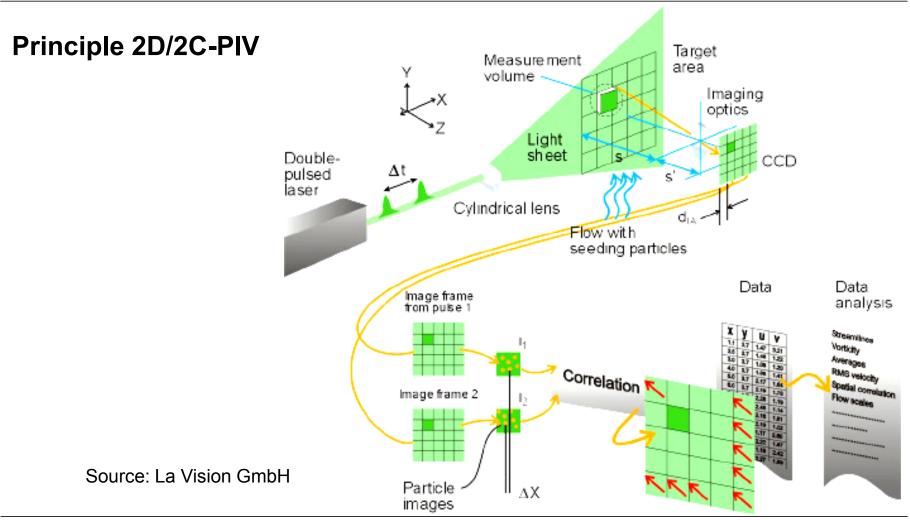


Laser based diagnostics

- Non intrusive
- High spatial and temporal resolution
- High accuracy and precision
- Simultaneous measurement of several quantities multi-parameter diagnostics

Gas Velocity	Flame Front Position	Gas Temperature	CO Concentration
(Stereo) Particle Image Velocimetry (PIV)	Planar LIF of OH radical Flame front from OH gradient	ro-vibrational ns- CARS	Two Photon LIF of CO molecule
2 D/3 Components Rep. Rate: 10 kHz	2 D Rep. Rate: 10 kHz/10 Hz	0 D Rep. Rate: 10 Hz	0 D Rep. Rate: 10 Hz

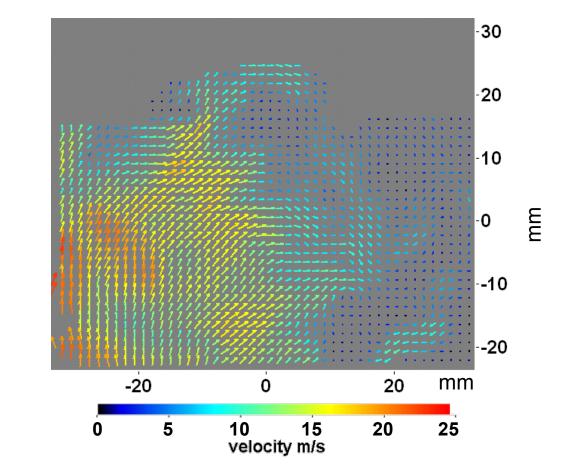






TECHNISCHE

Particle Image Velocimetry – PIV



Particle Image Velocimetry – PIV

TECHNISCHE UNIVERSITÄT DARMSTADT

Visualization

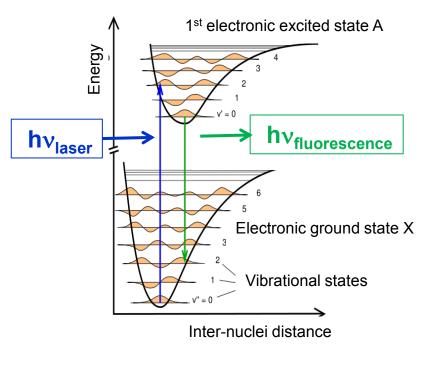
In-cylinder meas.



Laser Induced Fluorescence – LIF

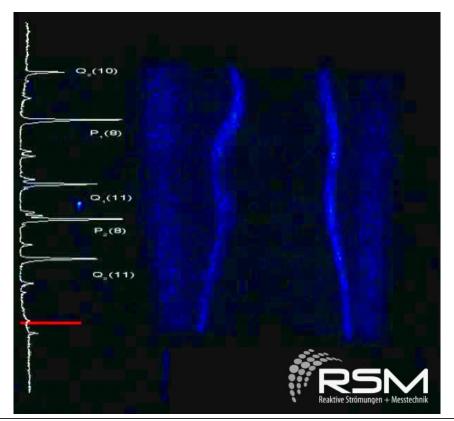


Schematic of LIF (single-photon)



Rotational sub-states not shown

OH planar LIF in fuel rich Bunsen flame \rightarrow Flame front tracking



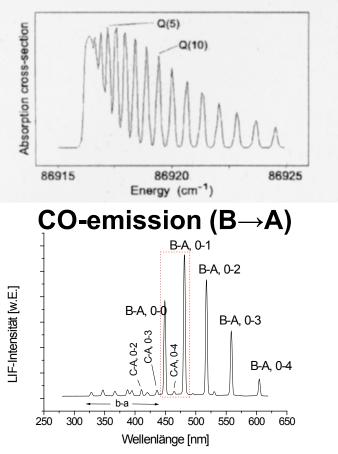


CO LIF



2-photon excitation Q(5) Absorption cross-section $B^2\Sigma$ photoionization collisional quenching $= \chi^2 \Sigma^1$ $b^{3}\Sigma$ B ¹Σ* 86915 triplet LIF **A**¹Π emission co а³П excitation LIF-Intensität [w.E.] X 1Σ* B-A, 0-0 C-A, 0-3 C-A, 0-2 3 b-a

CO-absorption ($B \leftarrow \leftarrow X$)





Coherent anti-Stokes Raman spectroscopy (1)



- Non-linear polarization $P_{i} = \varepsilon \left(\chi_{ij}^{(1)} E_{j} + \chi_{ijk}^{(2)} E_{j} E_{k} + \chi_{ijk}^{(3)} E_{j} E_{k} E_{j} + \dots \right)$
 - P_i : Polarization
 - E_i : Electrical field
 - $\chi^{(n)}$: Susceptibility of n-th order
 - Non-linear effects are observable only at high electrical field strength

 $\approx 10^{-12} \approx 10^{-12} \approx 10^{-23}$

➡ Pulsed LASER is prerequisite

In Gases :

$$\chi^{(2)} = 0$$



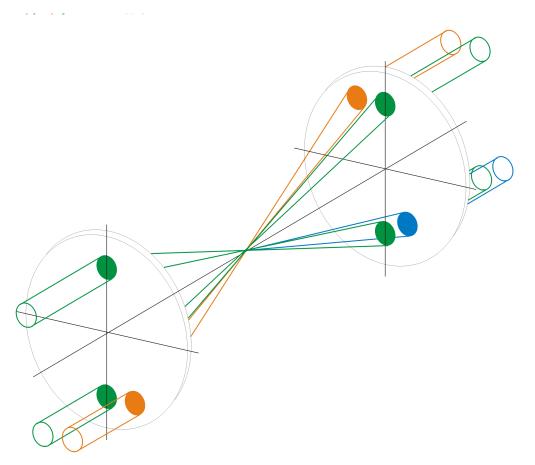
TECHNISCHE CARS: energy and momentum conservation UNIVERSITÄT DARMSTADT Pump laser Pictorial view of CARS Stokes laser Energy balance: $\omega_3 = 2\omega_1 - \omega_2$ CARS signal (anti-Stokes) Selection rules ω \mathcal{O}_1 ω_{2} \mathcal{O}_{2} \mathcal{W}_1 \mathcal{O}_1 ω_3 ω_{2} $\Delta J = 0, \pm 2$ $\Delta v = 1$ ω_{R} Momentum balance: $k_3 = k_1 + k_1 - k_2$ Termed phase matching k_1 k_1 \vec{k}_{2} \vec{k}_3 k_{3} **Co-linear CARS** BOX CARS: preferred, higher spatial resolution



CARS: phase matching



- Realization of phase matching
 - Pump laser: 532 nm (frequency-doubled Nd:YAG)
 - Stokes laser: 607 nm (broadband dye laser)
 - CARS signal: 473 nm

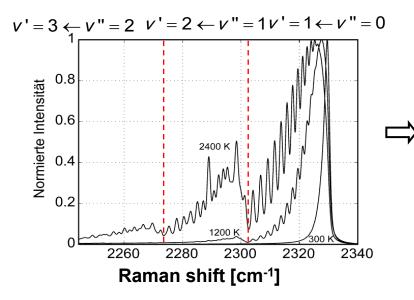




CARS: thermometry



• Typical application in turbulent flames: ro-vibronic N₂-broad band CARS



Temperature obtained by fitting CARS spectrum to experimental spectrum

Temperature information is contained in line-strength~ N_i^2 (in χ^3 -tensor)

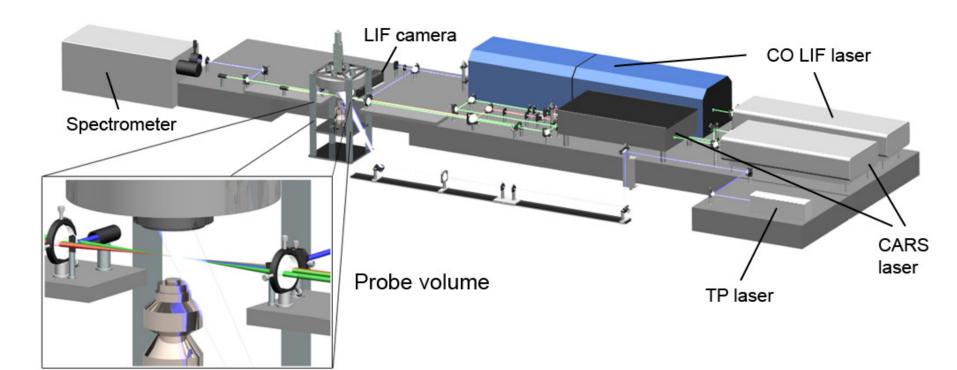
Based on Boltzmann distribution

$$\frac{N_i}{\sum_i N_i} = \frac{g_i e^{-E_i/kT}}{\sum_i g_i e^{-E_i/kT}}$$



Combined CARS – CO LIF – setup







Measurement techniques



Fluid Velocity	Flame Front Position	Fluid Temperature	CO Concentration
Particle Image Velocimetry (PIV)	Planar LIF of OH molecule Flame front from OH gradient	Coherent Anti Stokes Raman Spectroscopy (CARS)	Two Photon LIF of CO radical
2 D/2 Components Repetition Rate: 10 kHz	2 D Repetition Rate: 10 kHz	0 D Repetition Rate: 10 Hz	0 D Repetition Rate: 10 Hz
Resolution: Wall-nearest loc.: ~0.4 mm	Resolution: Wall-nearest loc.: ~0.1 mm	Resolution: Wall-nearest loc.: ~0.05 mm	Resolution: Wall-nearest loc.: ~0.1 mm
Precision and Accuracy: similar to PIV far from walls	Uncertainty: ±0.05 mm	Precision: 2.5 – 8%	Precision: 8 – 11 % Accuracy: ≤20% in most regions
Challenge: Too few particles very close to wall, beam steering	Challenge: Noisy signal, IRO blurring	Challenge: Resolution in beam wise direction, 0D extension to 1D	Challenge: Spatial resolution, calibration, 0D extension to 1D feasible
simultaneously simultaneously			



Outline

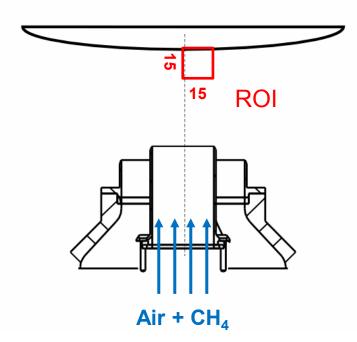


- Motivation of Flame-Wall Interaction (FWI) Research
- Experimental Approach at RSM/TU Darmstadt
- Head-on Quenching
 - Flame dynamics of turbulent flames
 - Thermo-chemical states
- Side Wall Quenching
 - Flame dynamics of turbulent flames
 - Flame surface density
 - Mean reaction rate modelling
 - Thermo-chemical states
 - Laminar flames
 - Turbulent flames



Unsteady flame-wall interaction





- Flame is **ignited** by a laser spark over the nozzle
- Flame propagates towards the wall
- Re = 5000, 10 000; Φ = 0.83, 1.0;
 with and w/o TG
- Region of interest (ROI): 15 x 15 mm²
- Measured: CO, T, Velocity and

Flame Front Position

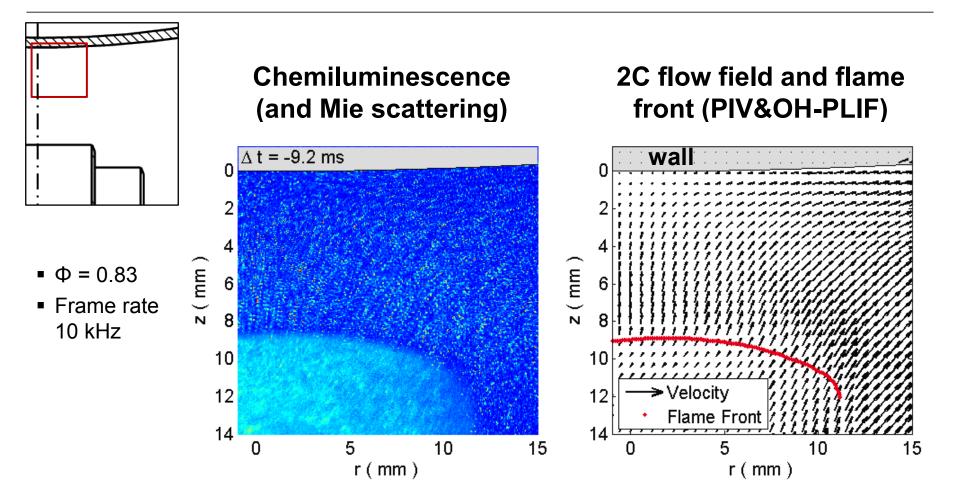
Unburned gas between flame and

wall



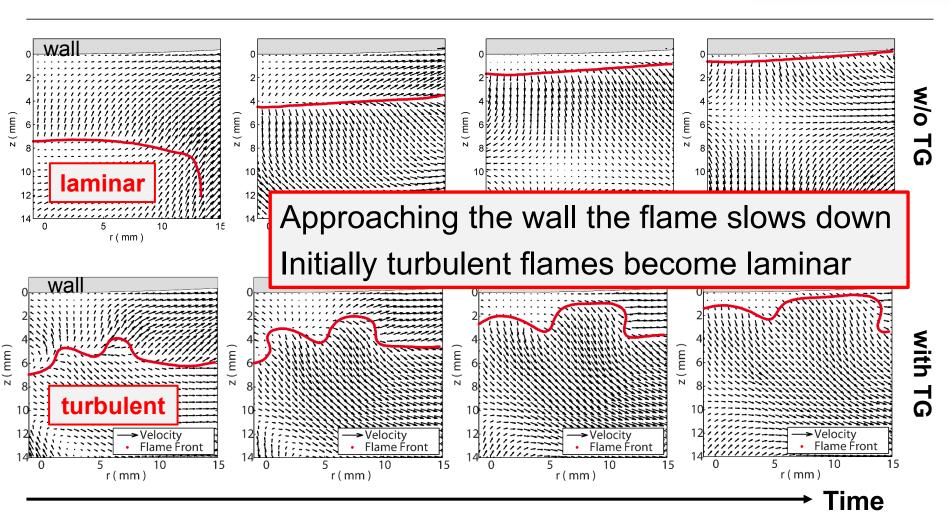
Laminar flame propagation and wall impingement







Unsteady flame-wall interaction (Re = 5000, Φ = 1.0, with and w/o TG)





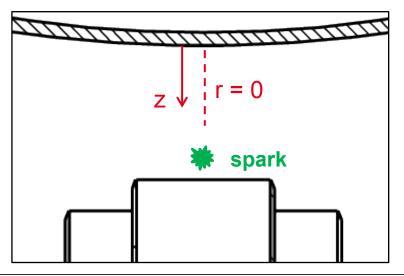
TECHNISCHE UNIVERSITÄT

DARMSTADT

Phase-resolved temperature and CO concentration measurements for HOQ - laminar



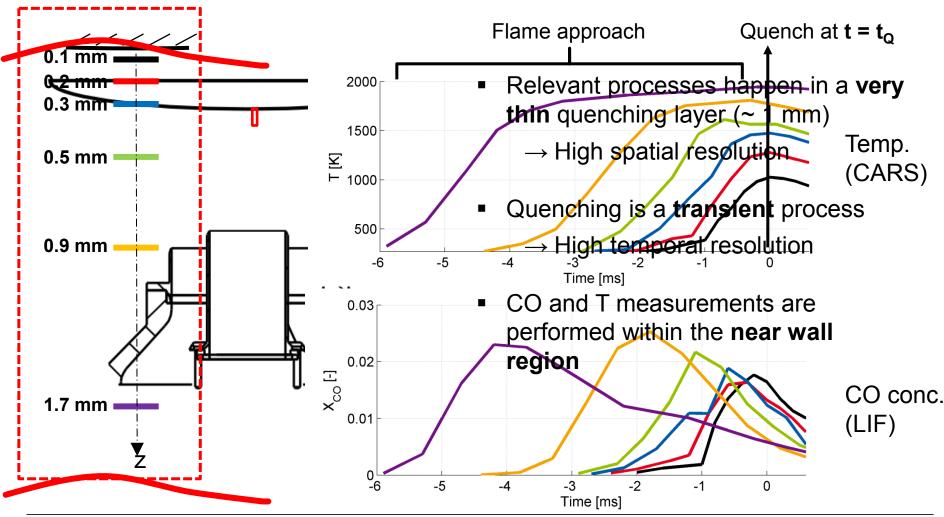
- Laser spark 2 mm above nozzle
- Phase-fixed CO-T-measurements relative to spark
 - 6 probe volume (PV) locations spanning from $0.1 \le z \le 1.7$ mm
 - Focus on near wall region
- Time delay: Variation of time in steps of $\Delta t = 100 \ \mu s$
- 200 single-shots at each PV
- Example: Φ = 0.83, Re = 5000





Time-resolved temperature profiles for HOQ - laminar



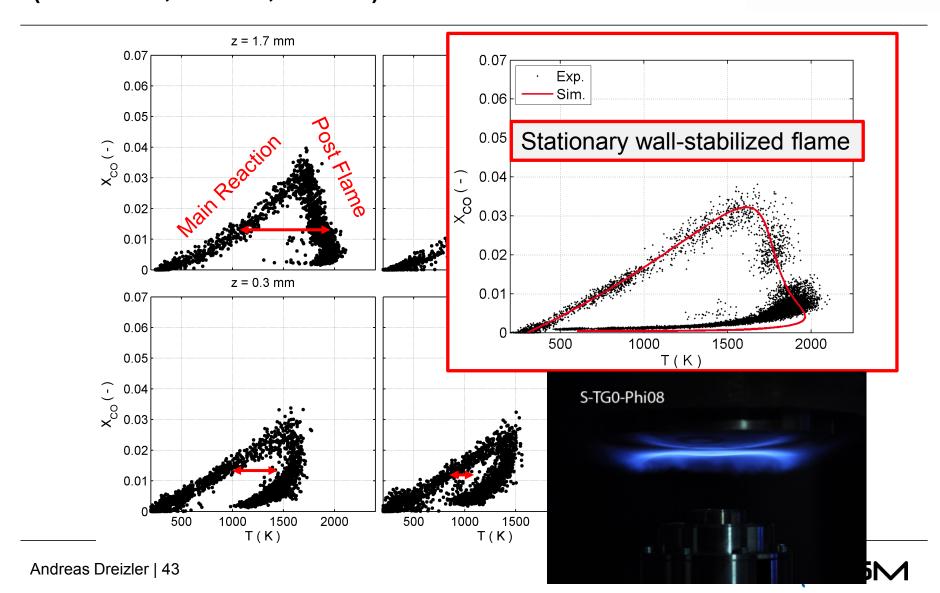




Laminar thermo-kinetic states (Re = 5000, Φ = 1.0, w/o TG)

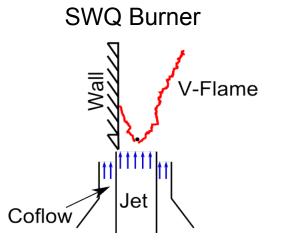


TECHNISCHE UNIVERSITÄT DARMSTADT



Outline

- Motivation of Flame-Wall Interaction (FWI) Research
- Experimental Approach at RSM/TU Darmstadt
- Head-on Quenching
 - Flame dynamics of turbulent flames
 - Thermo-chemical states
- Side Wall Quenching
 - Flame dynamics of turbulent flames
 - Flame surface density
 - Mean reaction rate modelling
 - Thermo-chemical states
 - Laminar flames
 - Turbulent flames





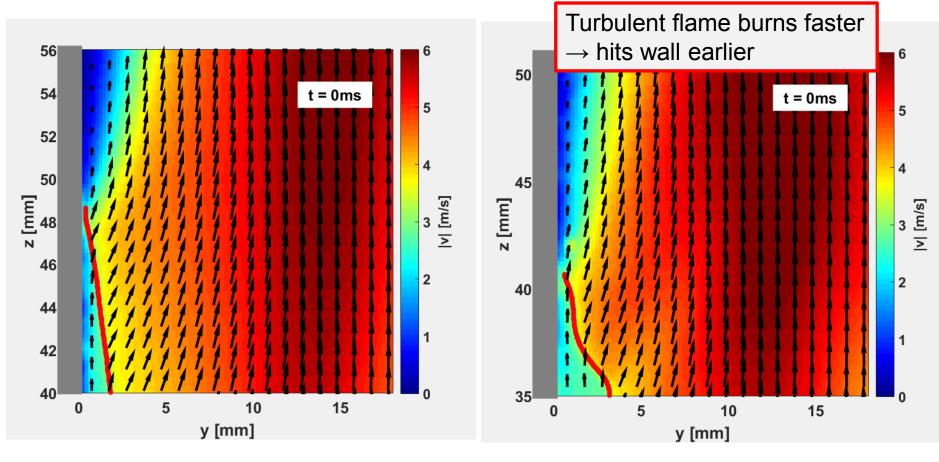


Laminar vs. turbulent flame



laminar, $\phi = 1.0$



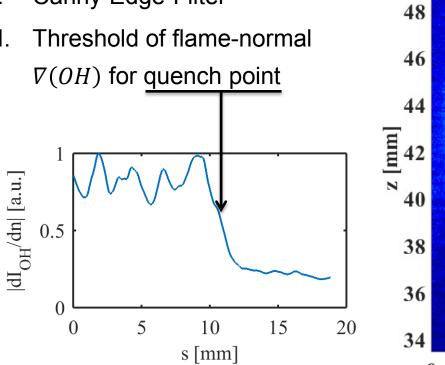


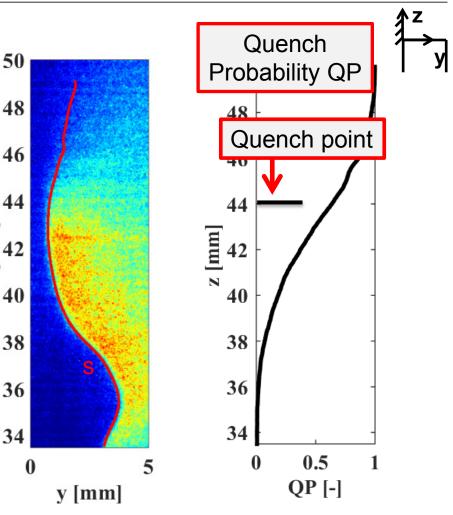


Post-processing of OH PLIF

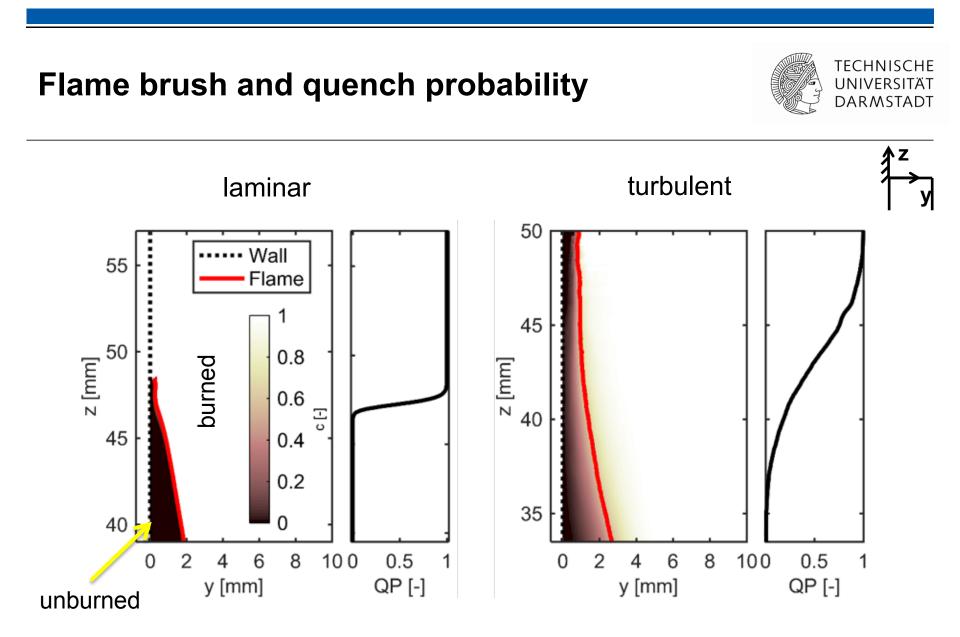


- Flame front detection:
 - Canny-Edge-Filter Ι.
 - Ш. Threshold of flame-normal











Modelling of turbulent premixed flames



- Flame surface density (FSD) model requires mean reaction rate $\overline{\dot{\omega}_R}$:
 - 1. turbulent flame \rightarrow ensemble of laminar flamelets
 - 2. flame-flow interaction \rightarrow local consumption speed $s_l \star$ flame surface density Σ

Density and fuel mass fraction of unburned mixture – known

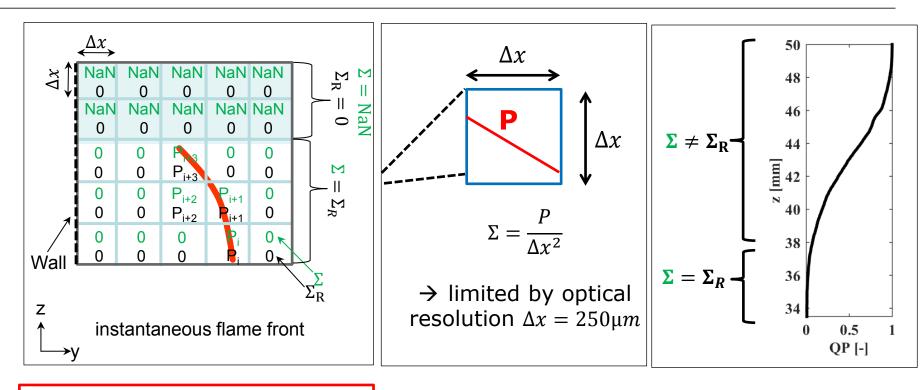
$$\overline{\dot{\omega}_R} = \rho_1^0 Y_1^0 s_l \Sigma$$
OH PLIF OH PLIF
& PIV



Flame surface density – definition

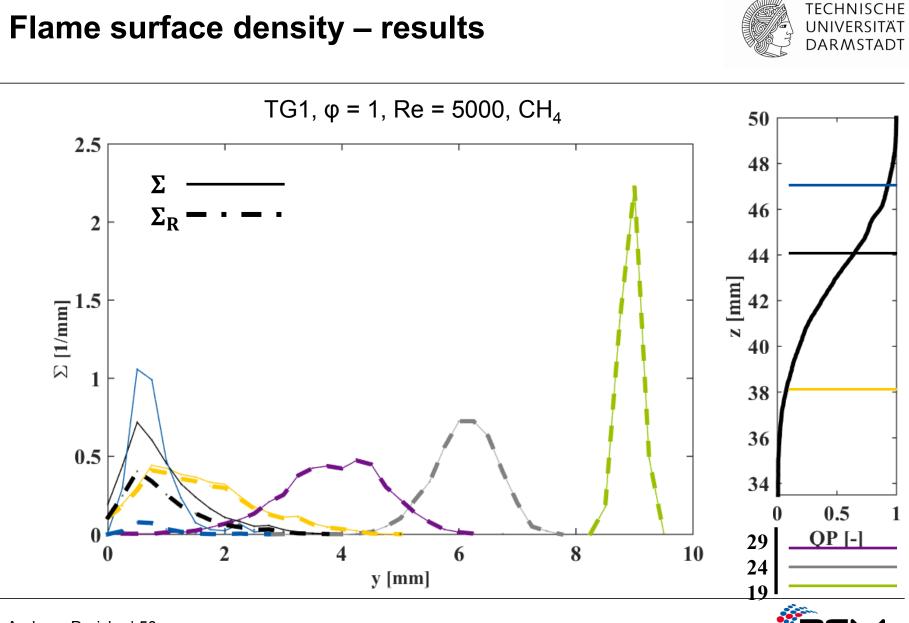


TECHNISCHE UNIVERSITÄT DARMSTADT



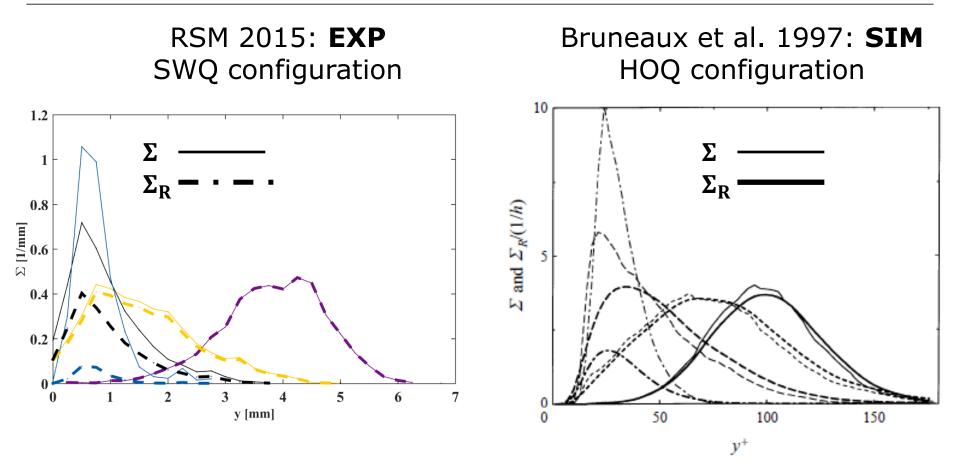
Σ **ignores** quenching Σ_R **considers** quenching Probability of quenching as function of height z over nozzle exit





Flame surface density – comparison to DNS



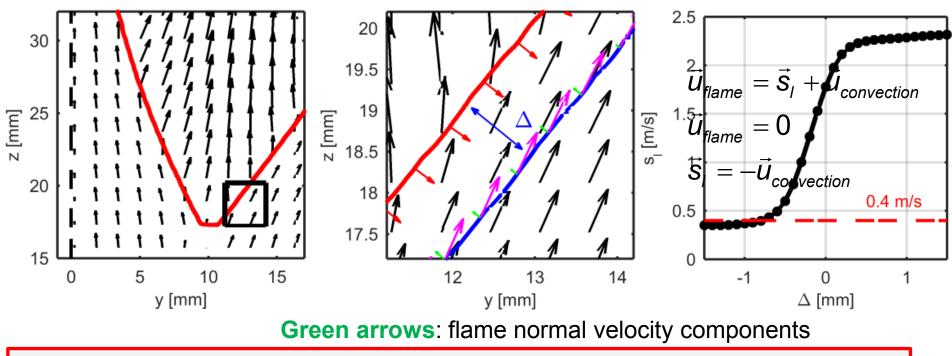




Flame consumption speed s_l - undisturbed



- *s*_l determined from **laminar configuration**
- Use of undisturbed flame branch



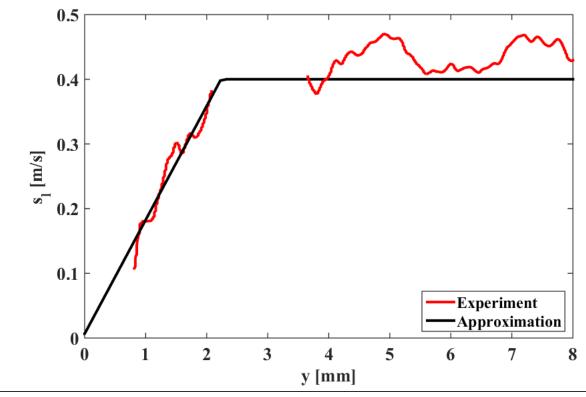
1 mm ahead of flame front flame normal velocity matches laminar burning velocity



Flame consumption speed s_l - during wall approach



 wall closest point @ y = 1mm, because of s_l refers to unburnt mixture

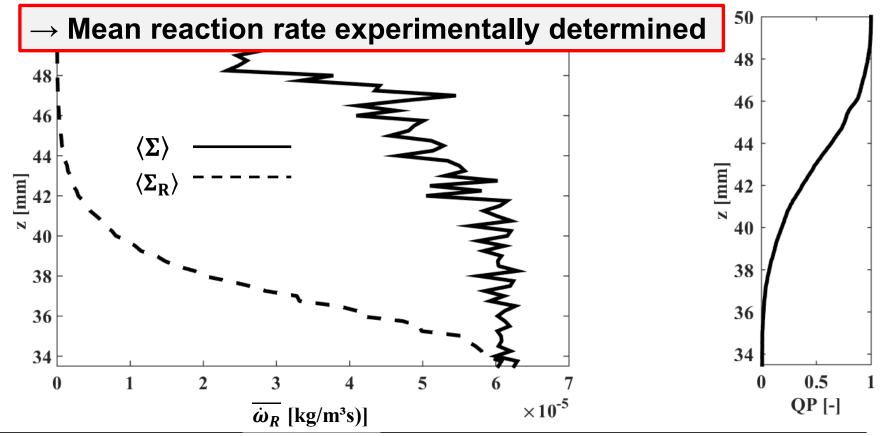




Mean reaction rate $\dot{\omega}_R$



$\overline{\dot{\omega}_R}(z) = \rho_1^0 Y_1^0 \langle s_l(y) \Sigma(y, z) \rangle$





Conclusions from PIV-OH PLIF measurements



- Impact of turbulence on FWI in SWQ-configuration:
- 1. Analysis of FSD Σ reveals:
 - Relaminarization of the flame near the wall
 - "Reacting" FSD Σ_R necessary for correct SWQ description and modelling
- 2. Mean reaction rate $\overline{\dot{\omega}_R}$:
 - Deduced from flame surface density
 - Important quantity for modelling
- Comparison to literature:
 - Good agreement with HOQ DNS from Bruneaux (1997)
 - FSD Σ_R agrees qualitatively well with model based on velocity fluctuations from Watkins (1996) see Jainski et al., PCI 2017



Outline



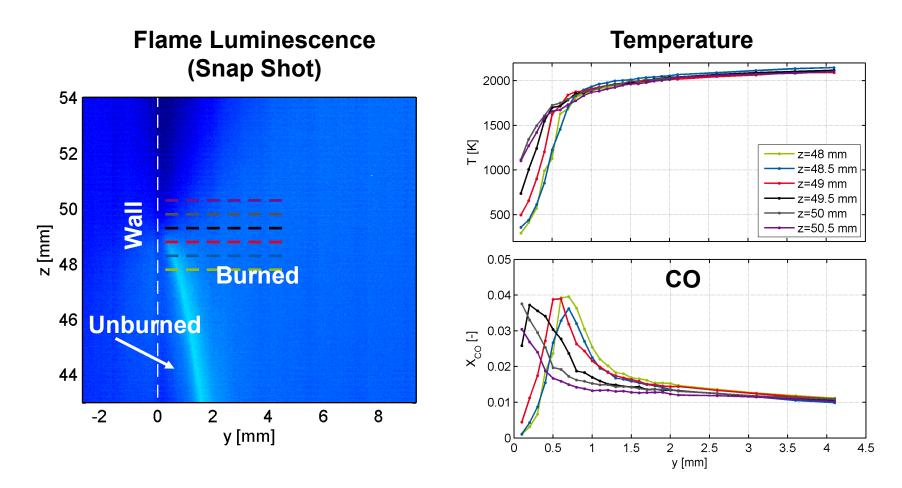
- Motivation of Flame-Wall Interaction (FWI) Research
- Experimental Approach at RSM/TU Darmstadt
- Head-on Quenching
 - Flame dynamics of turbulent flames
 - Thermo-chemical states
- Side Wall Quenching
 - Flame dynamics of turbulent flames
 - Flame surface density
 - Mean reaction rate modelling
 - Thermo-chemical states
 - Laminar flames
 - Turbulent flames

Jainski et al., Combust. Flame 2017



Laminar side wall quenching (Re = 5000, Φ = 1.0, w/o TG)

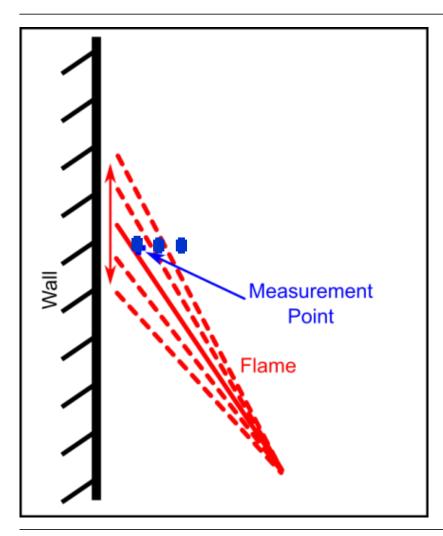






Space-fixed measurement of thermochemical states – laminar case



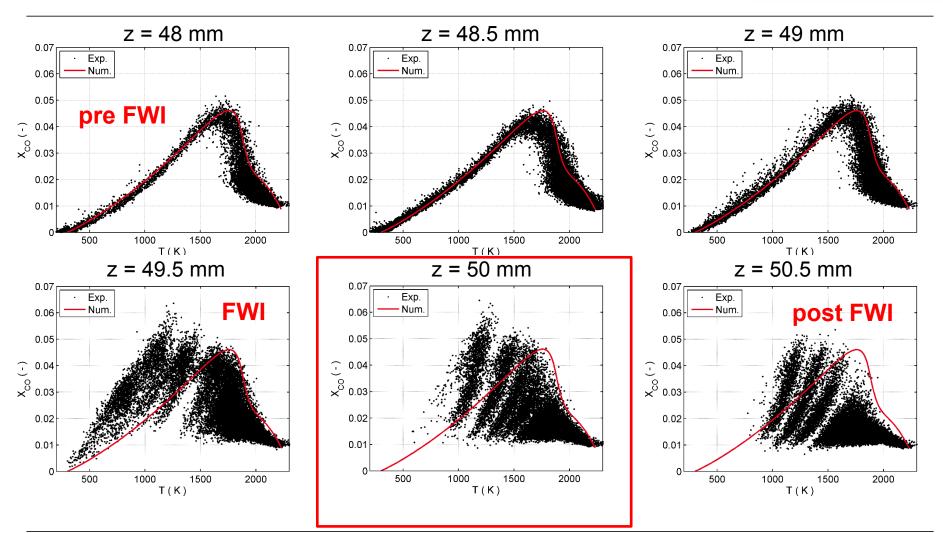


- Fixed axial positions spanning across the FWI-zone
- Scatter plots containing data from all distances to wall



Thermo-chemical states – laminar (Re = 5000, Φ = 1.0, w/o TG)

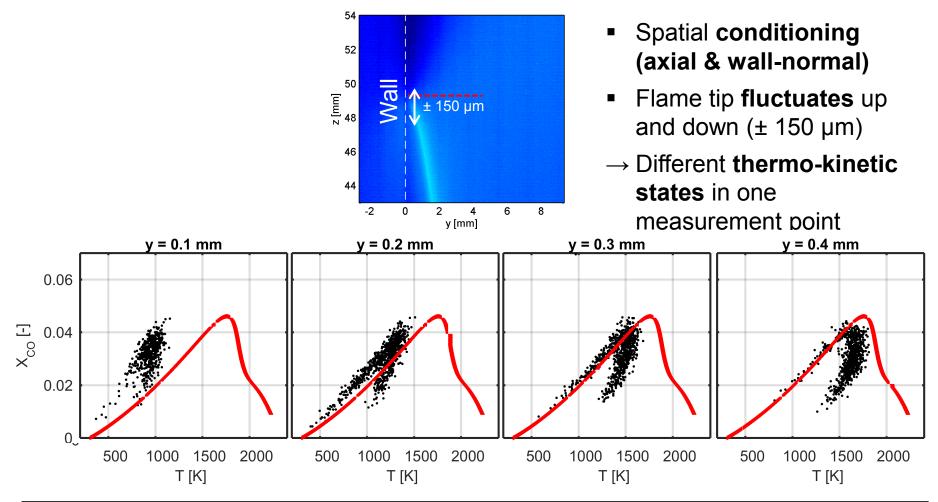






Thermo-chemical states for z = 50.0 mm (Re = 5000, Φ = 1.0, w/o TG)

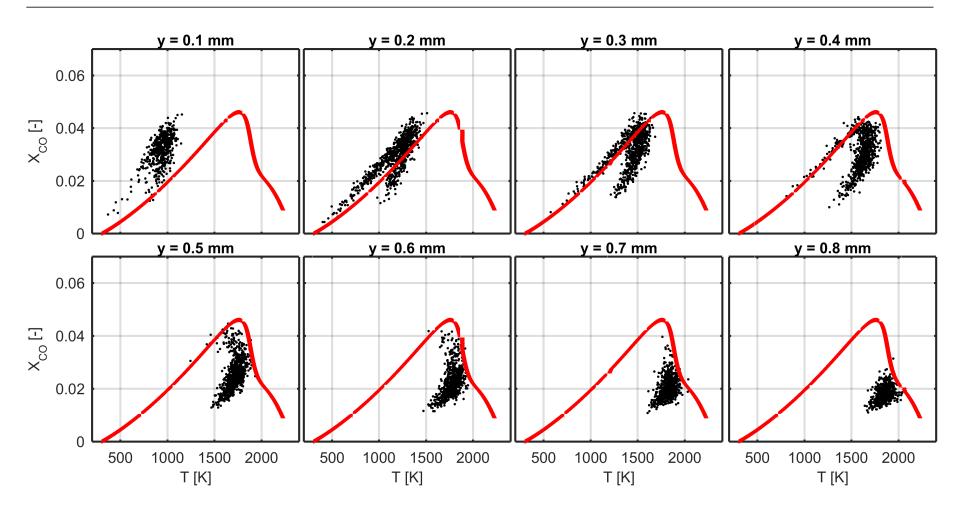






Thermo-chemical states for z = 50.0 mm (Re = 5000, Φ = 1.0, w/o TG)





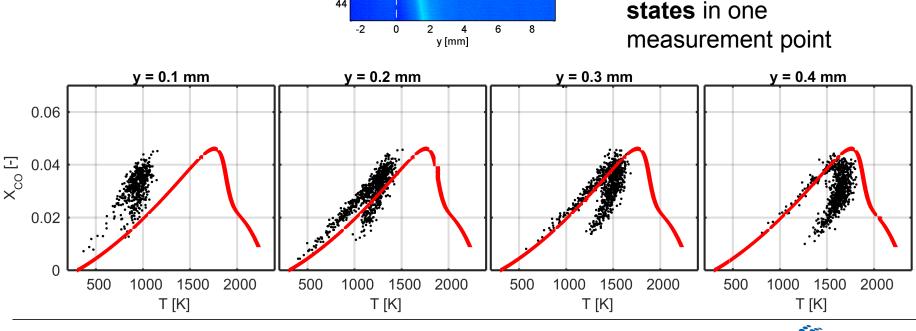


Thermo-chemical states for z = 50.0 mm (Re = 5000, Φ = 1.0, w/o TG)



enno-kinelic

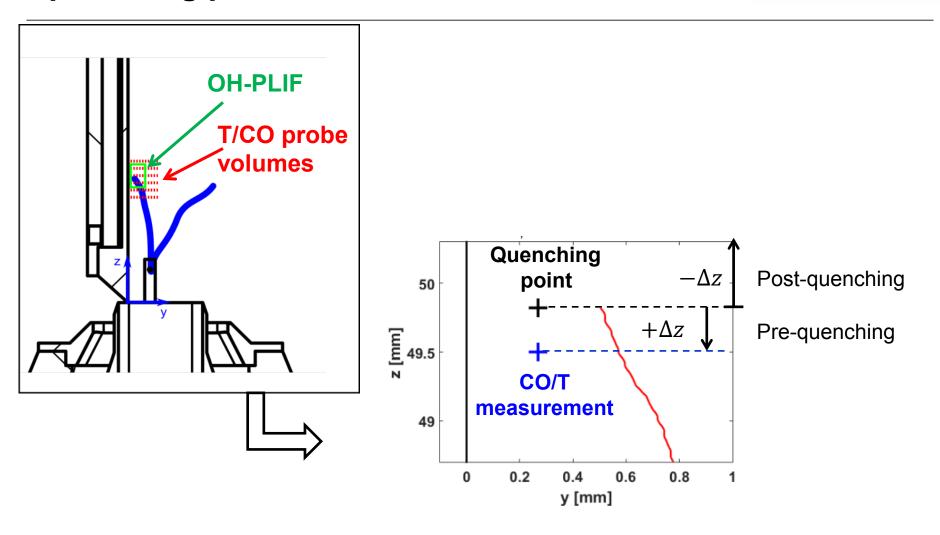
- **CO-consumption branch**: strongly influenced for wall distances y < 0.8 mm
- CO-production branch: influence starts for $y \le 0.2$ mm
- Time-scales of CO-consumption a factor of 100 larger than for CO-production
- → Heat losses more pronounced for CO-consumption branch





Analysis of thermo-chemical states relative to quenching point – flame fixed

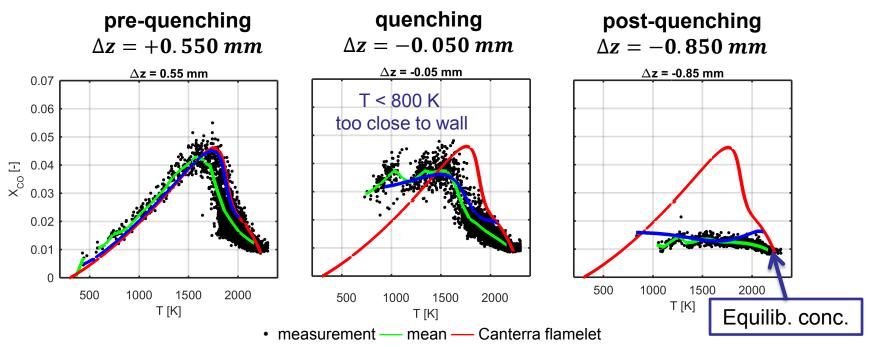






Conditioning on quenching – flame fixed analysis





Pre-quenching: undisturbed flame

Quenching and **post-quenching**: strong deviation from undisturbed flame

S. Ganter, G. Kuenne, J. Janicka: Comparison to 2D-DNS reveals dominance of diffusion over kinetic effects that cause this observation



Time scale analysis



Time scale of heat transfer¹

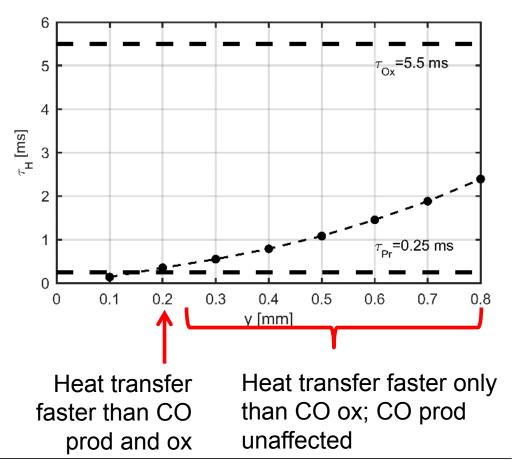
 $\tau_H = \frac{L^2}{\lambda} \rho c_p,$

- *L* represents the wall-normal distance *y*
- λ heat conductivity

Chemical time scales, from

1D calculations

- CO production $\tau_{Pr} = 0.25 ms$
- CO oxidation $\tau_{0x} = 5.5 ms$

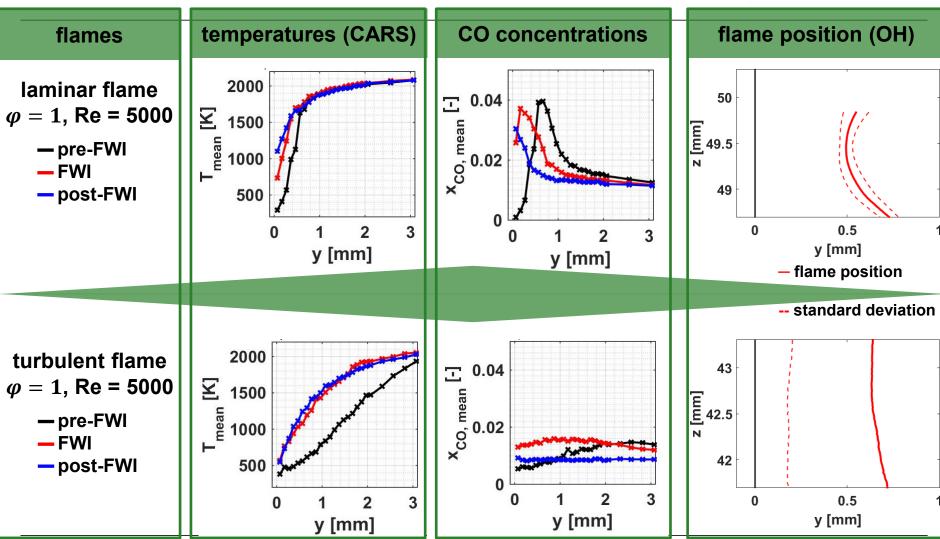


¹ E. Marín, Characteristic dimensions for heat transfer, Latin-American Journal of Physics Education 4 (2010) <u>56–60</u>



Mean quantities reveal significant differences between laminar and turbulent flames

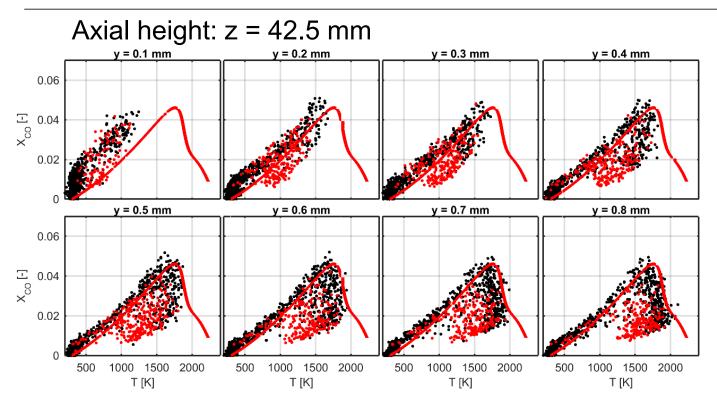






Turbulent flame – space fixed analysis ($\varphi = 1$, Re = 5000, with TG)





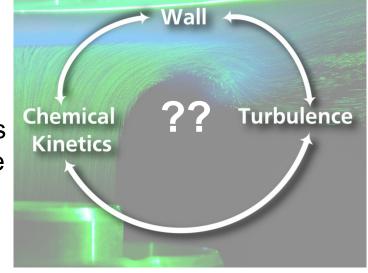
- upstream instantaneous quenching point
- downstream instantaneous quenching point
- Canterra flamelet simulation

→ Similar to laminar case but with more intermediate states
→ CO-consumption more influenced than CO-production
CO-consumption takes place at time-scales significantly longer than time-scales typical for heat transfer



Conclusions – thermo-chemical states

- Significant differences of CO-T-scatter plots compared to adiabatic flames
- Comparison to 2D DNS (not shown) and time-scale analysis reveals for CH₄-flames that diffusion rather than low temperature chemistry is dominant
- Quenching of flames near walls is observed at small spatial scales
- \rightarrow Implication for combustion modeling:
- High resolution required
- Appropriate turbulence-chemistry-interaction models needed to account for heat loss in the presence of a wall

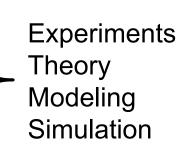






Open issues for flame-wall interaction (1)

- For steady and unsteady flame-wall interaction a more detailed understanding is required with regard to...
 - ...Structure of velocity boundary layers
 - ...Structure of thermal boundary layers
 - ... Structure of concentration boundary layers
- Unsteady heat transfer and impact of turbulent heat flux
- \rightarrow Valid models for near-wall turbulent combustion to be developed
- Understanding the influence of
 - Wetted surfaces (fuel or oil films)
 - Deposits







Open issues for diagnostics needs (2)



- Information lacking for:
 - Instantaneous structure of thermal boundary layers
 - \rightarrow Need for measurement of 1D-temperature profiles \rightarrow 1D fs/ps CARS
 - Unsteady heat transfer and impact of turbulent heat flux
 - \rightarrow Simultaneous temperature and velocity measurements near walls



Improved spatial resolution (< 50 μ m). • Automatically overlapped pump/Stokes fields, CARS temporally and spatially, makes the technique more robust and higher pulse energy available. PBS CL BD Probe S-branch BD Δv=0 ΔJ=2 Energy condition, DB-RCARS Combustion CL Research θ FACILIT HWP CL Probe Imp/Stokes 40 mJ / pulse @ 532 nm (~70 ps), 20 Hz 👂 4.5 mJ / pulse @ 800 nm (~45 fs), 1-10 kHz Time synchronized femtosecond (fs) and picosecond (ps) laser system, phase locked to an external 100 MHz RF source

TECHNISCHE UNIVERSITÄT DARMSTADT

(A. Bohlin, C. Kliewer – CRF Sandia Livermore, USA)

Two-beam fs/ps hybrid 1D-CARS

